On the Design of a European Bioeconomy that Optimally Contributes to Sustainable Development

Dissertation

zur Erlangung des akademischen Grades

Dr.-Ing.

eingereicht an der

Mathematisch-Naturwissenschaftlich-Technischen Fakultät

der Universität Augsburg

von

Lars Wietschel

Augsburg, Januar 2022

Universität Augsburg
Mathematisch-Naturwissenschaftlich-Technische Fakultät

Erstgutachter:	Prof. Dr. Axel Tuma
Zweitgutachter:	Prof. Dr. Andreas Rathgeber

Datum der Disputation: 07.04.2022

Abstract

The inevitability for a change in humankind's resource and fossil energy consumption is demonstrated by global crises such as the climate change, disturbances of natural cycles, and the loss of biodiversity. The sun provides sufficient energy to generate electricity and by photosynthesis, solar radiation is converted into energy chemically bound in biomolecules, which provide building blocks for the production of various materials, chemicals, or fuels. The *bioeconomy* puts biomass at the center of an economy that attempts to cover resource and energy demand by renewable materials to address the global challenges. However, the finiteness of the terrestrial surface limits renewables, requiring a prioritization of use. The Sustainable Development Goals (SDGs) provide a common ground for global peace, prosperity, improved health and education, reduced inequality, and spur economic growth while tackling climate change and biodiversity loss, making it the most comprehensive framework for defining objectives in the design of the bioeconomy. Against this background, this dissertation is particularly dedicated to the design of bioeconomic value chains based on agroforestry residues in the European Union, considering economic, environmental, and social objectives to optimally exploit the potential to contribute to a sustainable development. All objectives are matched to SDGs to unveil congruencies, conflicts and trade-offs between different goals, and to provide aggregated insights and courses of action in the agroforestry residue-based bioeconomy to politics, the scientific community, and corporate decision-makers.

The availability of agroforestry residue volumes and their current uses is the first major concern of a bioeconomy aligned with the SDGs to be assessed in this work. Key findings are that the most promising agricultural residue in the EU is wheat straw, followed by maize stover, barley straw, and rapeseed straw, which together account for about 80% of EU's cereals and oil crops residues. In forestry, waste bark from the two coniferous species, spruce and pine, are most promising with the highest supplies in Scandinavia and central EU. The time-series-based forecast model predicts a total increase of the bioeconomic potential of the prioritized agricultural feedstocks from 113 Mt in 2017 to 127 Mt in 2030. The forecast indicates the largest increase of all investigated crops for corn stover at up to 20% until 2030, while rapeseed straw production is forecasted to decrease in many regions.

To take environmental and social aspects into account on a regional level, along with international competitiveness, this dissertation develops a multi-criteria strategic network design model for the planning of bioeconomic value chains. The environmental and social objectives are derived by means of Life Cycle Assessment and Social Life Cycle Assessment, respectively. The developed set of 35 economic, environmental, and social objective functions allows for the consideration of 16 of the 17 SDGs. The model

is applied for the planning of a second-generation bioethanol production network based on agricultural residues in the EU. Single-criteria optimization shows that sustainably available agroforestry residues could substitute up to 22% of the petrol demand in the EU in 2018 under optimal production networks for certain objectives (i.a., *global warming*). For environmental objectives, the decision to substitute petrol or edible crops-based ethanol has the highest impact. The greenhouse gas benefits could amount to up to 59 Mt CO_2 eq., conforming to about 1.35% of the EU's 2018 total emissions. However, *global warming* optimization leads to opportunity costs for other objectives. While for *ecosystem quality*, for example, the achieved value reaches 50% of its optimum, other categories like *land use* and *water consumption* could even be net deteriorated by optimizing *global warming*. For objectives such as *land use*, only 19% of the total agroforestry residues is used to substitute 100% of the edible crops-based ethanol, which would free up 11.7 billion m^2 crop land. Social objectives lead to large and labor-intensive production networks distributed all over the EU. Depending on the social objective, the value creation slightly shifts regionally. To optimize *local employment*, the network relocates to regions with high unemployment rates, such as Spain, Italy, and parts of France. Economically strong metropolitan regions are at a disadvantage in favor of weaker regions of Central and Eastern EU when optimizing economic development. At best, up to 140,000 new jobs could be created in the EU while 12,000 jobs could be lost due to substitution of reference products. In terms of network extend, most socially and environmentally optimal production networks are similar, although the substitution decision has little impact for social objectives. This means that interesting trade-offs between social and environmental objectives can be found with only minor sacrifices. Economically optimal networks are much smaller and more centralized than environmental ones, and lead to costs of about 0.75 €/l second-generation ethanol. Environmental optimization results in cost between 0.88 €/l to 2.00 €/l, which implies that large-scale bioethanol production is not economically feasible with today's oil prices and taxes.

While the single-criteria optimization reveals conflicts within and between the environment, social, and economic dimensions, Pareto optimization is conducted to unveil trade-offs between conflicting goals. Significant environmental and social benefits can often be realized with only small economic detriments, and vice versa, economic profitability can substantially be improved at low environmental opportunity cost. Furthermore, the applied Pareto optimization shows that the endpoints *human health* and *ecosystem quality* are suitable aggregators of environmental impact categories, wherefore they could serve as representative of the environmental dimension in decision-making. Nonetheless, a transparent consideration of a broad range of impacts and knowledge about the categories' contributions remains indispensable to reveal possible negative consequences of a decision. In a final step, the objective functions are

matched to SDGs, and opportunity cost between the objective functions are calculated to unveil congruencies and conflicts between different goals. The assessment of relationships between the different SDGs supports the perception that different aspects of sustainability are not equally directed. Sustainability, expressed by the SDGs, is rather case-specific and varies between a multitude of interdependent social, environmental, and economic criteria. Decision-makers, whether at the corporate level pursuing one or more business objectives or at the policy level, using the SDGs as a framework, should be aware of the reciprocities between the different criteria. The dissertation shows that the European bioeconomy has a great potential to contribute to sustainable development. Multi-criteria optimization models enable sound trade-off decisions that are aligned to the SDGs.

Acknowledgments

My dissertation has been written in the last years during my time as research associate at the Chair of Production & Supply Chain Management at the University of Augsburg. I want to thank all the people who motivated, challenged and supported me during this time.

I would especially like to thank Prof. Dr. Axel Tuma for his supervision, discussions, and support throughout my doctoral studies. Many thanks also to Prof. Dr. Andreas Rathgeber, who agreed to serve as second reviewer of the thesis. A special thanks to Dr. Andrea Thorenz for her excellent leadership of the working group Resource Lab I am part of, and with whom together I was privileged to accompany the EU-fundet project REHAP during my time as a research associate. Many thanks also to Dr. Aitor Barrio, who did a great job in leading the multinational project consortium and making the REHAP project a success.

Many thanks to all my direct colleges Amelie, Aykut, Chantal, Christian, Christoph, Lukas, Martin, Sandra, and Stefan. In particular, I would like to thank Lukas, with whom I have worked closely on research projects over the past few years, where we have learned from each other and achieved great results together. In Christoph I found a good friend who I could approach with any problem and with whom I often discussed passionately.

I thank all my friends for many good moments together and their support. Very special thanks to my parents Jutta and Martin, and my siblings Johanna, Marie, and Felix, who gave me the necessary support and confidence in every situation of life. And finally, I want to thank my wife Jenny and my daughter Paula. In Jenny, I found a great partner with whom life is for sure not getting boring. We already managed many projects together, I am looking forward to all those that are still waiting for us. Paula, our wonderful daughter warms my heart every day with her nature and gives me the great joy of discovering the world anew through her eyes.

Table of contents

List of figures

List of tables

1 Introduction

1.1 Motivation

The last 150 years of humankind have been characterized by rapid developments in almost every area of life. The extensive use of fossil energy, which is solar energy transformed via photosynthesis into biomass and stored over millions of years, has been a major driver of this rapid progress. Already in 1896, Arrhenius raised the theory that the combustion of fossil fuels and the associated emissions could influence the temperatures on earth (Arrhenius, 1896). With the publication of 'Limits to Growth' in 1972, the discussion about the sustainability of human activity has become a matter of public debate at the latest (Meadows et al., 1972). Even though humankind took another 50 years to internalize, today, it is unequivocal that humans' consumption of fossil energy and the associated greenhouse gas emission has warmed the atmosphere, ocean, and land with rapid changes to almost every sphere (IPCC, 2021). To limit climate change to a certain level, cumulative CO_2 emissions must be limited (IPCC, 2021). In the Paris agreement, 196 states declared to limit climate change to "well below 2, preferably to 1.5 degrees Celsius" which means emissions must reach at least net-zero by mid-century (UNFCCC, 2015).

The imperative for a change in humankind's resource and energy consumption is shown by global warming and the transgression of various planetary boundaries, whereof a significant share can be attributed to the extensive use of fossil energy (Rockström et al., 2009). This raises the necessity of transforming our primarily fossil energy and mineral resources-based economy towards an economy that is mainly based on renewable sources. Even though the problem of climate change has had public attention since 1988 at the latest, with the establishment of the IPCC (IPCC, 1992), one of the most prosperous confederations of states such as the European Union, has not been able to liberate itself from fossil energies yet. Fig. 1 shows the per capita primary energy consumption by source and the CO_2 emissions of countries part of the EU27, relative to 1990 (Eurostat, 2021o; Global Carbon Project, 2021). CO_2 emissions per capita slightly declined over the past decades due to increased renewable energy production and the deactivation of the most emission-intensive fossil power plants in exchange for less emission-intensive ones (Eurostat, 2021o; World Bank, 2021a). Even though most technologies became more energy efficient in the last decades, the average primary energy consumption per capita fluctuated only slightly in a narrow band of $\pm$ 7% within the previous 30 years (EIA, 2021), which signifies that on a broader picture, rebound effects and increasing needs canceled out efficiency gains entirely. The energy

consumption is slowly decoupling from CO_2 emissions, but only reached a spread of 20% compared to 1990. The recent IPCC (2021) report clarified that global warming would exceed 1.5° and 2°C during the 21st century unless CO_2 and other greenhouse gas emissions are drastically reduced in the coming decades. Humanity has only a certain carbon budget remaining, depending on the probability of limiting the temperature increase to a certain level. Among a vast array of necessary measures to mitigate climate change, reducing carbon intensity of energy towards zero and reducing the energy intensity of processes that serve our material needs are among the most important (IPCC, 2014).

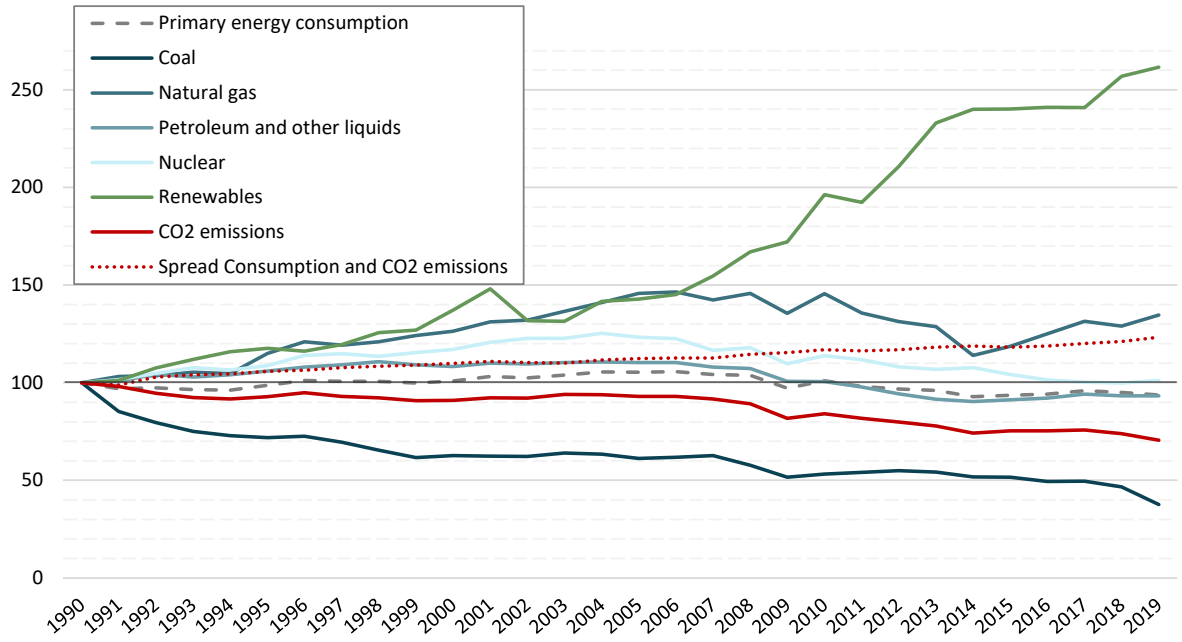

Fig. 1: Per capita primary energy consumption by source relative to 1990 in the EU.
Own depiction based on EIA (2021), Eurostat (2021m), and Global Carbon Project (2021)

Renewable energies and renewable materials are based on the flow of solar radiation, wherefore their use does not destroy low-entropy resources at the cost of climate active emissions. Georgescu-Roegen stated in 1971 the inevitability that the survival of humankind requires that it lives within the limits of what the sun provides annually in free energy (Georgescu-Roegen, 1971). After many years have been lost in transforming the economic system, limiting climate change to a tolerable level depends on whether humankind manages to base its consumption on renewable materials and energy within the next few decades.

The earth has three renewable sources at its service: solar radiation, geothermal and tidal energy. The sun is by far the most important contributor; geothermal and tidal energy have a subordinate role in renewable energy provision (Quaschning, 2020). Solar radiation can be transformed directly into usable energy via photovoltaics and solarthermics or by using natural transformations of the sun, such as wind or the water

cycle (Quaschning, 2020). The direct use of solar radiation via photovoltaics and its natural transformations via wind turbines, for example, are nowadays associated with mostly low environmental impacts (Hertwich et al., 2015) and economic costs (Edenhofer et al., 2013; Kost et al., 2021). By photosynthesis, solar radiation is converted into energy chemically bound in biomolecules everywhere on the earth's surface. Photosynthesis is the main driver of the earth's oxygen cycle and provides most energy for life on Earth. Fig. 2 shows some of the most important biomolecules of plant-based biomass that result from photosynthesis and their various services for humankind. Biomass has provided humanity with food, materials, and energy since time immemorial. Additionally, it offers the great advantage that it can provide building blocks for the production of various materials, chemicals, pharmaceuticals, or fuels. Besids the provision of resources and energy to fullfill human demands, plants provide a wide range of services, such as climate regulation, flood protection, a refuge for humans and animals, and biodiversity preservation. The various aspects of biomass services, conservation, and utilization are strongly interdependent and any system changes impact the other aspects.

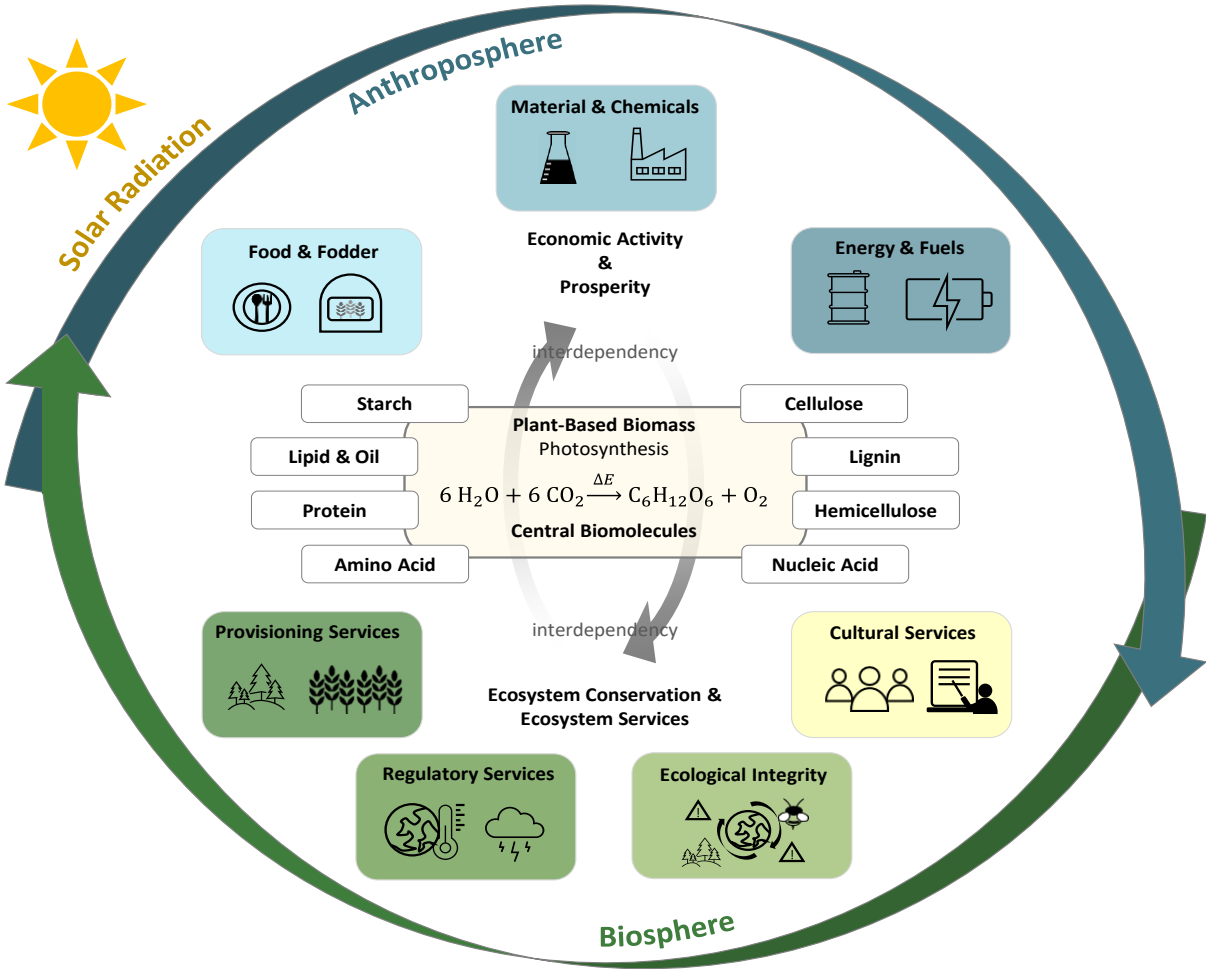

Fig. 2: Circular Bioeconomy with plant-based biomolecules as central feedstock for the different biomass services. Own depiction based on Burkhard et al. (2012), EFI (2020), NREL & PNNL (2004)

The so-called *bioeconomy* puts biomass at the center of an economy that attempts to cover resource and energy demand by renewable materials to address the global challenges, inter alia, the preservation of the biosphere (Stegmann et al., 2020). Due to the strong interdependency between the different stakeholders of biomass and its provision, using biomass for energy and material production is much more challenging than directly using solar radiation or natural transformations such as wind (Tilman et al., 2009; Pfau et al., 2014). Terrestrial land for renewable, plant-based resources is limited, wherefore food, fodder, energy, material production, and the various ecosystem services compete. Furthermore, the current anthropogenic land management is unsustainable regarding biodiversity preservation and soil maintenance (Rockström et al., 2009; Lewandowski, 2015).

To adequately guide the use of renewable raw materials and balance the various stakeholders, the European Commission launched 2012 the strategy "Innovating for Sustainable Growth: A Bioeconomy for Europe". The strategy is a comprehensive approach to address environmental, energy, food supply, and other natural resource conflicts related to the use of renewable, plant-based raw materials (European Commission, 2012). Funds have been available to support bioeconomic research and innovation projects under the EU's Horizon 2020 funding program. In 2018, the European Commission updated the 2012 Bioeconomy Strategy to reflect societal and political developments (European Commission, 2018c). The refocusing was primarily due to the lack of appropriate approaches that can adequately reflect the different environmental-techno-socio-economic aspects of biomass utilization and a missing alignment to political agendas such as the Sustainable Development Goals, the Paris Climate Agreement, and other EU initiatives (European Commission, 2018c).

In November 2019, the EU presented the European Green Deal intending to make the EU climate neutral by 2050. The Green Deal is the last and largest call under Horizon 2020 and is particularly characterized by environmental, social, and economic issues being thought of together for all parts of the EU (European Commission, 2021a). In 2015, the United Nations formulated the Sustainable Development Goals (SDG), probably the most comprehensive approach to meeting our time's various challenges (United Nations, 2015). They provide a common ground for global peace, prosperity, improved health and education, reduced inequality, and spur economic growth while tackling climate change and biodiversity loss. Fig. 3 shows all 17 Sustainable Development Goals intended to promote a global ecologically, socially, and economically sustainable development. Each SDG is further specified by a range of sub-targets and indicator suggestions to quantify and monitor the progress of sustainable development (United Nations, 2015). Bioeconomic activities are at the center of tension between food supply, energy demand, raw material requirements, and environment and, therefore, directly interfere with at least 11 sustainable development goals (Heimann,

2019). While some goals like *Zero Hunger, Affordable and Clean Energy, Responsible Consumption and Production,* or *Climate Action* are directly addressed by bioeconomic activities, depending on the design of bioeconomic value chains, any of the 17 goals may be addressed.

Fig. 3: Sustainable Development Goals of the United Nations
(United Nations, 2015)

1.2 Problem formulation

The meaning of the term *bioeconomy*, often also termed *biobased economy*, varies between the different stakeholders. It can either refer to all biotechnological advances, biotechnology in life science, or the use of biomass as a substitute for fossil resources (Pfau et al., 2014). This work understands the bioeconomy as an economy that bases its demand for materials, chemicals, and energy on biomolecules derived from renewable biomass resources to substitution conventional resources (McCormick and Kautto, 2013). A sufficient supply of biomass to serve food, feed, materials, and energy is a prerequisite for a bioeconomy that contributes to global sustainable development. Staffas et al. (2013) investigated different national bioeconomy strategies and ascertained a lack of policies for securing the biomass supply. The introduction of an EU-wide policy framework for the production of biofuels based on edible crops, for example, came without a dedicated resource strategy (Staffas et al., 2013) and an insufficient assessment of the various social and environmental repercussions of the use of edible biomass (Lewandowski, 2015). When planning bioeconomic value chains, it thus is essential to know the current regional feedstock availability and forecasts of the future development of regional raw materials availability, and it is inevitable to understand the environmental and social implications of their use. In the case of biofuel

production based on edible biomass, the intricate ecological and social interrelationships have been disregarded in favor of the exclusive goal of CO_2 reduction.

Humanity's use of fossil raw materials led to a global climate change with far-reaching consequences for life on Earth. This makes climate change mitigation one of the most urgent global challenges (IPCC, 2021). However, the various other transgressions of planetary boundaries and social challenges caused by humankind's lifestyle must also urgently be incorporated into global agendas (Rosenbaum et al., 2018). A bioeconomy that uses edible biomolecules such as starches, oils, or proteins to produce fuels and materials might mitigate climate change, but also has huge land requirements which implies the risk of increase social inequality and has massiv environmental consequences, such as biodiversity loss. A bioeconomy based on non-edible biomolecules such as cellulose, hemicellulose, or lignin has the potential to avoid such conflicts. Agroforestry residues, suche as straw, bark, or sawdust, as feedstock for basic building blocks in materials, chemicals, and energy provision, for example, are neither directly in competition with food production nor indirectly through land competition. Furthermore, various studies showed the environmental superiority of agroforestry residues over raw materials, particularly grown for material, chemical, or energy provision in most of the assessed ecological impact categories (Muñoz et al., 2014; Morales et al., 2015).

Nonetheless, the extraction of agroforestry residues entails various challenges that need to be addressed, like a low density, its spread over the area with associated long-distance transportation, and varying environmental effects depending on regional conditions such as soil type and quality, et cetera (Budzinski et al., 2019). The large absolute transportation quantities combined with the low specific material value of agroforestry residues and the economies of scale of chemical production sites render regional location and transport decisions very important. The importance of regional value chain characteristics while simultaneously taking into account the triple bottom line of economic, environmental, and social aspects necessitates decision models capable of addressing regionality and a variety of different objectives.

Production network planning models are applied in the decision-making process regarding production locations and the associated supply and product transportation flows. In addition, such models can be configured with different objectives, allowing economic goals to be considered alongside environmental and social objectives. Strategic network design typically encompasses structural, strategic decisions like plant locations and capacities and operative decisions like material flows between the plants and demands (Goetschalcks and Fleischmann, 2008). An ideal bioeconomy takes environmental, social, and health aspects alongside international competitiveness as the basis for business goals (Lewandowski, 2015).

The SDGs provide a common ground for humanity's most urgent challenges; however, they do not provide already operationalized and readily applicable quantitative indicators. The concept Life Cycle Sustainability Assessment (LCSA) divides sustainability into the three pillars economic, social, and environment, and adopts a life cycle perspective (UNEP, 2011). It operationalizes the three pillars and allows the identification of potential trade-offs between them (Valdivia et al., 2021). The environmental pillar is addressed by Life Cycle Assessment (LCA), particularly suited for a holistic evaluation of various environmental impacts. The social dimensions is addressed by Social Life Cycle Assessment (SLCA). Many studies in the field of strategic network design have addressed the economic feasibility and LCA-based environmental impacts in optimization models (Eskandarpour et al., 2015). The application of social sustainability into quantitative models is more intricate due to a lack of social data readily applicable and a lower maturity in terms of user-friendliness of tools, open methodological issues, interpretation of results, and a lack of best-practice approaches (Valdivia et al., 2021).

1.3 Research questions and outline of this thesis

To make the most of the opportunities offered by bioeconomic activities to contribute to the achievement of the Sustainable Development Goals, this dissertation is particularly dedicated to the strategic network design of bioeconomic value chains based on agroforestry residues, considering economic, environmental, and social objectives. The work provides different courses of action in the design of bio-based value chains and gives insights about congruencies and trade-offs between different investigated objectives. In a final step, all investigated objective functions are assigned to SDG targets to show conflicts and congruencies at the SDG level to provide aggregated insights to politics, the scientific community, and corporate decision-makers. Since the investigation requires a detailed understanding of various underlying regional aspects, this work takes the European Union as the system boundary. Against this background, this dissertation sets out to address the following five research questions:

- *RQ1*: Which agroforestry residue streams in the European Union are the most promising feedstocks for bio-based value chains, and how are they regionally distributed?
- *RQ2*: How will the set of prioritized agricultural feedstock potentials develop at the regional level by 2030?

- *RQ3*: How needs a multi-criteria optimization model for the strategic planning of bio-based value chains be designed to integrate economic and environmental objectives?
- *RQ4*: What is a best-practice approach for a structured and transparent selection of quantitative and operationalizable social indicators for bio-based value chains?
- *RQ5*: What are the social, environmental, and economic benefits of optimal biorefinery networks, and which Sustainable Development Goals are affected?

Fig. 4 shows the thesis structure with an assignment of the research questions to the corresponding chapters. The motivation, problem formulation, and research questions are followed by the state of research, which gives a brief background to the historical development of the European bioeconomy and addresses current challenges. Furthermore, the most important methods for answering the research questions are introduced. The third chapter investigates **RQ1** by assessing the regional potentials of a large set of different feedstocks. The fourth chapter examines and answers **RQ2** by providing a spatially explicit forecasting approach for a prioritized set of agricultural resources. The fifth chapter investigates **RQ3** and develops a multi-criteria optimization model that integrates supply chain network optimization and Life Cycle Assessment. The model is applied to the value chain for second-generation bioethanol production; however, it could, in principle, be applied to various strategic network design problems in the bioeconomy. The sixth chapter investigates **RQ4** and developes an approach for integrating social indicators into quantitative models. To answer **RQ5**, the derived social indicators are applied in an extended version of the network optimization model proposed in chapter 5. Especially in the social dimension, existing approaches have not yet gone far enough to quantitatively capture a larger number of different indicators in optimization models. This is necessary to eventually perform an Life Cycle Sustainability Assessment to show how bioeconomic value chains that substitute fossil products contribute to sustainable development and the expected trade-offs between different SDGs. In chapter seven, the findings of this thesis are critically discussed. Finally, chapter 8 briefly concludes the work and gives an outlook on future research fields.

Several research papers have been published within the scope of the research on which this dissertation is based. Parts of Chapters 3 to 6 were jointly published in peer-reviewed articles with coauthors as part of a regular scholarly research discourse underlying this thesis. Parts of Chapter 3 conform with Thorenz et al. (2018), parts of Chapter 4 conform with Wietschel et al. (2019), and parts of Chapter 5 conform with Wietschel et al. (2021). Parts of Chapter 6 conform with the manuscript *Assessing the Social Dimension in Strategic Network Design for a Sustainable Development: The*

Case of Bioethanol Production in the EU (Messmann et al., forthcoming), which is currently under review at the Journal of Industrial Ecology.

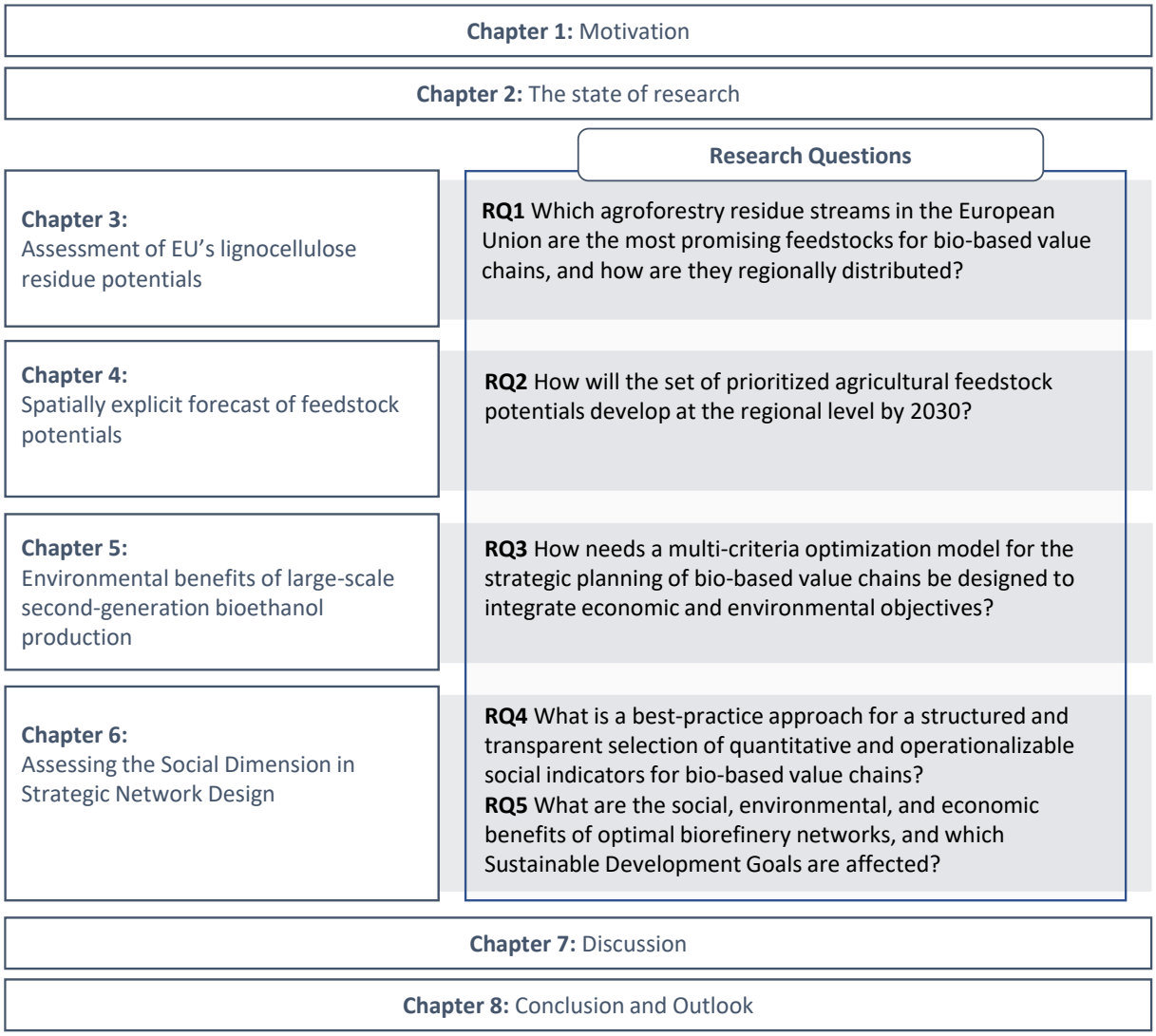

Fig. 4: Structure of the dissertation

2 The state of research

The state of research gives an overview of methods and findings to answer the research questions presented and indicates where further research is needed. The multidimensionality of this thesis requires a range of methodologies of different research fields. Chapter 2.1 gives a brief overview of the history of the bioeconomy and its recent development. Since methods for the environmental and social assessment of bioeconomy measures are needed, chapter 2.2 introduces the Life Cycle Assessment. Chapter. 2.3 briefly introduces Strategic Network Design, which allows the consideration of regional aspects in the decision-making process on the design of supply chains. Eventually, chapter 2.4 introduces Multi-objective Mixed Integer Linear Programming, which enables the mathematical formulation and optimization of decision problems under consideration of multiple goals.

2.1 Bioeconomy

Georgescu-Roegen can be seen as one of the founders of the bioeconomy and described in *The Entropy Law and the Economic Problem* industrial production and the associated resource consumption from a thermodynamic perspective (Georgescu-Roegen, 1971). In his work *Selections from "Energy and Economic Myths",* he describes a "minimal bioeconomic program", in which he makes several proposals on how humankind can ensure a long existence (Georgescu-Roegen, 1975). A major part of his critique stems from the extensive use of the confined terrestrially stored sun in fossil fuels and ordered material structures. Those low-entropy resources guarantee humankind's high energy and intensive material consumption to the cost of irrecoverable destruction of low-entropy. On the one hand, the stock will ultimately be exhausted, and on the other hand, using these resources leads to harmful pollution.

For this reason, he urges humanity to live within the limits of what the sun provides annually in free energy (Georgescu-Roegen, 1971). While Georgescu-Roegen understood the term "bioeconomy" to encompass the entire interplay of the economy, society, and the environment, the term has a different emphasis in today's perception. The argument of the scarcity of fossil resources has lost urgency due to many new explorations, especially given the much larger problem of climate change associated with fossil resource consumption. Until the mid-2000s, the term bioeconomy was used primarily in reference to economic activities in biotechnology (European Commission, 2007). Subsequently, the term was extended, and the OECD figured out three main characteristics of the bioeconomy: the use of biotechnology for new processes and

products, the use of renewable biomass, and the integration of biotechnology across sectors (OECD, 2009). The EU framed the term bioeconomy again even broader and focused on exploiting biological resources for securing healthy food, animal feed, and bio-based materials and fuels for a post-petroleum society (European Commission, 2012). Staffas et al. (2013) analyzed different bio-based economy and bioeconomy strategies and policies from countries all over the globe[1]. The authors ascertained a shortcoming of the discussion on biomass availability in almost all analyzed reports. The issue that sustainably available biomass will not be sufficient to fully replace fossil feedstocks, which would require prioritization of bio-applications, is poorly addressed. The authors plead for a better focus on environmental components in bioeconomy approaches, especially in the context of biomass supply (Staffas et al., 2013).

In principle, bio-based products are classified by three generations of biomass feedstocks shown in Table 1, especially in the context of biofuels (Lee and Lavoie, 2013). First-generation bio-based products are produced from edible biomass. Either starch-rich materials are used to produce ethanol by fermentation of C6 sugars (mostly glucose), or oily plants and seeds are used to extract plant-based oil (triacylglycerol) for further refinement of biodiesel, for example. Second-generation bio-based products encompass a wide array of different feedstocks, which have in common especially the non-edibility. Lavoie et al. (2011) distinguish three categories of second-generation feedstocks: homogeneous feedstocks, such as roundwood wood used for high-end products, quasi-homogeneous feedstocks, which mostly encompass agroforestry residues of fluctuating quality, and non-homogeneous feedstocks of low value like municipal solid waste. Lignocellulose residues as feedstock for high added value products have received the most attention in recent years due to their comparatively low price and high abundance. Third-generation bio-based products are produced from cultivated algae. The microorganism algae have a high yield and high lipid contents, which can be used for different products like biodiesel. The benefits of algae are their fast growth and comparably low area requirements. Challenges such as dewatering of the algae, lipid extraction, and large area and water requirements for a scaled-up production limit the potential of third-generation bio-based materials. Some studies additionally mention fourth-generation bio-based materials separately. Fourth generation feedstocks are genetically modified algae that have higher CO_2 capturing properties and higher lipid production (Dutta et al., 2014).

1 There are slight differences in the use of the terms “bioeconomy” and “bio-based economy”. Bioeconomy rather refers to the biotechnology sector and bio-based economy to the transformation of the whole economy to one that is based on biomass for food, feed, material, and fuel production (Staffas et al., 2013). In this work, the terms bioeconomy and bio-based economy are used interchangeably.

Table 1: Different generations of feedstocks for bio-based materials
with pros and cons (based on Abdullah et al., 2019; Dutta et al., 2014; Lee & Lavoie, 2013)

Generation	Feedstock	Pro	Con
I	• Starch-rich food crops • Oily plants and seed (triacyglycerol) • Animal fats	• Simple conversion technology • Profitable	• Food, energy, environment trilemma • Low biomass yield • Expensive feedstock • Direct and indirect land use change
II	• Homogeneous: round wood • Quasi-homogeneous: agroforestry residues, e.g., straw and bark • Non-homogeneous: municipal solid waste, waste cooking oil	• No direct nor indirect food competition • Utilization of residues and waste • Environmental benefits compared to conventional products in many impact categories	• Expensive pretreatment (esp. lignocellulose) • Marginal profitability due to advanced technological requirements • Risk of lowering soil organic carbon (SOC)
III	• Algea	• High growth rate • High lipid yield • No direct nor indirect food competition	• High energy demand (e.g., dewatering, lipid extraction) • High cost if grown in photo-bioreactor • Contamination if grown in open ponds • Not profitable yet
VI	• Genetically modified algea	• High production rate • High CO_2 capture ability • High lipid yield • No direct nor indirect food competition	• Risk of gene transfer to the environment • Legislative barriers • High initial investment • Still under research • Not profitable yet

Besides some niches, lignocellulosic residues currently have the largest potential to replace conventional products in various bio-based applications with a significantly better environmental footprint while being economically viable at the same time. In recent years, great progress has been made in developing bio-based materials based on lignocellulosic residues. However, as these compete against petrochemicals that have been optimized over decades, most bio-based products are still on the verge of economic viability. If the economic viability is given, the concepts developed so far on laboratory or pilot scale will be increasingly upscaled, which again raises the question of the availability of feedstocks and the prioritization of feedstock utilization. Since a sufficient biomass supply to serve the different demands is a prerequisite to sustainable development, various works and projects have investigated the issue of raw material availability in recent years in the European Union (Scarlat et al., 2010, 2019; Dees et al., 2017; Thorenz et al., 2018). To the best of the authors' knowledge, forecasts on the development of the availability of lignocellulosic residual materials are virtually non-existent to date.

2.2 Life Cycle Assessment

Various instruments are available to science, industry, and politics to quantify the environmental impacts of products, services, and processes. The globally recognized and widely used Life Cycle Assessment (LCA) method is particularly well suited for a holistic environmental evaluation of products, services, or process chains based on modeled material and energy flows (Hauschild, Rosenbaum, et al., 2018). LCA enables the evaluation of the entire life cycle of a product, from the acquisition or extraction of raw materials, through production, the use phase, to the end-of-life treatment. For this purpose, the product is standardized to a so-called Functional Unit (FU), such as the product itself, the service of the product (i.e., the product function), or the mass (Frischknecht, 2020). The procedure of a Life Cycle Assessment is described in ISO standards 14040 and 14044 and consists of four iterative phases. Fig. 5 shows the four phases with brief examples, starting with the Goal and Scope definition, the *Life Cycle Inventory*, the *Life Cycle Impact Assessment*, and the *Interpretation* of the results (ISO, 2006a).

An LCA begins with a thoroughly considered definition of its goal. This includes a justification of reasons for the study with a precise description of its intended application and the possible recipients. An accurate goal definition is the basis for the scope definition, where the LCA is further framed and outlined. The scope of the study includes the definition of a *Function Unit* (FU), which is a quantitative description of the function of the assessed object and the basis for scaling the inputs and outputs in step two, the life cycle inventory analysis (LCI) (Hauschild, Rosenbaum, et al., 2018). Furthermore, it includes defining the decisive processes, the cut-off criteria, and the system boundaries (Frischknecht, 2020).

The LCI gathers all inputs and outputs that arise to deliver the defined functional unit. Inputs are typically energy, raw materials, intermediate products, air, auxiliaries, and different others. Outputs are the intentionally produced functional unit, and many unintentional emissions like excess heat, wastewater, exhaust gases, and many others are further separated in the environmental compartments water, air, and soil to which the emissions are released. There are two principally different modeling approaches for the LCI: attributional and consequential. The attributional approach asks the question, "which environmental impact can be attributed to a product system or process", wherefore it tries to isolate the production system from the rest of the technosphere (Bjørn et al., 2018; Frischknecht, 2020). Determining the share is the big challenge in this approach and, to a certain extent, always subjective since no product can completely be isolated from the rest of the economy. Consequential modeling came up around 2000 and tried to eliminate this weakness by asking the question of the actual environmental consequence of a decision or the consumption of a product (Bjørn et al.,

2018). The difficulty with this approach is making predictions about the future consequences of a decision and identifying the "true" cause-and-effect chains. In contrast to the attributional approach, marginal processes are used instead of average processes for determining the in- and outputs (Bjørn et al., 2018).

The LCI is followed by the impact assessment, divided into seven sub-steps (ISO, 2006b; Frischknecht, 2020). (1) selects the relevant impact categories with a representative indicator and the applied impact assessment model that can quantify the impact of an elementary flow[2] on the indicator (e.g., the impact category *greenhouse gas emissions* with the IPCC impact assessment model and the reference substance CO_2). (2) allocation of the LCI results to environmental impact categories (e.g., both CO_2 and methane contribute to the greenhouse effect; furthermore, methane contributes to ground-level ozone formation, wherefore methane is also classified for this impact category). (3) calculation of the impact category results, also called *characterization*. All substances relevant for one impact category are aggregated based on the selected reference substance (e.g., the global warming potential quantifies the greenhouse gas effect with CO_2 as reference substance. Therefore, all greenhouse gas effective substances are characterized by their impact in relation to the reference. Methane is about 30 times as greenhouse effective as CO_2, wherefore 1 kg emitted methane corresponds to 30 kg CO_2 equivalents). While those first three steps are mandatory in every LCA, the following steps are optional: (4) The results of the impact characterization can be normalized to a set of common references. (5) the normalized impacts can be further classified (grouped) to impact pathways, which summarize impacts on humans, the environment, or economic systems (e.g., both impact categories global warming and land use (next to others impacts) contribute to a loss of harvest and are therefore responsible for an *increase in malnutrition*). (6) the impact pathways can again be normalized and aggregated to damages to the society or the environment, also called *Areas of Protection* (AoP). For example, the ReCiPe method uses the AoPs *human health, ecosystem quality,* and *resource scarcity*. By grouping the impacts to damage categories, it is possible to compare the severity of the different impacts. The grouping is particularly relevant for decision support (Hauschild, 2018). (7) finally, the data quality can be analyzed by evaluating the effect of the uncertainties on the results.

The interpretation of the results follows the LCIA with the determination of the LCI and LCIA in relation to the goal and scope of the study. The most important processes, assumptions, and elementary flows are determined. They are analyzed by sensitivity and scenario analysis regarding their impact on the final result of the LCA study. Based

[2] Input elementary flow: Material or energy that enters the system under study, that has been drawn from the environment without previous human transformation. Output elementary flow: Material or energy that is released from the studied system into the environment without subsequent human transformation (ISO, 2006a).

on the interpretation, conclusions, limitations, and recommendations are drawn for the stakeholder of the study (Hauschild, Bonou, et al., 2018). Summing up, Life Cycle Assessments are based on quantitative methods and make assertions on potential (and not actually observed) environmental impacts. LCA studies can be used for material and product design, strategic network planning, determination of political guidelines, marketing, and balancing of companies, among others (Frischknecht, 2020).

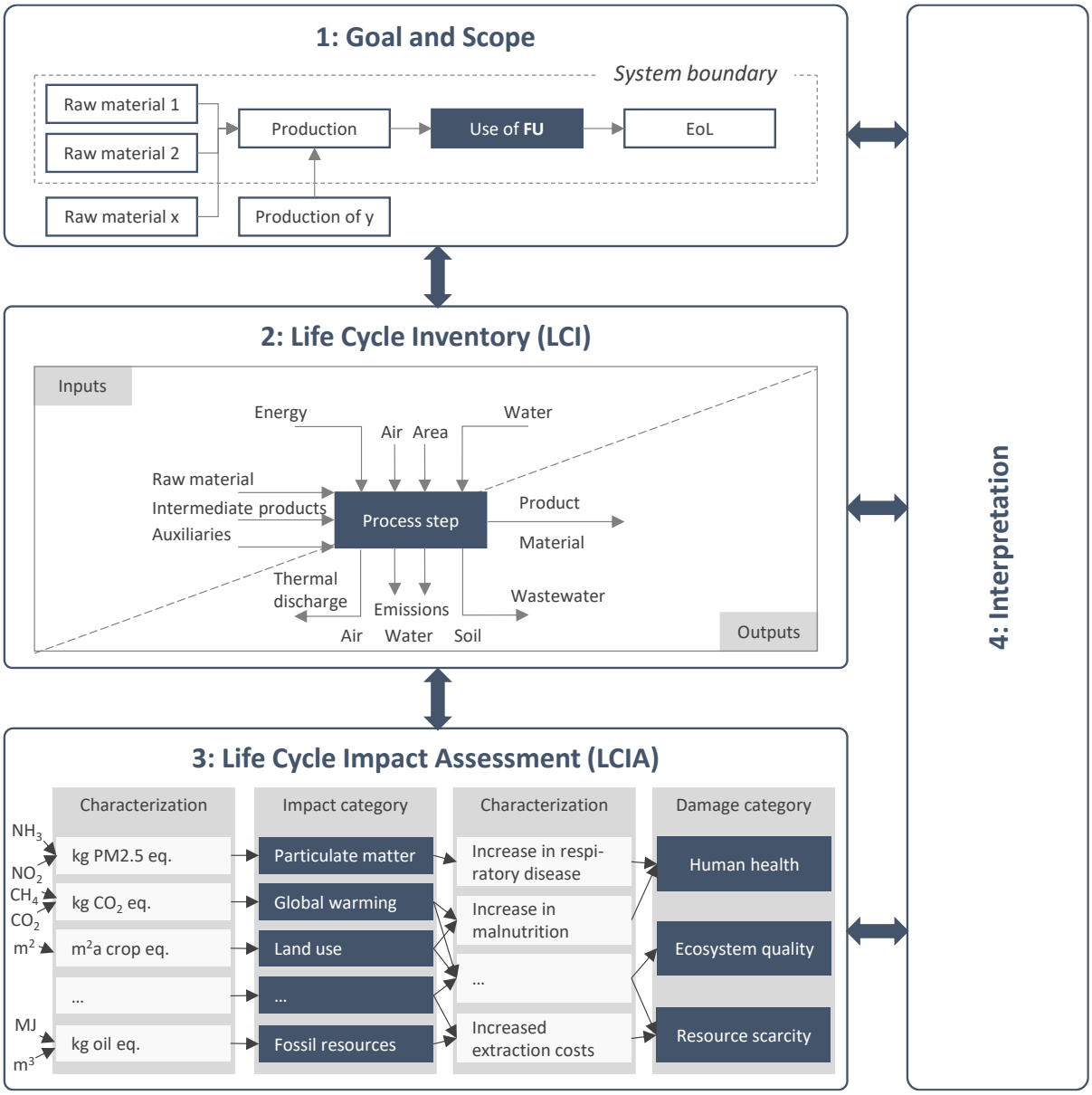

Fig. 5: Framework for Life Cycle Assessments
with four phases based on ISO 14040 (ISO, 2006a). The depiction of the *Goal and Scope* and the *Life Cycle Inventory* is based on notional examples. The *Life Cycle Impact Assessment* is illustrated by four possible impact categories with examples for the impact characterization. The three damage categories are based on the LCIA method ReCiPe 2016 with examples for the damage characterization. Own illustration based on Huijbregts et al. (2016), Frischknecht (2020)

Many studies in bioeconomy research deal with the environmental aspects of biomass processing. There is a broad consensus in the scientific community that life cycle assessment is one of the best methods for assessing bio-based products' environmental impacts and damages (Cherubini et al., 2009). Research in this field differentiates in the feedstocks, the products considered, the scope of the study, the system boundaries, the assumptions made, the life cycle impact assessment methodology, the impact and damage categories chosen, and the data basis. Bio-based products are a highly diverse group of different products whose environmental performance compared to conventional alternatives is case-specific and depends to a large extent on the feedstock used. To date, more studies have been published on biofuels than on biobased products, and many studies are still based on first-generation biomass (Hjuler and Hansen, 2018). S. Kim & Dale (2005) investigated the environmental impacts of using first- and second-generation biomass to substitute conventional energy for bioethanol production. Studies on first-generation bio-based products often neither adequately address the consequences on food production and related social issues nor direct and indirect land use changes and associated greenhouse gas emissions (Dias De Oliveira et al., 2005; Wiloso et al., 2012). Although a significant amount of first-generation biomass continues to be used for bio-based products, researchers showed that if greenhouse gas emissions from land use change (direct and indirect) are taken into account, the balance often even turns in favor of the petrochemical alternatives (Hjuler and Hansen, 2018). Summing up, first-generation feedstocks for the production of fuels, chemials and materials are likely to thwart the achievement of several SDGs.

In contrast, many studies show that second-generation organic products have significantly higher greenhouse gas savings than first-generation and petrochemical products (Cherubini and Strømman, 2011). Bright & Strømman (2009) use four impact categories to analyze the production system of ethanol refineries from Scandinavian wood and compare the environmental impacts of two bioethanol technologies with conventional gasoline. The work is based on the well-to-wheel approach and uses the CML 2 baseline 2000 method for impact assessment. Cherubini & Ulgiati, 2010 compare the supply chain of bioethanol from crop residues with that from fossil resources, also using the impact categories according to the CML 2 baseline 2000 approach. Muñoz et al., 2014 chose LCA on the one hand to identify the main factors influencing the environmental impact of ethanol production based on different feedstocks and geographical regions, and on the other hand to compare ethanol to conventional alternatives. The system boundaries follow a cradle-to-gate approach, and six ReCiPe impact categories and seven additional novel impact categories on biodiversity and ecosystem services are considered.

The literature review shows a comprehensive set of diverse approaches for including LCA-based environmental impacts into mathematical strategic supply networks

optimization models (Eskandarpour et al., 2015). The case of social sustainability is more complex: while for the economic and environmental dimension, making or not making a decision has quantifiable effects, social consequences of a decision are not always clear beforehand. Furthermore, the application of social indicators into quantitative models is exacerbated due to a lack of social data readily applicable (Valdivia et al., 2021). The tools for assessing the social dimension have lower maturity in terms of user-friendliness of tools, they have open methodological issues, the interpretation of results is immature, and best-practice approaches are still rare (Valdivia et al., 2021). Site-or product-specific social assessment frameworks, such as the Sustainability Reporting Standards (GRI, 2021) or the ISO 26000 (ISO, 2011), are valuable for evaluating the actual social state of a value chain but difficult to include in mathematical optimization models. Messmann et al. (2020) reviewed 91 publications with social objective functions in strategic network design models and concluded that three-quarters of the reviewed articles do not cite one of the existing social frameworks. Of all reviewed articles, only 14% identify relevant social indicators by referencing to social frameworks (Ghaderi et al., 2018; Mota et al., 2015a; Soleimani et al., 2017). They further figured that there are only a few constantly applied indicators, and only some articles consider more than a few social indicators at once (Pishvaee et al., 2014; Anvari and Turkay, 2017; Zhu and Hu, 2017). The indicator *Job Creation* is the only one that is taken into account regularly and in the majority of works applied by the total number of jobs created (Miret et al., 2016; Roni et al., 2017; Mousavi Ahranjani et al., 2018; Lin et al., 2019). Finally, almost no work takes a multi-dimensional approach to consider the economic, environmental, and social dimensions simultaneously. A few studies apply, for example, the AHP method to weight and aggregate the triple bottom line (Jakhar, 2015; Shokouhyar and Aalirezaei, 2017; Sahebjamnia et al., 2018).

2.3 Strategic Network Design

Strategic network planning (SNP) is the cornerstone for companies to maximize their business goals over time (Goetschalcks and Fleischmann, 2008). The strategic network design typically encompasses structural, strategic decisions like decisions on locations or capacities of a production plant and operative decisions like material flows between the plants and demands. Strategic network design decisions are the basis of all planning levels of a company: the strategic (long-term), tactical (mid-term), and operational (short-term) and therefore have a great lever on achieving the business goals. In particular, SNP encompasses decisions on the most important products, the number and location of production and storage facilities, production processes, the output capacity per facility, the most important sales markets, raw material and product

supplier selection, and the flow of goods in procurement, production, and product distribution (Eskandarpour et al., 2015). Accordingly, SNP models contain binary structure variables on the one hand and continuous flow variables on the other, wherefore those decision models belong to the class of mixed-integer models, which are often difficult to solve optimally (Goetschalcks and Fleischmann, 2008).

Supply chains that process agroforestry residues face different challenges compared to typical industrial supply chains, particularly in raw material procurement. Due to the low density and economic value of agroforestry residues, feedstock transportation is challenging, and long transportation distances are neither economical nor environmentally beneficial, wherefore biorefinery locations and output capacities are closely coupled to feedstock supplying regions. While an iron ore mine can produce a constant output under normal circumstances, agroforestry residues only occur at certain times of the year, and the quantities produced can vary significantly from year to year due to weather events. Furthermore, those raw materials are more or less equally distributed in the area and cannot be obtained at discrete locations. Finally, there are almost no 'big players' which would supply huge feedstock volumes, but often small farms, wherefore raw material procurement must be negotiated in many small and local contracts without relying on large collaborations. Fig. 6 shows the Supply Chain Planning Matrix (SCPM) with a specification of strategic network design decisions in particularly relevant for bioeconomic value chains. In procurement and production, decisions must be made on the type of processed feedstock and the associated biorefinery technology. In order to produce economically and environmentally efficient, supply regions with high and constant raw material volumes must be selected. Due to the mentioned challenges in feedstock transportation, the biorefinery locations and capacities need to be in spatial proximity to the feedstock supply. The political intention to promote bioeconomic applications and the associated subsidization can significantly influence strategic sales planning. The decision on product program, the selection of markets, and the magnitude and duration of subsidies paid can be decisive for reaching business goals.

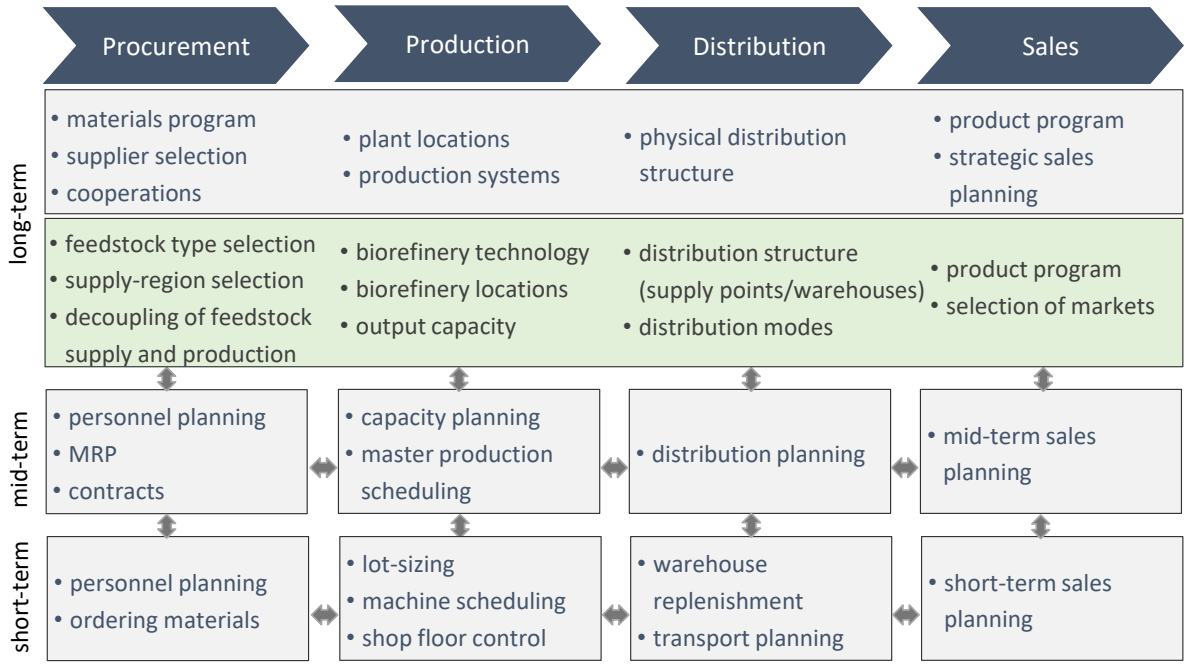

Fig. 6: Supply Chain Planning Matrix
extended by strategic decisions relevant in the bioeconomic context. Own illustration based on Fleischmann et al. (2008)

Hitherto, the business goals of most companies that were intended to be achieved through Strategic Planning have been confined to ensuring economic performance (costs, net present value, profitability, or net cashflow), service level, risk minimization, or flexibility (Goetschalcks and Fleischmann, 2008). The largest subset of bio-based supply chain planning literature addresses exclusively economic goals. The works vary in terms of the methodology used, geographic reference, databases, considered end products, the production technologies, fixed plant capacities or site constraints, and other assumptions. Bowling et al. (2011), Huang et al. (2010), J. Kim et al. (2011), Marvin et al. (2013), Walther et al. (2012), and Zamboni et al. (2009), for example, use mixed-integer linear programming for planning bio-based supply chains under consideration of economic objectives such as cost minimization, profit maximization, or net present value maximization. Osmani & Zhang (2013) explicitly considered various uncertainties to which the supply chain is exposed by extending the MILP approach by stochastic programming. Other works such as Corsano et al. (2011), Lauven et al. (2018) Singh et al. (2014) use mixed integer nonlinear programming for the economic optimization of the supply chain and biorefinery configuration.

Most companies are aware that economic performance and other goals can only be guaranteed if climate change is limited, ecosystems do not deteriorate too much, and social cohesion is ensured (PwC, 2019). In recent years, one of the main trends in the scientific literature on strategic network design is considering the triple bottom line, including economic aspects, environmental performances, and social responsibility

(Eskandarpour et al., 2015). Especially the environmental performances and the social contributions of a supply chain can only be assessed with models that can take regional aspects into account. This is especially true for bio-based applications, since the feedstock provision and transportation are the most sensitive factors in the success of bio-based value chains (Budzinski et al., 2019). Due to the urgency to consider a larger number of objectives in strategic planning, multi-objective models continue to gain further importance.

2.4 Multi-objective Mixed Integer Linear Programming

In order to take decisions in companies and organizations in such a way that optimality of the set goals is achieved with the available scarce resources (Schweitzer, 1994), decision problems need to be formulated as optimization models. Optimization models from operations research enable the presentation and analysis of complex real-world decision problems through abstract models. Optimization models are usually composed of one or more decision variables (degrees of freedom of the decision-maker), an objective function (goal of the decision-maker), and any number of constraints (restrictions) (Suhl and Mellouli, 2013). Based on the model structure and the associated applicability of different approaches, optimization models can be divided into different categories:

- *Linear Programming* – The objective function and all model constraints are linear combinations of the decision variables.
- *Nonlinear Programming* – The objective function and/or restrictions contain nonlinearities.
- *Integer Programming* – All decision variables are subject to integer constraints.
- *Mixed Integer Programming* – Some variables are subject to integer constraints.

In all mentioned approaches, the given objective function can either be minimized or maximized, and the restrictions can be equations or inequalities. Mixed-integer programming is often applied in practical problems when the divisibility of resources is not given. When the objective function and the constraints of a mixed-integer optimization model are also linear, it is called a Mixed Integer Linear Program (MILP) (Suhl and Mellouli, 2013).

Almost all real-world decisions problems require consideration of multiple and often conflicting goals, with the decision-maker deciding which objectives are relevant in a given problem (Zimmermann and Gutsche, 1991). Multi-objective optimization deals with optimization problems that consider more than one objective, focusing on approaches to find trade-offs in case of conflicting objectives. Different objectives can

be *complementary*, *conflictory* (contrary), or neutral (Domschke et al., 2015). No conflict of objectives arises if one has only complementary objectives in a decision problem and the set of solutions contains at least one vertex representing an optimum for each objective. For conflictory objectives, the goals compete with each other, and improving one objective leads to a deterioration of another. The degree of *objective achievement* can be expressed by

$$\frac{z_i^* - z_i(x)}{z_i^*} \tag{1}$$

where z_i^* is the optimal objective value of objective i and $z_i(x)$ the achieved value at a solution x regarding objective i (Domschke et al., 2015). In the case of neutrality, a change in the degree of objective achievement of one objective does not change the degree of objective achievement of the other objectives.

Multi-criteria optimization models for real-world problems usually do not have a simultaneously optimal solution in all considered criteria, making the problems considerably more difficult. Typically, multi-criteria optimization models are based on the concept of Pareto-optimality. A Pareto optimum (also called Pareto efficient solution) is a (best possible) state in which it is impossible to improve in one property without having to worsen another property at the same time (Mavrotas, 2009). The economic, environmental, and social dimensions do not have a uniform unity and are fundamentally different, so a multi-criteria approach is required. When comparing only two objective functions, it is possible to visualize the set of Pareto-optimal solutions graphically in a two-dimensional coordinate system using a so-called Pareto frontier, from which the decision-maker can choose.

Two of the best-known methods for generating Pareto-optimal frontiers of multi-objective optimization problems are the weighted sum and the ε-constraint method, briefly introduced by a maximization problem in the following. In the fairly intuitive weighted sum method, the individual objective functions $f_i(x)$ with $i \in p$ of the basic multi-criteria model (2) are multiplied with specific, varying weighting factors $w_i > 0$ and combined into the weighted sum model (3). The weighted sum objective function (3) is then maximized, taking into account the problem constraints. If the weights are $w_i = e_i$, the standard basic vector, the weighted sum method is equivalent to maximizing f_i. In order to use the weighted sum method, the objective functions have to be normalized ex-ante.

Basic multi-criteria model $$\max_{x \in X} f_1(x), \dots, f_p(x) \tag{2}$$

Weighted sum model $$\max_{x \in X} \sum_{i=1}^{p} w_i \times f_i(x) \tag{3}$$

It has been shown that the weighted sum method produces efficient solutions under convexity assumptions (Ehrgott, 2005). However, the advantage of its simple implementation comes with the disadvantage that the results obtained are highly dependent on the applied weights that have to be specified before the optimization process starts. Furthermore, the weighted sum method may work poorly for nonconvex problems (Ehrgott, 2005).

These challanges can be avoided by using other scalarization methods like the ε-constraint method. The ε-constraint method is probably the best-known technique to solve multi-objective optimization problems besides the weighted sum approach (Mavrotas, 2009). Instead of an objective aggregation, only one of the original objectives is optimized, while all other objective functions are transformed to constraints. The original multi-objective problem (2) is substituted by the ε-constraint problem (4).

$$\begin{aligned} &\text{ε-constraint problem} && \max_{x \in X} f_j(x) && && \\ &\text{subject to:} && f_i(x) \leq \varepsilon_i && i = 1, \dots, p && j \neq i \end{aligned} \tag{4}$$

The procedure of the ε-constraint method is explained by the simple example of two objective functions to be maximized and five constraints (5).

$$\begin{aligned} &&& \max_{x \in X} \ (f_1(x), f_2(x)) \\ &\text{subject to:} && constraint\ 1-5 \end{aligned} \tag{5}$$

First, the boundary values of the Pareto curve are calculated by optimizing each of the two objective functions, taking into account the five problem-specific constraints while neglecting the second objective function, yielding in $f_1^*(x)$ and $f_2^*(x)$, respectively. In the next step, the ε value is set to the resulting objective value. The second objective function, neglected first, is now optimized to calculate the Pareto point. In addition to the other constraints, the solution space is also restricted by ε, i.e., the objective value of the first objective function. Consequently, Pareto point 1 is composed of the objective function values of the optimization of f_1 and that of the ε-restricted optimization of f_2 and Pareto point 2, in turn, results from the objective function value of the optimization of f_2 and that of the ε-restricted optimization of f_1. Adding more Pareto points to the solution set is necessary to approximate the entire Pareto frontier. These can be calculated by iteratively fitting Epsilon with a continuous absolute increase within the two limits. The increment interval of ε is to be chosen by the decision-maker. With a diminution of the increment interval, i.e., with the execution of additional iterations, the accuracy of the Pareto curve increases. All solutions calculated in this way correspond to Pareto efficient solutions.

Table 2: General procedure of the ε-constraint method

Step	Boundary 1	Boundary 2
I	$\max_{x \in X} f_1(x)$	$\max_{x \in X} f_2(x)$
	subject to: $constraint\ 1-5$	subject to: $constraint\ 1-5$
II	$\varepsilon = f_1^*(x)$	$\varepsilon = f_2^*(x)$
III	$\max_{x \in X} f_2(x)$	$\max_{x \in X} f_1(x)$
	subject to: $constraint\ 1-5$	subject to: $constraint\ 1-5$
	$f_1(x) \geq \varepsilon$	$f_2(x) \geq \varepsilon$

The Pareto frontier serves to visualize the trade-offs between two conflicting objective functions. Based on the frontier, the decision-maker can select the best alternative based on the preferences. In most cases, it is not straightforward for decision-makers to choose a single preferred solution based on a set of Pareto-optimal solutions. Multi-criteria decision-making (MCDM) methodology can systematically select a single preferred solution out of a set of Pareto-optimal solutions. Multi-objective optimization problems usually exhibit points on their Pareto front, which can be characterized as superior to other Pareto points (Deb and Gupta, 2010). Fig. 7 briefly outlines a suggestion for a possible compromise point, which in this case is defined as the shortest relative Euclidean distance from the so-called "Utopia point", i.e., a point where both objectives are at the same time at their optimal values.

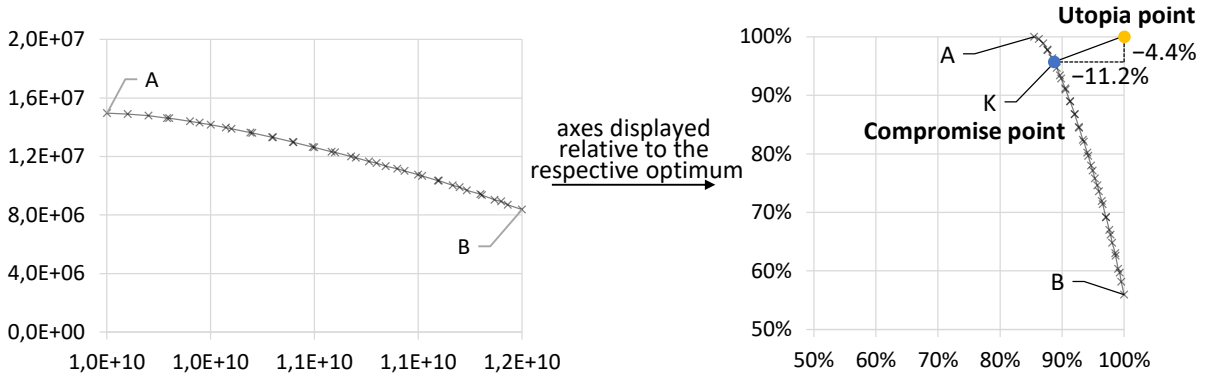

Fig. 7: Visualization of an exemplary Pareto-optimal frontier
in a two-dimensional maximization problem and a theoretical "Compromise point", i.e., point of shortest relative Euclidean distance from the "Utopia point"

Multi-criteria models have been increasingly used to simultaneously consider economic, environmental, and social objectives in planning bio-based value chains. Several papers have been published in the subfield of environmental and economic biorefinery location and transportation planning. The studies differentiate in the products considered, the applied optimization methodology, the ecological life cycle impact assessment method, the impact and damage categories considered, the system boundaries, the geographic

reference, and the assumptions made. Most research on multi-criteria optimization that implicitly performs an LCA consider the minimization of greenhouse gas emissions exclusively (Zamboni et al., 2009; You and Wang, 2011; Gong and You, 2014; Osmani and Zhang, 2014) of which a few additionally include the social dimension (You et al., 2012; Budzinski et al., 2019). Some research works chose environmental single scores and here, especially the eco-indicator-99, which is composed of the normalized and aggregated damage categories human health, ecosystem quality, and resource availability (Santibañez-Aguilar et al., 2011, 2014; Bairamzadeh et al., 2016; Babazadeh et al., 2017; Wheeler et al., 2018). The large-scale reorganization of a production and consumption system like biofuel consumption instead of petrochemical fuel would have global implications. A few studies linked their detailed and site-specific optimization approach to global value chains by hybrid LCA (Yue et al., 2016; Budzinski et al., 2019). The investigated and optimized system is considered a normal LCA model with detailed knowledge of the corresponding processes and site-specific data. Throughout an Input-Output (IO) model, the foreground LCA model is linked to the different sectors of the global value chains, avoiding arbitrary cut-offs (Watanabe et al., 2016). Almost all mentioned references apply the *a posteriori epsilon-constraint* method as a multi-criteria optimization approach to generate Pareto efficient trade-off solutions.

2.5 Research gaps

The state of research illustrates the open research gaps in the context of a European bioeconomy aligned to the major human challenges. The availability of agroforestry residue volumes and their current uses is the first major concern of a bioeconomy aligned with the SDGs, and many existing works and political bioeconomy strategies still lack adequate policies for securing the biomass supply. Moreover, there are hardly any approaches that forecast the future availability of agroforestry residues. A growing number of publications in the field of bioeconomic supply chain design consider economic, environmental, and social dimensions. However, most articles base the respective dimensions on one or only a few goals (e.g., *global warming potential* in the environmental dimension and *job creation* in the social dimension) without being transparent about the reasons for selecting the respective objective function. Thereby, many important environmental and social issues remain unconsidered, and the repercussions of decisions among the different biomass services may be disregarded. Especially the operationalization of social issues is not yet methodologically sound for inclusion into mathematical optimization models. Consequently, existing approaches are insufficient to align the planning of bioeconomic value chains with a large set of Sustainable Development Goals.

3 Assessment of EU's lignocellulose residue potentials

The prerequisite for a sustainable bioeconomy is a sufficient biomass supply to serve the different societal needs (Lewandowski, 2015). During the past decades, the separation between food and feed provision on the one hand and energy and material provision on the other was more clear-cut: Agriculture was responsible for food and feed supply, and mining and oil production for energy and material supply. With the transformation toward a decarbonized economic system, the sun is increasingly important as an energy supplier. One way of exploiting solar energy in materials and energy is via photosynthesis and thus via biomass. The challenge is to use the available biomass as sustainably as possible for food, feed, materials, and energy needs. An ideal bioeconomy considers the triple bottom line of environmental and social aspects alongside the competitiveness of biobased products (Lewandowski, 2015). Several nations have published bioeconomy strategies in recent years, but these are characterized by a lack of securing biomass supply (Staffas et al., 2013).

This chapter deals with the biomass supply in the European Union. Many previous works on the sustainability of bio-based products based on first-generation feedstocks have shown that, when land use change is adequately considered, these products perform worse than conventional products in many environmental categories (Hjuler and Hansen, 2018). For this reason, this work exclusively deals with lignocellulosic residues, which can be assigned to the class of second-generation renewable feedstocks.

The transformation of traditional industrial processes to sustainable patterns is compulsory given limited resources and adverse environmental effects. In this context, establishing a biobased economy is a major responsibility. Concepts for biobased economies aim to substitute emission-intensive and non-renewable resources with renewable resources (McCormick and Kautto, 2013).

This chapter assesses the resource potential for the biobased chemical industry in the European Union. The chemical industry is one of the largest sectors in the EU-28, with over 500 billion EUR revenues, a fuel and power consumption equivalent to 52.6 million tonnes of oil, and greenhouse gas emissions of approximately 130 million tonnes CO_2 equivalent (CEFIC, 2017). Many innovative products and materials based on renewable input sources—so-called "biomaterials"—have already been developed within the concept of a biobased economy. Using biobased materials on a large scale, significant oil shares can be substituted by renewables. The supply of lignocellulose feedstock (LCF) needs to be secured sustainably as the main constituents of the considered biomass, lignin, cellulose, hemicellulose, and tannin, are suitable for transforming into high added-value applications. The most promising sources are by-products from

agricultural and forestry activities, containing large amounts of industrially interesting substances (Kamm and Kamm, 2004). A future-oriented bioeconomy, where basic building blocks from renewable resources replace oil-based materials and chemicals, can meet important environmental, social, and economic requirements for sustainable development.

Additionally, such a transformation supports the geostrategic goals of the European Union: by substituting oil with agroforestry products, the EU gains independence from oil-exporting countries and intensifies utilization of domestic resources. However, misuse of industrial utilization of biomass can also be associated with ecological and ethical concerns. For instance, arable land for growing biomass feedstock is limited, and thus industrial applications may compete with food production, and strain on environmental resources may negatively affect humans, animals, and plants. Therefore, it is crucial to analyze EUs LCF potentials, considering sustainability issues and competitive application.

Terminology in the current discussion of concepts for assessing biomass potential is inconsistent in the existing literature (Hennig et al., 2016). Despite this, some initiatives guide the harmonization of the potential calculations (Vis and van den Berg, 2010; Thrän and Pfeiffer, 2015; Brosowski et al., 2016). Brosowski et al. (2016) recently published a comprehensive review of publications on the biomass potential of wastes and residues in Germany. The study compiles the status quo for the theoretical and technical potential and proposes the reference unit "metric tonnes of dry matter." However, research that focuses on the energy use of biomass residues, either for direct combustion or, with increasing interest, to feed advanced biofuel production (Edwards et al., 2005; Ericsson and Nilsson, 2006; Scarlat et al., 2010; Vis and van den Berg, 2010; Kretschmer et al., 2012; Brosowski et al., 2016). Thrän and Pfeiffer (2015) and BTG (2010) suggested potential analysis in energy reference units (e.g., joule), which are less useful outside energy analyzes. Therefore, Hennig et al. (2015) call for a reassessment of contemporary concepts of energy utilization of biomass, which must be assessed when those already "tapped" raw materials are more beneficial in high-value applications.

The reviewed research on biomass potential concentrates on energy utilization. Research analyzing the potential of biobased industrial transformations that considers economic and ecological strains are rare, and comprehensive studies on the regional dispersal of sources and interdependencies with primary production processes are lacking (Scarlat et al., 2010). No research is available for the determination of the potential of agroforestry waste for high value-added applications addressing regional arising, competitive applications (e.g., animal bedding, horticulture), and the content

of focal substances (e.g., lignin, tannin, cellulose, hemicellulose), which are essential for the design of biopolymers as a precursor of high value-added industrial products. Consequently, no potential levels are described for biomass utilization other than energy. Against this background, we herein apply a method for the assessment of regional agroforestry residue potentials products as input for a European bioeconomy and investigate the following research question:

> ***RQ1*: Which agroforestry residue streams in the European Union are the most promising feedstocks for bio-based value chains, and how are they regionally distributed.**

The following two sub-research questions further specify the main research question of this chapter:

- *Q1:* How must agroforestry residue potentials be categorized, considering their current application, volumes, and biochemical composition?
- *Q2:* How large is the sustainably available potential of prioritized agroforestry residues on a regional level in the EU-28?

Chapter two introduces the applied method, and our approach's specifics are described in detail. In section three, we present the results of our research. Starting with a general overview of all considered biomass, the bioeconomic potential of the most promising sources is presented on a regional basis. At the end of the chapter, a sensitivity analysis consolidates our results. Chapter four discusses the results, and in chapter five, we give a conclusion and perspective.

3.1 Methods

To thoroughly address the research questions, a structured research process is implemented. The applied method sets out to quantify the bioeconomic potential for the use of high added-value bio-products, taking into account sustainable farming, forestry practices, and competitive applications. Kretschmer et al. (2013) noted that existing literature on biomass arisings is discordant in classifying available potentials. Therefore, a transparent distinction between three levels of biomass potential, based on BTG (2010) and Pfeiffer and Gröber (2011), is provided.

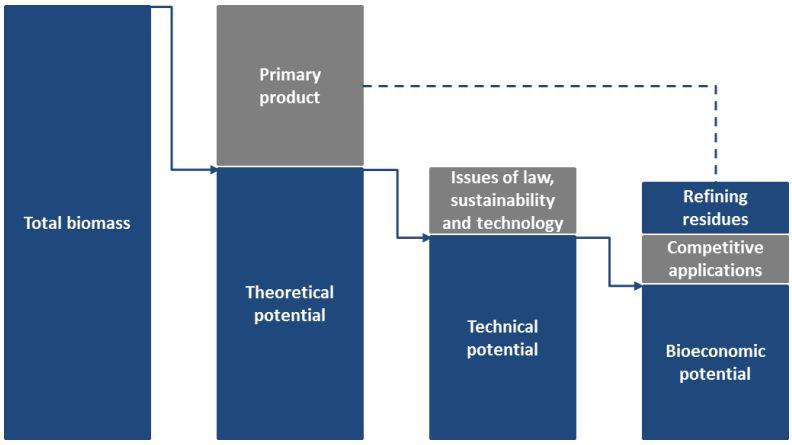

Fig. 8: Definition and context of resource potentials

Theoretical potential includes all parts of the harvested biomass that have no direct use in food, feed, or industrial production. The primary product (e.g., industrial roundwood or grains) plus the theoretical potential sum up to the total biomass. Due to factors such as sustainable harvesting practices (e.g., balancing humus quality, see Helwig et al. (2002), Münch (2008a)) and legislation (e.g., restriction of the removal of treetops and small branches from forests), only a fraction of the theoretical potential is accessible for further utilization. These facts are considered in calculating the technical potential, which we define as the amount of residue that can be technically, legally, and sustainably removed from the field or forest. The bioeconomic potential is the share of technical potential that is not necessarily used in competing applications. Additionally, refining residues of the primary product can add to the bioeconomic potential.

3.1.1 Identification of theoretical potential

In the first step, we identify all relevant agroforestry sources (cereals, oil crops, sugar crops, fiber plants, coniferous and broadleaf) of lignocellulose-based biomass. We assess the total residue potentials based on the main product, the residue-to-crop ratio, and the concentration of focal substances (lignin, celluloses, hemicellulose, and tannin) within the residues.

Crop production values serve as a proxy for calculating the theoretical potential of the lignocellulose feedstock. The crop production data is obtained from Eurostat using the regional level NUTS 1 (Nomenclature des unités territoriales statistiques). The theoretical residue potential is calculated with the residue-to-crop ratio derived from literature. The ratio has numerous influence factors and is therefore difficult to estimate. Seed type, soil condition, weather events, and other factors may influence the ratio. A good basis for the derivation of the residue-to-crop ratio (R:C ratio) is the well-investigated harvesting index (HI) (share of primary products in relation to total biomass aboveground). Equations (6) shows the connection of the HI to the R:C ratio.

Research on the harvesting index addresses questions about the biophysical maximum, which is estimated to be 0.65 for wheat. An HI of 0.65 translates to an R:C ratio of 0.53. However, despite the theoretical limit of 0.65, observed values for the harvesting index are approximately 0.5 for wheat, resulting in an average residue-to-crop ratio of 1. This value has been constant since the early 1990s (Foulkes et al., 2011). In contrast to the HI, crop yield has significantly increased in the last years, leading to higher straw yields (Foulkes et al., 2011). The other R:C ratios for agricultural products can be found in Appendix A.1.

$$R{:}C\ ratio = \frac{residue\ (\frac{t}{ha})}{yield\ (\frac{t}{ha})} = \frac{1}{HI} - 1 \tag{6}$$

To quantify the share of focal substances, we also review the identified residues' biochemical composition. The composition of agricultural harvesting residues is similar for most sources, with approximately 15-20 % lignin, 30-45 % cellulose, and 20-25 % hemicellulose (Bakker et al., 2013; Kamm and Kamm, 2004). The results of the reviewed studies differ due to factors such as the measuring method, pre-treatment of the material, and varying climatic conditions in different world regions (Buranov and Mazza, 2008). The presented values are derived from studies referring to multiple laboratory tests of different samples and must not be confused with data from samples from isolated industrial processes (Monteil-Rivera et al., 2013). The literature study on the biochemical composition of agricultural and forestry residues can be found in Table A 2 and Table A 3, respectively, of Appendix A.1.

3.1.2 Identification of technical potential

The technical potential is the amount of biomass that can be removed from consideration of technical, legislative, or sustainability constraints. An example of technical limitations is a combined harvester, which leaves certain plant parts on the field (e.g., stubble). A certain share of residue must be left on the field as natural fertilizer, delivering important nutrients for humus formation. Plants gather nutrients containing carbon, nitrogen, phosphor, potassium, magnesium, and sulfur during growth. Nutrients taken from the ground for plant growth must be replaced to sustain soil quality. On cultivated land, this is achieved by animal manure, synthetic fertilizers, incorporation of harvest residues, catch crops during winter, and fruit rotation (VLK, 2015). Incorporating agricultural residues into the soil is important for sustaining humus quality (Kretschmer et al., 2012). However, information about removal rate may vary for different soils, locations, crops, production concepts, and years. Therefore the removal rate of residues depends on a combination of factors, such as equipment limitations, crop variety, harvest height, R:C ratios, water supply, soil, and location

(Scarlat et al., 2010). The applied sustainable removal rates of different crops are found in Table A 4.

The German Institute for Energy and Environmental Research Heidelberg (IFEU) recommends an average sustainable removal rate (SRR) of approximately one-third, with a range of 10 % to 60 % depending on the location, crop rotation, and amount and fertilizer type (Münch, 2008). Organic compost fertilization can be an important step for attaining higher sustainable removal rates (Münch, 2008; VHE, 2014). Organic farms even return up to 100 % of straw residues to the soil. However, the positive effects of incorporating harvesting residues can be limited, especially in dry regions where soil humidity is too low to decompose residues. Applied sustainable removal rates are presented by Scarlat et al. (2010).

3.1.3 Identification of the regionalized bioeconomic potential

Two factors influence bioeconomic potential: (a) competitive applications further restrict technical potential, and (b) residues from subsequent refining steps of the primary product can add to bioeconomic potential. An in-depth understanding of each value chain is needed, and knowledge of current concepts for managing agroforestry waste. Therefore, we analyze statistical data (e.g., number of horses, cattle in a certain region) and review the literature and industry reports. The literature revealed that grain refining residues are still rich in nutrients and therefore constitute an important component of animal fodder (e.g., press cake from oil seeds or bran from cereals). In addition, refining residues of roundwood processing are also already substantially used in many cases (e.g., particleboard), whereas refining residues are not considered further. According to the scope of this work (assessment of lignocellulose feedstock potentials for the European bioeconomy) NUTS 1 regions (Nomenclature des unités territoriales statistiques) are the most appropriate grid level for regionalization. Since the regional demand for straw in competing applications can exceed regional supply, some regions' bioeconomic potential can also be negative.

As already described, the most important step in the identification of bioeconomic potential is the analysis of competing applications. Competing application of bark includes combustion and mulching, which we consider to be of lower value than a substantial recovery in high value-added products (e.g., insulating foams; Lacoste et al., 2015). Agricultural residues are predominantly used in three sectors: agriculture, energy, and industry; the agricultural sector itself has the largest demand for straw.

Animal bedding accounts for the largest straw demand (Edwards et al., 2005) and is expensive and labor-intensive. Alternatively, cattle may be kept in slatted housing units without straw, and horse bedding may be realized by means of alternative material, such as shredded paper or wood chips (RPS-MCOS, 2004). For sheep and pigs, straw

is even less important, as only a few farms use straw in pig bedding (Scarlat et al., 2010). Due to its low nutritive value, the use of straw as animal fodder is limited and regulated by European law (López et al., 2005, European Commission, 2013b). However, with modern straw treatment techniques, it is possible to improve its nutritive value, enabling feed containing straw to be combined with other forages, such as hay or silage (Heuzé et al., 2016). Tuyttens (2005) outlines a recommended minimum of 10 % long fibre roughage in the cattle diet, which is assumed to be satisfied by bedding material that also serves as roughage fodder. For these reasons, there is no significant demand for straw as animal fodder. Industrially cultivated mushrooms are grown on a certain compost normally composed of straw, dust and poultry litter, which serve as the nutrient basis (RPS COS 2004). The mushroom yield is approximately 20 % of the straw mass. Strawberries require straw cover for improved water balance and protection of the fruits against dust and weeds. Straw also protects the soil from erosion. After strawberry harvesting, it is incorporated into the soil as fertilizer. Straw mulching is important in the growing field of ecological farming. Interviews with farmers revealed that up to 100 % of the produced straw on the farm is used for surface mulching. Straw delivers important nutrients, improves humus development, prevents soil erosion, and reduces the use of artificial fertilizers. For frost prevention in horticulture, no figures are available, but they are assumed to be rather small compared to the other applications.

Several reports have been published assessing the potential of straw in the energy sector (Edwards et al., 2005; Kretschmer et al., 2012; Lal, 2005; Scarlat et al., 2010). According to our research, 15 large combined heat and power plants (CHP) are operating in the EU, most of which are located in Denmark. Power plants in Hungary and Germany were recently opened. Scarlat et al. show their straw demand based on the low heating value (LHV) of straw dry matter, which is 17.5 MJ/kg (Scarlat et al., 2010). Straw burning in combined heat and power plants is a growing field. Our analysis neglects small plants for household heat production, as well as the co-firing of straw in coal-fired power plants, due to the lack of reliable data. As inputs in the energy sector, agricultural residues may also serve as second-generation biofuels. These biofuels rely on LCF such as straw and wood residues, in contrast to contemporarily produced first-generation biofuels produced by fermentation and distillation of crops (De Santi et al., 2008). Contemporarily, biofuel production from waste LCF is mostly at the pilot plant stage, with no significant consumption in the EU. One plant in Northwest Italy (Crescentino) is producing large amounts of cellulosic bioethanol, with an annual consumption of approximately 200 kt of straw (mainly wheat straw). The overall consumption of LCF by biofuel production is currently very small but is likely to increase in the future (EBTP, 2017; Gregg et al., 2017).

In the industry sector, straw can be utilized as input for the production of pulp and paper in some plants as well as in traditional building material. In recent decades, efforts have been undertaken by researchers and companies to produce pulp from straw (McKean and Jacobs, 1997). Nevertheless, efforts to commercialize pulp made from straw are negligible, especially within the EU (FAO, 2014). Straw as a traditional building material, e.g., as insulation or roof thatching, is widely substituted by modern materials. In addition to very limited applications, the building sector absorbs minor amounts of straw (Kretschmer et al., 2012; RPS-MCOS 2004).

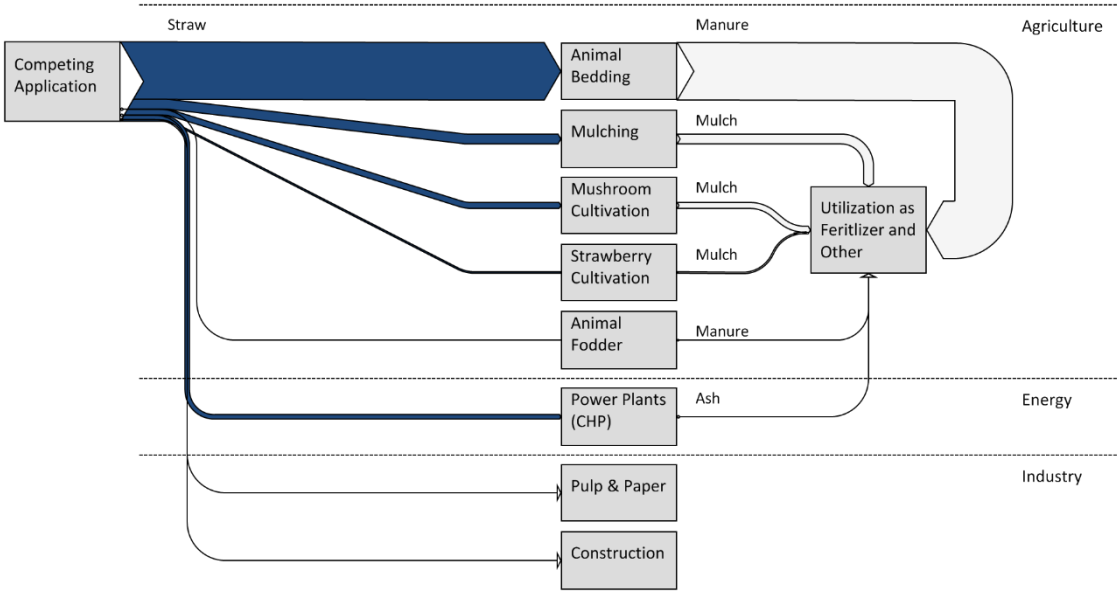

Fig. 9: Sankey diagram for competitive applications of straw

Fig. 9 shows competitive applications for straw. All analyzed competing applications can consume various types of straw and are not dependent on a single type. Therefore, bioeconomic valorization techniques can concentrate on the residue source with the most promising biochemical properties without compromising the needs of competing applications or sustainable farming practices.

Table 3: Assessment of EU-28 agroforestry lignocellulose feedstock (Ø 2010 – 2014)
All residue volumes are given as dry matter (DM)

Crop, EU-28 (Ø 2010-2014)	**Crop production (kt)**	**Area (1000 ha)**	**Type of LCF residue**	**Theoretical potential (kt)**	**Technical potential (kt)**	**Bioeconomic potential (kt)**	**Lignin (%)**	**Cellulose (%)**	**Hemicellulose (%)**	**Tannin (%)**	**Total focal substances(%)**
Agriculture											
Cereals											
Wheat and spelt	141,772	26,121	Wheat Straw	141,772	56,709	46,333	17.8	37.3	28.7	N/A	83.8
Grain maize and corn cob mix	65,434	9,365	Maize Stover and Cob	73,940	36,970	30,783	16.7	37.3	25.5	N/A	79.5
Barley	55,321	12,288	Barley Straw	51,449	20,580	16,154	17.2	39.6	24.7	N/A	81.5
Oats	10,840	3,795	Oats Straw	12,250	4,900	3,683	16.1	37.8	28.3	N/A	82.2
Triticale	11,084	2,709	Triticale Straw	10,529	4,212	3,507	19.2	36.3	21.0	N/A	76.5
Rye	8,840	2,462	Rye Straw	9,723	3,889	3,198	12.3	37.0	24.0	N/A	73.3
Rice	3,064	455	Rice Straw	5,208	N/C	N/C	15.2	37.1	25.1	N/A	77.4
Sorghum	689	1316	Sorghum Straw	896	N/C	N/C	15.5	36.0	18.0	N/A	69.5
Green maize	212,072	5,796	No Residue	0	N/C	N/C	N/A	N/A	N/A	N/A	N/A
Legumes											
Soybean	1,294	467	Soybean Straw	1,941	N/C	N/C	17.6	25.0	11.9	N/A	54.5
Oil crops											
Rape- and turnip rapeseed	19,197	6,697	Rapeseed Straw	32,636	16,318	13,883	19.8	40.9	24.4	N/A	85.1
Sunflower seed	7,961	4,296	Sunflower Straw	21,496	10,748	9,533	25.2	34.8	21.8	N/A	81.8
Sugar crops											
Sugar beet	117,001	1,613	Sugar Beet Pulp	26,910	N/C	N/C	5.9	18.4	14.8	N/A	39.1
Fibre plants											
Fibre flax	487	76	Flax Shives	146	N/C	N/C	25.3	38.4	18.0	N/A	81.7
Cotton fibre	321	349	Cotton Stalk	707	N/C	N/C	N/A	N/A	N/A	N/A	N/A
Hemp	68	10	Hemp Hurds	120	N/C	N/C	17.6	43.8	N/A	N/A	61.4
Forestry											
Coniferous	110,500	N/A	Bark	13,748	13,748	13,748	30.9	25.8	8.7	10	75.3
Broadleaf	106,836	N/A	Bark	8,917	8,917	8,917	34.9	10.7	11.2	5	61.8

3.1 Results

The assessment of Europeans bioeconomic potential is based on the described approach. The analysis covers all relevant cereals, oil, sugar, fiber, coniferous, and broadleaf crops cultivated in Europe. Identifying competitive applications is based on a value chain analysis, actual research on farming issues, and statistical data at the regional level. Table 3shows the theoretical, technical, and bioeconomic potential as well as the content of focal substances of different lignocellulose feedstock. Fig. 10 compares absolute quantities of lignin, cellulose, hemicellulose, and tannin available from bioeconomic potentials of considered residues and underlines the importance of wheat straw, maize stover, barley straw, rapeseed straw, and coniferous bark as input sources to value-adding bio-refinery systems. Contemporary discussion of the potential of agroforestry residues for a biobased economy lacks information on industrially available magnitudes of lignin, cellulose, hemicellulose, and tannin (Hennig et al., 2016). The numbers reveal the opportunity for substantial recovery of agroforestry residues and show the annual production of residues.

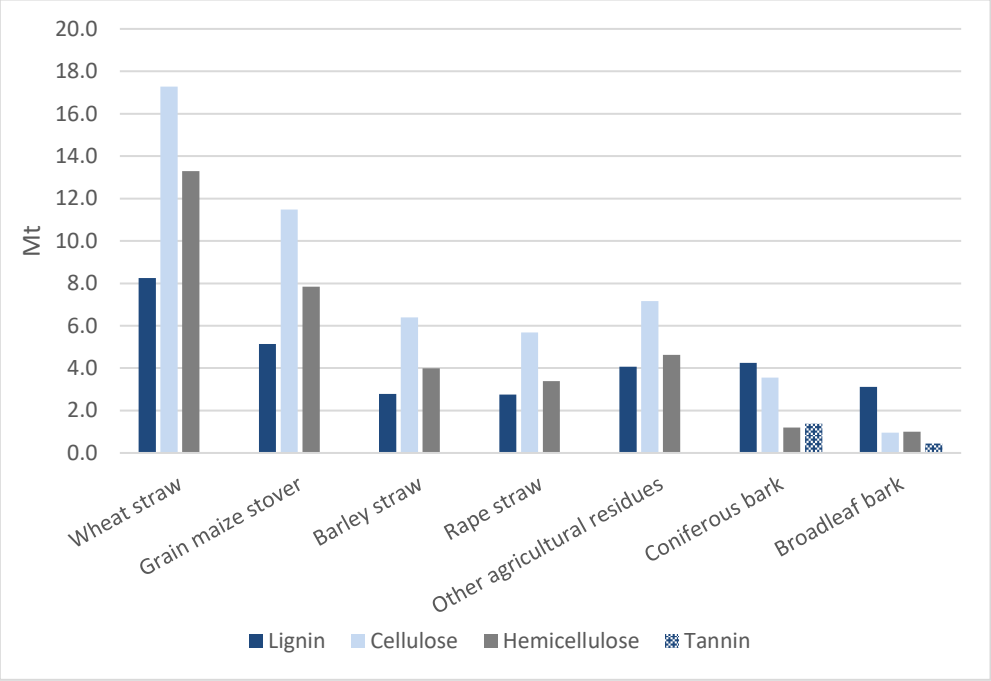

Fig. 10: Absolute quantities (d.m.) of focal substances is agroforestry residues available from the bioeconomic potential of agroforestry residues in the EU28 (Ø 2010-2014)

3.1.1 Agriculture

The **agricultural sector** produces large amounts of residues utilizable for bioeconomic purposes. Straw shows the highest potential, with approximately 95 Mt of LCF, of which the most promising is wheat straw (46 Mt), barley straw (16 Mt), and rapeseed

seed straw (14 Mt). Apart from straw, significant quantities of maize stover (31 Mt) can be extracted from grain maize production. Fig. 11 shows the theoretical, technical, and bioeconomic potential of the most promising agricultural species in Europe (EU-28). The lignocellulose content for these is 80 % to 85 %.

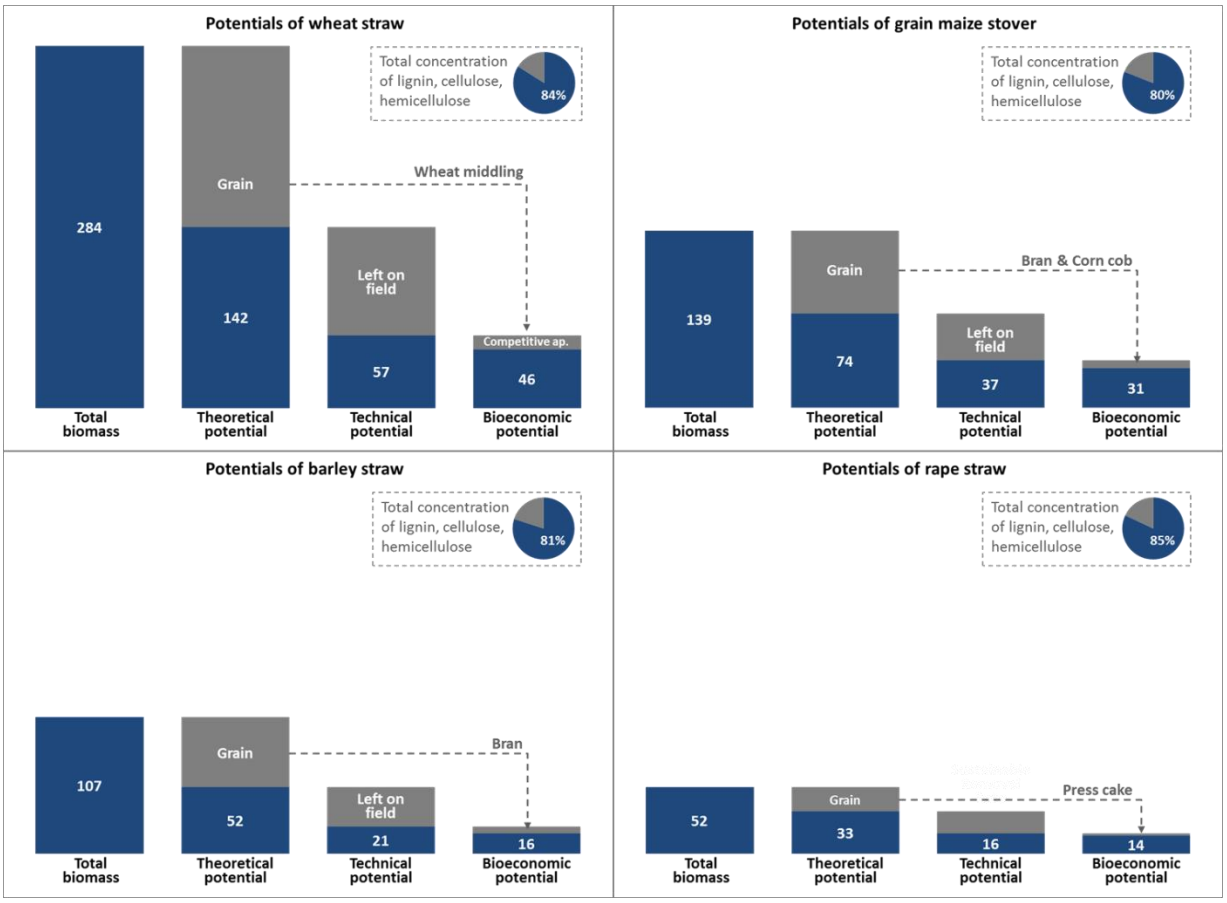

Fig. 11: Theoretical, technical, and bioeconomic potential in agriculture for the most promising residue sources (all values in Mt DM)

The agricultural sector must be developed as a supplier for a biobased economy to utilize this potential. Farmers tend to use residues within their premises, and trading these goods is uncommon. Indeed, farmers may perceive the development of a bioeconomy as an opportunity to generate profit from residues that they regard as low-value input materials. Farmers will trade when straw prices exceed the opportunity cost of substituting these materials in contemporary applications (e.g., animal bedding). For instance, soil quality may be balanced using organic compost fertilization instead of straw (DBFZ, 2011). Currently, less than 10 % of straw is recovered from fields, although most sustainable agriculture experts agree that a larger share of straw can be removed from fields without compromising soil quality (Münch, 2008).

Regional bioeconomic potential

To establish future biomass supply chains for an agroforestry residue-based bioeconomy in Europe, potentials must be calculated on a regional level. The starting point is the identification of regional crop arisings from the most promising sources (wheat, maize, barley rapeseed). The theoretical and technical potential is then calculated on a regional level. Due to a lack of regional data, the R:C ratio and the sustainable removal rate are homogenous in Europe, and values are from a consolidated literature review (see chapter 2). In contrast, the demand from competitive applications (e.g., wheat straw) depends on regional characteristics. Therefore, we gathered regional information on local livestock, organic farms' number and size, and the cultivated land use for strawberry production. Table 4 shows calculations for the straw demand for different agricultural applications. The demand from industry (e.g., power plants) is also considered.

Table 4: Demand of straw for competitive applications

Agricultural Application	**Calculation**	**Reference**	**Total demand 2014, EU-28 (kt DM)**
Demand bedding cattle	$D_r = 1.5\,[\frac{kg}{d}] \times \frac{1}{4}\,Head_r \times 365\,[\frac{d}{a}]$	Scarlat et al. (2010)	12,093
Demand bedding horse	$D_r = 1.5\,[\frac{kg}{d}] \times Head_r \times 365\,[\frac{d}{a}]$	Scarlat et al. (2010)	2,194
Demand bedding sheep	$D_r = 0.1\,[\frac{kg}{d}] \times Head_r \times 365\,[\frac{d}{a}]$	Scarlat et al. (2010)	3,102
Demand pig bedding	$D_r = 0.5\,[\frac{kg}{d}] \times \frac{1}{8}\,Head_r \times 365\,[\frac{d}{a}]$	Scarlat et al. (2010)	3,382
Animal fodder	No additional demand	Assumption*	-
Demand mushroom compost	$D_r = \frac{5}{3} \times m_{r,\,mushroom}[\frac{kg}{a}]$	Own calculation**	2,172
Demand strawberry production	$D_r = 5\,\frac{t}{ha} \times Area_{r,\,strawberry}\,[\frac{ha}{a}]$	Own calculation***	547
Straw mulching	$D_r = 0.025 \times TP_r[\frac{kg}{a}]$	Own calculation****	3,563
Energy	Number of large plants in the EU-28	Reference	Demand 2014 (kt)
Combined heat and power plants	15	(Scarlat et al., 2010; Pannonpower, 2014; BEKW, 2016)	1,622
Second-generation biofuels	Pilot plants only		N/A
Industry	Negligible demands		N/A
Total			28,675

*: Roughage requirements of animals are covered by straw from bedding.

**: Straw as one of the three most important bulk ingredients and mushroom yield of 20 % compost.

***: Based on the assumption that on average, 5 tonnes of straw per hectare are used for strawberry cultivation.

****: Based on the assumption that around 2.5 % of the cereal production is cultivated organically (European Commission, 2013), those farms return 100 % of the technical potential (TP) into the soil.

Most competing applications can use different agricultural residues (e.g., wheat straw vs. barley straw). Therefore, we analyzed three scenarios to reflect changing demand patterns due to variable conditions such as legislation, subsidies, or prices.

The *Base case scenario* allocates the type of straw to applications based on production shares. For instance, if wheat straw represents 40 % of the straw produced in a region, we assume that the straw demand for competing applications is also satisfied to 40% by wheat straw. This approach accounts for the fact that straw is consumed regionally. The transport of straw is limited due to its large volume and low value.

The *Lower bound scenario* assumes that demand from competing applications is first satisfied with the considered source (e.g., the total demand from the competing application is fulfilled by wheat straw). Other kinds of straw are only used when the preferred source is already depleted in this region. Hence, the amount of this source available after considering competing applications represents the minimum bioeconomic potential.

The *Upper bound scenario* assumes that demand from competing applications is first satisfied with substitutes. The source under consideration is only used when other straws are depleted in this region, which results in a maximum bioeconomic potential.

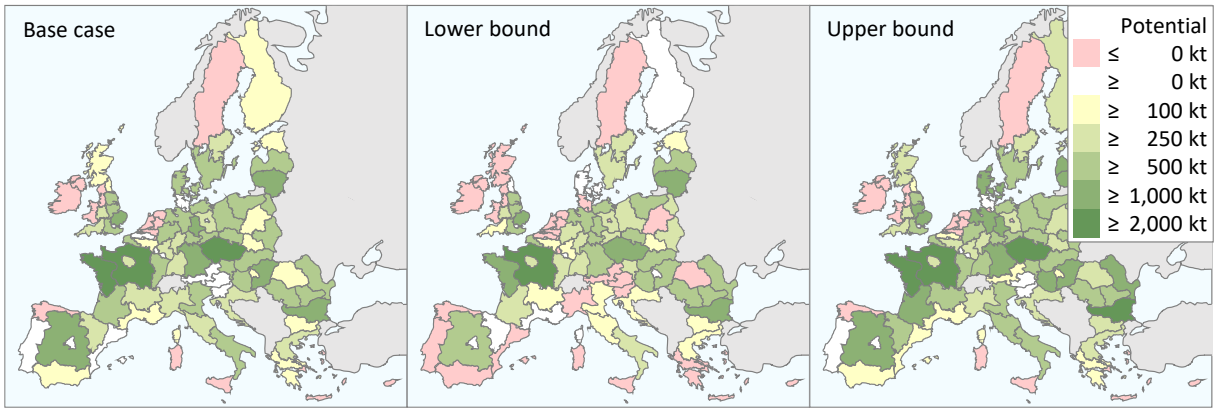

Fig. 12: Wheat straw's regionalized bioeconomic potential
for the base case scenario and the lower and upper bound scenarios

Fig. 12 shows the regionalized bioeconomic potential for wheat straw depending on the scenario. It is evident that from a sourcing perspective, the area around Paris (region "Bassin Parisien") is the most promising region. Crosschecks with trade data confirm our calculations. Regions with an undersupply of straw (red) tend to import to satisfy straw demand (UN Comtrade, 2016). Table 5 shows the NUTS 1 regions with the highest bioeconomic potential for straw, namely stover, from wheat, maize, barley, and rapeseed seed within the EU-28.

Table 5: Bioeconomic straw potentials in selected NUTS 1 regions

Crop	Selected NUTS1 region with bioeconomic potential in kilo tonnes (DM)				
Wheat straw	Bassin Parisien (FR2)	Ouest (FR5)	Czech Republic (CZ0)	Severna I Yugoiz-tochna Bulgaria (BG3)	East of England (UKH)
	6,848	2,389	1,660	1,617	1,305
Maize stover	Sud-Ouest (FR6)	Nord-Est (ITH)	Ma´croregiunea Doi (RO2)	Nord-Ovest (ITC)	Ouest (FR5)
	2,121	1,913	1,870	1,783	1,766
Barley straw	Bassin Parisien (FR2)	Centro (ES4)	Danmark (DK0)	Scotland (UKM)	Bayern (DE2)
	1,936	1,537	782	674	625
Rapeseed straw	Bassin Parisien (FR2)	Severna I Yugoiz-tochna (BG3)	Czech Republic (CZ0)	Mecklenburg-Vorpommern (DE8)	Sachsen-Anhalt (DEE)
	1,944	1,271	954	708	543

3.1.2 Forestry

In the **forestry sector**, the bioeconomic potential of bark from conifers (approximately 14 Mt) is dominant compared to broadleaf plants (Fig. 13).

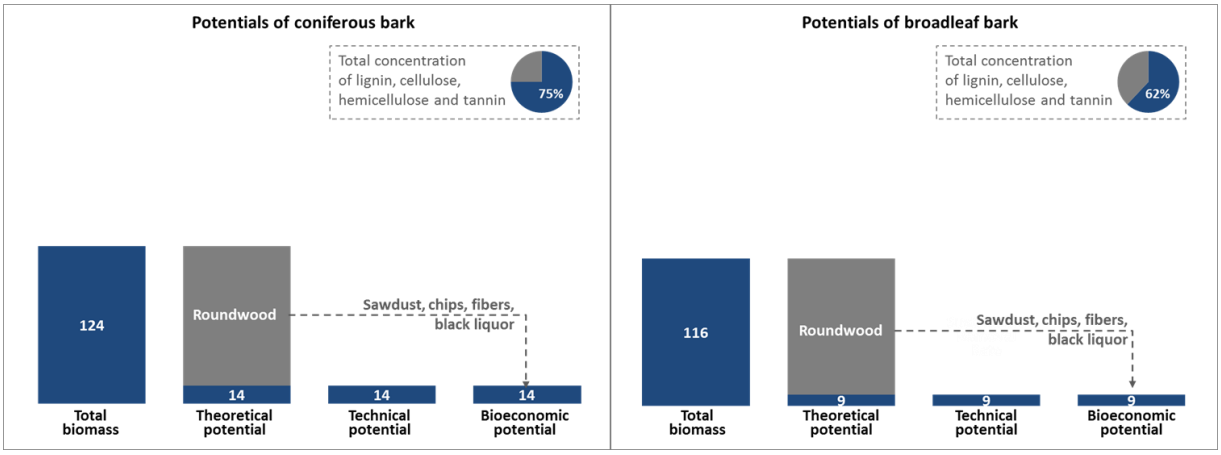

Fig. 13: Theoretical, technical, and bioeconomic potential in forestry for the most promising sources (values in Mt)

Coniferous bark is advantageous because the wood category of coniferous trees mainly includes two species, spruce, and pine, making it a homogeneous material stream compared to broadleaf trees. Secondly, coniferous bark is perceived as waste and is often directly combusted, leading to low prices, reduced opportunity cost of alternative fuels, and high availability (Kemppainen et al., 2014; Ogunwusi, 2013). Thirdly, bark accumulates in large amounts at discrete locations, such as sawmills and pulp mills, facilitating collection for integration into high value-added processes. These patterns make coniferous bark a very promising source of LCF, although the overall bioeconomic potential is lower than the amount acquirable from the agricultural sector.

Our calculations of the bark share to harvested roundwood based on Eurostat production data and crosschecks with literature recommend a bark-to-wood ratio of 0.1 to 0.15 (Kemppainen et al., 2014; Eurostat, 2016b). All weight calculations suppose a dry matter density of 380 kg/m^3 for spruce bark and 400 kg/m^3 for pine bark (Kemppainen et al., 2014). Table 6 shows the regional distribution of bark from conifers on a country level (average 2005-2014).

Table 6: Geographic distribution of coniferous bark in Europe
(literature study in Table A 5 of Appendix A.1)

EU-28, (Ø 2005-2014)	**Spruce (%)**	**Pine (%)**	**Other (%)**	**Bark (1000 m3)**	**Spruce (1000 m3)**	**Pine (1000 m3)**	**Bark (kt)**	**Spruce (kt)**	**Pine (kt)**
Coniferous				36,179			13,748		
Sweden	63.4	36.6	0.0	9,048	5,737	2,100	3,020	2,180	840
Finland	52.0	48.0	0.0	5,600	2,912	1,398	1,666	1,107	559
Germany	69.3	23.3	7.4	5,313	3,682	858	1,742	1,399	343
Poland	9.1	84.6	6.3	3,128	285	241	205	108	96
France	21.1	30.1	48.8	2,443	515	155	258	196	62
Austria	69.0	N/A	N/A	1,733	1,196	N/A	N/A	454	N/A
Czech Republic	51.5	16.7	31.8	1,805	930	155	415	353	62
Other countries	N/A	N/A	N/A	7,109	N/A	N/A	6,442	N/A	N/A
Broadleaf				14,861			8,917		

The most abundant regional arisings are concentrated in the region of "Manner-Suomi" (Finnland), "Norra-Sverige" and "Södra-Sverige" (Sweden), as Table 7 shows.

Table 7: European regions with the highest coniferous bark potentials

Coniferous bark	**Manner-Suomi (FI1)**	**Norra Sverige (SE3)**	**Södra-Sverige (SE2)**	**Czech Republic (CZ0)**	**Bayern (DE2)**
Total	2,111	1,600	1,343	686	610
Spruce	1,098	1,014	851	353	423
Pine	1,013	586	492	333	187

Therefore, we conclude that future feasibility studies for bioeconomic development in Europe should concentrate on LCF sourced from wheat, grain maize, barley, rapeseed, and coniferous trees. Fig. 14 depicts the bioeconomic potential and total concentration of focal substances of the considered lignocellulosic residues.

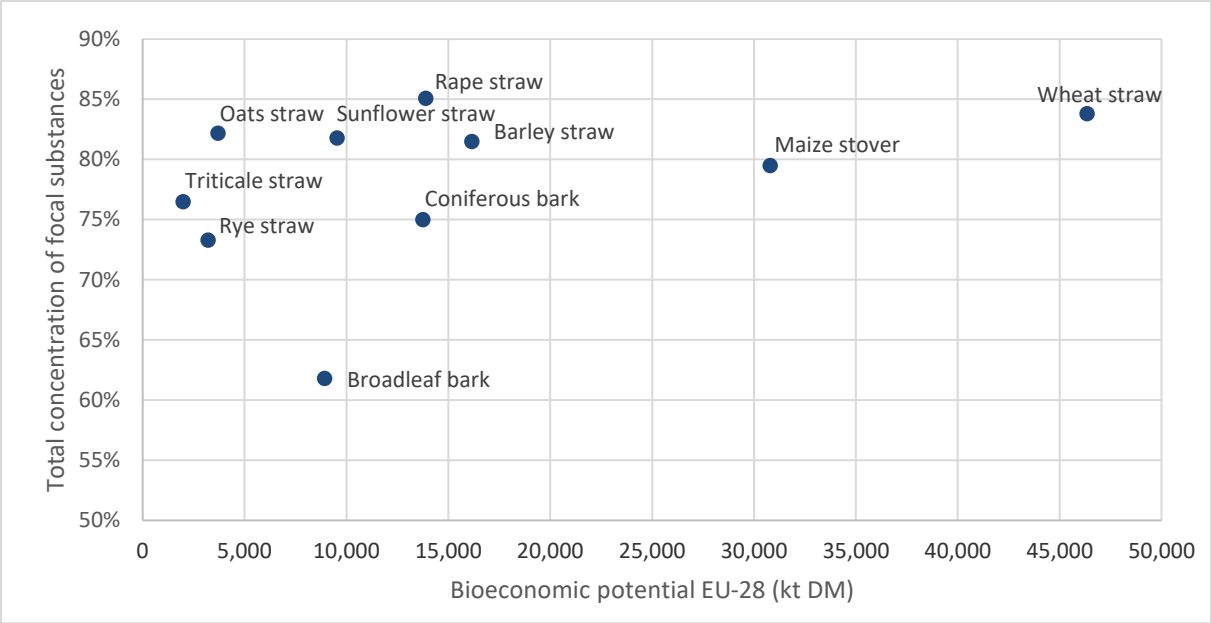

Fig. 14: Bioeconomic potential versus total concentration of focal substances for different agricultural residues

3.1.3 Sensitivity analysis

Calculation of bioeconomic potential depends on crop and wood production data and assumptions of the R:C ratio and sustainable removal rate. To address these uncertainties, sensitivity analysis enhances the understanding of central assumptions and demonstrates the results' robustness. Additionally, varying assumptions reveals the most important opportunities and risks for increasing and decreasing potentials and can highlight actions for policy makers. Table 8 shows the effect of altering parameters, such as increasing the sustainable removal rate, in the case of wheat straw. Positive drivers for bioeconomic potential are increased removal rates, increased R:C ratios, and substitutions concerning competing applications, especially in animal bedding. Vis versa, a lower sustainable removal rate has the potential to significantly reduce the bioeconomic potential.

Coniferous bark from industrial processes, especially bark from spruce and pine, shows a large and comparatively easily accessible bioeconomic potential. As bark is an already-available waste stream in certain industries, the bioeconomic potential should be less volatile than agricultural goods. The bioeconomic utilization of bark from other applications should be less critical, as the contemporary application fields are of low value. A major concept for increasing biomass from forestry is promoting the cascading use of wood, along with decreased combustion of valuable wood resources.

Table 8: Sensitivity analysis for wheat straw

Description	Effect on wheat straw bioeconomic potential	Description and field of activity
Opportunities		
Increase in sustainable removal rate by 10 % to an average of 50 %	+ 14 Mt (total: 60 Mt)	Substitution by organic compost fertilization
Utilization of crop species with higher residue-to-crop ratios (+10 %)	+ 5 Mt (total: 50 Mt)	Substitution of high crop yield cultivations by cultivation with higher residue-to-crop ratios
Switching animal bedding technology (slatted housing)	+ 10 Mt (total: 56 Mt)	Promotion/subsidization of straw-free bedding technologies
Substitution of wheat straw in energy production	+ 1 Mt (total: 47 Mt)	Promotion/subsidization of renewable energies not based on biomass feedstock
Reduction of livestock by 10% (alteration of societal diet patterns)	N/A	Less straw demand due to reduction in livestock
Threats		
Lower sustainable removal rate of 30 %	- 14 Mt (total: 32 Mt)	New research insights into the SRR
Crop species with lower residue-to-crop ratios (-10 %)	- 5 Mt (total: 40 Mt)	New cereal cultivations with lower ratios
50 % additional demand for agricultural applications	- 5 Mt (total: 40 Mt)	Changing demand patterns
Duplication of energy production in straw-burning combined heat and power plants (CHP)	- 1 Mt (total: 45 Mt)	Expansion of contemporary energy production from straw

The fraction of roundwood currently used for energy could be directed to substantial recovery in bioeconomic applications, which would free additional potential (approximately 11 Mt of roundwood (over bark)). A major risk is the continued utilization of bark for combustion or gardening material (Table 9).

Table 9: Results of sensitivity analysis for coniferous bark

Description	Effect on coniferous bark bioeconomic potential	Description & field of activity
Opportunities		
Increase in coniferous wood consumption by industry of 20 %	+2.8 Mt (total 16.5 Mt)	Promotion of natural building materials
Utilization of black liquor (refining residues)	N/A	Promotion of substantial recovery instead of energy recovery. Worldwide up to 50 Mt lignin from black liquor (Müssig and Carus, 2014)
Expansion of substantially used wood with less wood used for energy generation	+ 11 Mt of	Promotion of cascading use of wood
Threats		
Decrease of coniferous wood consumption by 20 %	- 2.7 Mt (total: 11 Mt)	Climate change can lead to diminishing conditions for coniferous trees, which can affect spruce populations
50 % bark demand of competing applications of technical potential	-6.8 Mt (total: 6.9 Mt)	Deviating demand

3.2 Discussion and conclusion on the agroforestry residue assessment

Theoretical potential includes all parts of fully harvested biomass that have no direct use in food, feed, or industrial production. To calculate the theoretical potential, R:C ratios are required. These depend on agricultural research and yield expectations. In principle, a decreased R:C ratio increases yield. However, this comes with a less robust structure of the plant and a higher risk of losing part of the harvest due to critical wheatear events. The R:C ratios are a trade-off between profit and risk issues and must be decided by each farmer. Therefore, general data is not applicable, and the calculation is based on averages.

Due to factors such as sustainable harvesting practices (e.g., balancing humus quality) and legislation (e.g., restriction of treetops and small branch removal from forests), a fraction of the theoretical potential is not accessible for further utilization. These facts are considered in the calculation of *technical potential*. Sustainable removal rates differ between species (40% - 50%). There is also an ongoing discussion about whether farmers tend to over-fertilize their acreage, which results in reduced technical potential.

Bioeconomic potential is the share of technical potential that is not necessarily used in competing applications such as animal bedding. All data regarding bioeconomic potential, except R:C ratio and sustainable removal rate, are measured on a regional level (NUTS 1).

For wheat straw (the most promising source of lignocellulose in Europe, with a total biomass of 284 Mt) (average in the EU-28 from 2010 - 2014), we found an R:C ratio of 1 and a sustainable removal rate of up to 57 Mt. Competing applications that demand straw can be found in the agricultural sector, with consumption of 27 Mt, and the energy sector (straw-based power plants) with a demand of 1.6 Mt. For wheat straw alone, this translates to consumption of 10.4 Mt by competing applications within the base case scenario (the demand pattern of straw from competing applications follows the distribution of regional production). This leaves 46 Mt as bioeconomic potential. The lower bound is 28.6 Mt, and the upper bound is 54.6 Mt. All results are based on averaged historic values. Development over time and geographical trends necessitates statistical forecasting of future waste arisings with good explanatory power. Robust forecasting of future waste arisings is crucial for an industrially scalable bioeconomy.

The scope of this chapter is twofold. First, a methodology for assessing the bioeconomic potential of agroforestry waste for biopolymers as precursors of high value-added products is developed. Based on this approach, the bioeconomic potential of endemic sources (cereals, oil crops, sugar crops, fiber plants, coniferous and broadleaf) is determined on a regional level (NUTS 1). The most promising source in the agricultural

sector is wheat straw (46 Mt), followed by maize stover (31 Mt), barley straw (16 Mt), and rapeseed straw (14 Mt), all containing a total lignocellulose content of more than 80 %. The NUTS 1 regions with the highest bioeconomic potential for wheat straw are the North of France (Bassin Parisien: 6.8 Mt; Ouest: 2.4 Mt) and the Czech Republic (1.7 Mt). Grain maize is most abundant in France (Sud-Ouest: 2.3 Mt; Ouest: 2.0 Mt) and Northeast Italy (Nord-Est: 2.0 Mt). The main arisings of barley straw are located in the Paris region (Bassin Parisien: 2.1 Mt), Central Spain (Centro: 1.8 Mt), and Denmark (1.3 Mt). In the forestry sector, waste bark from two coniferous species, spruce, and pine is the most promising source, with a bioeconomic potential of 15 Mt and a 70 % concentration of focal substances. Scandinavian countries (Manner-Suomi: 2.1 Mt; Norra-Sverige: 1.6 Mt; Södra-Sverige: 1.3 Mt) and central Europe show the most stable supplies of coniferous bark. By analyzing the procurement and supply chain patterns of bark (centralized supply at observed mills) and agricultural residues (decentralized supply by multiple farmers, some of which are new to the straw trading business), the disadvantages of relatively fewer arisings of bark compared to agricultural residues appear to be compensated by easier procurement and lower procurement costs.

To prove the robustness of the results, sensitivity analysis concerning alternative removal rates, R:C ratios, changes in farming technologies, and competing applications are applied. The sensitivity analysis of wheat straw (the agricultural source with the highest overall potential) and coniferous bark proves the robustness of our results. An increasing removal rate may enhance the amount of straw available for bioeconomic use. A major concept for increasing the amount of biomass available from forestry is promoting the cascading use of wood, along with decreased combustion of valuable wood resources. Further work covers the design of an economically and ecologically optimized European Supply Chain with robust collection networks to establish a sustainable European bioeconomy.

4 Spatially explicit forecast of feedstock potentials

Chapter four deals with the forecasting of prioritized feedstock potentials on the spatially explicit NUTS 1 level. The methods section develops an approach to forecast the theoretical, technical, and bioeconomic potential of lignocellulose residues. The approach is applied to the feedstocks wheat straw, corn stover, barley straw and rapeseed straw.

In 2012, the European Commission launched the European Bioeconomy Strategy (European Commission, 2012). The strategy was set up to enforce further the European bioeconomy, which was already one of the biggest and most important sectors in the EU. Limited natural resources, food security, and the advancing climate change in light of an increasing world population urge society to deal smarter with available resources. With this background, the European Commission advocated for a renewable resource strategy that, on the one hand, secures healthy food and animal feedstuff, and on the other hand, helps to move Europe towards a post-petroleum age where materials and biofuels are made of renewable sources. Better incorporation of underutilized materials like agricultural residues needs to be achieved (European Commission, 2012).

Lignocellulose materials are considered as a major feedstock for a second-generation bioconversion industry. Those materials are likely to play an important role as raw materials for various industries that do not compromise food or feedstuff production (Moreno et al., 2017). Especially agricultural harvesting residues like wheat straw, corn stover, barley straw, and rapeseed straw show large sustainably-available potentials (cf. chapter 3). The valorization of lignocellulose feedstock into intermediates, products, and biofuels will occur in biorefineries with different conversion routes. The variety of possible products from biorefineries is large and could be placed on the traditional petrochemical market and a future bio-based market (Kamm et al., 2010). Key challenges in the material and biofuel utilization of lignocellulose include its resistance to breaking down into its components cellulose, hemicellulose, and lignin; the large variety of different structures and chemical compositions due to genetic and environmental influences; as well as the large variety of released sugars from the breakdown of cellulose and hemicellulose (Balat, 2011). According to the recently published review of the *2012 European Bioeconomy Strategy*, significant progress has been achieved in extracting sugars from lignocellulose and its conversion to biochemicals and biofuels (European Commission and European Union, 2017). Another challenge is the supply chain cost, including collecting, distributing, and storing lignocellulose materials with low density (Balat, 2011). Hennig et al. (2015) claimed that the sustainable feedstock potential and its provisional cost are the major

limitations for a bio-based economy. Therefore, long-term monitoring of harvesting residues is required to ensure the efficient and sustainable utilization of this important feedstock in the future (Brosowski et al., 2016).

This work widens the knowledge base on the availability of lignocellulose biomass potentials concerning the spatial distribution in the European Union and its development over time. To successfully implement the utilization of lignocellulose feedstock on an industrial scale, one has to answer questions about feedstock availability: What feedstock shows the highest potential? Where is the feedstock spatially allocated? How will the supply develop in the future? This research was set out to answer these questions for the EU28 on NUTS 1 level. In the light of the increasing demand for biomass residues available for material and energy use, information on current and future potentials is gaining importance (Brosowski et al., 2016). The current production of primary agricultural goods is well investigated, and different future predictions exist. The annually published Agricultural Outlook is one of the most important global reports on food and feedstuff production (Asia et al., 2017). The Organisation for Economic Co-operation and Development (OECD) and the Food and Agricultural Organization (FAO) of the United Nations bring together their commodity, policy, and country expertise for a collaborative assessment of future agricultural commodity markets (OECD and FAO, 2015).

For the EU, the model is adapted by the European Commission, which annually publishes the EU Agricultural Outlook (Asia et al., 2017; European Commission, 2017a). In contrast to crops, future predictions on lignocellulose residue potentials are rarely found in the literature (Hennig et al., 2016). This chapter extends the approach for assessing agroforestry residue potentials introduced in chapter 3 (Thorenz et al., 2018)by a forecast of residue potentials. Since eheat straw (common wheat and durum wheat), corn stover, barley straw, and rapeseed straw make up to 80 % of cereals and oil crops harvesting residues, this chapter focuses on the future predictions on the lignocellulose feedstock potential of those prioritized resources. The forecasting horizon is until 2030, based on the time horizon of the EU Agricultural Outlook (European Commission, 2017a). Against this background, the following main research question is addressed by chapter 4 of this thesis:

> **RQ2: How will the set of prioritized agricultural feedstock potentials develop at the regional level by 2030?**

Answering the main research question takes place stepwise by answering the following sub-research questions:

- *Q1:* What are the underlying variables determining the future development of agricultural harvesting residues?

- *Q2:* What are suitable methods for providing a spatially explicit annual forecast of agricultural residues until 2030?
- *Q3:* How will agricultural residues' theoretical, technical, and bioeconomic potential develop in the EU28?

This research set out to answer these questions by reviewing existing literature and analyzing historic time series. With the developed methodology, potentials were forecasted on a spatially explicit level (NUTS 1 level) until 2030. With a sensitivity analysis and an out-of-sample test, the results' robustness was verified.

4.1 Methods

This research aims to develop a spatially explicit prediction model of agricultural residues' theoretical, technical, and bioeconomic potentials. The forecasting horizon is medium-term and covers the period from 2017 to 2030. As a spatial resolution, the 98 NUTS 1 regions (French: Nomenclature des unités territoriales statistiques) of the European Union were chosen based on national administrative subdivisions, mainly for the collection development and harmonization of European regional statistics. Datasets which are important to this work are available on NUTS 1 level, and the spatial resolution proved to be sufficient for the regionalization of agricultural residue potentials. Chapter 3 applied a methodology to calculate agroforestry residues' theoretical, technical, and bioeconomic potential, which provides the basis for this work. The work at hand extends the approach with an annual forecast of the potentials until 2030. Regional crop production, and consequently the available agricultural residues, depends on several factors such as market development and weather extremes or pandemics, often leading to high volatility in the regional annual production volumes. The results of this work display regional forecasts on the assumption that crop yields, crop areas, and other factors follow an average trend. A distinction is made between the three different levels, *theoretical potential*, *technical potential*, as well as *bioeconomic potential*, which are described as follows (Thorenz et al., 2018):

1. The theoretical potential (ThP) of agricultural residues is a function of the cultivated area of the primary crop, yield of a primary crop, and the residue to crop ratio of the specific crop.

$$ThP_{c,r,t} = Yield_{c,r,t} * Area_{c,r,t} * R{:}C\ ratio_c \quad (7)$$

$Yield_{c,r,t}$ denotes the yield in t/ha for the crop c in region r in the year t. The $Area$ (in ha) has the same indices and the $R{:}C\ ratio_c$ is assumed to be variable for different crops but is supposed to be constant within the considered time frame and regions.

2. The technical potential (TP) of agricultural residues considers that only certain shares of residues can be recovered due to technical, legislative, and sustainability criteria. These criteria are combined in the Sustainable Removal Rate (SRR), reducing the theoretical potential.

$$TP_{c,r,t} = SRR_c * ThP_{c,r,t} \quad (8)$$

SRR_c denotes the Sustainable Removal Rate for crop species c.

3. The bioeconomic potential (BP) calculates by the consideration of competing applications. The most important competing application of straw is the bedding of animals (cattle, horse, pig, etcetera) and other agricultural uses like horticulture and mushroom cultivation (Data repository D.1, Table 5).

$$BP_{c,r,t} = TP_{c,r,t} - CA_{c,r,t} \quad (9)$$

$CA_{r,c,t}$ denotes competing applications for crop species c, region r, and year t.

These three potentials provide the independent variables *area, yield, residue to crop ratio, sustainable removal rate (SRR),* and *competing applications.* Equations 1 to 3 describe the mathematical relation of the independent variables and the potentials. The independent variables need to be forecasted to perform forecasts on a dependent variables, which are the three afore described residue potentials.

4.1.1 Forecasting approach

This section deals with analyzing and explaining the independent variables and the applied time series models. Chapter 3 identified the crop yield, the cultivated area, the residue to crop ratio, the sustainable removal rate, and competing applications as independent variables determining the different potentials. Each variable shows specific peculiarities, requiring a careful selection of applied time series models. The historic time series of the analyzed independent variables showed patterns like a linear trend, no trend, a logistic trend, or exponential decay. For each time series, different appropriate time series models were fitted with a final selection of the most suitable model according to quality measures, which are further described in the following section.

Cultivated crop area: Regional forecasts on the *cultivated crop area* of different species are rarely found in the literature. The EU Agricultural Outlook annually projects the most important values in agriculture production in the European Union, including projections on cultivated crop area (European Commission, 2017a). The outlook is based on the Aglink-Cosimo Model, a comprehensive partial equilibrium model for

global agriculture (OECD and FAO, 2015). A large set of macro-economic assumptions considers several developments such as population change, oil price, EU inflation, and currency exchange rates. For specific species, external factors like changing consumption patterns, biofuel policy, and land use changes are considered (European Commission, 2017a). On the downside, the outlook differentiates only in EU-15, the EU member states before 2004, and EU-N13, EU members that joined in 2004 or later (Data repository D.1, Table 7).

The cultivated crop area is subject to a complex nexus of aforementioned factors such as population change, oil prices, changing consumption patterns, agro-policies, and others, whereby the outlook's projections provided the basis for the independent variable *cultivated crop area*. Simply disaggregating the outlook's area projections to the regional level would bias the regional prognosis. As the last observed value is the basis for future predictions, regional extremes of the last observed value would strongly bias the prediction. To address this inaccuracy, statistical time series models were applied to smooth the first year (2017). Historic time series for the cultivated crop area of each species are available on NUTS 1 level (Eurostat, 2016a). For data without trend, simple exponential smoothing (ES1) and data with linear trend, Holt's linear trend method (ES2) was applied (Hyndman and Athanasopoulos, 2013). As data was investigated annually, seasonal variations were ruled out, and seasonal time series models were excluded. All models were parameterized by optimizing Theil's inequality coefficient (U). Theil's inequality coefficient compares the quality of a prognosis to the quality of the naïve prognosis, and the optimal U minimizes the forecasting error e_t (Theil, 1966). If the optimised U is larger than 1, the quality of a forecast is worse than the naïve prognosis which leads to a rejection of the model (see eq. (10)).

$$U = \sqrt{\frac{\frac{1}{K}\sum_t^K e_t^2}{\frac{1}{K}\sum_t^K (y_t - y_{t-1})^2}} \tag{10}$$

The Tracking Signal indicates systematic errors if the model systematically under- or overestimates data. The tracking signal calculates as the sum of all errors divided by the Mean Average Error (MAE). A model is only applied in case the Tracking Signal ranges between $-0.5 < TS < 0.5$ (Thonemann, 2010) (see eq. (11)).

$$TS = \frac{\sum e_i}{MAE} \tag{11}$$

In the case of simple exponential smoothing for data without trend, the area forecast $\hat{y}_{t+1}$ depends on the smoothing parameter α. It can take values between 0.05 and 1, with low values giving more weight to old area observations, depicted by $\hat{y}_{t-1}$, and high values giving more weight to the last observed crop area y_t.

$$\hat{y}_{t+1} = \alpha * y_t + (1 - \alpha) * \hat{y}_{t-1} \tag{12}$$

For each time series, α is selected by minimizing the quality measure U (Theil's inequality coefficient). For time series with trend, the tracking signal of simple exponential smoothing is larger than 0.5, respectively smaller than -0.5. Holt's linear trend method applies in the case of time series with a linear trend. The forecast $\hat{y}_{t+h|t}$ is made of one smoothing equation for the level l_t and one for the trend b_t (Hyndman and Athanasopoulos, 2013).

$$\hat{y}_{t+h|t} = l_t + hb_t \tag{13}$$

$$l_t = \alpha y_t + (1 - \alpha)(l_{t-1} + b_{t-1}) \tag{14}$$

$$b_t = \beta^*(l_t - l_{t-1}) + (1 - \beta^*)b_{t-1} \tag{15}$$

The smoothing parameters α and β range from 0.05 to 1, with small parameters giving more weight to old area observations and large parameters giving more weight to recent data (Schlittgen and Streitberg, 2001). The parameter h is the h-step-ahead forecast, which linearly multiplies the last estimated trend variable. In case none of the models fitted the investigated data accurately, a naïve prognosis was applied.

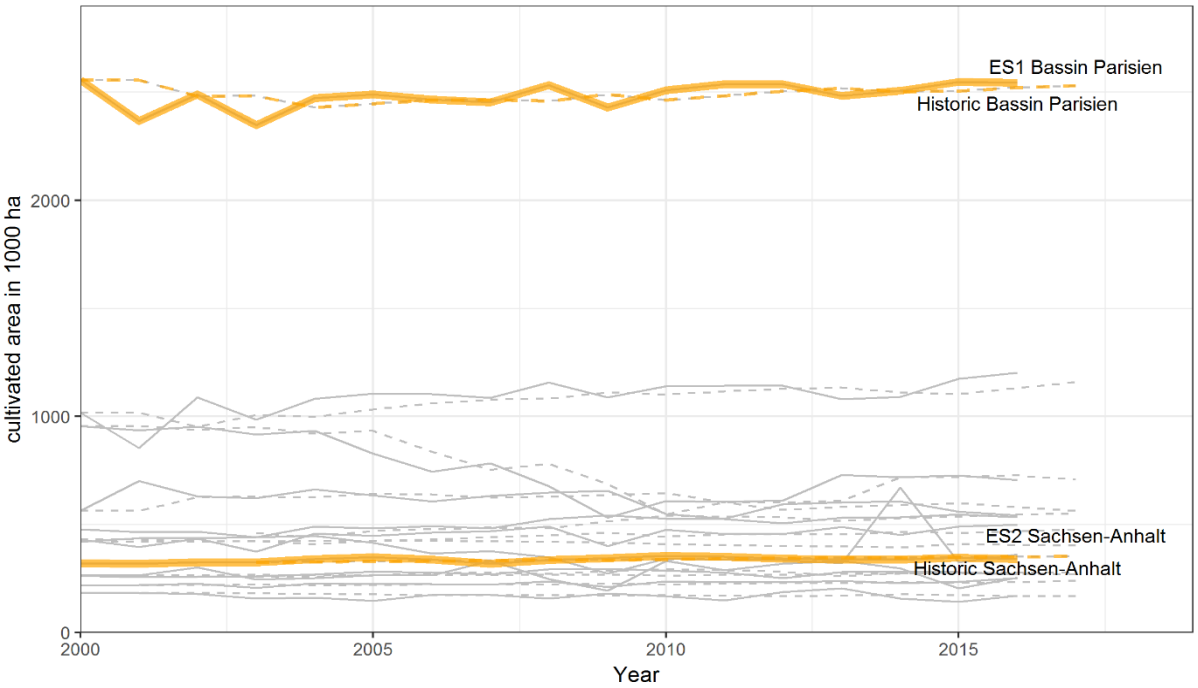

Fig. 15: Plot of the cultivated area of wheat grain.
The solid lines represent historically cultivated areas; the dashed lines depict the applied time series model results. Bassin Parisien (France) is highlighted exemplarily for regions where simple exponential smoothing (ES1) applies, and Sachsen-Anhalt (Germany) is highlighted for regions where Holt's linear trend method (ES2) applies

Grain yield: The agricultural database of Eurostat (2017) provides historic time series of the annual *grain yield* of each species on NUTS 1 level. Grain yields are limited by an agro-economic saturation, which arises from plant-specific biophysical properties and the limited provision of the crops with key resources like nutrients, sunlight, water, and growing space. Table 10 shows the saturation levels for agricultural crop yields (European Commission, 2016).

Table 10: Agro-economic yield saturation of relevant crops

Agricultural products	**Agro-economic yield saturation (in t/ha)**	**Residue-to-Crop ratio**	**Sustainable Removal Rate**
Wheat grain	7.0	1.00	40 %
Corn grain	10.4	1.13	50 %
Barley grain	5.3	0.93	40 %
Rapeseed	3.9	1.70	50 %

Fig. 16 shows a log-log plot of all available historic wheat grain production values and corresponding cultivated areas (98 NUTS 1 regions and 16 historic years). The red line represents the average yield saturation of 7.0 t/ha assumed for wheat grain. The blue lines constitute historic average wheat yields of the whole EU (in 2000, 4.89 t/ha and in 2015, 5.73 t/ha) and the highest historically observed wheat grain yield (10.66 t/ha, Ireland in 2015). The historically achieved yield maximum of 10.66 t/ha is distinctively higher than the expected agro-economic yield saturation. Ireland benefits from stable and good rainfall and a lack of extreme weather events like cold winters or hot summers. Combined with expensive disease control, Ireland is the world leader in wheat yields (Jones, 2015). In the last 15 years, the average yield increased by nearly one tonne per hectare.

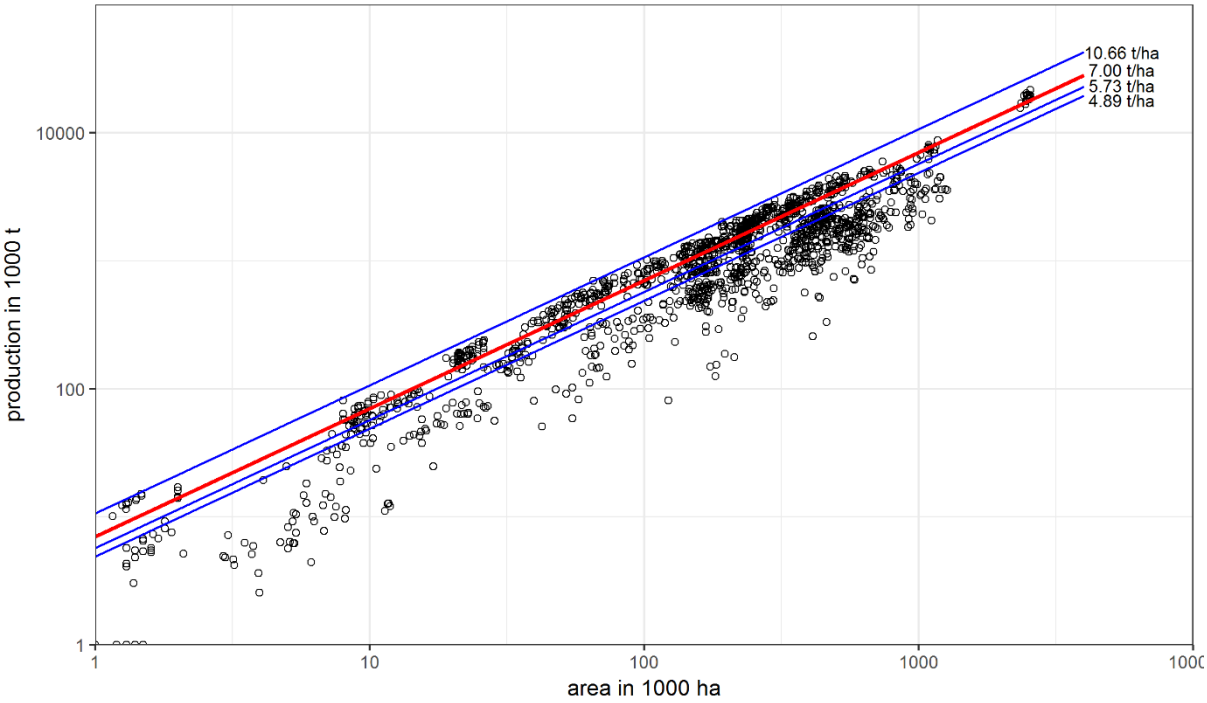

Fig. 16: Log-log plot of wheat grain production
and cultivated area with equi-yield lines. The red line represents the assumed agro-economic yield saturation of wheat grain. The upper blue line represents the highest historically achieved wheat yield (10.66 t/ha, Ireland in 2015). The 5.73 t/ha yield line corresponds to the average wheat grain yield in 2015, and the 4.89 t/ha yield line corresponds to the average wheat grain yield in 2000

Logistic growth models apply very well to the case of limited resources (Rye et al., 2013). Therefore, future yields were forecasted with logistic growth models, including region-specific parameters. Eq. (16) shows the logistic growth function with $\hat{y}_t$ being the prognosis in period t. The yield asymptotically approaches the saturation level, which implies decreasing growth rates. Estimates for the starting value y_0, the saturation level S, and the growth factor k can be retrieved from literature or acquired by parametric rating.

$$\hat{y}_t = \frac{S}{1 + \left(\frac{S}{y_0} - 1\right) * e^{-k*S*t}} \tag{16}$$

In principle, a saturation value for crops exists in the agro-economic yield saturation. The parameters k and y_0 were estimated by a linearisation of eq. (16). The slope m and the y-intercept b in eq. (17) were derived from the linearised model by the least-squares method (linear regression).

$$f(t) = \ln\left(\frac{S}{y(t)} - 1\right) = \ln\left(\frac{S}{y_0}\right) - kSt = b + mt \tag{17}$$

The original nonlinear model's missing parameters k and y_0 were then calculated by inverse transformation shown in eq. (18) and eq. (19).

$$k = -\frac{m}{S} \tag{18}$$

$$y_0 = \frac{S}{1 + e^b} \tag{19}$$

For each of the 98 NUTS 1 regions, the saturation S of the logistic growth model corresponds to the yield saturation. The growth factor k and the initial value y_0 were calculated from historic data (2000 - 2016). Time series with strong growth in the past have a higher growth factor, and regions with slow or no growth were parameterized with lower growth factors leading to almost stable future yields. Due to advantageous conditions like deep rich soils, good rainfall, very few extreme weather events, or expensive disease control (Jones, 2015), some regions exceeded this assumed saturation, whereby the saturation level of those regions was adjusted to their respective historic maximum. In the case of constant historic yields, the logistic growth model did not project the data properly, wherefore, in this case, simple exponential smoothing performed well. This was especially true for regions with already very advanced agriculture and thus high yields. In case no model fitted, the data naïve prognosis was applied.

Fig. 17 shows the historic and forecasted wheat grain yields of selected 28 EU countries. The region Niedersachsen in Germany belongs to the regions with already very high grain yields where the results indicate no significant increase in the future whereby simple exponential smoothing had better forecasting quality. Romania, on the contrary, substantially increased its grain yield in the last years. The logistic growth model was parameterized with this data, which led to a high growth factor k resulting in fast approximation towards the saturation level.

Residue to crop ratio and sustainable removal rate: The *residue to crop ratio* and the *sustainable removal rate* were assumed to be constant over time and region. According to Foulkes et al. (2011), the harvesting index and, thereby, cereal plants' residue to crop ratio has been constant since the early 1990s. Chapter 3 reviewed several studies on residue-to-crop ratios, and the results are displayed in Table 10. Sustainable removal rates of harvesting residues ensure the incorporation of nutrients to sustain the humus quality. The rate depends on various factors like the kind of soil, farming patterns, soil fertilisation, water supply and other factors making it difficult to give region-specific rates (Scarlat et al., 2010). For reasons of simplicity, in this work the sustainable removal rate was supposed to stay constant over time and region.

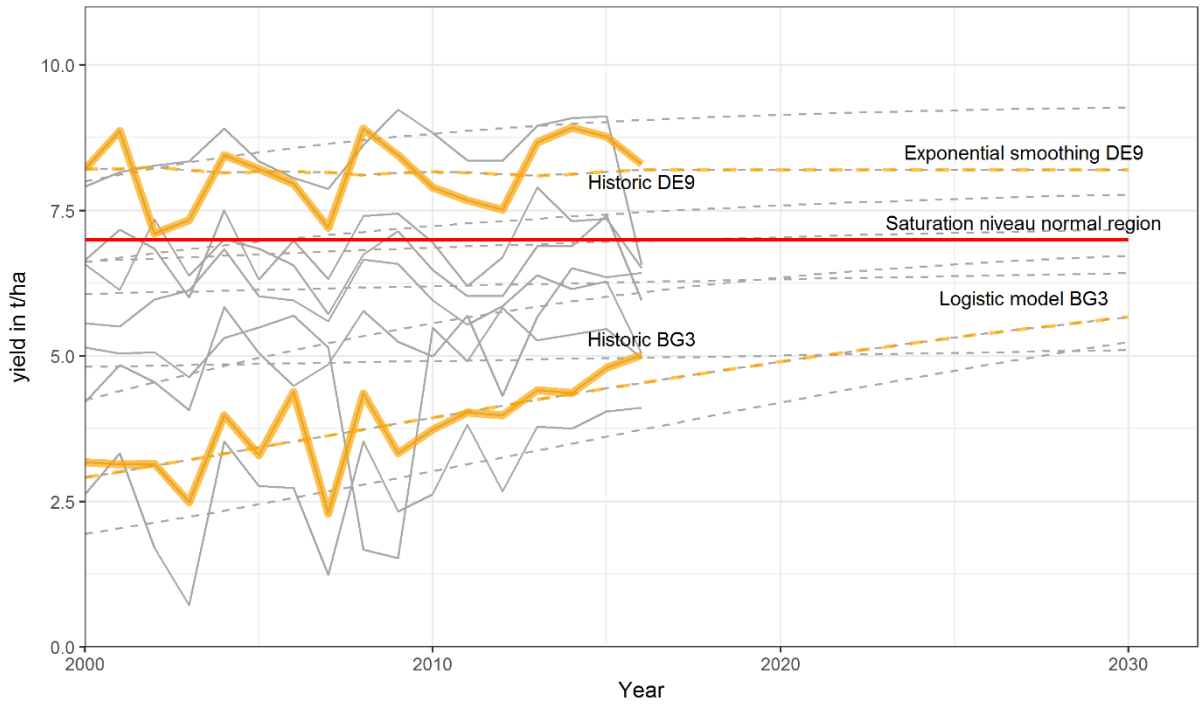

Fig. 17: Historic and future wheat grain yields by NUTS 1 regions.
The solid lines represent documented historic yields of NUTS 1 regions, emphasizing DE9 (Niedersachsen) and BG3 (Severna I Yugoiztochna Bulgaria). The dashed lines depict the forecasting until 2030, emphasizing DE9 (simple exponential smoothing) and BG3 (logistic model)

Competing applications: The demand for *competing applications* is the last factor required to calculate the bioeconomic potential. According to the results of chapter 3, competing applications consume nearly 30 Mt residual straw annually. The most important competing applications for straw are the bedding of animals like cattle bedding with a share of about 41 % of the straw consumed by competing applications, pig bedding with about 12 %, sheep bedding with about 11 %, and horse bedding with about 6 %. Apart from animal bedding, surface-mulching accounts for about 12 % of the demand, the production of compost for mushroom cultivation accounts for 10 % of the straw demand from competing applications, the energy production in combined heat and power plants (CHP) accounts for 6 % and the covering of strawberries for about 2 %. Calculation specifications for the straw demand of competing applications were based on Scarlat et al. (2010) and the results of chapter 3. This chapter assumed that the calculation specifications would remain constant in the period under review. As for the variables introduced before, the forecasting of the straw demand from competing applications is based on historic time series. Simple exponential smoothing was applied with stable future demand for data without trend. Holt's linear trend method was applied for data with a positive trend with increasing future demand. Holt's linear trend method was applied to the logarithmical demand to address the circumstance that demand cannot become negative for time series with negative trend.

Fig. 18 shows Poland's historic and future straw demand of selected competing applications. Holt's linear trend method forecasted the future demand of cattle bedding and mushroom cultivation. Strawberry covering fluctuated in the past around a stable level, wherefore simple exponential smoothing was selected. Pig bedding distinctively decreased in the past 15 years, wherefore Holt's linear trend method was applied to the logarithmical straw demand of pig bedding. The forecasting results for every NUTS 1 region can be found in Data Repository D.1, Table 5.

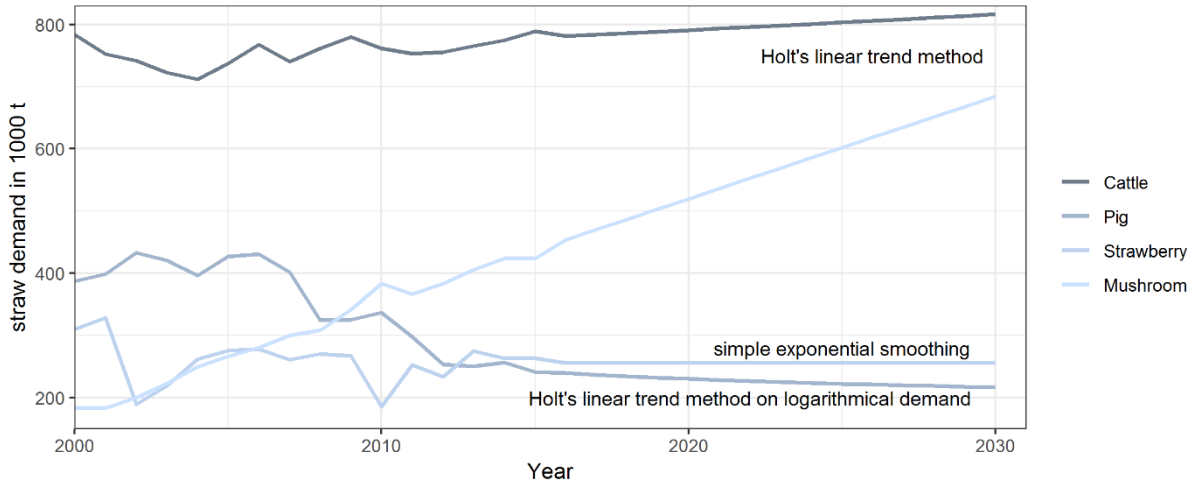

Fig. 18: Historic and future straw demand
of cattle bedding, pig bedding, strawberry covering, and mushroom cultivation in Poland

4.1.2 Data preparation

Eurostat provides historical data of cultivated crop area, crop yields, and agricultural crop production on NUTS 1 level with some data gaps from 2000 to 2016. Where necessary, data gaps were filled by appropriate methods. Country data (NUTS 0) is available on Eurostat without gaps, wherefore, in the case of missing NUTS 1 level data, country data is used to calculate the missing NUTS 1 data. Data gaps were filled by multiplying the historic average NUTS 1 share with the country data of the missing year. In-data tests indicated a good performance of this method.

Historical data for calculating competing demand were obtained from Eurostat for cattle, pig, and sheep on NUTS 1 level (Eurostat, 2016a). For the strawberry and mushroom production and the number of horses, data were obtained from FAO Stat with the disadvantage that figures are only available on NUTS 0 level (FAO, 2017). To disaggregate country data of those applications, the area share of each NUTS 1 region within the country is used as a disaggregation proxy.

4.2 Results

Harvesting residues of wheat grain (common wheat and durum wheat), corn grain, barley grain, and rapeseed represent about three-quarters of the annually accumulated lignocellulose residues from EU's fields. Results of each feedstock type are discussed in detail in the following sections. All forecasts and results were calculated on NUTS 1 level. For a comprehensible depiction of the results, most of the diagrams and tables are displayed on an aggregated level (EU28 or country level). Detailed forecasting results on NUTS 1 level of theoretical, technical, and bioeconomic potentials until 2030 are found annually in the data sheets of Data Repository D.1, Table 1, Table 2, and Table 3.

Fig. 19 displays aggregated values of the historic and forecasted bioeconomic potential for the EU28. Results indicate that the most important agricultural residue wheat straw further increases in the future. Also, corn straw is likely to continue its positive trend in the next years. This is mainly due to their competitiveness on the world market and comes at the expense of crops like oats and rapeseed (European Commission, 2016, 2017a). The cultivated area of barley is expected to stay rather stable. Together with only marginal increases in barley yields, the theoretical potential of barley straw increases marginally. The strong growth rates of rapeseed production, mainly due to expansions in the cultivated area, seem to reach a plateau with rather decreasing production volumes in the years to come.

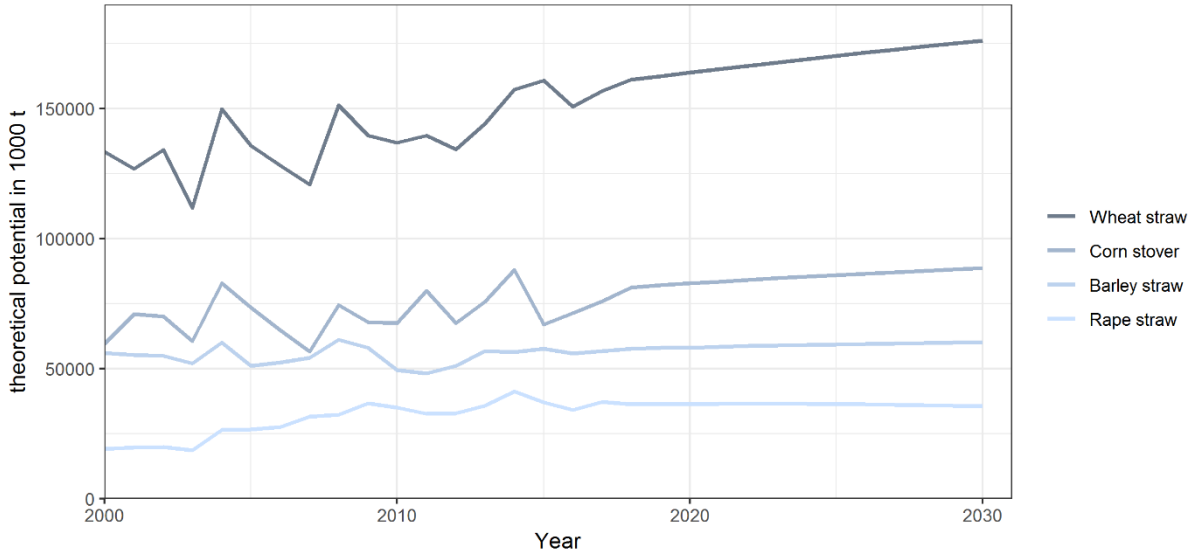

Fig. 19: Aggregated historical (2000-2016) and forecasted theoretical potential of lignocellulose feedstocks

The results indicated that the overall theoretical potential of considered agricultural residues rises from 326.8 Mt in 2017 to approximately 360.6 Mt in the year 2030, corresponding to an increase of about 10.3 %. The bioeconomic potential calculates at

113.0 Mt in 2017 and will rise to approximately 127.0 Mt in 2030. This increase is mainly due to increasing yields in central-eastern European countries. Especially for common wheat, increases in the cultivated area could come at the expense of other cereals (European Commission, 2017a). Results show a rather stable demand of competing applications for agricultural residues of about 30 Mt. For the years ahead, the results do not show significant changes in demand of the largest straw consumer cattle bedding, pig bedding, and sheep bedding (Data Repository D.1, Table 5).

Table 11 is an aggregated summary that compares the 2017 potentials with the forecasted potentials in 2030. According to the results, the overall bioeconomic potential of corn stover will increase by nearly 20 %. Simultaneously, the amount of rapeseed straw is supposed to decrease slightly (Data Repository D.1, Table 3).

Table 11: Comparison of the average 2017 data with forecasted 2030 data

Agricultural harvesting residues	**2017 Theoretical potential (kt)**	**2017 Bioeconomic potential (kt)**	**2030 Theoretical potential (kt)**	**2030 Bioeconomic potential (kt)**	**Change Theoretical Potential**	**Change Bioeconomic potential**
Wheat straw	156,880	50,097	176,144	57,227	12.3 %	14.2 %
Grain corn stover	75,961	30,429	88,642	36,503	16.7 %	20.0 %
Barley straw	56,664	16,666	60,251	18,098	6.3 %	8.6 %
Rapeseed straw	37,281	15,807	35,584	15,205	-4.6 %	-3.8 %

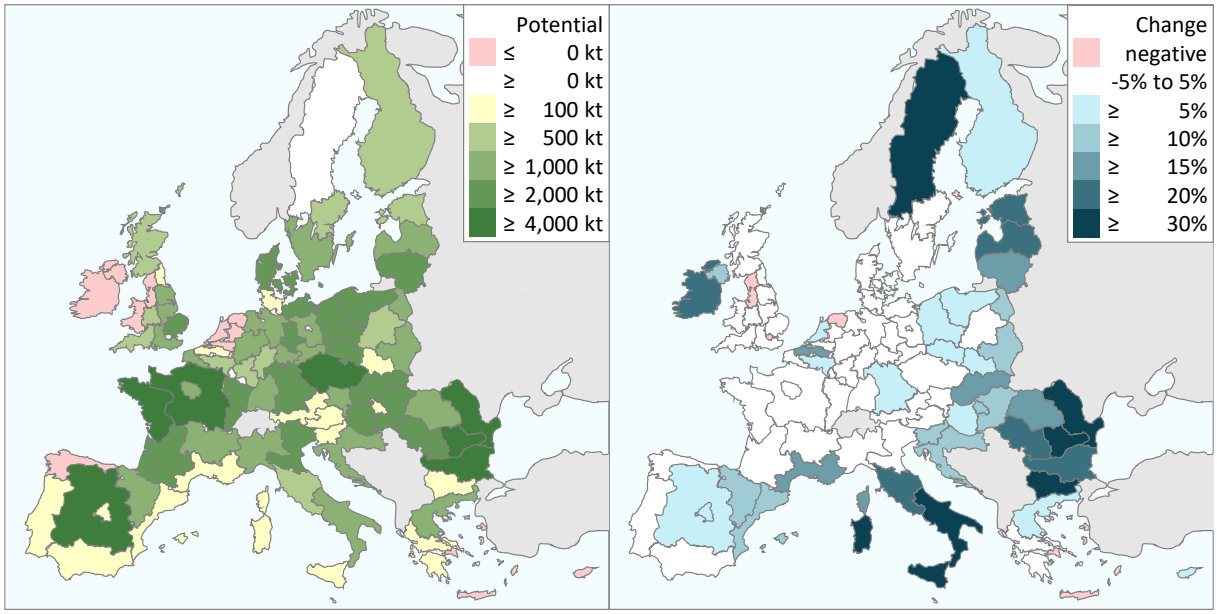

Fig. 20: (a) Total bioeconomic potential of the four considered agricultural residues wheat straw, corn stover, barley straw and rapeseed straw in the year 2030. (b) shows the forecasted percentage change in the residue availability

4.2.1 Wheat straw

According to the results, wheat straw from common and durum wheat remains the most important agricultural lignocellulose residue in the European Union. The growth rate of the cultivated area is expected to stay rather small, with an average annual growth of around 0.1 % (European Commission, 2017a, Data Repository D.1, Table 7). In countries with a long EU membership, yields tend to be on average higher than in countries with more recent EU accession. On the contrary, this implies in many cases that yields are already around the agro-economic saturation with little or no potentials for further increasing yields. In countries like Belgium, Denmark, France, Germany, or the Netherlands, the models predict growth rates between 0 % and well below 3 to 4 % over the whole period under observation, which implies nearly constant yields. Central and Eastern European Countries with more recent EU accession like Bulgaria, Estonia, Poland, and Romania show yield growth rates up to 30 % between 2017 and 2030. Those countries currently undergo advances in farming technology and attain more efficient resource management (European Commission, 2017a).

4.2.2 Corn stover

Like wheat, corn production is also likely to expand further in the coming decade. Fig. 21 shows the EU map with the bioeconomic potential of corn stover in 2017 (a) and 2030 (b) (without the oversee regions). The main driver for the increase in corn stover potentials is the increasing crop yields. Like wheat, most noticeably Bulgaria, Romania, and Slovakia are catching up with farming techniques, increasing crop yields between 1.5 t/ha and 2.3 t/ha, resulting in up to 7 – 9 t/ha. Those countries are likely to register distinctly larger residue potential growths of up to 25 – 30 % than most other regions.

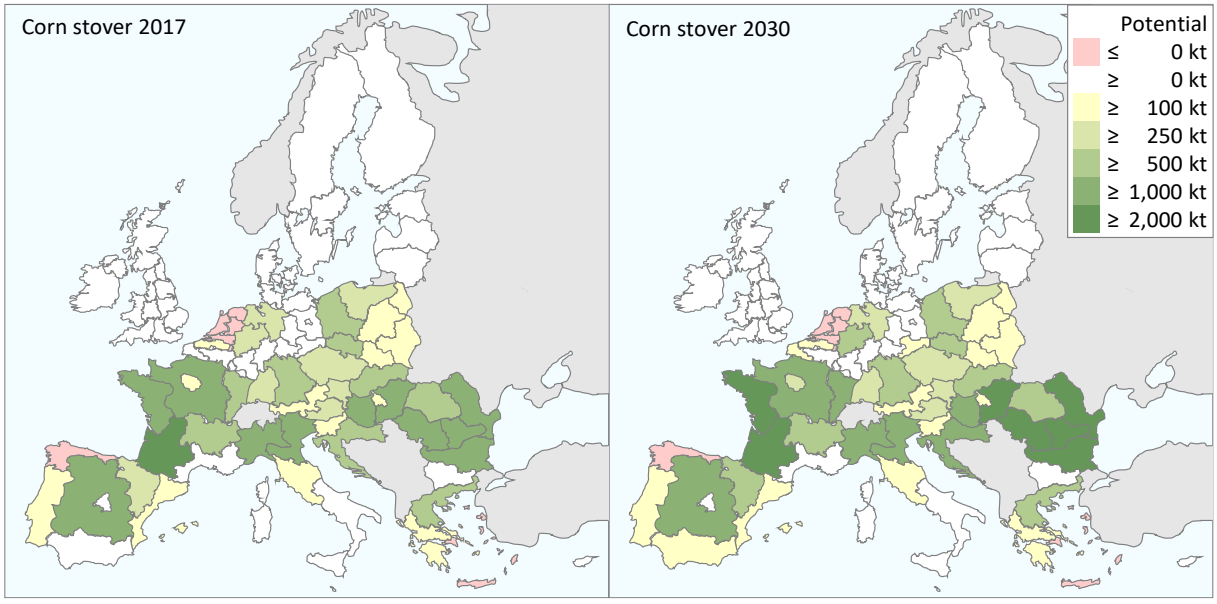

Fig. 21: (a) Bioeconomic potential of corn stover 2017 and (b) bioeconomic potential of corn stover 2030

According to the 2017th Agricultural Outlook, from 2020 onward, the cultivated corn grain area is expected to decrease by 0.1 to 0.2% per year (European Commission, 2017a) slightly. In countries with stagnating yield growth rates like France or Italy, this means stable or even slightly falling production volumes. Romania, already the second-largest producer of corn, could catch up with France by 2030 as the largest producer. Even though the cultivated corn grain area could slightly decrease in the decade after 2020, the overall production volumes are expected to increase until 2030.

4.2.3 Barley straw

It is predicted that the barley straw potential will have the most stable supply in the coming years. In the historic period under consideration, in nearly all regions of the EU, barley production stayed rather constant or had a slightly negative trend. According to the European Commission (2017b), the annual changes in the cultivated area are expected to fluctuate around 0 % (Data Repository D.1, Table 7). The models predict yield increases in EU regions with a more recent EU accession. As those countries only produce minor volumes of barley, the increase in yield carries little weight for the overall production volumes. To sum up, in the EU28, theoretical barley straw potentials are expected to increase by about 6 % until the year 2030.

4.2.4 Rapeseed straw

Compared to the results of the other investigated feedstocks, rapeseed straw volumes will decrease in the next ten years in most regions. According to the European Commission (2017), the total rapeseed area in the EU will decrease by about 0.5 to 0.9 % annually. The contraction is driven by the decrease in demand for vegetable oil and decreasing demand for first-generation biofuels. Additionally, a shift from rapeseed towards imported soybean can be observed at the moment (European Commission, 2016). The decreasing cultivated land share of rapeseed has especially strong effects on production volumes in countries with already high grain yields like France or Germany. In countries that currently undergo advances in farming practices, the expected area decrease is compensated by growing grain yields (like Romania or the Czech Republic). Fig. 22 plots the theoretical potential of rapeseed straw for each EU country, emphasizing France and Romania. France includes the regions that have already reached yield saturation, and Romania represents regions that still face strong increases in the achievable yield. For the whole EU28, the 2030 theoretical potential of rapeseed straw is supposed to drop by 4.6 % and the bioeconomic potential by 3.8 % compared to 2017. Detailed results for each species and region are found in Data Repository D.1, Table 1.

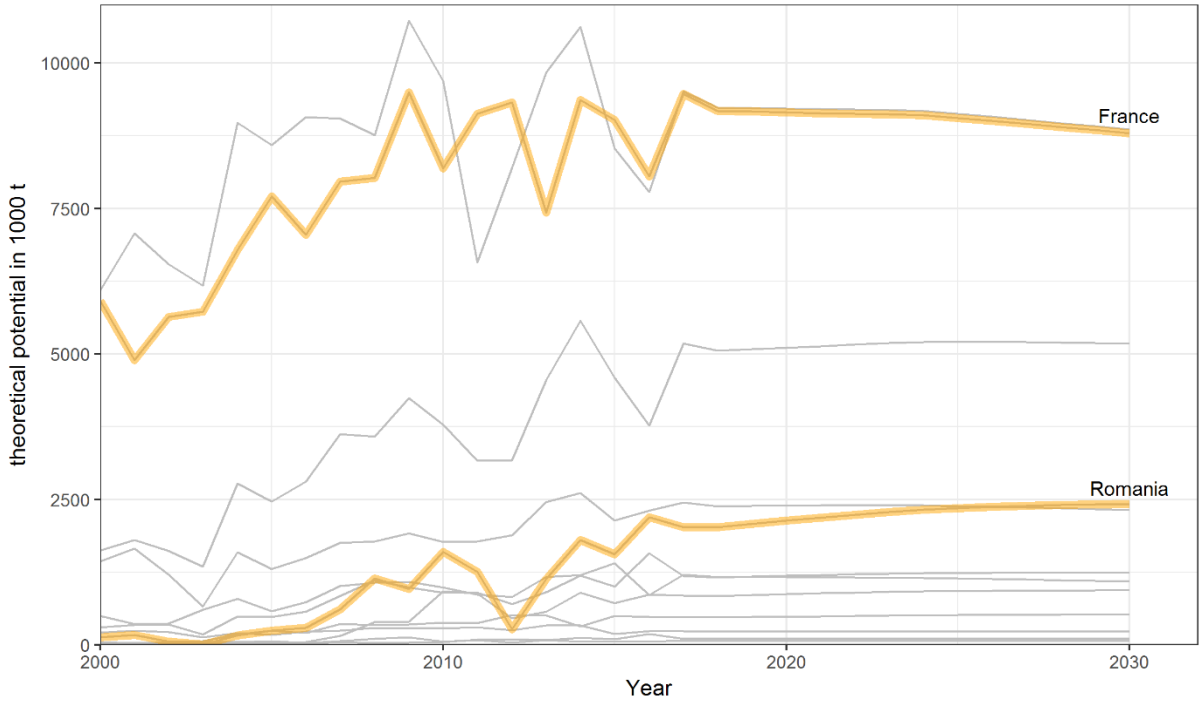

Fig. 22: Development of theoretical potentials of rapeseed straw from 2016 to 2030.
France is representative for countries with forecast of negative development and Romania for countries with a positive development

4.3 Discussion and conclusion on the forecasting approach

This work forecasted agricultural residue potentials of lignocellulose matter until the year 2030. Wheat (common and durum), corn, barley, and rapeseed are the crops with the largest production volumes in the EU, yielding the highest amounts of harvesting residues. Up to 80 % of lignocellulose residues from agricultural harvesting (cereals and oil crops) arise from those species (cf. chapter 3). Based on historic data (2000 – 2016), the cultivated area of the year 2017 was forecasted with fitted time series models. From 2018 to 2030, the EU Agricultural Outlook adopted annual percentage change in the cultivated area. This approach was chosen as exogenous macro-economic factors that affect the cultivated area are not considered by applying time series-based models only. To prove the robustness of model assumptions, the cultivated area forecasted by the EU Agricultural Outlook was compared to a time series-based forecast of the cultivated area (Data Repository D.1, Table 6 and 7). For wheat straw and corn stover, the results hardly differ. In the time series-based area forecast, barley straw residue potentials are expected to decrease in the next decade. In many regions, barley area contracted in the last years and time series-based models predict that this will continue. Conversely, rapeseed areas developed positively between 2000 and 2016, resulting in increasing area forecasts. The sensitivity analysis regarding the cultivated area development confirms that time series-based forecasts do not include exogenous information, although they strongly affect the future.

Forecasts of crop yields are based solely on fitted models, and especially in regions with more recent EU membership, the logistic model fitted very well and identified a positive development of yields in the observed years. In regions where the yield fluctuated around a stable level in past years, simple exponential smoothing applied better (see chapter 2.1.2). To prove the results, they were compared with the EU Outlook's predictions. The regionalized yield forecasts of in this work were aggregated to the EU-15 and EU-N13 levels, based on the production share of a region. For wheat and corn, the results show good comparability (difference in the 2030 yield forecast well below 3 to 4 %). While barley yields on the EU-N13 level are similar, yields on the EU-15 level differ by nearly 15 %. This difference is the historic barley yields, which already differ by around 15 % between the EU Agricultural Outlook and the Eurostat data used in this work. For EU-15 countries, rapeseed yield forecasts are almost similar. In contrast, for the EU-N13 aggregation, the yield forecast is higher, and in 2030 the prediction exceeds the Outlook's prediction by 15 % (further information on the comparison is found in the Data Repository D.1, Table 4, and Table 7).

The residue to crop ratio and the sustainable removal rate were assumed to stay constant during the period under consideration. This assumption is a limitation of this study, as the residue to crop ratio and the sustainable removal rate depend on regional and terrain-specific features. The sustainable removal rate is an important factor for the humus quality and thereby sustainable and long-term-oriented agriculture. In Germany, the Association of German Agricultural Assessment and Research Organisations provides a methodology for calculating field-specific humus balance, which provides a basis for calculating regionalized sustainable removal rates (VDLUFA, 2014). However, the methodology requires specified information, which is difficult to acquire in assessments on a macro level, wherefore we used a sufficiently high average sustainable removal rate (Scarlat et al., 2010).

To verify the robustness of the presented results, this study completes an out-of-sample test for 2017, where forecasted residue volumes were compared with actual recorded values of 2017. Beginning of the year 2018, the first datasets on 2017 crop production were published on NUTS 0 level (EU28 countries) by EUROSTAT (Eurostat, 2018a). Accordingly, the forecasted theoretical potentials were compared to the actual potentials of the year 2017. While the forecasted theoretical potential of wheat straw in the EU28 summed up to 156.9 Mt, the actual wheat straw potential was 152.7 Mt, which corresponds to a deviation of 2.7 %. Corn stover deviates by 2.5 % (Forecast: 76.0 Mt, actual volume: 74.1 Mt). Barley straw was forecasted with 56.7 Mt and the actual volume summed up to 55.1 Mt, which corresponds to a deviation of 2.8 %. The same small deviation holds for rapeseed straw with a forecast of 37.3 Mt and an actual volume of 37.0 Mt (deviation of 0.6 %). As a result of the out-of-sample test on aggregated EU level for the year 2017, it may be noted that the time series models

show a high prognosis accuracy. However, it is noticeable that the forecast overestimated the observed production in 2017.

On the country level, larger deviations between forecasts and actual volumes were registered (see Fig. 23). Deviations between forecasted and actual potentials are small for all large producers of wheat straw. Romania, the fifth-biggest wheat straw producer in the EU, showed the largest deviation with about a 20 % higher theoretical potential than forecasted. The exemplary development in 2017 was due to favorable weather, government subsidies, proper fertilizer management, and disease prevention (Dobrescu, 2017). Due to poor weather conditions during the growing campaign in 2017, the largest wheat crop producer, France, stayed about 3.5 % behind the forecasted volumes (Houghton, 2018). Again, for corn stover, the actual 2017 volumes in Romania strongly exceeded the forecast (about 25 %), making Romania the second-largest corn stover producer in the EU in 2017. The results indicate that Romania's production will catch up with France as the biggest producer in 2030. However, also for corn, the development in Romania in the year 2017 was exceptionally positive (Dobrescu, 2017). Other important corn-producing countries like France, Italy, or Spain significantly produced less than forecasted.

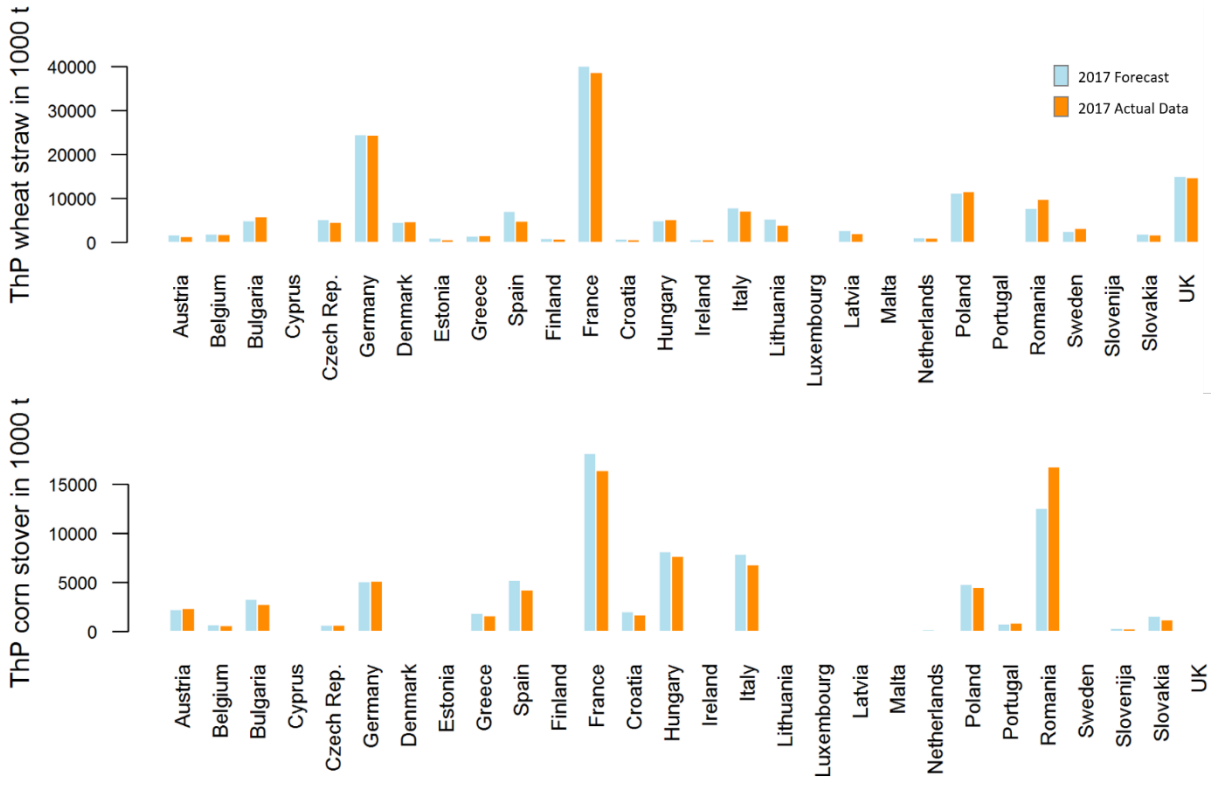

Fig. 23: Comparison of the 2017 forecast and actual data
of the theoretical potential of wheat straw and corn stover

For barley straw, the 2017 forecast of the largest producers is fairly accurate (deviation in Germany: 2.7 %, France: 0.7 %, UK: 0.8 %). The forecast exceeded the actual

production by about 21 % in Spain, the fourth-largest producer. A severe drought hit Spain, leading to distinctively smaller barley grain yields (Rehman, 2017). While for rapeseed straw on NUTS 0 level, the difference of the forecast and the actual values is close to zero, on NUTS 1 level, large differences are noted (see Fig. 24). Especially the largest producers, France and Germany, showed remarkable differences between forecast and actual volumes. While rapeseed straw volumes in 2017 in Germany were about 25 % less than forecasted, in France, the actual volumes exceeded the forecasted potentials by about 12 %, which partly counterbalanced the sum. The German rapeseed production suffered from negative temperatures after sowing, heat waves during the growth phase, and very wet phases during the harvest, which altogether led to the remarkable drop (Krauß, 2017). In France, rapeseed yields in 2017 reached a record level-high due to optimal growing conditions leading to higher than forecasted straw potentials (Trompiz, 2017).

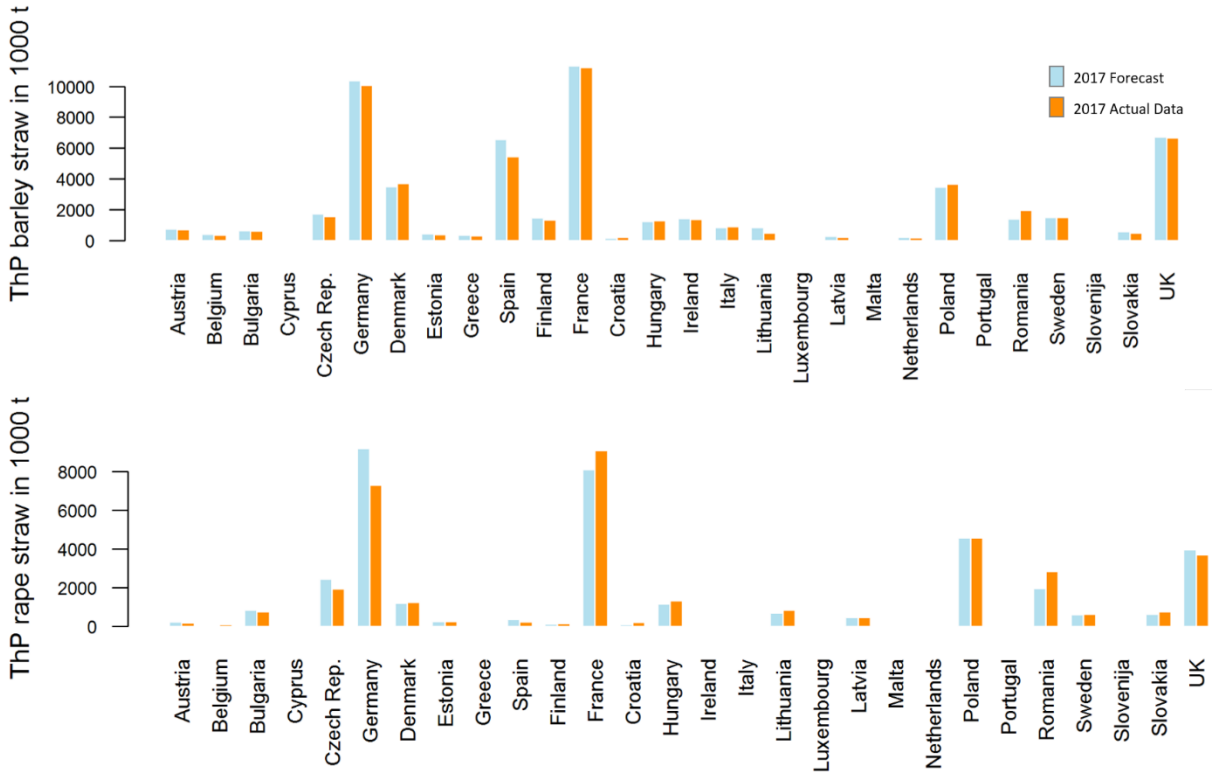

Fig. 24: Comparison of the 2017 forecast and actual data
of the theoretical potential of barley straw and rapeseed straw

On EU28 aggregation, the out-of-sample test reveals robust forecasting results as regional anomalies are compensated. At the regional level, larger deviations between the forecast and actual production were observed. These deviations are mainly driven by annual weather events that strongly influence crop yields (Lesk et al., 2016). Weather events appeal from very small- to large-scale, whereby they are not confined

to a given political region or a country. In 2003, almost the whole EU faced extremely unfavorable weather conditions with heatwaves and droughts in many regions leading to a severe drop in agricultural productivity (Ciais et al., 2005). Likewise, precipitation can strongly impact grain volumes, as seen in 2016 in Northern France. Wheat and corn grain production collapsed by about 35 % due to extreme precipitation during the growth phase (Agrifrance, 2017). However, extreme weather events do not show long-term effects on crops, and production returns to normal the year after the event (Lesk et al., 2016).

Annual regional variations due to weather are difficult to anticipate. The more spatially detailed forecasts are, the stronger impacts of such events are. The latest report by the Intergovernmental Panel on Climate Change (IPCC) leaves little doubt for an accumulation of climate anomalies in the coming years. Events with negative effects on crop yields like heatwaves, droughts, or extreme precipitation during the growth phase are likely to occur more frequently and intensely (IPCC, 2014). Lesk et al. (2016) point out that the intensified agriculture of high-income countries with yield-maximizing strategies is more susceptible to extreme weather events than less developed regions that use risk-minimizing strategies. That supports the inference that future weather anomalies could strongly impact annual regional residue potentials, especially in high-income countries.

Lignocellulose materials from agricultural harvesting residues are expected to become an important renewable resource for materials and biofuel of the post-petrol era. Many issues still have to be addressed before lignocellulose can be applied on a large scale. On the one hand, technical issues like the resistant nature of lignocellulose or the large variety of sugars derived from hemicellulose and cellulose have to be addressed (Balat, 2011). On the other hand, economic questions have to be answered. Currently, neither a transparent market nor a transparent price for agricultural harvesting residues exists in the EU. The question about sustainably available feedstock potentials is also still an object of discussion (Hennig et al., 2016). This work contributes to a future perspective on the available potentials in the EU. Before investments in large-scale biorefineries occur, decision-makers from politics and business need to know where to expect the largest and most stable feedstock supply. The variety of feasible lignocellulose materials is much broader and covers, for example, grasses like miscanthus, pruning residues, forest thinning residues, and others. The introduced methodology can also be applied to a broader range of resources by adapting the assessed feedstock.

As the out-of-sample test shows, the 2017 forecast of the theoretical potential of agricultural residues proved to be adequate at the EU28 level. However, annual fluctuations on regional level are difficult to address. Future studies may focus on determining the impacts of weather events on agricultural production, respectively, on

agricultural residue potentials. For example, simulated future daily weather data derived from climate change scenarios could be considered. Duveiller et al. (2017), for example, recently published simulated near (2020) and medium-term (2030) daily weather data that is ready to be applied to crop modeling studies. This work broadens the knowledge about feedstock potentials from agricultural residue potentials available for the transition towards a bioeconomy. As biomass supply chains seem to be more effective on a regional scale, this work aims to predict potentials on a regional basis.

5 Environmental benefits of large-scale second-generation bioethanol production

Chapter five develops a multi-criteria optimization model that integrates supply chain network optimization and Life Cycle Assessment to assess the environmental and economic benefits of a bioeconomic value chain that substitutes conventional products. The model is applied to the value chain for second-generation bioethanol production and takes decisions on the substitution of petrol and first-generation bioethanol.

The promotion of pilot-scale technologies to industrial-scale has characterized the field of second-generation bioproducts in recent years. After decades of research and repeated setbacks, lignocellulosic bioethanol is on the verge of commercialization (Hauschild et al., 2018; Clariant, 2020). Successful large-scale production of second-generation bioethanol as a substitute for liquid fuels and base chemicals haseco the potential to reduce environmental pressure significantly (Morales et al., 2015). Several studies investigate economic, environmental, or social aspects of lignocellulose biorefineries. However, these dimensions have mostly been assessed independently (Cherubini and Strømman, 2011; Morales et al., 2015; Patel et al., 2016). Existing studies can be clustered into techno-economic evaluations (Hamelinck et al., 2005; Lauven et al., 2018), life cycle assessments (LCA) to compare different production pathways (Bright and Strømman, 2009; Watanabe et al., 2016), LCAs to compare the environmental performance of different feedstocks (Kim and Dale, 2005; Muñoz et al., 2014), and network optimization models (Dunnett et al., 2008; Leduc et al., 2010).

In existing multi-dimensional approaches in the field of advanced biofuels, environmental considerations are often limited to greenhouse gas (GHG) emissions (Zamboni et al., 2009; You et al., 2012; Budzinski et al., 2019) or are represented by an aggregated score like the eco-indicator 99 (Santibañez-Aguilar et al., 2014; Babazadeh et al., 2017). Although climate change is considered one of the most urgent global challenges, the limitation to global warming bears the risk of neglecting other environmental impacts (Cherubini and Ulgiati, 2010; Hauschild et al., 2018). The politically intended implementation of first-generation biofuels in the EU showed the complex interconnection in the "food, energy, and environment trilemma" (Lewandowski, 2015, p. 37) and the problem of fixation to the single goal *climate change mitigation*. LCAs that cover a wide range of impact and damage categories do not allow a clear statement about the advantageousness of bio-products compared to their conventional counterparts (Borrion et al., 2012), especially in categories such as *eutrophication*, *stratospheric ozone depletion*, *acidification*, and *human* and *terrestrial*

toxicity. In order to avoid problem shifting, it is essential to include all relevant impact categories in decision-making processes (Hauschild, Rosenbaum, et al., 2018). Environmental "single scores" might address societal interests better than a single impact category. However, these scores lack the necessarytransparency without full data documentation and intermediate results (Goedkoop and Spriensma, 2001; Rosenbaum et al., 2018). Understanding competing for economic, environmental, and social aspects in regional biomass provision is the central aspect in optimizing bioeconomic value chains (Lewandowski, 2015).

Agricultural residues as feedstock for biorefineries neither compete directly with food production nor indirectly through land competition, thus avoiding the "food and energy" dilemma. Other studies have shown the environmental advantageousness of agricultural residues compared to feedstocks cultivated particularly for energy use (Muñoz et al., 2014; Morales et al., 2015). For the production of fuels and base chemicals, these considerations render agricultural residues superior to other feedstock and fuels. Nevertheless, the utilization of agricultural residues entails environmental impacts that need to be addressed. The low density and economic value of lignocellulose render feedstock transportation challenging in planning production networks. In contrast to large fossil refineries, the disproportionately increasing feedstock transportation cost for large biorefineries may overcompensate economies of scale of refineries, which is why biorefinery production networks tend to be more decentralized with smaller individual refineries (Lauven, 2014). Most existing approaches are based on process analysis with fixed parameters. However, especially in the bioeconomy, environmental repercussions are particularly dependent on regional characteristics of the value chain, such as feedstock availability (Budzinski et al., 2019).

The specific challenges in the assessment of biofuels require models capable of weighing economic and environmental criteria against each other and, at the same time, take regional value chain aspects into account. Decisions have to be made as to whether feedstock is sourced from a certain region, whether biorefineries have to be built and with which capacity, and whether it is worthwhile to transport the final product to sales markets; an echelon of decisions for which multi-objective mixed-integer linear programming is a proven tool in Operations Research (Govindan et al., 2015). This work develops a multi-objective production network optimization model, where second-generation bioethanol is produced to substitute first-generation bioethanol and fossil petrol in the European Union. The environmental dimension is addressed by optimizing a broad range of impact and damage categories, considering regionalized life cycle inventories of different steps in the value chains. The consideration of endpoints and midpoints alike and the regionalization of environmental aspects is novel in the field of strategic network design (Messmann et al., 2019). Economically, the price of fossil fuels does not represent the accruing societal cost of fossil fuels (World Bank, 2019), and

advanced biofuels still lack competitiveness vis-à-vis conventional fuels. However, if profitability increases, advanced biofuels like ethanol could be an important element in tackling greenhouse gas reduction targets and other environmental problems related to fossil fuel consumption (Giuntoli, 2018). Therefore, the economic dimension is addressed by profit maximization, considering different excise and carbon tax scenarios, which reflect possible policy instruments to support alternative fuels. This work contributes to existing literature on advanced biofuels by the application region (European Union), by the distinction between substitution of petrol and first-generation ethanol, by the large number of environmental objectives and economic scenarios, and the model's regionalized character. This broad spectrum of perspectives allows deriving insights into the various environmental and economic consequences of different advanced biofuel strategies, which could interest European policy-makers and companies. Chapter 5 sets out to answer the following main research question:

> **RQ 3: How needs a multi-criteria optimization model for the strategic planning of bio-based value chains be designed to integrate economic and environmental objectives?**

Since the network design and economic and environmental properties are highly case-specific, this chapter uses second-generation bioethanol as a case study. Therefore, the main research question is further divided into the following sub-research questions:

- *Q1*: What are the benefits of optimal second-generation ethanol production network configurations to substitute petrol and first-generation ethanol, considering different environmental and economic aspects?
- *Q2*: Which environmental objectives are congruent, and which are conflicting considering LCIA mid- and endpoints?
- *Q3*: Which taxation scenario supports the scale-up of a second-generation ethanol production network in the European Union?

The methods section introduces key parts of the optimization model and the life cycle assessment. The results section shows the optimal design of large-scale bioethanol production in the EU, based on economic and different environmental objectives, as well as Pareto-efficient trade-offs between different objective functions. In the last section, we discuss the implications of the results for policy-makers, the benefits of the applied methodology, and limitations in the tangibility of the results.

5.1 Methods

This section includes a detailed description of the considered value chain for the production of second-generation bioethanol, the assumptions made regarding feedstock supply and bioethanol demand, as well as brief presentations of the LCA carried out for the parameterization of the optimization model, the experiment design, and the multi-objective optimization model.

5.1.1 Value Chain

The value chain includes (1) feedstock cultivation and harvesting, (2) feedstock sourcing, (3) the bioethanol production process, (4) ethanol distribution to demand regions, where (5) second-generation bioethanol (2G EtOH) substitutes fossil petrol or first-generation bioethanol (1G EtOH) (see Fig. 25). To obtain meaningful results at the regional level, a high level of regional disaggregation is desirable.Since the complexity of the model increases disproportionately with regional granularity, the 98 NUTS-1 regions of the EU, which correspond to the major socio-economic areas, are used as spatial resolution. Every region represents a potential supply, production, and demand region. In the first step of the value chain, the harvested agricultural residues are baled to facilitate storage and transportation. At the biorefinery, the feedstock is converted in several process steps to bioethanol and the by-products electricity and biomethane.

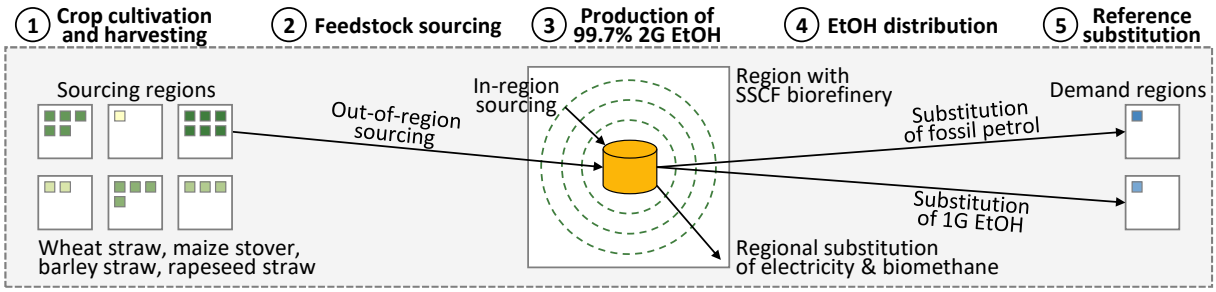

Fig. 25: Simplified illustration of the value chain structure

The bioethanol production process is state-of-the-art and can be described as steam explosion pre-treatment and simultaneous saccharification and co-fermentation (SSCF) with integrated enzyme production (Appendix B.1). Pre-treatment includes mechanical shredding and (acid-free) hydrothermal cracking to separate cellulose and hemicellulose from lignin (Gupta and Verma, 2015). An enzyme mixture produced in an integrated production step hydrolyzes cellulose and hemicellulose chains into sugar monomers (hexoses and pentoses). The hexose and pentose are fermented to ethanol and finally distilled to purified ethanol (>99%) by micro-sieves during fermentation. Separated lignin is used to generate electricity and process heat by cogeneration, and excess

electricity is fed into the regional grid. The distillation residue stillage is valorized to biomethane via anaerobic digestion. Distribution of purified ethanol to the regional markets and substitution are the last considered operation.

5.1.2 Feedstock availability and bioethanol demand

Lignocellulose typically consists of 30% to 45% cellulose, 15% to 30% hemicellulose, and 15% to 30% lignin, therefore, all lignocellulose biomass can generally be used for bioethanol production (Balat, 2011). A high degree of flexibility concerning the feedstock is desirable for a biorefinery, however, especially pre-treatment needs a certain focus on a biomass class (Taherzadeh and Karimi, 2008; Gupta and Verma, 2015). This work focuses on the main agricultural crop residues (in terms of volume) in the EU, wheat straw, maize stover, barley straw, and rapeseed straw. Estimates on the theoretical energy content of agricultural residues in the EU range from 3,673–6,389 PJ (Scarlat et al., 2019), of which only certain shares are available. The bioeconomic potential considers a large array of accessibility limitations, such as technical limitations, sustainable removal rates to sustain soil organic carbon and privileged local biomass demands by applications such as animal bedding. It therefore can be considered a conservative scenario. Data on the *bioeconomic potential* primarily comes from the results of chapter 4, with 2018 as a reference. Where necessary, the database is amended by data from the S2BIOM project, which assume slightly higher potentials (Dees et al., 2016).

Fig. 26 shows the absolute bioeconomic potential in 2018 for the four considered feedstocks, with wheat straw being the most widespread across EU regions. Maize stover potentials are found in the southern temperate and northern subtropical zones. Barley and rapeseed straw potentials are almost exclusively found in the temperate zone.

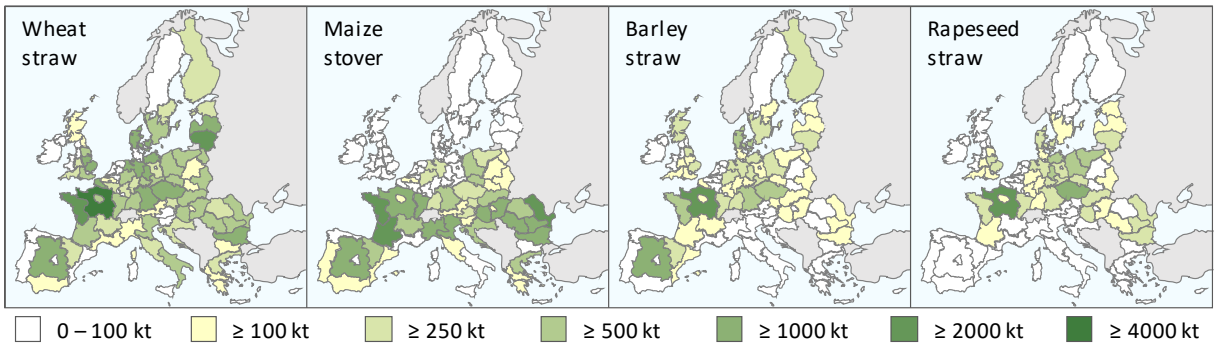

Fig. 26: Bioeconomic feedstock availability on NUTS-1 level in 2018
of wheat straw, maize stover, barley straw, and rapeseed straw in metric kilotonnes (based on results of chapter 4). Feedstock potentials and demands are zeroed for the four overseas regions (ES7, FR9, PT2, PT3) among the 98 NUTS-1 regions. Underlying data used of this figure can be found in the Data Repository D.2

Second-generation bioethanol can substitute fuels in the transportation sector (both fossil petrol and first-generation bioethanol) and industrial ethanol in the chemical sector. As a fuel, 2G EtOH can substitute petrol either entirely (E100) in specifically designed spark-ignition engines or partly in a blend, which is currently the common practice (Thangavelu et al., 2016). In 2018, the fuel ethanol consumption of the transportation sector in the EU was 4.33 Mt (million metric tonnes) and 0.47 Mt in the industrial sector, which was covered almost entirely by first-generation sources (ePure, 2018). The consumption of petrol amounts to 75 Mt in 2018, equivalent to about 120 Mt of EtOH (Eurostat, 2019c). While substitution between 1G and 2G EtOH is possible without technical adjustments, the use of E100 in vehicles would require engine adjustments, the implications of which are not considered in the scope of this work.

5.1.3 Life Cycle Assessment

The main objective of the model is the maximization of environmental benefits in the EU by upscaling second-generation ethanol production and the respective substitution of petrol and first-generation bioethanol. The assessment of environmental benefits is carried out based on Life Cycle Assessment. The Life Cycle Inventory (LCI), i.e., the inputs and emissions associated with the environmental parameters, is modeled in SimaPro 9, assessing the ecoinvent database Version 3.5 (Wernet et al., 2016). The Life Cycle Impact Assessment (LCIA), i.e., the characterization of the inventory in terms of impact and damage categories, is carried out using ReCiPe 2016 (H) v1.1 (Huijbregts et al., 2017). This section provides a brief overview of the assumptions taken for the LCA (assumptions in Appendix B.3, LCI in Data Repository D.2).

The system boundary of the work at hand is depicted in Fig. 27 and can be described as cradle-to-tank. It includes feedstock cultivation and transportation, production, and final distribution to the demand region. The functional unit of the model is the **producible volume of second-generation bioethanol per year** (in metric tonnes, the references are adjusted by energy equivalence) in the resulting production network. The model optimizes the substitution of the **same function** (i.e., the same energy) of the two reference products, petrol and first-generation bioethanol. To facilitate a fair comparison between fossil-based and bio-based fuels, biogenic carbon stored in the bio-based fuel is modeled negatively in the carbon balance (Appendix B.3).

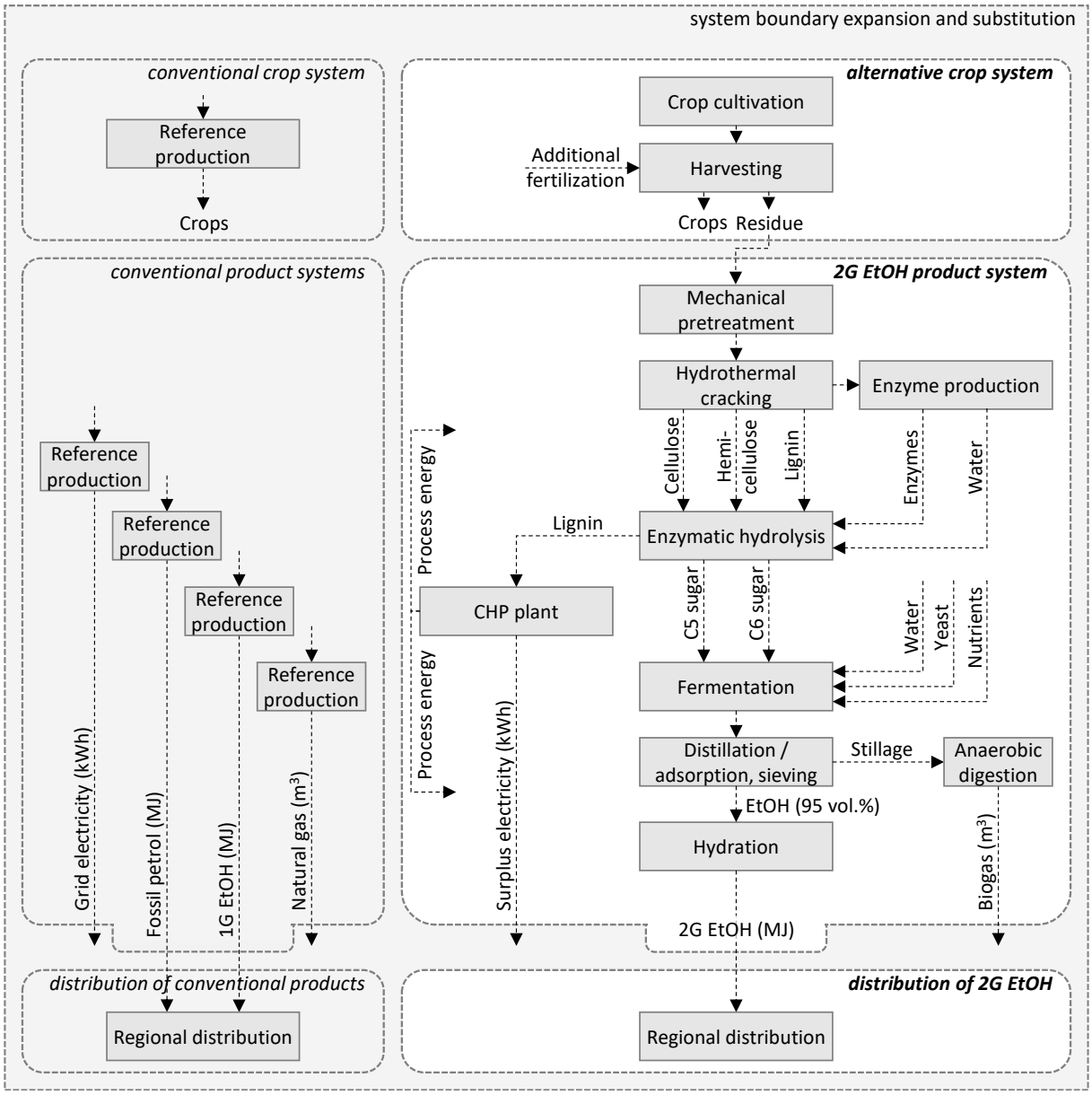

Fig. 27: System boundaries and simplified flow diagram

The environmental dimension comprises the 18 midpoints and three endpoints of the LCIA method ReCiPe 2016. Midpoints describe environmental impacts, which can optionally be normalized and aggregated towards endpoints. Endpoints provide information on the damages to the respective areas of protection and can thus be considered more meaningful to the society in decision-making processes. A short description of the considered midpoints and endpoints, their units, and midpoint-to-endpoint aggregation are provided in Table B 5. By providing both midpoints and endpoints, the consequences of decisions become visible and support the interpretation of results (Rosenbaum et al., 2018). The *environmental benefits* of the production network are assessed by system boundary expansion and substitution (see Fig. 27). The feedstock system and the biorefinery process are multi-functional processes, which

requires an allocation of their environmental implications. The conventional counterpart needs to be selected carefully, as it is a critical step in the system boundary expansion and substitution approach (Heijungs and Guinée, 2007). We assume the complete incorporation of straw into the soil for the conventional agricultural system. In the alternative system, additional N-P-K fertilization is assumed to compensate for the nutrient loss through straw evacuation, based on Cherubini and Ulgiati (2010). The co-products biomethane and electricity are expected to be fed into the regional gas and electricity grids, respectively, substituting natural gas and the regional electricity mix (referring to the same function). For the multiple biorefinery outputs, this approach assumes a direct substitution of reference products currently on the market with a given environmental burden, wherefore this model can be considered consequential LCA (Majeau-Bettez et al., 2018). Equation (20) illustrates that the total environmental benefit calculates as the difference between avoided burdens of all products and the total production impacts.

$$environmental\ benefit^{LCIA} = \sum_{product} avoided\ burden^{LCIA}_{product} - production\ impact^{LCIA} \qquad (20)$$

Where possible, environmental impacts are regionalized in their inventory to account for regional characteristics (e.g., electricity mix or water use).

5.1.4 Multi-objective model and experiment design

Table 12 lists the key elements of the optimization model with the indices, the decision variables, the generic formulation of the objective functions, and the considered scenarios. The complete mathematical formulation with all parameters, objective functions, and constraints is provided in the following sections. The first set of decisions represents the choice of locations and capacity levels of biorefineries. The capacity-dependent investment cost and impacts of biorefinery construction are nonlinear, scale-dependent parameters. Biorefineries can be supplied with the four feedstock types, wheat straw, maize stover, barley straw, and rapeseed straw, converted to the main product 2G EtOH, and the two by-products electric energy and biogas. Feedstock can either be sourced from another region or transported to a refinery region. Alternatively, it can be sourced within the same region of the biorefinery. In the latter case, larger plant capacities require larger sourcing areas, which leads to nonlinear transportation costs (Wright and Brown, 2007; Lauven et al., 2018). The produced 2G EtOH is then shipped from refineries and substitutes either 1G EtOH or fossil petrol demand. The transport of both feedstock and EtOH can be carried out with different transportation modes. The optimization model is implemented as a multi-objective mixed-integer linear program (MILP) and either maximize the profit ($\max O^{econ}$), or one of 21 LCIA midpoints and endpoints ($\max O_l^{env}, \forall\, l \in L$). The originally nonlinear scale-dependent

parameters (capacity-dependent investment costs and impacts, and sourcing costs and impacts) are stepwise linearized.

As part of the economic assessment, this work examines in five scenarios which taxation policy can promote the role-out of large-scale 2G EtOH production (Table 12). Tax scenario T1 represents the current taxation for petrol and bioethanol, where excise tax abatements exist in some countries, while others raise taxes for all three considered products equally (European Commission, 2020). Tax scenarios T2 and T3 assume a uniform excise tax abatement of 50% and 100% respectively in every country. Scenarios T4 and T5 assume additional carbon taxes of €50 (moderate taxation) and €375 (high taxation) respectively per emitted metric ton of CO_2 eq. T4 corresponds to the minimum price needed in 2020 to be consistent with achieving the temperature target of the Paris agreement of "well below 2°C" (World Bank, 2019). T5 is based on Ricke et al. (2018), who estimated the median social cost of carbon emission at about €375. Tax scenarios T2-T5 improve the competitiveness of second-generation bioethanol compared to petrol. The carbon taxation of scenarios T4 and T5 additionally increases transport costs.

A multi-dimensional consideration follows the single-objective optimization based on the equidistant ε-constraint method with a calculation of Pareto-optimal frontiers. As described in chapter 2.4, this method allows the simultaneous consideration of different objectives to gain insights into their interrelationships. Between the economic and an environmental categories, the Pareto-optimal frontier presents marginal economic costs to achieve environmental benefits transparently. The environmental dimension is characterized by a plethora of impacts with complex cause-effect chains, which makes it particularly important to point out trade-offs between the different conflicting environmental objectives.

The MILP model is implemented in IBM ILOG CPLEX Optimization Studio 12.8.0.0. The optimization is carried out on an Intel® Core™ i7-2600 CPU with four physical cores at 3.40 GHz and 32 GB RAM, and an Intel® Xeon® CPU E5-2690 with eight cores at 2.90 GHz and 64 GB RAM. The set MIP gap tolerance is 10^{-6} for single-objective optimization (exception: economic T5 runs out of memory at around 10^{-2}). For epsilon-constraint optimization, the gap can be higher to ensure solvability on the used systems.

Table 12: Formal model description
with indices, decision variables, verbal descriptions of objective functions, and scenario definitions

Indices		
Indices	Definition	Description
$R = \{1 \dots 98\}$	regions	NUTS-1 level regions in 28 EU member states
$C = \{1 \dots 37\}$	capacity levels	25,000, ..., 3,000,000 metric tonnes (output)
$F = \{1 \dots 4\}$	feedstock	wheat straw, maize stover, barley straw, rapeseed straw
$P = \{1 \dots 2\}$	by-products	surplus energy, biomethane
$M = \{1 \dots 100\}$	sourcing annulus	5 km, ..., 500 km
$T = \{1 \dots 3\}$	transport modes	farm tractor, truck, rail
$L = \{1 \dots 21\}$	LCIA categories	ReCiPe 2016 endpoints (E1-3) and midpoints (M1-18), Table B 5
Decision variables		
Variable	Domain	Definition
$B_{r,c}$	$\in \{0,1\}$	construction of a biorefinery in region $r \in R$ with capacity level $c \in C$
$F^{in}_{r,m,f,t}$	$\in \mathbb{Q}_0^+$	transported amount of feedstock $f \in F$ within region $r \in R$ from sourcing sector $m \in M$ to biorefinery with transport mode $t \in T$
$F^{out}_{r,s,f,t}$	$\in \mathbb{Q}_0^+$	transported amount of feedstock $f \in F$ from region $r \in R$ to biorefinery in region $s \in R$ with transport mode $t \in T$
$P^{1G}_{r,s,t}$	$\in \mathbb{Q}_0^+$	transported amount of 2G bioethanol from biorefinery in region $r \in R$ to demand in region $s \in R$ with mode $t \in T$, substituting 1G bioethanol
$P^{FF}_{r,s,t}$	$\in \mathbb{Q}_0^+$	transported amount of 2G bioethanol from biorefinery in region $r \in R$ to demand in region $s \in R$ with mode $t \in T$, substituting petrol (fossil fuel, FF)
Objective functions		
Economic objective: $\max O^{econ}$		Environmental objectives: $\max O^{env}_l, \forall\, l \in L$
$= revenues\ (substituted\ 1G\ EtOH)$		$= benefits\ (substituted\ 1G\ EtOH)$
$+ revenues\ (substituted\ fossil\ fuel)$		$+ benefits\ (substituted\ fossil\ fuel)$
$+ revenues\ (substituted\ by\text{-}products)$		$+ benefits\ (substituted\ by\text{-}products)$
$- refinery\ costs\ installation$		$+ benefits\ (carbon\ storage)$
$- refinery\ costs\ personnel\ \&\ others$		$- refinery\ impacts\ installation$
$- refinery\ costs\ processes$		$- refinery\ impacts\ processes$
$- feedstock\ costs$		$- feedstock\ impacts$
$- collection\ costs\ fixed$		$- collection\ impacts\ fixed$
$- collection\ costs\ variable$		$- collection\ impacts\ variable$
$- distribution\ costs\ fixed$		$- distribution\ impacts\ fixed$
$- distribution\ costs\ variable$		$- distribution\ impacts\ variable$
Scenarios		
Scenario	Verbal definition	Manipulated parameters
Tax scenario T1	Current tax situation per country	α^{FF}_r
Tax scenario T2	Half (50%) excise tax abatement in every country	α^{FF}_r
Tax scenario T3	Full (100%) excise tax abatement in every country	α^{FF}_r
Tax scenario T4	Carbon tax of €50 per metric ton of CO_2 eq.	$\alpha^{FF}_r, \varepsilon^{var}_t, \eta^{var}_t$
Tax scenario T5	Carbon tax of €375 per metric ton of CO_2 eq.	$\alpha^{FF}_r, \varepsilon^{var}_t, \eta^{var}_t$
Feedstock sc. 2018	Feedstock potential as determined for 2018 (chapter 4)	$\psi_{r,f}$, $\mu_{r,f}$
Feedstock sc. 2030	Feedstock potential as forecasted for 2030 (chapter 4)	$\psi_{r,f}$, $\mu_{r,f}$

Linearization of transport costs

With increasing capacities, biorefineries require a larger catchment area around the biorefinery. The catchment area of a biorefinery is modeled as a circle with the assumption of evenly distributed feedstock within a region. The amount of collectible

feedstock grows with the square of the radius. $\psi_{r,f}$ (in metric tons) is the total regional feedstock potential, $\mu_{r,f}$ (in $\frac{t}{km^2}$) is the specific feedstock potential of feedstock $f \in F$ in region $r \in R$, A_r is the area of the region r and ρ_r is the radius of the region (based on the assumption that the region is a circle):

$$\mu_{r,f} = \frac{\psi_{r,f}}{A_r} \tag{21}$$

$$\psi_{r,f} = A_r \times \mu_{r,f} = \pi \times \rho^2 \times \mu_{r,f} \tag{22}$$

If the whole feedstock of a region were sourced, the average sourcing distance would be:

$$average\ sourcing\ distance_{r,f}^{circle} = \sqrt{\frac{\psi_{r,f}}{\pi\ \mu_{r,f}}} \times \upsilon \times \tau_r \tag{23}$$

Where τ_r is the regional tortuosity factor based on the regional road network, and $\upsilon = \frac{2}{3}$ corresponds to the geometric factor for the average distance from the center of a circle to each area point within the circle. Eq. (24) depicts this geometric relationship (in Eq. (24) R and r correspond to *radius*):

$$\frac{\int dA\ r}{\int dA} = \frac{\int_0^R dr\ r \int_0^{2\pi} d\varphi\ r}{\int_0^R dr\ r \int_0^{2\pi} d\varphi\ 1} = \frac{2\pi \int_0^R dr\ r^2}{2\pi \int_0^R dr\ r} = \frac{2}{3}R \tag{24}$$

To calculate the transport costs, the *average sourcing distance* is multiplied by the amount of collected feedstock (decision variable $F_{r,m,f,t}^{in}$), the variable transport cost ε_t^{var} and factor 2 to account for pendulum tours. Equation (25) shows that this relation results in nonlinear transport costs with degressive specific transportation costs and progressive total collection costs (Wright and Brown, 2007; Lauven et al., 2018). The parameter must be linearized since nonlinear parameters and functions cannot be applied in a linear program. Therefore, the term is linearized stepwise in annuli of the same width ρ. Index $m \in M$ is introduced to count the annuli. The total transport costs are calculated as the sum over all annuli of which feedstock is sourced (26).

$$transport\ cost_{r,f,t} = \sqrt{\frac{F_{r,f,t}^{in}}{\pi\ \mu_{r,f}}} \times \upsilon \times \tau_r \times F_{r,f,t}^{in} \times \varepsilon_t^{var} \times 2 \tag{25}$$

$$transport\ cost_{r,f,t} = \sum_{m \in M} \upsilon_m \times \rho \times \tau_r \times F_{r,m,f,t}^{in} \times \varepsilon_t^{var} \times 2 \tag{26}$$

Fig. 28 exemplifies the stepwise linearization of the transport cost. Transportation distances are assumed to be fixed for feedstock sourcing within each "sourcing annulus". The incremental annulus width ρ allows the adjustment of the granularity of the linearization; the smaller the width, the more accurately the actual course is

approximated. However, with decreasing width, the calculation time of the model increases significantly, which is why in this work, a compromise solution with a step-width of 5 km was chosen after several experiments. The index $m \in M$ counts the annuli and υ_m represents the geometric factor for the average distance between the center and the annulus m (in Eq. (27) r corresponds to *radius*):

$$\upsilon_m = \frac{2\pi \int_{(m-1)\rho}^{m\rho} dr\, r^2}{2\pi \int_{(m-1)\rho}^{m\rho} dr\, r} = \frac{2}{3}\frac{3m^2 - 3m + 1}{2m - 1} \tag{27}$$

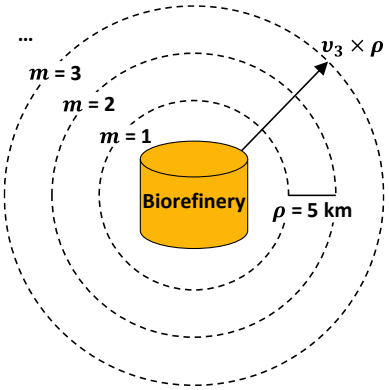

Fig. 28: Stepwise linearization of transport cost

The feedstock supply per annulus is limited, which requires one additional constraint. Equation (28) shows the relation between the radius of the whole region, the annulus width ρ, and the maximum number of annuli n. This equation is solved for ψ.

$$\sqrt{\frac{\psi_{r,n,f}}{\pi\, \mu_{r,f}}} = n \times \rho \tag{28}$$

$$\psi_{r,n,f} = \rho^2 n^2\, \pi\, \mu_{r,f} \tag{29}$$

The $\mathit{amount\ per\ annulus}_{r,m,f}$ for each region, sourcing annuli m and feedstock f can then be calculated by simply computing the total amount of feedstock available to annuli m minus the total amount of feedstock available to annuli m-1 (Eq. (30).

$$\mathit{amount\ per\ annulus}_{r,m,f} = \rho^2 m^2 \pi\, \mu_{r,f} - \rho^2 (m-1)^2 \pi \mu_{r,f} = \pi\, \rho^2\, \mu_{r,f}\, (2m-1) \tag{30}$$

In the next step, this relation is transformed into a constraint (Eq. (31), applied in the model. The sum over all transport modi $t \in T$ for decision variable $F^{in}_{r,m,f,t}$ must be smaller than the available feedstock in each annulus (see Table 15).

$$\sum_t F^{in}_{r,m,f,t} \leq \pi\, \rho^2\, \mu_{r,f}\, (2m-1) \qquad \forall\, r \in R, m \in M, f \in F \tag{31}$$

Linearization of capacity dependent parameter

Due to economies of scale, we assume nonlinearly decreasing marginal investment costs and environmental impacts with increasing biorefinery capacity. Towler and Sinnott (2013) give a range for the scale parameter λ in chemical plants from 0.7 to 0.9. As

cellulose ethanol production requires physical pre-treatment, this work uses 0.8 as scale parameter for the construction-based investment costs and environmental impacts. We use the same scale parameter for environmental impacts, as we assume scale effects due to a more efficient use of construction resources.

$$Investment\ costs_c = \left(\frac{capacity_c}{capacity_0}\right)^{\lambda} \times Investment\ costs_0 \quad (32)$$

Discrete capacity steps $c \in C$ are introduced, based on the relation shown in Eq. (32). Similar to the transportation costs, the step-width of capacity levels C strongly affect the model run time. To adequately address the model run time and model precision trade-off, the step-width is 25,000 t for small capacities (25,000 to 300,000 t), 50,000 t for medium capacities (300,000 t to 1,000,000 t), 100,000 t for high capacities (1,000,000 to 1,500,000 t), and 250,000 t to account for outliers of maximum optimal capacity (1,500,000 to 3,000,000 t). The smallest capacity level matches the capacity of a pilot plant (Clariant, 2021b), the maximum capacity of 3 Mt is twice the optimal biorefinery capacity found by other studies (Lauven et al., 2018).

Set of parameter

Table 13 provides the nomenclature, the unit, and a brief description of all general, economic and environmental data and parameters of the model. The background of the general data and parameters, the underlying assumptions, calculations, and references can be found in Annex B.1, and values for these parameters are given in the Data Repository D.2. The background of the economic parameters, the underlying assumptions, calculations, and references can be found Annex B.2 and values for these parameters are given in the Data Repository D.2. Furthermore, the table provides the nomenclature of the 21 environmental categories and a brief description of the environmental parameters of the model. The background of the environmental parameters, the underlying assumptions, calculations, and references can be found Annex B.3, and values for the environmental parameters and the Life Cycle Inventory are given in the Data Repository D.2. The Life Cycle Inventory (LCI), i.e., the inputs and emissions associated with the environmental parameters, is modeled in SimaPro 9, assessing the ecoinvent database version 3.5 (Wernet et al., 2016). The procedure "allocation at the point of substitution" (APOS) is chosen for the impact allocation. The Life Cycle Impact Assessment (LCIA), i.e., the characterization of the life cycle inventory in terms of impact and damage categories, is carried out using ReCiPe 2016 (H) v1.1 (Huijbregts et al., 2017).

Table 13: Set of general, economic, and environmental parameters

Parameter	Unit	Definition
General data and parameter		
$\delta_{r,s}$	km	distance between regions $r \in R$ and $s \in R$
ζ_r^{1G}	t	current demand for 1G bioethanol in region $r \in R$
ζ_r^{FF}	t EtOH eq.	current demand for petrol in region $r \in R$ expressed in metric tons EtOH equivalent
$\psi_{r,f}$	t	total available feedstock $f \in F$ in region $r \in R$
$\mu_{r,f}$	t / km^2	specific feedstock potential for feedstock $f \in F$ in region $r \in R$
θ_f	t EtOH / t	transformation factor from feedstock $f \in F$ to bioethanol
θ_p^{byp}	t / t EtOH	co-production factor from bioethanol to by-product $p \in P$
σ_c	t EtOH	capacity of a biorefinery with capacity level $c \in C$
τ_r		regional road network tortuosity factor of region $r \in R$
ρ	km	width of sourcing annuli
υ_m		geometric factor for the average distance between the center and annulus $m \in M$
Economic parameter$^+$		
α_r^{1G}	€ / t	competitive revenues of 2G EtOH in region $r \in R$ for substitution of 1G EtOH
α_r^{FF}	€ / t	competitive revenues of 2G EtOH in region $r \in R$ for substitution of fossil petrol
$\alpha_{r,p}^{byp}$	€ / t	revenues of by-products $p \in P$ in region $r \in R$ when substituting references
κ_c^{depr}	€ / BR	annual costs (depreciated) of installing a biorefinery with capacity level $c \in C$
κ_c^{pers}	€ / BR	annual costs for personnel of a biorefinery with capacity level $c \in C$
κ_c^{oper}	€ / BR	annual fix costs of operating a biorefinery with capacity level $c \in C$
κ^{var}	€ / t	variable costs of refining bioethanol at a biorefinery
$\varphi_{r,f}$	€ / t	costs of feedstock $f \in F$ at farms in region $r \in R$
ε_t^{fix}	€ / t	fixed costs of transporting feedstock with transport mode $t \in T$
ε_t^{var}	€ / tkm	variable costs of transporting feedstock with transport mode $t \in T$
η_t^{fix}	€ / t	fixed costs of transporting bioethanol with transport mode $t \in T$
η_t^{var}	€ / tkm	variable costs of transporting bioethanol with transport mode $t \in T$
γ_r^{inv}		investment cost factor in region $r \in R$
γ_r^{lab}		labor cost factor in region $r \in R$
γ_r^{tra}		transport cost factor in region $r \in R$
Environmental Parameter ($\forall\, l \in L$)*		
$\tilde{\alpha}_l^{1G}$	impact* / t	saved impact when substituting 1 metric ton of 1G bioethanol
$\tilde{\alpha}_l^{FF}$	impact* / t	saved impact when substituting 1 metric ton of fossil petrol
$\tilde{\alpha}_{l,r,p}^{byp}$	impact* / MJ; impact*/m^{3}gas	saved impact when substituting 1 MJ conventional electricity or 1 m^3 conventional gas by by-product $p \in P$ in region $r \in R$
$\widetilde{\omega}_l^{CO2}$	benefit* / t	benefit from CO_2 stored in 1 metric ton of 2G EtOH
$\widetilde{\omega}_l^{CH4}$	benefit* / t	benefit from CO_2 stored in CH_4 per metric ton of produced 2G EtOH
$\tilde{\kappa}_{l,c}^{depr}$	impact* / BR	annual impacts of installing a biorefinery with capacity level $c \in C$
$\tilde{\kappa}_l^{var}$	impact* / t	variable impacts of refining 1 metric ton of 2G bioethanol at a biorefinery
$\tilde{\varphi}_{l,f}$	impact* / t	impacts of 1 metric ton of feedstock $f \in F$ at farm (dry matter)
$\tilde{\varepsilon}_{l,t}^{fix}$	impact* / t	fixed impacts of transporting 1 metric ton of feedstock with transport mode $t \in T$
$\tilde{\varepsilon}_{l,t}^{var}$	impact* / tkm	variable impacts of transporting 1 metric ton feedstock with mode $t \in T$ over 1 km
$\tilde{\eta}_{l,t}^{fix}$	impact* / t	fixed impacts of transporting 1 metric ton of bioethanol with mode $t \in T$
$\tilde{\eta}_{l,t}^{var}$	impact* / tkm	variable impacts of transporting 1 metric ton of bioethanol 1 km with mode $t \in T$

[+] $\alpha_r^{FF}, \varepsilon_t^{var}, \eta_t^{var}$ vary depending on the tax scenario (see section 5.2.4)

*All environmental parameters exist for each of the 21 environmental categories, $\forall\, l \in L$, see Table B 5. The unit of the 'impact' depends on the category and parameter; for example, for global warming and the parameter $\tilde{\kappa}_l^{var}$, the unit is kg CO_2 eq. per ton of 2G bioethanol, and for human health, it is DALY per metric ton of 2G bioethanol.

Objective function and constraints

Table 14 provides the objective functions, the decision expressions, and the mathematical formulation of the expressions. The economic model is made upon 12 decision expressions, where three expressions represent the revenues that can be generated by selling second-generation bioethanol to substitute first-generation bioethanol or fossil petrol and selling excess electricity and biogas. Nine expressions represent costs related to activities required to generate the revenues.

Table 14: Objective functions and decision expressions

Function	Expression	Formulation
$\max O^{econ}$	$= revenues\ (1G)$	$= \sum_{r \in R} \sum_{s \in R} \sum_{t \in T} P_{r,s,t}^{1G}\ \alpha_s^{1G}$
	$+ revenues\ (FF)$	$+ \sum_{r \in R} \sum_{s \in R} \sum_{t \in T} P_{r,s,t}^{FF}\ \alpha_s^{FF}$
	$+ revenues\ (by-products)$	$+ \sum_{r \in R} \sum_{s \in R} \sum_{t \in T} \sum_{p \in P} \left(P_{r,s,t}^{1G} + P_{r,s,t}^{FF}\right) \alpha_{r,p}^{byp}\ \theta_p^{byp}$
	$- refinery\ costs\ installation$	$- \sum_{r \in R} \sum_{c \in C} B_{r,c}\ \kappa_c^{depr}\ \gamma_r^{inv}$
	$- refinery\ costs\ personnel$	$- \sum_{r \in R} \sum_{c \in C} B_{r,c}\ \kappa_c^{pers}\ \gamma_r^{lab}$
	$- refinery\ costs\ others$	$- \sum_{r \in R} \sum_{c \in C} B_{r,c}\ \kappa_c^{oper}$
	$- refinery\ costs\ process$	$- \sum_{r \in R} \sum_{s \in R} \sum_{t \in T} \left(P_{r,s,t}^{1G} + P_{r,s,t}^{FF}\right) \kappa^{var}$
	$- feedstock\ costs$	$- (\sum_{r \in R} \sum_{m \in M} \sum_{f \in F} \sum_{t \in T} F_{r,m,f,t}^{in}\ \varphi_{r,f}\ + \sum_{r \in R} \sum_{s \in R} \sum_{f \in F} \sum_{t \in T} F_{r,s,f,t}^{out}\ \varphi_{r,f})$
	$- collection\ costs\ fixed$	$- (\sum_{r \in R} \sum_{m \in M} \sum_{f \in F} \sum_{t \in T} F_{r,m,f,t}^{in}\ \varepsilon_t^{fix} + \sum_{r \in R} \sum_{s \in R} \sum_{f \in F} \sum_{t \in T} F_{r,s,f,t}^{out}\ \varepsilon_t^{fix})$
	$- collection\ costs\ variable$	$- (\sum_{r \in R} \sum_{m \in M} \sum_{f \in F} \sum_{t \in T} 2\ F_{r,m,f,t}^{in}\ \varepsilon_t^{var}\ \gamma_r^{tra}\ \upsilon_m\ \rho\ \tau_r + \sum_{r \in R} \sum_{s \in R} \sum_{f \in F} \sum_{t \in T} 2\ F_{r,s,f,t}^{out}\ \varepsilon_t^{var}\ \gamma_s^{tra}\ \delta_{r,s})$
	$- distribution\ costs\ fixed$	$- \sum_{r \in R} \sum_{s \in R} \sum_{t \in T} \left(P_{r,s,t}^{1G} + P_{r,s,t}^{FF}\right) \eta_t^{fix}$
	$- distribution\ costs\ variable$	$- \sum_{r \in R} \sum_{s \in R} \sum_{t \in T} 2 \left(P_{r,s,t}^{1G} + P_{r,s,t}^{FF}\right) \eta_t^{var}\ \delta_{r,s}$
$\max O_l^{env}$	$= benefit\ (1G)$	$= \sum_{r \in R} \sum_{s \in R} \sum_{t \in T} P_{r,s,t}^{1G}\ \tilde{\alpha}_l^{1G}$
	$+ benefit\ (FF)$	$+ \sum_{r \in R} \sum_{s \in R} \sum_{t \in T} P_{r,s,t}^{FF} \tilde{\alpha}_l^{FF}$
	$+ benefit\ (by-products)$	$+ \sum_{r \in R} \sum_{s \in R} \sum_{t \in T} \sum_{p \in P} \left(P_{r,s,t}^{1G} + P_{r,s,t}^{FF}\right) \tilde{\alpha}_{l,r,p}^{byp}\ \theta_p^{byp}$
	$+ benefit\ (carbon\ storage)$	$+ \sum_{r \in R} \sum_{s \in R} \sum_{t \in T} \left(P_{r,s,t}^{1G} + P_{r,s,t}^{FF}\right) (\widetilde{\omega}_l^{CO2} + \widetilde{\omega}_l^{CH4}\ \theta_2^{byp})$
	$- refinery\ impacts\ installation$	$- \sum_{r \in R} \sum_{c \in C} B_{r,c}\ \tilde{\kappa}_{l,c}^{depr}$
	$- refinery\ impacts\ process$	$- \sum_{r \in R} \sum_{s \in R} \sum_{t \in T} \left(P_{r,s,t}^{1G} + P_{r,s,t}^{FF}\right) \tilde{\kappa}_l^{var}$
	$- feedstock\ impacts$	$- (\sum_{r \in R} \sum_{m \in M} \sum_{f \in F} \sum_{t \in T} F_{r,m,f,t}^{in}\ \tilde{\varphi}_{l,r,f} + \sum_{r \in R} \sum_{s \in R} \sum_{f \in F} \sum_{t \in T} F_{r,s,f,t}^{out}\ \tilde{\varphi}_{l,r,f})$
	$- collection\ impacts\ fixed$	$- (\sum_{r \in R} \sum_{m \in M} \sum_{f \in F} \sum_{t \in T} F_{r,m,f,t}^{in}\ \tilde{\varepsilon}_{l,t}^{fix} + \sum_{r \in R} \sum_{s \in R} \sum_{f \in F} \sum_{t \in T} F_{r,s,f,t}^{out}\ \tilde{\varepsilon}_{l,t}^{fix})$
	$- collection\ impacts\ variable$	$- (\sum_{r \in R} \sum_{m \in M} \sum_{f \in F} \sum_{t \in T} 2\ F_{r,m,f,t}^{in}\ \tilde{\varepsilon}_{l,t}^{var}\ \upsilon_m\ \rho\ \tau_r + \sum_{r \in R} \sum_{s \in R} \sum_{f \in F} \sum_{t \in T} 2\ F_{r,s,f,t}^{out}\ \tilde{\varepsilon}_{l,t}^{var}\ \delta_{r,s})$
	$- distribution\ impacts\ fixed$	$- \sum_{r \in R} \sum_{s \in R} \sum_{t \in T} \left(P_{r,s,t}^{1G} + P_{r,s,t}^{FF}\right) \tilde{\eta}_{l,t}^{fix}$
	$- distribution\ impacts\ variable$	$- \sum_{r \in R} \sum_{s \in R} \sum_{t \in T}\ 2 \left(P_{r,s,t}^{1G} + P_{r,s,t}^{FF}\right) \tilde{\eta}_{l,t}^{var}\ \delta_{r,s}$
$\forall\ l \in L$		

The environmental model is made upon 11 decision expressions. Four expressions correspond to environmental benefits due to the substitution of first-generation bioethanol or fossil petrol by second-generation bioethanol and the substitution of the average regional electricity grid mix and natural gas by excess electricity and co-produced biogas. Seven expressions correspond to environmental impacts due to activities required to generate the environmental benefits. The environmental model comes up with two constraints less than the economic model since it is assumed that neither personnel nor other operational processes have environmental impacts.

Table 15 represents the nine constraints of the model. Constraint (1) is the flow preservation between the feedstock input (in- and out of region sourcing) and the product output. Constraint (2) ensures sufficient biorefinery capacity to produce the product output to substitute first-generation EtOH and fossil petrol. Constraint (3) guarantees that the limited feedstock amount per region is not exceeded. Constraint (4) limits the collectible feedstock per sourcing annuli. Constraints (5, 6) assure that the demand for liquid fuels per region cannot be exceeded. Constraint (7) ensures that the transport decision variable for out of region sourcing is zero within the same region. Constraint (8) assures that farm tractor cannot distribute bioethanol. Constraint (9) ensures only one BR per region.

Table 15: Constraints

	Constraint	
(1)	$\sum_{m\in M}\sum_{f\in F}\sum_{t\in T} F^{in}_{s,m,f,t}\,\theta_f + \sum_{r\in R}\sum_{f\in F}\sum_{t\in T} F^{out}_{r,s,f,t}\,\theta_f \geq \sum_{u\in R}\sum_{t\in T}\,(P^{1G}_{s,u,t} + P^{FF}_{s,u,t})$	$\forall\, s \in R$
(2)	$\sum_{s\in R}\sum_{t\in T}\,(P^{1G}_{r,s,t} + P^{FF}_{r,s,t}) \leq \sum_{c\in C} B_{r,c}\,\sigma_c$	$\forall\, r \in R$
(3)	$\sum_{m\in M}\sum_{t\in T} F^{in}_{r,m,f,t} + \sum_{s\in R}\sum_{t\in T} F^{out}_{r,s,f,t} \leq \psi_{r,f}$	$\forall\, r \in R, f \in F$
(4)	$\sum_{t\in T} F^{in}_{r,m,f,t} \leq \pi\,\rho^2\,\mu_{r,f}\,(2m-1)$	$\forall\, r \in R, m \in M, f \in F$
(5)	$\sum_{r\in R}\sum_{t\in T} P^{1G}_{r,s,t} \leq \zeta^{1G}_s$	$\forall\, s \in R$
(6)	$\sum_{r\in R}\sum_{t\in T} P^{FF}_{r,s,t} \leq \zeta^{FF}_s$	$\forall\, s \in R$
(7)	$F^{out}_{r,r,f,t} = 0$	$\forall\, r \in R, f \in F, t \in T$
(8)	$P^{1G}_{r,s,1} + P^{FF}_{r,s,1} = 0$	$\forall\, r \in R, s \in R$
(9)	$\sum_{c\in C} B_{r,c} \leq 1$	$\forall\, r \in R$

5.2 Results

The first subsection discusses the results of economic optimization and the second subsection discusses the environmental results with a focus on the relevance of, and congruencies, and conflicts between the 21 environmental objective functions. Pareto optimization is carried out in the last subsection between different environmental and economic objectives.

5.2.1 Economic network planning

Fig. 29 presents optimal network configurations in all five tax scenarios, including the information on the substituted references first-generation bioethanol and fossil petrol, the total amount and location of sourced feedstock, and the number and total capacity of biorefineries. The production networks are rather central, concentrating on production capacities in countries with lower labor and feedstock costs.

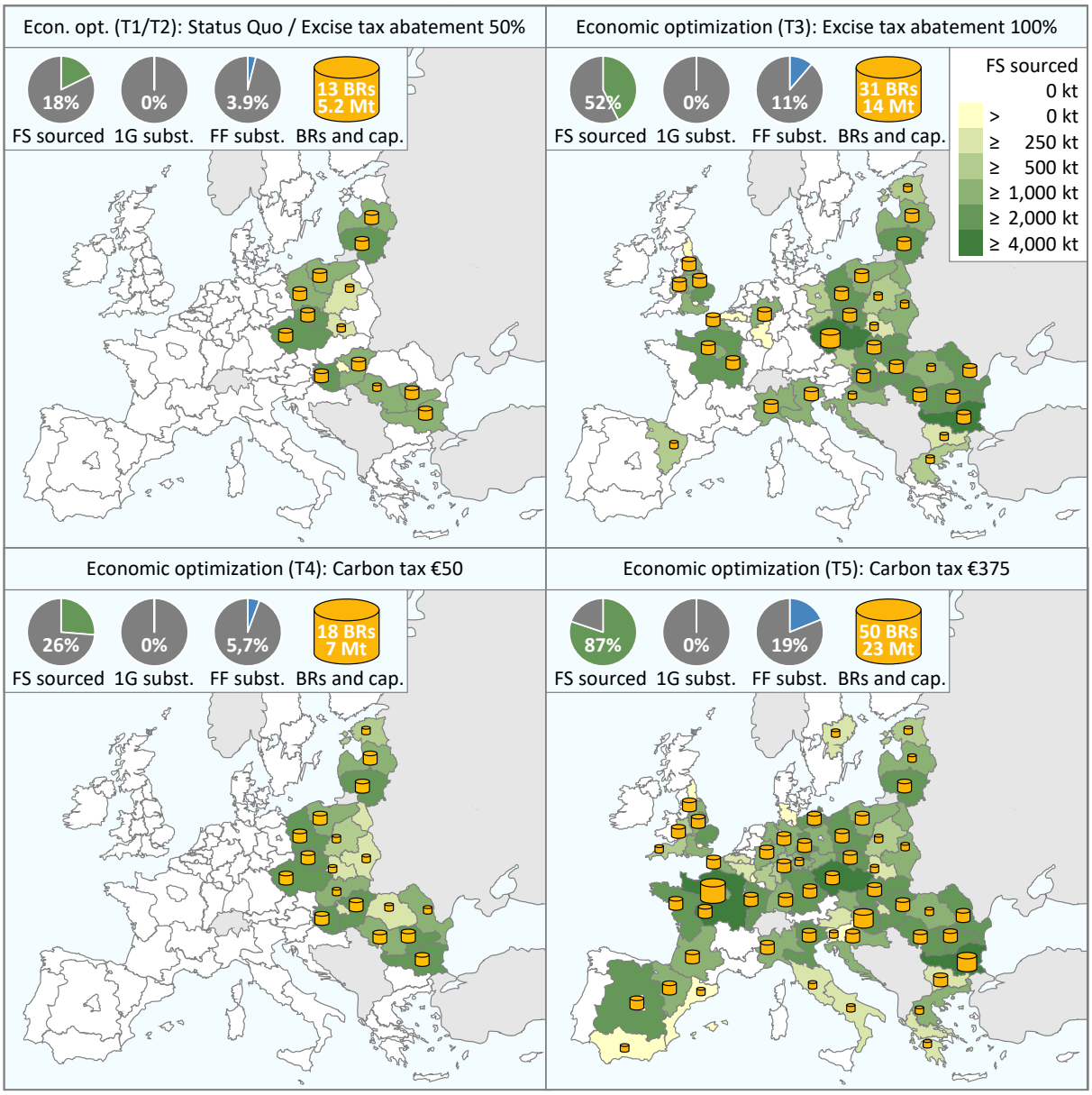

Fig. 29: Optimal biorefinery locations and capacities
(the size of cylinders corresponds to the capacity) and regional amounts of feedstock sourced (green shades) for economic objectives in five tax scenarios (with identical networks for T1 and T2). The legend also includes respective percentages of total feedstock collected (*FS sourced*), 1G demand substituted, and fossil petrol demand substituted (*subst. 1G* and *subst. FF*, pie charts), as well as total number and total capacity of biorefineries (*BRs and cap.*). Underlying data used to create this figure can be found in the Data Repository D.2

Revenues in scenario T1 are only slightly higher than the costs, which is why the profit margin of €275 million is small compared to the total costs (€4.43 billion). About 17.7% of the available feedstock is used to produce 4.7 Mt second-generation bioethanol, which substitutes 3.9% of the total petrol demand of 2018, but only in Sweden, Croatia, and Austria, where revenues are competitive due to already existing excise tax abatements. Economic optimization in T1 leads to environmental benefits of up to 17%

of the maximum achievable environmental values (see Fig. 32; e.g., GHG benefits of 10.13 Mt CO_2 eq). Scenario T2 yields the same results as T1, as competitive revenues remain insufficient with 50% tax abatement. An excise tax abatement of 100% (T3) has significant effects on production volumes (tripled to 13.7 Mt, approximately 365 PJ) and collection quotas (52.0% of all feedstock). Increasing production volumes are realized by larger production quantities in Central and Eastern EU countries and by biorefineries in feedstock-rich regions of England, France, and northern Italy. The objective value of €1.61 billion is about six times higher than for T1 and leads to positive environmental benefits in all three damage categories and some impact categories.

A carbon tax of €50 (T4) slightly increases the produced volumes compared to the status quo (T1). With 26% feedstock collection, the network is rather small, and the production takes place exclusively in Central and Eastern EU countries. Although the network is significantly smaller than T3, the economic objective value is almost similar with €1.53 billion. A carbon tax of €375 (T5) leads to a feedstock collection of 87% and a substitution of about 18.9% of the current petrol demand. The production volumes increase fivefold between scenarios T1 and T5, and the biorefinery network is dispersed across the EU. Unlike in T1, economic optimization in T5 leads to coincident environmental benefits of up to 85% of the maximum achievable environmental values (see Fig. 32, maximum M1 benefits of 59.17 Mt CO_2 eq.). In all economic scenarios, petrol is substituted exclusively as the tax abatements also apply to first-generation biofuels. Finally, the difference between revenues and cumulative magnitude of all cost elements is rather small for all economic scenarios, wherefore the economic dimension can be considered sensitive to parameter alterations. The results of the sensitivity analysis are thoroughly described in chapter 5.2.3.

5.2.2 Environmental network planning

Depending on the objective, different impact categories contribute differently to the respective damage categories. These contributions are influenced by the ReCiPe 2016 midpoint-to-endpoint aggregation and the decision taken and parameters used in this specific case (resulting from Life Cycle Inventories and Life Cycle Impact Assessment). This work focuses on those impact categories that, throughout all optimization runs, contribute the most to their respective damage categories. For example, if in one optimization run, the values of the midpoints mineral resource scarcity (M16) and fossil resource scarcity (M17) are (in the unit of their respective endpoint resource scarcity (E3)) $|-8\times10^6|$ and $|3{,}320\times10^6|$ USD2013 respectively, the sum of magnitudes of all contributions to E3 is $3{,}328\times10^6$ USD2013, which means a relative contribution by M16 and M17 of −0.25% and 99.75% respectively to the endpoint value. Fig. S1-2 shows the maximum (over all optimization runs) of magnitudes of the relative contribution of

each midpoint to its respective endpoint (i.e., to the total of magnitudes of relative contributions). In our opinion, this provides a reasonable estimate of the relevance of each midpoint in this application case, wherefore the main body of this work thus includes only those categories which contribute at least 5% (positively or negatively) to the respective endpoint in any optimization run.

Fig. 30 shows that these are most notably *global warming* (M1), *particulate matter formation* (M5), *land use* (M15), and *fossil resource scarcity* (M17), and to a lesser degree, *terrestrial acidification* (M7), *human non-carcinogenic toxicity* (M14), and *water consumption* (M18). Fossil resource scarcity (M17) is almost identical to its endpoint resource scarcity (E3); thus, only E3 is displayed in the result section. All other impact categories are considered irrelevant with regard to their respective damage categories and therefore not separately presented.

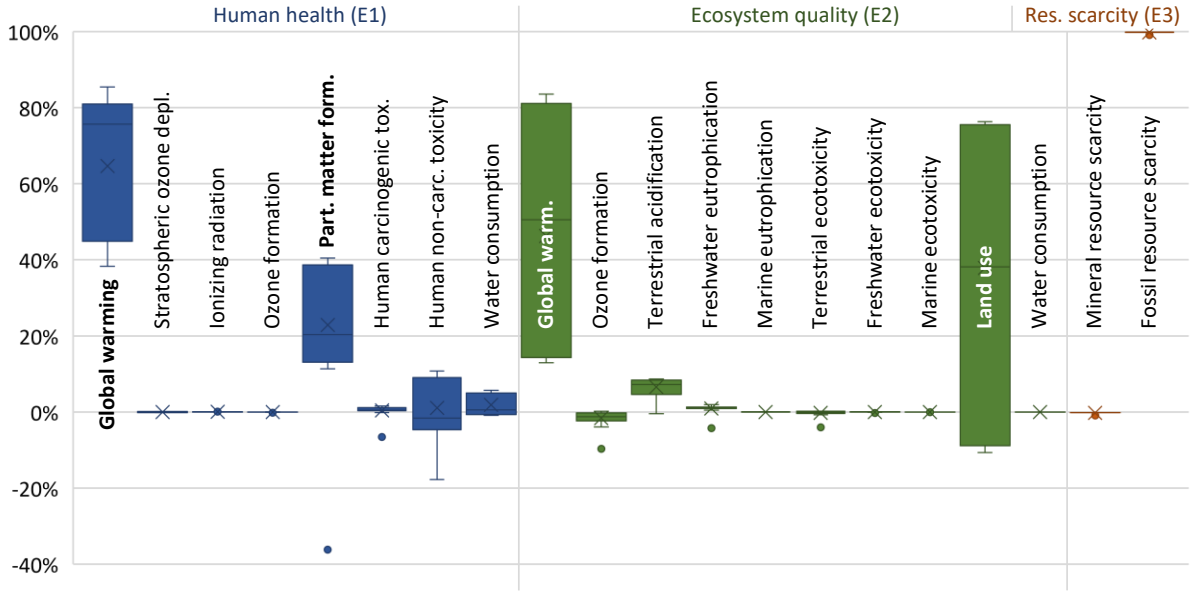

Fig. 30: Max relative contribution of each midpoint to the respective endpoint
(i.e., share of each midpoint to the sum of magnitudes of contributions to the respective endpoint; maximum over all optimization runs)

Fig. 31 presents all endpoints and relevant midpoints with their respective optimal objective value. It further displays the substitution decision and the environmental "opportunity cost", which refers to the percental deterioration of the optimal objective value when optimizing another objective. Eq. (33) generically displays the calculation of the percental opportunity cost between two objectives l and k ($l, k \in L$), with O_l^{env} being the optimal objective value of l, and $V_{l,k}^{env}$ being the value for l when optimizing k. Eq. (34 and (35) exemplify the opportunity cost calculation for the categories human health (E1) and land use (M15):

$$opportunity\ costs_{l,k} = \left(V_{l,k}^{env} - O_l^{env}\right)/O_l^{env} \qquad \forall\, l,k \in L \tag{33}$$

$$opportunity\ costs_{human\ health,land\ use} = \left(V_{human\ health,land\ use}^{env} - O_{human\ health}^{env}\right)/O_{human\ health}^{env} \tag{34}$$

$$opportunity\ costs_{human\ health,land\ use} = (1.44E4\ \text{DALY} - 6.33E4\ \text{DALY})\ /\ 6.33E4\ \text{DALY} = -77\% \tag{35}$$

Moreover, Fig. 31 clusters the endpoints and midpoints in groups of mutual congruencies, within which optimization of another objective function entails no or only small opportunity costs. This does not necessitate that all decisions are entirely equal for all categories within the same group or that all midpoints of the same group behave identically towards a third category.

Group 1 is characterized by a simultaneous substitution of 1G ethanol and petrol due to net environmental advantageousness of 2G bioethanol over both reference products. The opportunity costs of Group 1 categories range from −4% to −52% when optimizing Group 2 categories and from −39% to −79% when optimizing Group 3, which, despite the relative detriments, implies positive absolute benefits for Group 1 regardless of the selected objective. For instance, the optimal objective value of *human health* (E1) achieves benefits of 6.3E+4 DALY. With only −4 to −6%, the opportunity costs of *human health* are small compared to Group 2 categories, which can be explained by a high midpoint-to-endpoint characterization factor of *GWP* to *human health*. The opportunity costs of *human health* for Group 3 categories are with −78% substantially higher, which is due to much smaller networks with no substitution of petrol in optimal Group 3 solutions. Optimization towards *ecosystem quality* (E2) yields a maximum benefit of 2.6E+2 species years. Compared to E1, Group 3 objective functions' opportunity costs are lower, as *land use* contributes significantly to the damage category *ecosystem quality*. For Group 2 categories, the detriment is higher for E2 due to a lower midpoint-to-endpoint factor of *GWP* to *ecosystem quality*.

Group 2 is characterized by an exclusive substitution of petrol. The correlation to Group 1 categories is high, so optimization of Group 1 categories implies low opportunity costs (−7% to −13%) for Group 2 categories. The enormous opportunity cost when optimizing Group 3 categories indicate that the objective functions of Group 3 are mostly conflicting with Groups 1 and 2, resulting in different network decisions.

Group 3 optimization favors small production networks with exclusive substituting first-generation bioethanol, as the substitution of petrol by second-generation bioethanol is not desirable due to associated negative environmental benefits. When optimizing Group 2 categories, the opportunity cost is particularly high, with −117% to −314%. Since the optimal value is deteriorated by more than 100%, optimization of Group 2 objectives leads to an absolute deterioration of these categories. The opportunity costs vis-à-vis Groups 1 optimization are somewhat ambiguous with a

range of −14% to −178%. The consistently high opportunity costs of *human non-carcinogenic toxicity* can be explained by the additional fertilization. *Land use* has only low opportunity costs vis-à-vis Group 1 categories, which can be attributed to the substitution of 1G ethanol in Group 1. The finding that petrol can outperform second-generation ethanol in certain environmental categories is mostly consistent with existing LCA studies. Particularly *freshwater eutrophication*, *marine eutrophication*, *terrestrial acidification*, *fine particulate matter*, *land use*, and *water consumption* may be worse compared to petrol (Cherubini and Ulgiati, 2010; Borrion et al., 2012). For *freshwater* and *marine eutrophication* and *land* and *water use*, those findings are supported by the results of this work. The underlying technology is assumed to be based on acid-free pretreatment (most existing studies base their assessment on hydrolysis reactions, which are catalyzed by dilute sulfuric acid). This technological progress leads to environmental improvements in *terrestrial acidification* and *fine particulate matter formation* and thereby to benefits compared to petrol. Likewise, the optimization of group 3 objectives entails high opportunity costs for all damage and most impact categories (up to 94%). However, the optimal values of groups 1 and 2 are not deteriorated by more than 100%, which means a net positive contribution to those objectives, even though it can be very small.

Summing up, three groups of mutual congruencies are identified, within which opportunity costs are small. Between groups 1 and 2, the opportunity costs can be very small with only 4% and do not exceed 54%. Thus, pursuing objectives of the other group also leads to positive contributions in each case. The objective functions of group 3 are conflicting with groups 1 and 2, however, the magnitude of deterioration is heterogeneous. Depending on which objective function is considered, the opportunity costs in group 3 can exceed 100%, which would mean an absolute deterioration of these categories. For comparison purposes, the last column of the figure shows the environmental opportunity costs for economic T3 optimization. Economic optimization implies for group 2 the lowest opportunity costs with only about 50%, which means considerable benefits in this group for economic optimization. For group 3, the opportunity cost transcends 100%, which means an absolute degradation.

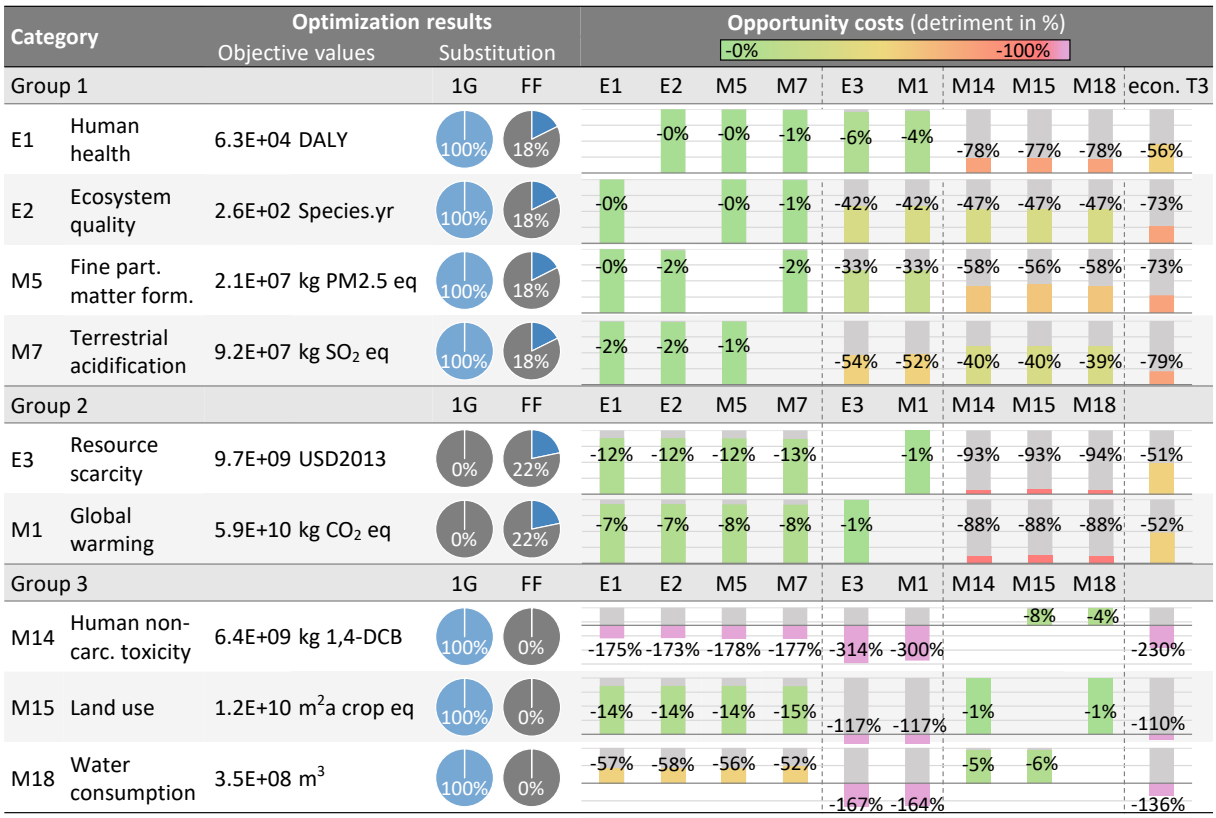

Fig. 31: Endpoints and relevant midpoints with their objective values and units clustered in groups of mutual congruencies (i.e., with similar substitution decisions, in percent of the total demand for 1G/FF). The figure also includes opportunity costs in each category to optimize the other environmental categories. For example, the objective value of *human health* (E1) is diminished by 77% when *land use* (M15) is optimized. Categories of one group have little or no opportunity costs to each other. The last column shows the environmental opportunity cost for economic optimization in tax scenario 3. *Fossil resource scarcity* (M17) is not listed separately, as it constitutes the endpoint *resource scarcity* (E3) by almost 100%. Underlying data used to create this figure can be found in the Data Repository D.2

Fig. 32 shows the environmental opportunity costs for economic optimization of the five different tax scenarios. The opportunity costs for both congruency groups one and two are very similar for the different tax scenarios and range from −14 to −91%. This means that an environmental advantage is achieved in groups one and two, even with economic network planning, although this benefit is sometimes very small (e.g., only 10% of the achievable value for *ecosystem quality)*. The environmental detriments can be explained by significantly smaller production networks and, therefore, lower petrol and 1G ethanol substitution volumes. For T3, for example, the total second-generation bioethanol production is with 13,7 Mt, only half the volume compared to production volumes of 27 Mt ethanol for Group 1 and 2 categories. For tax scenario 5, the detriments are much smaller due to the significantly higher ethanol production volumes. The opportunity costs are slightly smaller for environmental categories of group two (-83 to -14%) than group one (-91 to -19%), as the substitution decision

favors petrol for environmental categories of group two and the economic dimension. For environmental categories of Group 3, economically optimal results even lead to a net deterioration due to contrary substitution decisions. Economic optimization would favor the substitution of petrol by second-generation bioethanol. This would lead to a deterioration in categories like *land use*, as 2G EtOH has higher land use impacts than petrol. Especially the high opportunity costs of *human non-carcinogenic toxicity* of up to −288% stand out and can be explained by the additional fertilization, which would be required if large volumes of straw would be removed from agricultural land.

Category		Optimization results: Objective values	Substitution: 1G	Substitution: FF	Opportunity costs (detriment in %): econ. T1	econ. T2	econ. T3	econ. T4	econ. T5
Group 1			1G	FF	econ. T1	econ. T2	econ. T3	econ. T4	econ. T5
E1	Human health	6.3E+04 DALY	100%	18%	-84%	-84%	-56%	-77%	-19%
E2	Ecosystem quality	2.6E+02 Species.yr	100%	18%	-90%	-90%	-73%	-86%	-51%
M5	Fine part. matter form.	2.1E+07 kg PM2.5 eq	100%	18%	-89%	-89%	-73%	-85%	-45%
M7	Terrestrial acidification	9.2E+07 kg SO_2 eq	100%	18%	-91%	-91%	-79%	-88%	-61%
Group 2			1G	FF	econ. T1	econ. T2	econ. T3	econ. T4	econ. T5
E3	Resource scarcity	9.7E+09 USD2013	0%	22%	-83%	-83%	-51%	-75%	-14%
M1	Global warming	5.9E+10 kg CO_2 eq	0%	22%	-83%	-83%	-52%	-75%	-15%
Group 3			1G	FF	econ. T1	econ. T2	econ. T3	econ. T4	econ. T5
M14	Human non-carc. toxicity	6.4E+09 kg 1,4-DCB	100%	0%	-140%	-140%	-230%	-162%	-288%
M15	Land use	1.2E+10 m^2a crop eq	100%	0%	-103%	-103%	-110%	-105%	-115%
M18	Water consumption	3.5E+08 m^3	100%	0%	-110%	-110%	-136%	-117%	-157%

Fig. 32: The figure shows the opportunity costs for all relevant end- and midpoints for the optimization of the different tax scenarios. For example, the objective value of *global warming* (M1) is diminished by 52% when the economic *tax scenario3* is optimized

Fig. 33 presents optimal production networks of one representative objective per group and the economic T3 result. Environmental objectives result in disaggregated and spatially spread production networks in all categories, as transportation (feedstock collection and ethanol distribution) is the dominating impact. Optimizations of Group 1 and 2 leads to the collection of 100% of the available feedstock. While Group 1 objectives substitute 1G EtOH completely and then the maximum remaining possible volume of petrol, Group 2 solely replaces petrol. Optimization of Group 2 objectives leads to a substitution of 22% of the currently existing petrol demand, implying inter alia avoided GHG emissions of 59.17 Mt CO_2 eq. annually. Production networks of Group 3 objectives consist of many dispersed biorefineries with small capacities, which

is due to the fact that only 1G EtOH is substituted. 19% of the available feedstock is used to substitute 100% of the 1G EtOH demand, which has, in terms of *land use*, positive benefits of 11.7 billion m^2 annual crop land eq.

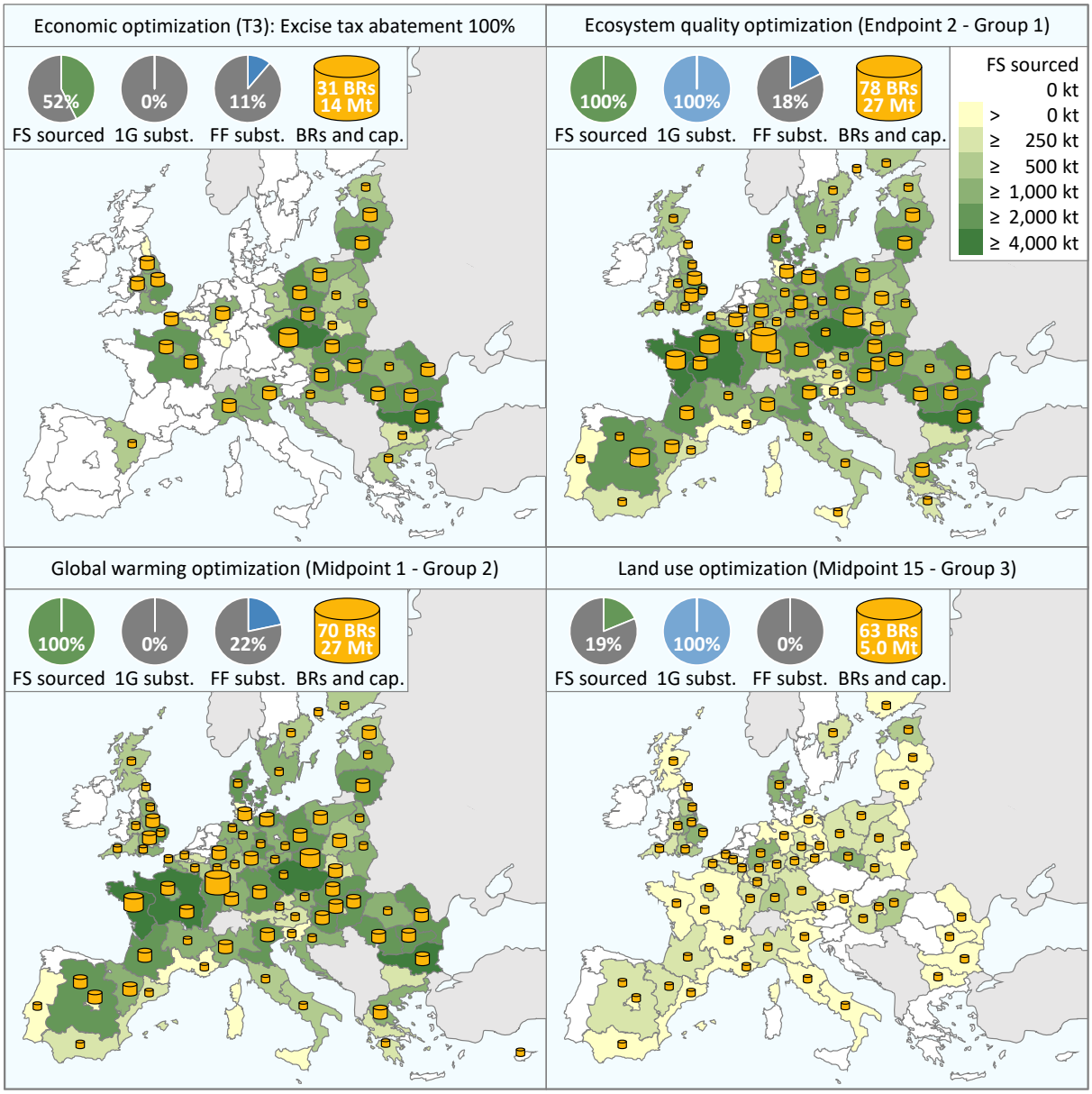

Fig. 33: Optimal biorefinery locations and capacities
(the size of cylinders corresponds to the capacity) and regional amounts of feedstock sourced (green shades) for economic objective (tax scenario 3) and three environmental objectives. The legend also includes respective percentages of total feedstock collected (*FS sourced*), 1G demand substituted, and fossil petrol demand substituted (*subst. 1G* and *subst. FF*, pie charts), as well as total number and total capacity of biorefineries (*BRs and cap.*). Underlying data used to create this figure can be found in the Data Repository D.2

Fig. 34 depicts the total costs per liter of second-generation bioethanol of optimal networks for all objectives and scenarios in ascending order within each congruency group. They are to be regarded as averages, as the particular costs per liter *per*

biorefinery are subject to deviations due to different costs structures in the different regions. The evaluation shows that the per-liter costs are similar for most objectives of one group with a few outliers within the three congruency groups. Economic optimization yields the lowest specific product prices, ranging from 0.75 to 0.87 €/liter. The specific product prices range from 0.88 to 1.00 €/liter for most environmental categories. The three objective functions *ionizing radiation* (M3), *freshwater eutrophication* (M8), and *marine eutrophication* (M9), lead to significantly higher specific prices. The explanation is not directly obvious and is provided by the co-products: for the *ionizing radiation* category, the entire production would take place in France, accepting very long transportation distances and higher costs, with the main objective to substitute as much grid electricity as possible through the co-produced electricity. France has by far the highest share of nuclear electricity in the EU, which is why the entire planning is driven by the substitution of this ionizing radiation-intensive electricity. Similar explanations apply to *freshwater eutrophication* and *marine eutrophication.* However, all three objectives are irrelevant in terms of their respective damage categories and are therefore considered not relevant in the context of decision making.

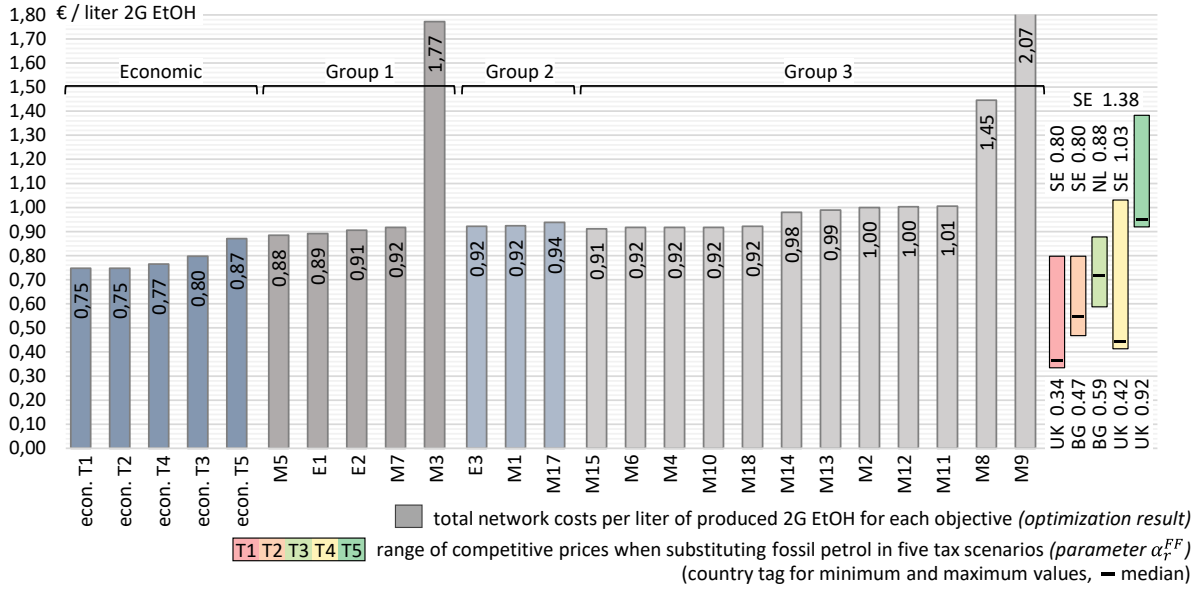

Fig. 34: Total network costs per liter of produced second-generation bioethanol for the different objectives in ascending order. Additionally, the figure depicts the range of average 2018-2019 petrol liter prices (in €/liter EtOH eq.) in the five tax scenarios with a country tag for the minimum and maximum and the median price. Underlying data used to create this figure can be found in the Data Repository D.2

For comparison, the figure also shows the range of competitive prices when substituting fossil petrol (α_r^{FF}) in the five tax scenarios on the right end of the figure. The competitive fuel prices are an important parameter for the economic dimension on which it depends whether substitution takes place or not. Above and below the colored

bars, the maximum and minimum values, respectively, with the corresponding country tag are indicated and the median value of the 28 countries (i.e., average between the 14th and 15th highest values). This illustrates why in scenario T1 (status quo), only very few countries (Sweden, Austria, and Croatia) have high enough competitive revenues to offset the network costs. It also shows that scenario T4 (€50 carbon tax) features a higher range of revenues between the countries and higher maximum revenue. However, overall profitability is higher in scenario T3 (100% excise tax abatement, also see Fig. 29), as the tax abatement has a larger effect on those countries in which bioethanol is currently very uncompetitive (e.g., UK), which is indicated by the higher minimum and median values. In scenario T5 (€375 carbon tax), the competitive price of fossil petrol is much higher in every country, wherefore this scenario can resolve many of the conflicts between the economic and various environmental objectives.

5.2.3 Sensitivity analysis

Many of the parameters used in this model are subject to uncertainty in practice. This section analyzes the repercussion of variations in key economic and environmental parameters in terms of optimal decisions and objective values. A full Monte Carlo simulation of environmental parameters, which is common practice in LCA studies, and their impact on the optimization outcome is not practical due to the computational times of the MILP model. An analysis of the contribution of the different revenue/benefit and cost/impact elements towards the respective objective value is given in Fig. 35.

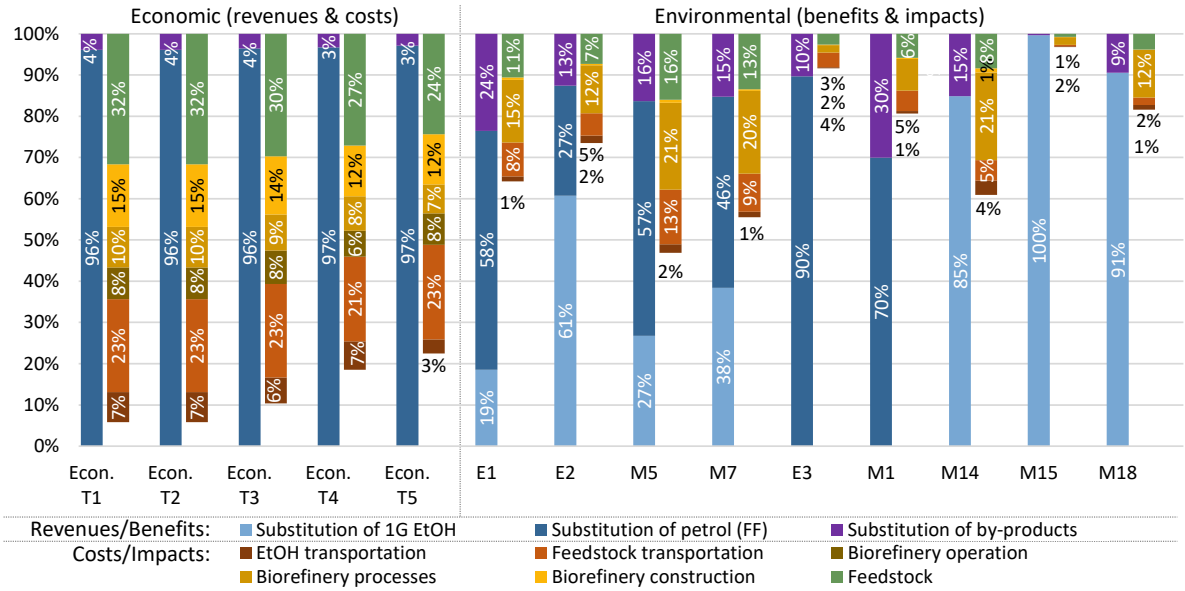

Fig. 35: Composition (revenues/benefits vs. costs/impacts) of objective values and relative contribution of different types of revenues/benefits and costs/impacts. Underlying data used to create this figure can be found in the Data Repository D.2

The most relevant elements of the environmental objective functions are feedstock impacts, impacts from production processes, and feedstock transportation impacts. Feedstock costs, biorefinery depreciation, and feedstock transportation are most relevant for economic objective functions. Together with the revenue/benefits parameters in each objective function, the model is suspected to be most sensitive towards changes in these parameters, which is why they are chosen for a sensitivity analysis. Moreover, the economic function is suspected to be more sensitive than the environmental ones, since the total revenues compared to the cumulative magnitude of all cost elements (≙ return on sales of 5.8% in T1 and 10.4% in T3) is much smaller than analogously in the environmental cases.

Table 16 lists the altered economic and environmental parameter changes (by ±10% and ±20%) and the resulting changes in objective values and in the number of biorefineries, displayed exemplary for economic (tax scenario T3; tax scenarios T1-T4 behave similarly, only T5 is much more robust) and ecosystem quality (E2) optimization. It shows that economic results are expectedly sensitive towards changes in the revenues, and the whole network turns unprofitable for reductions of 20% and almost completely unprofitable by reductions of 10%. Vice versa, revenues of +10% and +20% can increase the objective values by up to +278%. The high economic sensitivity towards the revenue (which is, to a significant degree, beyond the control of a company) could be one reason why only a few market participants have been active in the field of advanced bioethanol production to date. Decreasing feedstock and feedstock transportation costs have a large contribution to the economic objective value as well. A reduction of feedstock cost by 20% increases the network profit by +66%, and a reduction of transportation cost by 20% increases it by 54%, but likewise, increasing feedstock and feedstock transportation cost can diminish the objective value significantly. The sensitivity of the economic objective value is lowest for the variable production cost and the fix and variable product transportation cost.

Fig. 35 illustrates that the environmental benefits through reference substitution clearly exceed the environmental impacts, wherefore the environmental results are expectedly much more robust to parameter alterations. Table 16 shows that the environmental objective values behave almost linearly with parameter alterations and are mainly in the low single-digit percentage range. The most sensitive parameters are the environmental impacts of the substituted reference products, with an objective value decline of -9% when environmental impacts of 1G EtOH decrease by 20%. A variation of the construction impacts hardly affects the environmental objective value (0.1 to -0.1%), and also the change in the total number of biorefineries is low with one biorefinery more for a 20% reduction in impacts. Furthermore, it is noticeable that the number of refineries built decreases with decreasing transport impacts, since longer transport routes to larger refineries can be accepted.

Table 16: Changes in the objective values for sensitivity analysis of the economic T3 objective and the environmental E2 objective (objective values and number of biorefineries) when altering model parameters by ±20% and ±10%

	Altered economic parameters							**Altered environmental parameters**						
Parameter alteration	1) α_r^{1G}	2) α_r^{FF}	3) $\varphi_{r,f}$	4) κ_c^{depr}	5) κ^{var}	6) $\varepsilon_t^{fix}, \varepsilon_t^{var}$	7) $\eta_t^{fix}, \eta_t^{var}$	1) $\tilde{\alpha}_l^{1G}$	2) $\tilde{\alpha}_l^{FF}$	3) $\tilde{\varphi}_{l,f}$	4) $\tilde{\kappa}_{l,c}^{depr}$	5) $\tilde{\kappa}_l^{var}$	6) $\tilde{\varepsilon}_{l,t}^{fix}, \tilde{\varepsilon}_{l,t}^{var}$	7) $\tilde{\eta}_{l,t}^{fix}, \tilde{\eta}_{l,t}^{var}$
	Resulting changes in economic (T3) objective value							Resulting changes in environmental (E2) objective value						
−20%	±0%	-100%	66%	30%	18%	54%	12%	-9%	-4%	2%	0.1%	3%	2%	0.5%
−10%	±0%	-74%	31%	14%	9%	24%	6%	-5%	-2%	1%	0.1%	2%	1%	0.2%
+10%	±0%	118%	-26%	-13%	-8%	-20%	-6%	5%	2%	-1%	-0.0%	-2%	-1%	-0.2%
+20%	±0%	278%	-49%	-24%	-16%	-38%	-12%	9%	4%	-2%	-0.1%	-3%	-1%	-0.5%
	Resulting changes of the economic (T3) solution in the number of biorefineries							Resulting changes of the environmental (E2) solution in the number of biorefineries						
−20%	-1	-29	+10	+6	+2	± 0	+2	± 0	-1	+2	+1	± 0	-2	-1
−10%	± 0	-11	+4	+2	+1	± 0	+1	+3	+1	-1	+1	± 0	-1	-1
+10%	-1	+16	-7	-4	-1	-2	-1	+2	-1	± 0	± 0	± 0	+1	-1
+20%	± 0	+21	-9	-9	-2	-6	-2	± 0	-1	± 0	± 0	± 0	+2	+1

Parameters: 1) revenues/saved impacts of 1G EtOH, 2) revenues/saved impacts of 1G EtOH and fossil petrol, 3) feedstock costs/impacts, 4) construction and depreciation costs/impacts of biorefineries, 5) variable costs/impacts from processes in biorefineries, 6) fixed/variable costs/impacts of feedstock transport, 7) fixed/variable costs/impacts of 2G EtOH transport

To account for uncertainties and possible changes in the feedstock availability in the future, we computed the model with the feedstock volumes forecasted on NUTS-1 basis for 2030 (forecasting results of chapter 4). Overall, the 2030 feedstock scenario assumes an increase of feedstock potentials by 12.5% on average. Since the objective values of Group 1 and 2 are constraint by the limited feedstock supply, the objective values of those categories would almost linearly increase with the higher feedstock volume in 2030. The volumes of substitutable first-generation bioethanol limit the benefits of environmental objectives of Group 3, wherefore higher feedstock volumes almost do not affect the results in those categories. The economic objectives are much more sensitive towards changes in the feedstock potential, wherefore an increase of the feedstock volumes would result in distinctly higher economic objective values of up to 28% (for tax scenario T1 and 24% in T3). Higher feedstock potentials would slightly reduce conflicts between the economic and environmental categories. The comprehensive results of the sensitivity and scenario analyses for different objective functions can be found in the Data Repository D.2).

5.2.4 Pareto optimization

To ease finding trade-offs between the three environmental congruency groups and the economic objective, Pareto-optimal frontiers are calculated using the equidistant ε-constraint method. Between the optimal objective value of the first objective (optimum) and its value when optimizing the second objective (nadir point), 19 equidistant points (steps of 5%) are defined. These are then successively used as lower bounds of the second objective function. This is done for optimization of both objectives, resulting in 40 Pareto-efficient points, where the solution of one objective cannot be improved without deterioration of the others. From this set, a decision-maker can choose a preferential solution (Kenneth and Zammit-Mangion, 2013). For tax scenarios T1, T2, and T4, a reasonable trade-off between the economic and environmental criteria is intricate, as every environmental objective leads to a negative economic value. For T5, the network is almost always beneficial for economic and environmental objectives alike. Since scenario T3 (100% tax abatement) arguably provides the most interesting economic-environmental trade-offs, only T3 is shown in Fig. 36.

Fig. 36 includes six Pareto-optimal frontiers, one for each combination of Groups, and the economic dimension. The first and the last Pareto points correspond to the respective optimum when only one objective is optimized. Fig. 36 a shows that profitability declines moderately and eventually leaves the profitable zone with an increasing preference for ecosystem quality. With an increasing preference for *ecosystem quality* (E2), 1G EtOH is increasingly substituted at the expense of petrol substitution. The frontier for economic (T3) vs. *global warming* optimization (Fig. 36 b) behaves similarly however, the network remains profitable even for high *GWP* benefits due to low marginal costs (~€10 per metric ton CO_2 eq.), and petrol is replaced exclusively. A strong decline characterizes the end of the curve, translating to high marginal costs for increased *global warming* benefits (~€1,500 per metric ton CO_2 eq.), which is attributable to the much larger number of biorefineries. Fig. 36 c shows that with increasing preference for *land use*, 1G bioethanol is substituted instead of petrol. The total amount of produced second-generation bioethanol is constant for most Pareto points, with a sudden drop of production volumes close to the optimal solution for *land use*, where produced volumes decrease while the number of biorefineries doubles. In Fig. 36 a-c, it becomes clear that for economically optimal networks, the average biorefinery capacity is larger than for environmentally optimal solutions, translating to more centralized supply chains. Fig. 36 d reveals an almost linear frontier between Group 1 and Group 2 (depicted for E2 and M1) as the total feedstock is used to substitute either petrol only (Group 2) or both petrol and 1G ethanol (Group 1). The

production volumes, and subsequently the environmental benefits, are only limited by the limited feedstock base.

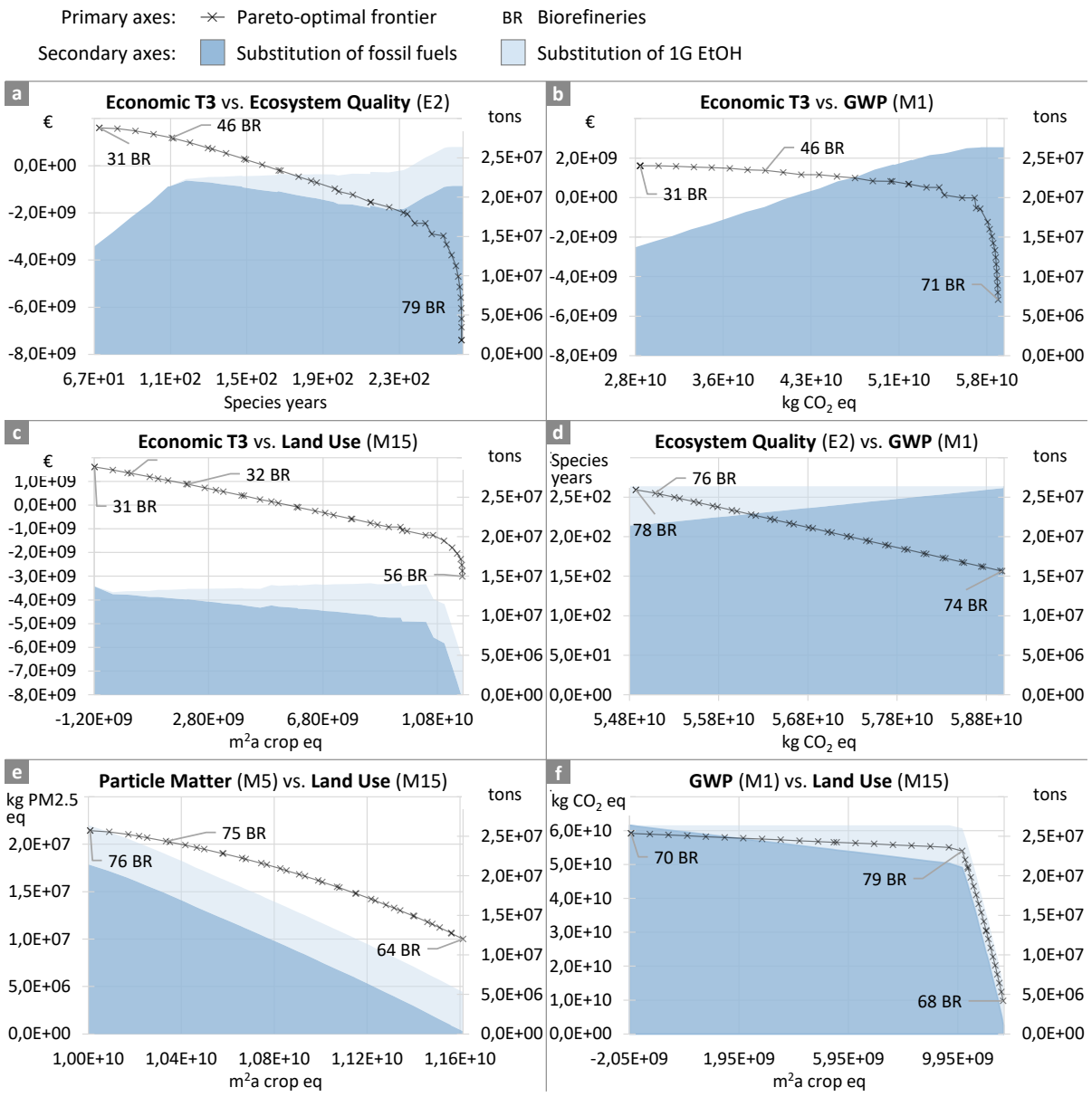

Fig. 36: Selected Pareto curves between economic and environmental objectives.
Fig. 36a to c show economic (in T3) vs. environmental (one representative per group) Pareto-efficient frontiers. Fig. 36d to f show frontiers between these three environmental objectives. The figure additionally includes the substituted volumes of first-generation bioethanol and petrol as stacked area plots and the number of biorefineries at the two respective optima and at the point of the shortest relative Euclidean distance to both optimum values (Compromise point, section 2.4). Underlying data used to create this figure can be found in the Data Repository D.2

Pareto curves between Group 1 and Group 3 (Fig. 7e) show that, with an increasing preference on Group 3, the demand for 1G EtOH is the limiting factor, rather than the feedstock supply. As noted above, only 1G EtOH substitution is beneficial for Group 3 categories. The Pareto frontier between *GWP* and *land use* (Fig. 36 f) is next to linear

at both ends, with high marginal costs for the less preferred objective. The Pareto frontier has a strong gradient change at the point where additional *land use* benefits can only be achieved by reducing 2G ethanol production. Interestingly, the Pareto-optimal solution at this point is almost identical to the solution for the endpoints *human health* and *ecosystem quality*. This shows that the endpoint-inherent normalization and weighting between different impact categories is a meaningful aggregator in environmental decision-making processes.

5.3 Discussion and conclusion on the optimization results

The results of this work indicate positive environmental benefits of substituting petrol and 1G bioethanol with 2G bioethanol in most impact and damage categories. Nonetheless, the different environmental categories are not unanimously congruent. We found conflicts between some environmental goals, leading to opposing optimal production networks and substitution decisions. Hence, the general assumption that GHG emissions fully reflect the environmental dimension falls short. Second-generation bioethanol indeed has the potential to avoid GHG emissions and the maximum achievable benefit of about 59.17 Mt CO_2 eq. corresponds to the total emissions of a country like Finland and 1.35% of the EU's total emissions in 2018 (Eurostat, 2020a). However, impact categories like *terrestrial acidification*, *particulate matter formation*, *human non-carcinogenic toxicity*, *land use*, and *water consumption* show high opportunity costs for optimization of *global warming*. This implies that, from a societal perspective, *global warming* is not sufficient as exclusive objective, as it is not entirely congruent with the areas of protection (health, ecosystems, and resources). While *global warming* optimization advises the exclusive substitution of petrol, optimization of the two endpoints *human health* and *ecosystem quality* indicates the advantageousness of a concurrent substitution of first-generation bioethanol and petrol. The feedstock production for 1G bioethanol in the EU (mainly maize, wheat, and sugar beet) requires substantial agricultural land, compromising biodiversity. Complete substitution of 1G ethanol would yield about 1.2 million hectares of land, which could be used for additional food production (about +5% wheat EU-wide) or as compensation areas to mitigate biodiversity loss. Additionally, substituting first-generation with second-generation ethanol would significantly reduce particulate matter emissions due to reduced ammonium application and use of agricultural machinery, thereby contributing to human health protection.

While a large-scale production of second-generation bioethanol is advantageous from an environmental point of view, it is hardly conceivable from an economic perspective. With today's oil prices and taxation, second-generation bioethanol production is barely competitive vis-à-vis fossil petrol. At best, 0.75 €/l of second-generation bioethanol

(production and distribution costs without excise taxes and other duties) is achieved, and for environmentally optimal networks, the price can be as high as 0.88 €/l. Currently, the combination of production in countries with low wages, feedstock, and transportation costs, as well as consumption in countries with excise tax abatement (e.g., Sweden, Croatia, or Austria) is only just or close to being profitable (also reflected in the high sensitivity of the economic model). Political guidance will be needed if EU countries decide to implement advanced biofuels as part of climate change mitigation measures. Our results show that already a carbon tax of €50 could double the volume of profitably produced 2G ethanol to 7.0 Mt, which corresponds roughly to today's total 1G ethanol consumption in the EU in 2018. An excise tax abatement of 100% for advanced biofuels could further increase economically profitable production to 13.7 Mt.

The Pareto optimization shows that additional environmental benefits can be realized with only small economic opportunity cost for many categories. Fig 7b exemplifies that about 85% of the maximum GWP benefits can be achieved in tax scenario 3 with a positive profit. Beyond a certain point on the Pareto frontier, the costs of additional environmental benefits increase disproportionally. This implies that an exclusive focus on environmental categories would render any network unprofitable. For a larger degree of congruency between economic and environmental objectives, the five tax scenarios show that significant changes in economic preconditions are required. In this application case, Pareto optimization between two environmental objectives (Fig. 7d-f) demonstrates the meaningfulness of endpoints in environmental decision-making processes. For example, the strongest gradient change on the Pareto-frontier between the two impacts *GWP* and *land use* seems to be a reasonable trade-off between the two (Fig. 7f). A sacrifice of about 10% of the optimal *GWP* value permits achieving 85% of the optimal *land use* value and >99% of the optimal values for *human health* and *ecosystem quality*, proving the endpoint-inherent normalization and weighting of different impact categories. Stefansdottir et al. (2018) propose different methods to reduce objectives in a multi-objective optimization problem, i.a., the δ-error method or using an LCIA-inherent weighting scheme. In model introduced in this chapter, the anticipated results of a δ-error method are somewhat preempted by grouping objectives into the three congruency groups with similar substitution decisions and low opportunity costs. Furthermore, Pareto optimization shows that the three ReCiPe endpoints are suitable aggregators of the 18 midpoints in this application case. Goal Programming is another possible approach to find a compromise solution between a number of objectives by minimizing the total Euclidean distance between the objectives and their single-optimization optima. Considering that a single environmental impact category hardly covers the whole environmental dimension, we suggest future works on multi-criteria decision-making to base decisions on damage categories rather than impact categories. However, a transparent presentation of all impacts and knowledge

about the categories' contributions remains indispensable to reveal possible negative consequences.

Bioethanol could play an important role in the transportation sector in the medium term (~2030), however, BEVs and hydrogen-based propulsion are likely to gain major shares in this sector. For heavy-duty vehicles, international navigation, and aviation, alternative environmentally-friendly solutions are rare, and hydrocarbon-based fuels may remain the only viable option in the next decades. Our results show that sustainably available agricultural residues are sufficient to substitute up to 17.2 Mt petrol, which equals 22% of the EU's demand in 2018 (or the entire first-generation ethanol and 18% petrol demand). In T3, 13.7 Mt bioethanol could profitably be produced to substitute petrol. This work focuses on the most abundant residues, and an expansion of the feedstock base can further increase production volumes. The project S2BIOM estimated about 20% higher agricultural residue potentials than applied in this work. Additionally, forestry residues could further serve as feedstock for bioethanol production (Dees et al., 2017). However, agricultural residues are increasingly sought-after by bio-based applications, and policy makers should carefully consider how to guide the utilization of this limited resource.

This approach of integrating different methods allows the simultaneous consideration of different research goals. By considering a broad set of environmental categories and a regionalization of the different value chain aspects, this work extends existing models for environmental decision-making in multi-objective network models. Furthermore, the model considers the nonlinear relationship between feedstock collection costs (agricultural residues are distributed in area) and refinery size (economies-of-scale) by step-wise linearization, which is a common approach in Operations Research literature (Lin et al., 2013), but has been neglected by most previous studies in the field of biorefinery configuration (Lauven et al., 2018; Budzinski et al., 2019).

The endpoint *human health* and the midpoint *land use* implicitly cover social aspects in the context of advanced biofuels (food-to-energy conflicts, Čuček et al., 2012). In particular, with regard to regional development, the additional explicit consideration of a social dimension is a desirable next step towards a holistic sustainability assessment in strategic network design. In addition, different research efforts indicate that the underlying biorefinery technology could improve efficiency in the future. A high added value valorization of residual lignin in bio-based products could further improve the environmental performance (Ghaffar and Fan, 2014), and environmental benefits could be augmented by a Carbon Capture and Storage/Use system for the fermentation emissions. Such technological development would significantly impact the carbon balance of second-generation bioethanol, and even a negative carbon balance of large-scale production, environmentally and technically, within the realms of possibility.

Future works should also consider a wider range of consequential aspects of the implementation of second-generation bioethanol, such as abated *land use*, or how a large-scale second-generation EtOH production would alter the overall market situation.

6 Assessing the Social Dimension in Strategic Network Design

This chapter develops an approach for the structured and transparent inclusion of social indicators in the strategic network design. The developed approach is applied to the case of second-generation bioethanol production in the European Union. Therefore, the model developed in Chapter 5 is extended by the social dimension. The resulting model can account for a variety of economic, environmental, and social objective functions in Strategic Network Planning. The presentation of results is completed by matching the objective functions to SDGs to be able to make assertions about the implications of the results on the SDGs.

For decades, most companies oriented their strategic supply chain design solely towards economic performance. To address the challenges of our time, the United Nations formulated the Sustainable Development Goals (SDGs; United Nations, 2015) to provide a common ground for peace, prosperity, health, and education, reduced inequality while tackling climate change and biodiversity loss. In 2019, 72% of over 1,000 globally acting companies mentioned the SDGs in their reporting, although only 1% measured their actual performance (PwC, 2019). Hence, companies are aware of their role in achieving sustainable development but not their actual impact. Incorporating operationalized environmental, economic, and social indicators as early as in strategic decision-making is the basis of aligning with the 17 SDGs.

While the SDGs are the "high-level shared blueprint" (Valdivia et al., 2021, p.1), the Life Cycle Sustainability Assessment (LCSA) framework (UNEP, 2011) divides sustainability into three pillars. For the environmental pillar, Life Cycle Assessment (LCA) is a formally defined concept (ISO, 2006a) that copes with both the product and the strategic, more aggregated level. Unlike product-specific or site-specific assessments, sustainable decision-making on a strategic and multi-regional scale, by nature, relies heavily on aggregated and often generic data. In the field of strategic supply network design, many studies have addressed both LCA-based environmental impacts and economic feasibility in mathematical optimization models (Eskandarpour et al., 2015). The case of social sustainability is more intricate: While taking or not taking a decision has quantifiable repercussions in the economic and environmental dimensions, the social implications of the decision are not always clear ex-ante. The complexity of social indicators, their subjective and often qualitative nature, and a lack of data (Valdivia et al., 2021) render their inclusion into quantitative decision-making models complex. Existing social frameworks, such as the ISO 26000 (ISO, 2011) or the

Sustainability Reporting Standards (GRI, 2021), focus on ex-post evaluations, which allow for site- or product-specific assessments (e.g., Kolotzek et al., 2018, Ren et al., 2015). In contrast, strategic network design is located on a more generic level of aggregation and includes Greenfield problems, where social considerations and their interconnectedness with environmental and economic criteria (Valdivia et al., 2021) need to be quantifiable before strategic decisions are taken.

Although general interest in the inclusion of social issues is observed in the literature (Mujkic et al., 2018), the state-of-the-art implementation of the social dimension is far from being on par with the economic and environmental dimensions (Barbosa-Póvoa et al., 2018). Recently, Messmann et al. (2020) reviewed 91 articles with social objective functions for strategic network design and concluded: 1) most of the reviewed articles (74%) do not cite any existing social framework, and only 14% use frameworks specifically for identifying relevant social issues or quantifiable indicators (Ghaderi et al., 2018; Mota et al., 2015a; Soleimani et al., 2017). Those articles that rely on frameworks tend to cover more social issues, but the reasoning behind the selection is often not transparent, and there is no "best practice" process to build upon. 2) There is only a small number of consistently applied indicators, and only a few studies include more than a couple at once (Pishvaee et al., 2014; Anvari and Turkay, 2017; Zhu and Hu, 2017). Job creation is the only issue that is reliably found in the majority (69%) of relevant literature, mainly expressed by the total number of jobs created (Miret et al., 2016; Roni et al., 2017; Mousavi Ahranjani et al., 2018; Lin et al., 2019). 3) There are hardly any attempts of impact assessment or multi-dimensional analyzes, e.g., multi-criteria optimization. Studies instead weight and aggregate the aspects by applying, e.g., the AHP method (Jakhar, 2015; Shokouhyar and Aalirezaei, 2017; Sahebjamnia et al., 2018). More quantitative approaches, such as the Social Hotspots Database (Benoît-Norris et al., 2018) or the Product Social Impact Life Cycle Assessment database (Ciroth and Eisfeldt, 2016), have not yet been applied in this field. Since both the selection of suitable indicators and their application are case-specific, we present our approach in a case study in the context of the bioeconomy. Agriculture claims the largest share of anthropogenically used land, which is why the use of renewable raw materials is subject to several tensions (Hennig et al., 2016; Thorenz et al., 2018; Eurostat, 2021l). Anthropogenic land use is not environmentally sustainable in its current state (Lewandowski, 2015). Utilizing biomass as a source for renewable energy and materials as substitutes for fossil-based counterparts competes for land with food security. The bioeconomy in general, and the second-generation bioethanol production in particular, represents a suspenseful application case for multi-criteria strategic network planning and is linked to many of the SDGs. Against this background, chapter 6 sets out to answer the two remaining research questions:

RQ4: What is a best-practice approach for a structured and transparent selection of quantitative and operationalizable social indicators for bio-based value chains?

RQ5: What are the social, environmental, and economic benefits of optimal biorefinery networks, and which Sustainable Development Goals are affected?

6.1 Methods

Subsection 6.1.1 first motivates and describes the case study. This is necessary, as the focal supply chain, the geographical and system boundaries, and the level of aggregation influence the outcome of the indicator selection, which is described in subsection 6.1.2. Subsections 6.1.3 and 6.1.4 then select social indicators and integrate them into the problem by formulating social objective functions and functions for social hotspot identification.

6.1.1 Problem description

The case study is based on and extends the model presented in chapter 5. Multi-criteria mixed-integer linear programming (MILP) is used to investigate environmental benefits and economic viability of second-generation (2G) bioethanol (EtOH) production networks for petrol and first-generation (1G) EtOH substitution in the EU. 2G bioethanol is based on lignocellulosic harvesting residues and thus avoids some of the environmental burdens and the conflict with food production linked to 1G bioethanol.

The environmental dimension comprises 18 impact and three damage categories of the LCIA method ReCiPe 2016. The economic dimension is addressed by profit maximization in five tax scenarios. Scenario T1 represents the current country-specific taxation of bioethanol. In scenarios T2 and T3, the excise tax is reduced by 50% and 100%, respectively. Finally, scenarios T4 and T5 assume EU-wide carbon taxes of €50 and €375, respectively. As T3 offers the most clear-cut economic-environmental trade-offs, this scenario represents the economic dimension in this chapter. The value chain includes feedstock provision and sourcing, bioethanol production and distribution to demand regions, to substitute petrol or first-generation bioethanol. The impact categories *global warming*, *fine particulate matter formation*, *land use*, and *fossil resource scarcity* were most affected. The results suggest that with current taxation, 2G bioethanol is hardly competitive vis-à-vis petrol, but environmentally beneficial production volumes become viable with a complete excise tax abatement for bioethanol or higher carbon taxes.

The societal "food, energy and environment" trilemma (Lewandowski, 2015, p.37) makes the given application case particularly relevant for including the social dimension. The environmental and economic objectives applied in chapter 5 already cover nine of the 17 SDGs (Table 22). Consequentially, seven socially-focused goals and many subordinate social targets of all SDGs are not represented. The approach presented in this section sets out to select and operationalize social indicators to fill the existing gaps and promote all SDGs (except SGD17).

6.1.2 Selection of issues and indicators

This work presents a structured selection approach (Fig. 37) to identify the relevant and quantifiable social issues in the given context. This ensures that the social dimension is not exclusively represented by a single and arbitrarily chosen issue and indicator but covers as many aspects associated with network decisions as possible. We differentiate between optimizable **social objective functions** (**SOF**; section 6.1.3), where decisions exert distinctly positive or negative impacts, and **social hotspot functions** (**SHF**; section 6.1.4), which provide ex-post insights on a plethora of potential social issues along the global value chains.

In step 1 of the approach, suitable social assessment frameworks are selected. In step 2, relevant and quantifiable social issues are identified, and the irrelevant ones are excluded with justification provided. Readily (case-specifically) applicable indicators proposed by the selected framework are directly adopted, and suitable operationalized indicators are developed for the remaining issues. In step 3, the SOFs and SHFs of the MILP model are formulated, using the social indicators as model parameters. In step 4, the model is computed. Trade-offs between different social, environmental, and economic categories are analyzed through multi-objective optimization, and social hotspots are evaluated. In the final step 5, the model categories are matched to the SDGs, and potentially positive and negative impacts on the attainment of the SDGs are investigated.

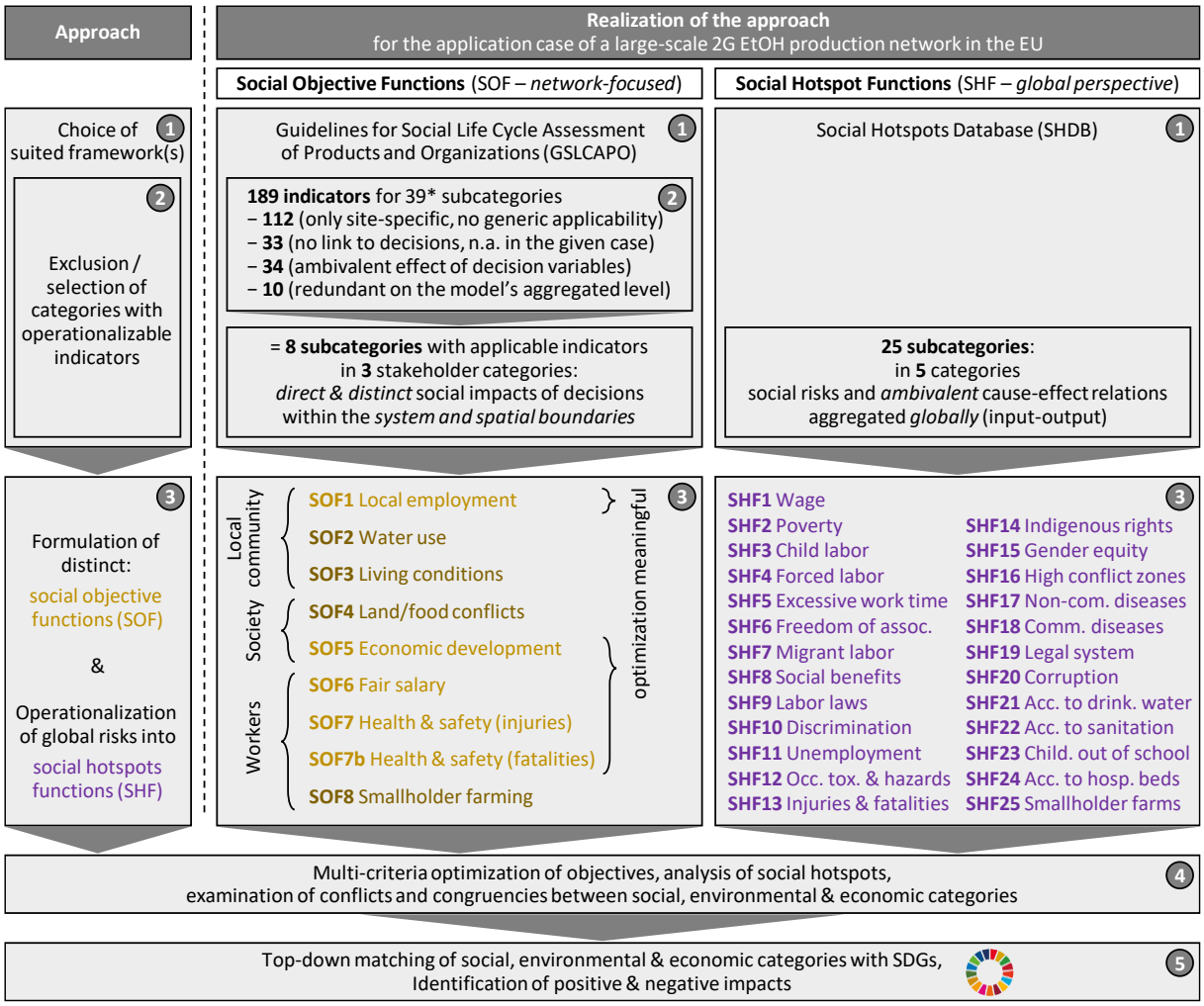

Fig. 37: Approach for social issue and indicator selection
operationalization and definition of indicators, formulation of social objective functions and social hotspot functions, and ex-post analyzes and matching with SDGs. *The methodological sheets (2013) list 189 indicators for the 30 subcategories of the GSLCAP (2009). The new GSLCAPO (2020) includes 39 subcategories

6.1.3 Social objective functions

While the SDGs are the overarching and globally accepted framework, their subordinate targets and indicators are not precisely designed to measure the impacts of specific supply chain decisions but rather to evaluate the progress of municipalities, countries, and humankind towards sustainable development. On the other end of the spectrum, there is a vast array of frameworks for evaluating social aspects in specific value chains and for certifying companies. Norms and standards such as the Sustainability Reporting Standards (GRI, 2021), the SA8000 (SAI, 1997), and the ISO 26000 (ISO, 2011) are among the most frequently cited frameworks in network design studies (Messmann et al., 2020), but often rather designed for site-specific assessments or auditing suppliers and companies' existing supply chains. While the Guidelines for Social Life Cycle Assessment of Products and Organizations (GSLCAPO; UNEP, 2020)

and the current version of the methodological sheets (UNEP SETAC, 2013) also feature site-specific and qualitative indicators, they explicitly focus on decision-making processes and are more product-focused through their kinship with environmental LCA. For the case of a bioethanol production network, the guidelines are viewed as a suitable foundation for quantifying distinctly positive or negative social impacts.

Table 17: Selected social issues and their indicators
as presented in the methodological sheets of the GSLCAP

Social issue (subcategory)	**Indicator proposed by the methodological sheets**	**Operationalized indicator(s) for the case of EU bioethanol production**	**Data sources**
Local employment	Unemployment statistics by country	Unemployment rate by region	Eurostat (2020c), World Bank (2021b)
Access to material resources	Levels of industrial water use	Local water use in the network; water stress level by country	FAO (2021)
Safe and healthy living conditions	Pollution levels by country	Local air emissions in the network; excess mortality from air pollution by region; population density by region	Anderson et al. (2004), EEA (2021), Eurostat (2021d), WHO (2021), Eurostat (2021e)
Prevention and mitigation of conflicts	Is the organization doing business in a sector that features linkages to conflicts [...]?	Local land occupation in the network; agricultural caloric yield by region	Eurostat (2021b), Lee et al. (2016)
Contribution to economic development	Economic situation of the country/region (GDP, [...])	GDP per capita by region	Eurostat (2020b), IMF (2021)
Fair salary	Non-poverty wage by country	Wages by country and sector; poverty threshold by country	Benoît-Norris et al. (2018), World Bank (2021a), Benoit-Norris et al. (2012), World Bank (2021a)
Health and safety	Number/percentage of injuries or fatal accidents in the organization [...]	Number of non-fatal accidents by days lost, country, and sector; number of employees by country and sector	Eurostat (2021a, 2021c), ILO (2021a, 2021b)
		Number of fatal accidents by country and sector; number of employees by country and sector	Eurostat (2021a, 2021c), ILO (2021c, 2021b)
Smallholders including farmers	*(new subcategory since 2020, no indicators available yet)*	Percentage of small & family-owned agricultural holdings by region	Eurostat (2020a)

The guidelines present 189 indicators in six stakeholder categories[3] from which the relevant indicators must be identified case-specifically. In the given case, 112 indicators are too site-specific with no generic applicability on the strategic level. 33 indicators are not affected by any strategic decision and do not apply to the case of bioethanol production. For 34, the effect of decisions on this indicator is ambivalent, and 10 indicators are redundant on the aggregated level of the model. The selection and exclusion process is detailed in the Data Repository D.3 (Details 1). This results in eight subcategories, i.e., social issues, which are the basis for developing social objective functions (SOF). For six of them, the GSLCAPO provides readily applicable indicators; for the others, indicators suited for this application case are developed in the course of formulating the SOFs (Table 17). Their operationalization and use as parameters in mathematical objective functions is based on existing approaches in this field (Kühnen and Hahn, 2017; Messmann et al., 2020) and own developments.

The social objective functions represent social fields of action, where strategic network decisions exert distinctly positive or negative impacts. Table 18 shows the nine SOFs with a semi-verbal definition of their calculation schemes. The optimizable SOFs are formulated as maximization functions as they consider the impacts and benefits of both the network itself and of substituting the two reference products.

- **SOF1** (*Local employment*) weights the number of jobs created by the network decisions with a parameter for the regional unemployment rate relative to the EU27 average. In this way, jobs created in regions with higher unemployment rates are favored (cf. Mota et al., 2015b; Zahiri et al., 2017; Zhalechian et al., 2016).
- **SOF2** (*Water use*), **SOF3** (*Living conditions*), **SOF4** (*Land-food conflict*) consider the direct, i.e., network-internal, impacts of the 2G EtOH network. SOF2 weights the water used in the network with the country-specific water stress level, which is also the indicator of SDG6.4 (FAO, 2021). SOF3 weights network-induced air emissions with regional population density and the calculatory marginal excess mortality per pollutant of each region. Finally, SOF4 is quantified by the regional grain yields to account for the potential loss in agricultural production by the network's regional land occupation.
- **SOF5** (*Economic development*) weights the regionally created economic value added by network decisions with a parameter for the regional GDP per capita

3 The methodological sheets of 2013 complemented the 2009 edition of the Guidelines for Social Life Cycle Assessment of Products (GSLCAP), and provided 189 indicators for the 30 subcategories and in five stakeholder categories. The new 2020 GSLCAPO add nine subcategories and a sixth stakeholder category (children). An according new version of the methodological sheets with complementing new indicators is planned (Life Cycle Initiative, 2021).

relative to the EU27 average. The regional GDP is one of the indicators proposed by the methodological sheets and used by the European Union in its cohesion reports (European Commission, 2017b). The economic value of network activities is assumed to mirror the cost elements of the economic objective function, i.e., higher costs contribute positively to SOF5. This assumption neglects the indirect and induced value that, e.g., a newly built facility may add to a local economy but ensures quantifiability (e.g., Govindan et al., 2016; Zhu & Hu, 2017).

- **SOF6** (*Fair salary*) weights regionally created jobs with the compound fraction between the average sector wage in a country, the country's poverty line, and the wage-poverty ratio on an EU27 average. Therefore, regions with high relative sector wages and a low relative poverty threshold are favored.
- **SOF7** and **SOF7b** (*Workers' health and safety*) use a 10-year average of lost employee-years and fatalities, respectively, per employee due to work accidents by country and sector to determine the number of employee-years and lives, respectively, that can be expected to be lost through network decisions or to be saved through substitution.
- **SOF8** (*Smallholder farming*) focuses on the value of feedstock sourced and weights it by the percentage of small and family- or communally owned farms in a region relative to the EU27 average.

For most modeled SOFs, explicit optimization is meaningful, but this is not the case for others in the given context. Although decisions exert distinctly positive or negative impacts in terms of the respective indicators (e.g., for SOF2, *water use*), the quantification and allocation of substitution quickly reveal limitations. For many processes, it is hardly possible to trace back more than one (or few) steps of their value chains. SOF2, SOF3, and SOF4 thus only assess regional impacts but no substitution benefits, while SOF8 only considers feedstock sourcing benefits but no adverse effects. Therefore, we only co-calculate these SOFs and refrain from explicitly optimizing them.

Table 18: Social objective functions.
DV_r generically represents all decision variables (detailed in Appendix C.3), broken down by region r, to illustrate the relation between network decisions and the various social parameters. DV_r thus may stand for feedstock provision and transportation, biorefinery construction, 2G bioethanol production and transportation, and substitution of 1G bioethanol or petrol. The complete mathematical formulation of the SOFs and the calculation and sources of the parameters are provided in Appendix C.2, and C.3.

Social objective function	**Generic formulation**
1) Local employment	$maximize\text{: } DV_r * job\ factor_r * \frac{unemployment\ rate_r}{unemployment\ rate_{EU27}}$
2) Water use	$DV_r * local\ water\ use * \frac{water\ stress\ level_r}{water\ stress\ level_{Europe}}$
3) Living conditions	$DV_r * local\ air\ emissions * \frac{excess\ mortality_r * population\ density_r}{excess\ mortality_{EU27} * population\ density_{EU27}}$
4) Land-food conflict	$DV_r * local\ land\ occupation * yield_r * caloric\ value\ of\ wheat$
5) Economic development	$maximize\text{: } DV_r * economic\ value_r * \frac{GDP\ per\ capita_{EU27}}{GDP\ per\ capita_r}$
6) Fair salary	$maximize\text{: } DV_r * job\ factor_r * \frac{daily\ wage_r}{daily\ wage_{EU27}} * \frac{poverty\ line_{EU27}}{poverty\ line_r}$
7a) Workers' health & safety	$maximize\text{: } DV_r * job\ factor_r * avg.employee\text{-}years\ lost_r$
7b) Workers' health & safety	$maximize\text{: } DV_r * job\ factor_r * avg.lives\ lost_r$
8) Smallholder farming	$DV_r^{feedstock} * \frac{economic\ value_r^{feedstock} * \%smallholders_r}{economic\ value_{EU27}^{feedstock} * \%smallholders_{EU27}}$

6.1.4 Social hotspot functions

The social objective functions are network-centered in their goal and scope, as global implications are mostly beyond the system boundaries of the decision-making process. However, regional decisions in a globalized economic system may also entail global implications. Therefore, and similar to Fürtner et al. (2021), the network-centered social objective functions are complemented by results from the Social Hotspots Database (Benoît-Norris et al., 2018), accessed via SimaPro 9.2.0.1. It provides country- and sector-specific social risks as well as an impact assessment method and is methodologically based on the GSLCAPO. The SHDB applies 160 indicators, data on labor intensity, and the underlying input-output model of the Global Trade Analysis Project (Aguiar et al., 2016) to calculate social risk values (so-called social hotspot indices; Benoît-Norris et al., 2018) for 140 countries and 57 sectors in 5 impact categories with 25 subcategories (cf. Table C 10). The results thus highlight existing social issues along global value chains. Risk values are expressed in medium risk hour equivalents (mrheq) per USD2011.

We compile the results into 25 social hotspot functions (SHFs) by composing a product/process system from the twelve different GTAP sectors that the network

activities (i.e., decision variables) comprise (Fig. 38). Table C 10 of Appendix C lists the 25 hotspot subcategories $h \in H$, for which social hotspot functions exist, as well as their respective top categories in the SHDB and Table 19 shows all elements of the social hotspot functions.

Table 19: Social hotspot functions[1] (basic quantity: economic value)

Function	Expression	Formulation
SHF_h	$= risk\ substuted\ with\ 1G$	$= \sum_{r\in R}\sum_{s\in R}\sum_{t\in T} P^{1G}_{r,s,t}\ \alpha^{1G}_{s}\ o^{chem}_{r}$
	$+ risk\ substuted\ with\ FF$	$+ \sum_{r\in R}\sum_{s\in R}\sum_{t\in T} P^{FF}_{r,s,t}\ \alpha^{FF}_{s}\ o^{petr}_{r}$
	$+ risk\ substuted\ with\ by\text{-}products$	$+ \sum_{r\in R}\sum_{s\in R}\sum_{t\in T}\sum_{p\in P} \left(P^{1G}_{r,s,t} + P^{FF}_{r,s,t}\right) \alpha^{byp}_{r,p}\ \theta^{byp}_{p}\ o^{byp}_{r,p}$
	$- risk\ from\ refinery\ installation$	$- \sum_{r\in R}\sum_{c\in C} B_{r,c}\ \kappa^{depr}_{c}\ \gamma^{inv}_{r}\ o^{const}_{r}$
	$- risk\ from\ refinery\ personnel$	$- \sum_{r\in R}\sum_{c\in C} B_{r,c}\ (\kappa^{pers}_{c-1} + \frac{\kappa^{pers}_{c} - \kappa^{pers}_{c-1}}{\sigma_c - \sigma_{c-1}})\ \gamma^{lab}_{r}\ o^{chem}_{r}$
	$- other\ risks\ from\ ref.operation$	$- \sum_{r\in R}\sum_{c\in C} B_{r,c}\ \kappa^{oper}_{c}\ o^{other}_{r}$
	$- risks\ from\ refinery\ processes$	$- \sum_{r\in R}\sum_{s\in R}\sum_{t\in T} \left(P^{1G}_{r,s,t} + P^{FF}_{r,s,t}\right) \kappa^{var}\ o^{chem}_{r}$
	$- risks\ from\ feedstock\ provision$	$- (\sum_{r\in R}\sum_{m\in M}\sum_{f\in F}\sum_{t\in T} F^{in}_{r,m,f,t}\ \varphi_{r,f}\ o^{agri}_{r}$ $+ \sum_{r\in R}\sum_{s\in R}\sum_{f\in F}\sum_{t\in T} F^{out}_{r,s,f,t}\ \varphi_{r,f}\ o^{agri}_{r})$
	$- fixed\ risks\ feedstock\ collection$	$- (\sum_{r\in R}\sum_{m\in M}\sum_{f\in F}\sum_{t\in T} F^{in}_{r,m,f,t}\ \varepsilon^{fix}_{t}\ o^{trans}_{r}$ $+ \sum_{r\in R}\sum_{s\in R}\sum_{f\in F}\sum_{t\in T} F^{out}_{r,s,f,t}\ \varepsilon^{fix}_{t}\ o^{trans}_{r})$
	$- var.risks\ feedstock\ collection$	$- (\sum_{r\in R}\sum_{m\in M}\sum_{f\in F}\sum_{t\in T} 2\ F^{in}_{r,m,f,t}\ \varepsilon^{var}_{t}\ \gamma^{tra}_{r}\ \upsilon_{m}\ \rho\ \tau_{r}\ o^{trans}_{r}$ $+ \sum_{r\in R}\sum_{s\in R}\sum_{f\in F}\sum_{t\in T} 2\ F^{out}_{r,s,f,t}\ \varepsilon^{var}_{t}\ \gamma^{tra}_{s}\ \delta_{r,s}\ o^{trans}_{r})$
	$- fixed\ risks\ EtOH\ distribution$	$- \sum_{r\in R}\sum_{s\in R}\sum_{t\in T} \left(P^{1G}_{r,s,t} + P^{FF}_{r,s,t}\right) \eta^{fix}_{t}\ o^{trans}_{r}$
	$- var.risks\ EtOH\ distribution$	$- \sum_{r\in R}\sum_{s\in R}\sum_{t\in T} 2\left(P^{1G}_{r,s,t} + P^{FF}_{r,s,t}\right) \eta^{var}_{t}\ \delta_{r,s}\ o^{trans}_{r}$
$\forall\ h \in H$		

[1] Formulated analogous to the economic and environmental objective functions, which are maximization functions, i.e., a positive value represents a net benefit of substituted risks versus risks accumulated from network activities

The SHDB-based risk entailed in a process is proportional to its economic value, mirroring the economic objective function. Thus, the risk value of a sector (converted to mrheq/EUR2020) in a country is multiplied by the economic value (in EUR2020) associated with decisions (e.g., biorefinery construction costs). For substituted products (e.g., petrol), the economic value can be interpreted as saved costs. The result is an absolute hotspot value (in mrheq), i.e., the aggregate of all risks entailed by all decisions taken in the production network. Therefore, production networks of different sizes are hardly comparable in absolute risk values, but the risk accumulated (or saved) per ton of 2G EtOH is more meaningful.

The social risks in different sectors or countries are explicitly *not* provided to induce divestment incentives from regions with high risks but instead aim to shed light on social issues to facilitate a positive development. This may imply that the greatest

opportunities for improving social issues can be found in regions with high social risks (Benoit-Norris and Norris, 2015). Due to ambiguous cause-effect relations and the uncertainty, whether activities, expressed by the model's decision variables, are levers for the better or reinforce adverse circumstances, the social hotspot values are also not optimized. This contrasts with those social (and economic and environmental) objective functions, where one unit of a decision variable has distinctly positive or negative effects on the respective social indicator. Instead, the 25 hotspot functions are quantified by co-calculation when optimizing other objective functions. This implies that the awareness of risks for e.g., questionable labor practices in a supply chain, enables a positive social development and due diligence of the respective operating companies.

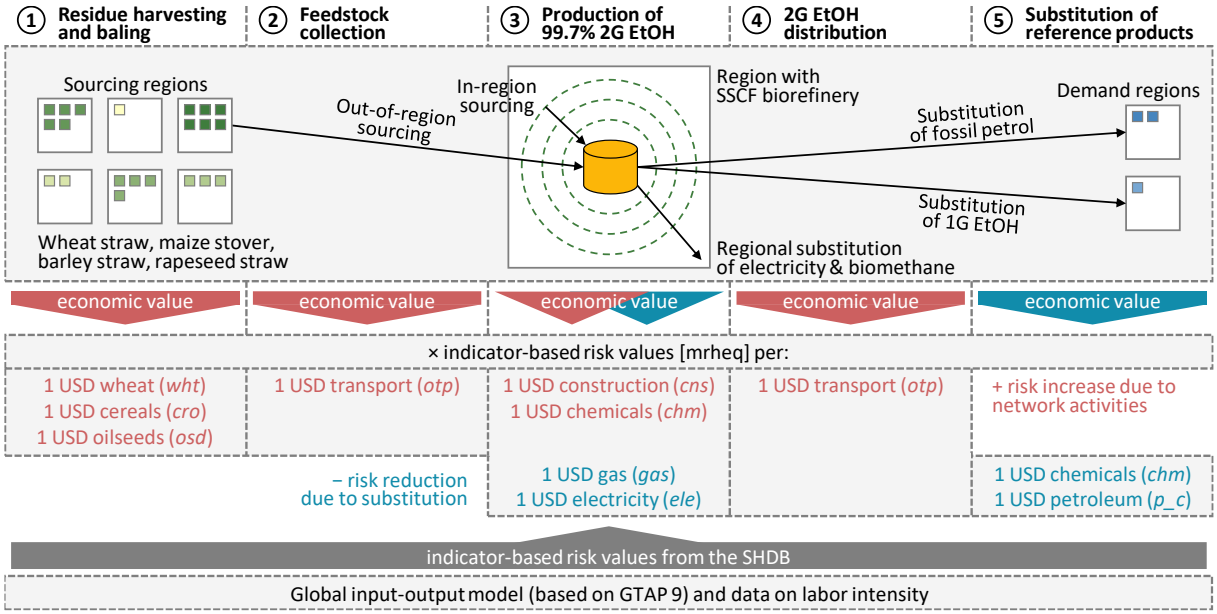

Fig. 38: Value chain activities and associated sectors

with increasing (through network decisions) or reducing (through substitution) risks, based on the underlying input-output model, the indicator values, and the impact assessment results retrieved from the SHDB. The sectors considered in the given context are wheat, cereal grains (nec.), oilseeds (nec.), transport (nec.), construction, chemical, rubber & plastic products, electricity, gas, as well as petroleum & coal products

6.1.5 Multi-objective model and experiment design

The mixed-integer linear program developed in chapter 5 is the basis for the model of this chapter and most indices, parameters, and decision variables remain the same. Table 20 provides the additional parameters that are required for the extension of the model.

Table 20: Formal description of extended social model
with additional indices, additional decision variables, and additional parameters

Additional Indices		
Indices	Definition	Description
$H = \{1 \dots 25\}$	SHDB subcat.	subcategories of the Social Hotspots Database (SHDB)
$Q = \{1 \dots 5\}$	pollutants	PM2.5, PM10, O3, NOX, BC
I	industry sectors	generic definitions based on GTAP 9 and NACE Rev. 2, depending on data availability[1]
Additional decision variables		
Variable	Domain	Definition
$B_{r,c}$	$\in \{0,1\}$	construction of a biorefinery in region $r \in R$ with fixed (i.e., facility-based) capacity level $c \in C$
$C_{r,c}$	$\in \mathbb{Q}_0^+$	variable (i.e., personnel-based) capacity of a biorefinery in region $r \in R$ with fixed capacity level $c \in C$
$S_{r,m,f}^{in}$	$\in \{0,1\}$	auxiliary variable: 1 if feedstock $f \in F$ is sourced within region $r \in R$ from sourcing annulus $m \in M$ to a biorefinery; 0 else
$S_{r,m,t}^{in}$	$\in \{0,1\}$	auxiliary variable: 1 if any feedstock is sourced within region $r \in R$ from sourcing annulus $m \in M$ to a biorefinery with transport mode $t \in T$; 0 else
$S_{r,s}^{out}$	$\in \{0,1\}$	auxiliary variable: 1 if any feedstock is sourced from region $r \in R$ and transported to a biorefinery in region $s \in R$; 0 else
$S_{r,s,t}^{out}$	$\in \{0,1\}$	auxiliary variable: 1 if any feedstock is sourced from region $r \in R$ and transported to a biorefinery in region $s \in R$ with transport mode $t \in T$; 0 else
Additional parameters		
Data	Unit	Definition
$\bar{\delta}_{r,s}$	-	gives the region index with the s-th shortest distance to region $r \in R$ (based on the distance matrix $\delta_{r,s}$ of the base model)
σ_c^{min}	-	gives the minimum required percental capacity utilization of the capacity that is added from one capacity level to another (differing between $c = 1$, and $c \in C/1$)
tts^{feed}	tkm	total allowed transport service (metric tons of feedstock × transportation distance) of feedstock
tts^{EtOH}	tkm	total transport service (metric tons of 2G EtOH × transportation distance) of 2G EtOH
δ_t^{min}	km	minimum required distance for transportation with transport mode $t \in T$
δ_t^{max}	km	maximum allowed distance for transportation with transport mode $t \in T$

Due to political realities, the United Kingdom was no longer included in the model compared to chapter five. For this reason, the size of the index set R changes to 91 (in chapter 5 it was 98). All other updates compared to the model presented in chapter 5 can be found in Table C 1 of Appendix C.1.

The mixed-integer linear programming model of this chapter builds upon the optimization model developed in chapter 5. The decision expressions remain similar but need to be slightly adapted for each Social Objective Function. Table 18 shows the generic formulation of the SOF, the mathematical formulation can be found in Table C 7, Table C 8, and Table C 9 of Appendix C.3. All linear constraints proposed in Table 15 (chapter 5.1.4) apply also in this model. To achieve reasonable results of some

of the newly introduced social objective functions, several new constraints need to be added (Table 21). This is the case for those objective functions, where negative and positive contributions to the objective value are opposite to the economic and environmental objective functions. For example, the environmental objective functions maximize the avoided burden of substituted products minus the impacts of the new production network, which means that these functions aim at achieving large substitution quantities while simultaneously limiting the impacts of the network, e.g., the number of biorefineries or transportation distances. For the social objective functions $SOF1$, $SOF5$, $SOF6$, and $SOF8$, however, larger networks and extended transportation amounts and distances lead to higher social benefits from the network, while substitution contributes negatively. Unrestrictedly, this would lead to unnecessarily large networks and unrealistically large transportation distances. Therefore, to achieve realistic and reasonable results, the following constraints have been introduced. All additionally introduced constraints are formulated to be non-binding for the solution spaces of economic and environmental objectives.

(10) ensures that the variable, personnel-dependent, capacity $C_{r,c}$ of a biorefinery with capacity level $c \in C$ is smaller than the difference between the fixed capacities σ_c and σ_{c-1}, i.e., the capacity provided by the personnel of a biorefinery with σ_{c-1} plus the additional variable capacity $C_{r,c}$ is not larger than the fixed, facility-dependent capacity of a biorefinery with σ_c.

(11) and (12) ensure that the output of a biorefinery is not larger than its capacity σ_c, and equals the fixed capacity of σ_{c-1} plus the variable capacity $C_{r,c}$. This ensures that only those jobs are created, which are required for the desired output (and not more, e.g., in $SOF1$). (11) thus renders the original constraint (2) (see Table 15) redundant. (13) and (14) ensure that no biorefineries with capacity $\sigma_1 = 0$ are built.

(15) forces the auxiliary variable $S^{in}_{r,m,f}$ to assume the value of 1 when in-region sourcing $F^{in}_{r,m,f,t}$ takes place. However, (16) and (17) ensure that in-region sourcing can only take place annulus by annulus in ascending order, i.e., sourcing from an annulus cannot take place until the feedstock potential of the previous annulus is completely sourced. This is done to prevent exclusive sourcing from the farthest possible distance within a region.

Analogously, (18) forces the auxiliary variable $S^{out}_{\delta_{r-1,s},s}$ to assume the value of 1 when out-of-region sourcing takes place between two regions. (19) and (20) ensure that out-of-region sourcing can only take place region by region in ascending order of distances, i.e., sourcing from a region to another cannot take place until the feedstock potential of all regions with shorter distances to the other region is wholly sourced.

Connecting (15) – (17) and (18) – (20), (21) ensures that out-of-region sourcing (i.e., sourcing beginning with the region with the shortest distance to the focal region) cannot take place until the feedstock potential of the focal region has been sourced.

Table 21: Additional model constraints to facilitate social objective functions

	Constraints	
(10)	$C_{r,c} \leq B_{r,c} * (\sigma_c - \sigma_{c-1})$	$\forall\, r \in R, c \in C: c > 1$
(11)	$\sum_{s\in R} \sum_{t\in T}\ (P_{r,s,t}^{1G} + P_{r,s,t}^{FF}) \leq \sum_{c\in C} B_{r,c}\ \sigma_c$	$\forall\, r \in R$
(12)	$\sum_{s\in R} \sum_{t\in T}\ (P_{r,s,t}^{1G} + P_{r,s,t}^{FF}) = \sum_{c\in C:c>1} (B_{r,c}\ \sigma_{c-1} + C_{r,c})$	$\forall\, r \in R$
(13)	$B_{r,1} = 0$	$\forall\, r \in R$
(14)	$C_{r,1} = 0$	$\forall\, r \in R$
(15)	$\sum_{t\in T} F_{r,m,f,t}^{in} \leq S_{r,m,f}^{in} * BigM$	$\forall\, r \in R, m \in M, f \in F$
(16)	$S_{r,m,f}^{in} \leq S_{r,m-1,f}^{in}$	$\forall\, r \in R, m \in M: m > 1, f \in F$
(17)	$S_{r,m,f}^{in} \leq \sum_{t\in T} \frac{F_{r,m,f,t}^{in}}{\pi \rho^2 \mu_{r,f}\ (2m-1)}$	$\forall\, r \in R, m \in M: m > 1, f \in F$
(18)	$\sum_{t\in T} \sum_{f\in F} F_{\bar{\delta}_{r-1,s},s,f,t}^{out} \leq S_{\bar{\delta}_{r-1,s},s}^{out} * BigM$	$\forall\, r \in R: r > 1, s \in R$
(19)	$S_{\bar{\delta}_{r,s},s}^{out} \leq S_{\bar{\delta}_{r-1,s},s}^{out}$	$\forall\, r \in R: r > 1, s \in R$
(20)	$\left(S_{\bar{\delta}_{r1,s},s}^{out} - 1\right) * BigM$ $\leq \sum_{u\in R} \sum_{t\in T} \sum_{f\in F} F_{\bar{\delta}_{r-1,s},u,f,t}^{out} + \sum_{u\in R} \sum_{t\in T} \sum_{f\in F} F_{\bar{\delta}_{r-1,s},m,f,t}^{in} - \sum_{f\in F} \psi_{\bar{\delta}_{r-1,s},f}$	$\forall\, r \in R: r > 1, s \in R$
(21)	$S_{\bar{\delta}_{2,s},s}^{out} \leq \frac{\sum_{m\in M} \sum_{f\in F} \sum_{t\in T} F_{s,m,f,t}^{in}}{\sum_{m\in M} \sum_{f\in F} \pi \rho^2 \mu_{s,f}\ (2m-1)}$	$\forall\, s \in R$
(22)	$\sum_{s\in R} \sum_{t\in T}\ (P_{r,s,t}^{1G} + P_{r,s,t}^{FF}) \geq \sum_{c\in C} B_{r,c}\ (\sigma_{c-1} + (\sigma_c - \sigma_{c-1}) * \sigma_c^{min})$	$\forall\, r \in R$
(23)	$\left(\sum_{r\in R} \sum_{m\in M} \sum_{f\in F} \sum_{t\in T} F_{r,m,f,t}^{in} \upsilon_m \rho \tau_r + \sum_{r\in R} \sum_{s\in R} \sum_{f\in F} \sum_{t\in T} F_{r,s,f,t}^{out} \delta_{r,s}\right) \leq tts^{feed}$	
(24)	$\sum_{r\in R} \sum_{s\in R} \sum_{t\in T}\ \left(P_{r,s,t}^{1G} + P_{r,s,t}^{FF}\right) \delta_{r,s} \leq tts^{EtOH}$	
(25)	$\sum_{f\in F} F_{r,m,f,t}^{in} \leq S_{r,m,t}^{in} * BigM$	$\forall\, r \in R, m \in M, t \in T$
(26)	$\sum_{f\in F} F_{r,m,f,t}^{in} \geq S_{r,m,t}^{in}$	$\forall\, r \in R, m \in M, t \in T$
(27)	$\sum_{f\in F} F_{r,s,f,t}^{out} \leq S_{r,s,t}^{out} * BigM$	$\forall\, r \in R, s \in S, t \in T$
(28)	$\sum_{f\in F} F_{r,s,f,t}^{out} \geq S_{r,s,t}^{out}$	$\forall\, r \in R, s \in S, t \in T$
(29)	$S_{r,m,t}^{in} \leq \frac{\upsilon_m\, \rho\, \tau_r}{\delta_t^{min}}$	$\forall\, r \in R, m \in M, t \in T$
(30)	$S_{r,m,t}^{in} \leq \frac{\delta_t^{max}}{\upsilon_m\, \rho\, \tau_r}$	$\forall\, r \in R, m \in M, t \in T$
(31)	$S_{r,s,t}^{out} \leq \frac{\delta_{r,s}}{\delta_t^{min}}$	$\forall\, r \in R, s \in S, t \in T$
(32)	$S_{r,s,t}^{out} \leq \frac{\delta_t^{max}}{\delta_{r,s}}$	$\forall\, r \in R, s \in S, t \in T$

Constraints (22) – (30) ensure economic, environmental, or practical feasibility and reasonability to prevent, e.g., maximum-sized biorefineries without output or straw transportation across the continent for the sake of, e.g., job maximization. Values for associated parameters were determined by maximum/minimum manifestations of these parameters in economic and environmental optimization. (22) requires that biorefinery capacity is utilized to a certain degree (parameter σ_c^{min}), differentiating between biorefineries with the smallest capacity level ($c = 1$), where σ_1^{min} corresponds to the minimum total utilization rate of the biorefinery's capacity, and larger capacity levels ($c > 1$), where σ_c^{min} is the minimum utilization rate of the additional capacity between

c and $c-1$. (23) and (24) limit the total transport service (in tkm) of straw and EtOH transportation, respectively, without limiting the economic or environmental functions while still retaining degrees of freedom for social objectives. (25) – (28) force the auxiliary variables $S^{in}_{r,m,t}$ and $S^{out}_{r,s,t}$ to assume the value of 1 when sourcing (in-region or out-of-region, respectively) takes place with transport mode $t \in T$, and (29) – (32) limit respective transportation distances to minimum (e.g., for rail) and maximum (e.g., for tractor) distances for each transport mode.

The MILP model is implemented in IBM ILOG CPLEX Optimization Studio 20.1.0.0. The optimization is carried out an Intel® Core™ i7-2600 CPU with four physical cores at 3.40 GHz and 32 GB RAM, and an Intel® Xeon® CPU E5-2690 with eight cores at 2.90 GHz and 64 GB RAM. The setup for single-optimization comprises 361,998 variables (100,282 of which are binary) and is limited by 400,402 constraints. The default MIP gap tolerance is 10^{-6} for single-objective optimization, with calculation times between a few hundred and 20,400 seconds. For M4, M6, M10, M14, M15, SOF1, and SOF6, the solving time is limited to eight hours (28,800s) to ensure solvability on the used systems with the given RAM, reaching MIP gaps between $1{\cdot}10^{-4}$ and $7{\cdot}10^{-3}$ within that time. For Pareto optimization, the gaps vary more strongly and range between 0.0 and $1.7{\cdot}10^{-1}$.

6.2 Results

Subsection 6.2.1 presents the socially, environmentally, and economically optimal production networks, and subsection 6.2.2 discusses the results of Pareto optimization between different pairs of objectives. Subsection 6.2.3 provides the results of the social hotspot assessment, and subsection 6.3 presents the impact of the objective functions on the SDGs semi-quantitatively.

6.2.1 Sustainable network planning

Fig. 39 presents production networks for selected objective functions of the three sustainability pillars. With economic optimization (displayed for tax scenario T3), the network of primarily high-capacity biorefineries is concentrated in countries of Central and Eastern Europe (CEE), with additional biorefineries in the EU's "breadbasket" in central France. Both are characterized by an abundant feedstock supply, and CEE countries additionally yield the economic advantage of below-average costs. The 26 biorefineries can valorize about 47% of the total feedstock potential to produce 11 Mt of second-generation bioethanol, which could substitute 10.8% of the total current petrol demand. The objective value of €1.54 billion (i.e., the profit) is relatively small compared to the network costs of €11.25 billion, which hints at a higher sensitivity towards model parameters.

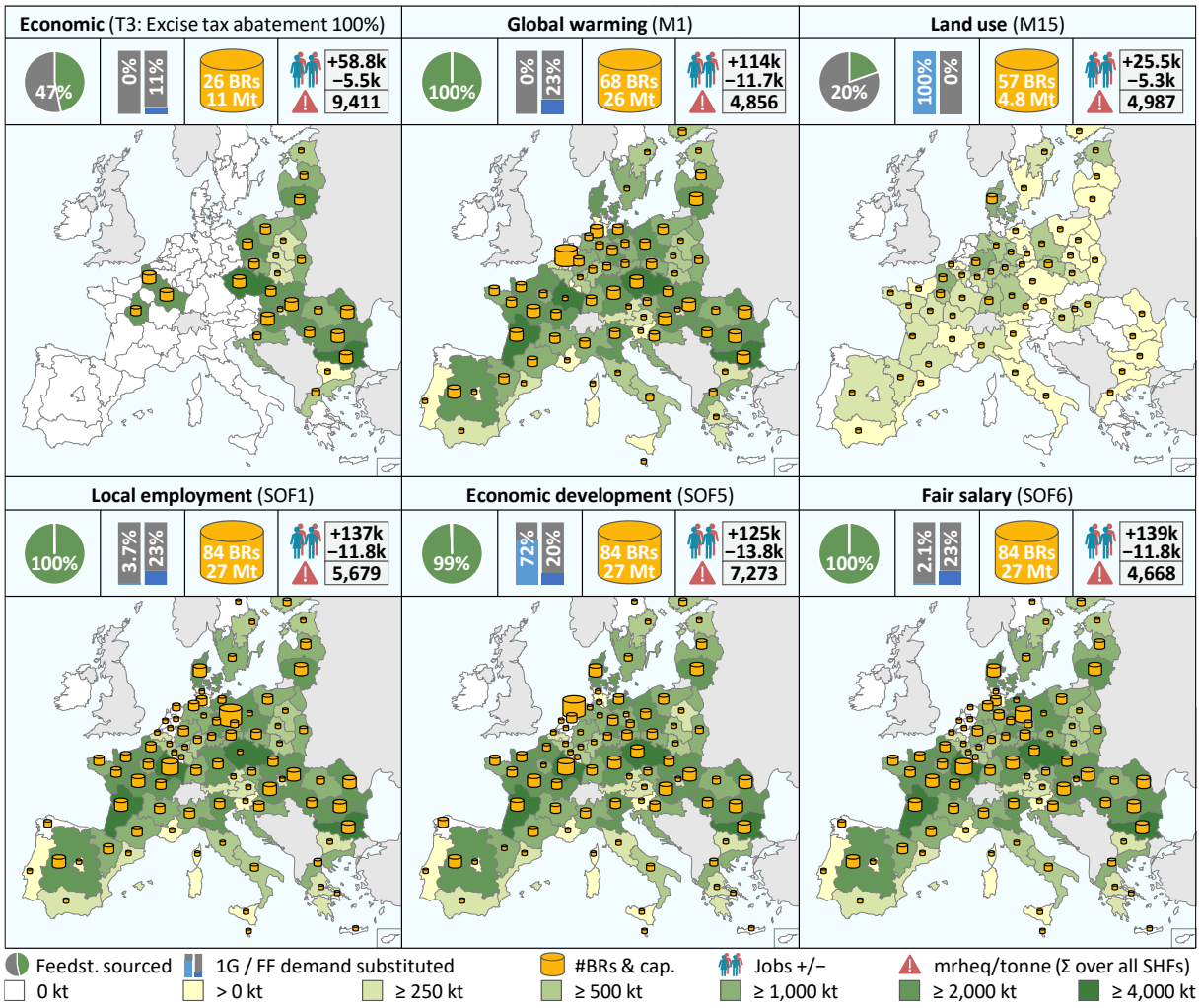

Fig. 39: Optimal biorefinery locations and capacities
(the size of cylinders corresponds to the capacity), and regional amounts of feedstock sourced (green shades, in metric kilotons) for six objectives. The legend also includes respective percentages of total feedstock collected (pie chart), the percentages of 1G demand and fossil petrol demand substituted (bar charts), the total number and total capacity of biorefineries (BRs & cap.), the number of jobs created and lost, as well as the total risk increase over all SHDB categories (in mrheq per ton). Figures C3-C14 in Appendix C.5 display analogous information for the economic objective in four tax scenarios, four environmental objectives (E2, M1, M5, M15), and four SOFs (1, 5, 6, 7), and in terms of amounts of feedstock sourced, jobs created, economic value created, and hotspot values accumulated

The environmental dimension is represented by the objectives *global warming* and *land use*, which are two relevant and conflicting environmental impact categories. While optimization of *global warming* leads to 100% utilization of the available feedstock to substitute as much petrol as possible, the objective *land use* exclusively substitutes first-generation ethanol, utilizing 20% of the available feedstock. Optimizing *global warming* results in a total benefit of 53.3 billion tons of CO_2 saved, while optimizing *land use* would only save 7.3 billion tons. Since the entire demand for 1G bioethanol is substituted with *land use* optimization, over 11.2 billion m^2 annual cropland eq. could be saved. In contrast, the optimization of *global warming* would increase the land use

impact of the network by 2.0 billion m^2 annual cropland eq. Apart from minor differences due to slightly adjusted parameters (cf. Table C 1), the results align with the results of chapter 5.

The results for the SOFs are mainly comparable to the results of the *global warming* optimization. While SOF1, SOF5, and SOF6 also suggest 100% feedstock sourcing, the substitution decision is less determined by the effects of the substitution itself. Instead, the social objectives aim to exploit opportunities, e.g., to create additional jobs or economic value where possible, and subsequently, substitute demand within the model's constraints. Even though optimization of SOF5 (*economic development*) results in the substitution of 72% of the 1G EtOH demand (compared 3.7% for SOF1 and 2.1% for SOF6), the values of SOF1 (*local employment*) and SOF6 (*fair salary*) deteriorate by only 22% and 21%, respectively, when SOF5 is optimized. The social objectives lead to distinctly negative economic objective values in every tax scenario, especially with SOF5 (T1/T2: −€19.6 billion, T3: −€8.88 billion, T5: −€5.17 billion). The total risk value (in mrheq per ton EtOH) reflects global social hotspots connected to the respective network design. A concentration on CEE countries (as for economic optimization) or a focus on underdeveloped regions (SOF5) entails significantly higher social risks than networks with large production capacities in Western European countries (cf. section 6.2.3).

6.2.2 Pareto optimization

Pareto optimization reveals the leverage of the different social parameters on the regional distribution of the activities. Regional differences are only discernible in nuances once 100% of the available feedstock potential is sourced (cf. Fig. 39). If the social dimension were not forced into a tight corset of constraints (cf. Table 21), the complete production would occur in the region with the highest social parameter value (e.g., the highest unemployment rate). When an economic constraint is introduced in Pareto optimization (applying the equidistant ε-constraint method), and less than 100% of the feedstock is sourced, regional social aspects emerge more clearly.

Fig. 40 displays Pareto-optimal frontiers between the economic objective (in tax scenario T3) and SOF1, SOF5, SOF6, and SOF7, visualizing network configurations at three points along the frontier in terms of created jobs. (a) corresponds to the Pareto point closest to 90% of the optimal economic objective value, (b) represents a numerical "compromise point" (i.e., with the shortest Euclidean distance to the two optima), and (c) is the last point with an economic profit.

The single-criteria economic optimization leads to 58,805 additional jobs, mainly in CEE countries and northern France (cf. Fig. 39), while 5,457 jobs are assumed to be lost due to the substitution of petrol. This net job creation of 53,348 already

corresponds to 42,5% of the value when maximizing SOF1 (*local employment*, 125,454). Once SOF1 is introduced as an additional objective (point a), the jobs start to shift to regions with high unemployment rates in Spain, Italy, and parts of France. However, despite exceptionally high unemployment, Greece hardly benefits from SOF1 due to its scarce feedstock supply. When sacrificing 11% profitability, the pure number of jobs created increases by 28% (from 53,348 to 68,314), but the objective value of SOF1 (in unemployment-weighted job equivalents) increases by more than 54% (from 40,067 to 61,866). These effects become more pronounced with increasing preference for SOF1 (point b). Beyond point (c), where close to 100% of the feedstock is sourced, the gradient of the Pareto frontier becomes steeper, meaning that marginal social gains are disproportionately expensive. Here, only a few regions with a combination of high costs and low unemployment rates are exempted (e.g., Southern Germany, Austria, the Netherlands).

Multi-criteria optimization between the economic objective and SOF5 (*economic development*) discriminates economically strong metropolitan regions such as most capital regions and countries such as Germany and Sweden, and favors regions in CEE countries and northern France (a and b). Even though regions of central and western Spain also have preferential model parameters due to a comparably low GDP per capita, these regions are not selected. The preference for CEE countries can be explained by the benefits in profitability *and* GDP, while costs indices in Spain hamper profitability. With a further preference for SOF5 (c), most feedstock is collected, and biorefineries are built in most regions. When higher SOF5 values are obtained, profit drops disproportionately to its lowest value in any of the curves with almost −€9 billion.

SOF6 (*fair salary*) favors regions with high sector wages relative to the poverty threshold. Regional differences in Pareto optimization are slightly more pronounced than with the other SOFs. Italy, in particular, profits from SOF6 but also selected regions in France, Spain, and Germany. The Pareto-optimal frontier has, in large parts, only a small gradient, meaning that SOF6's objective value can be tripled while remaining profitable (point c). After that point, the value again drops disproportionately.

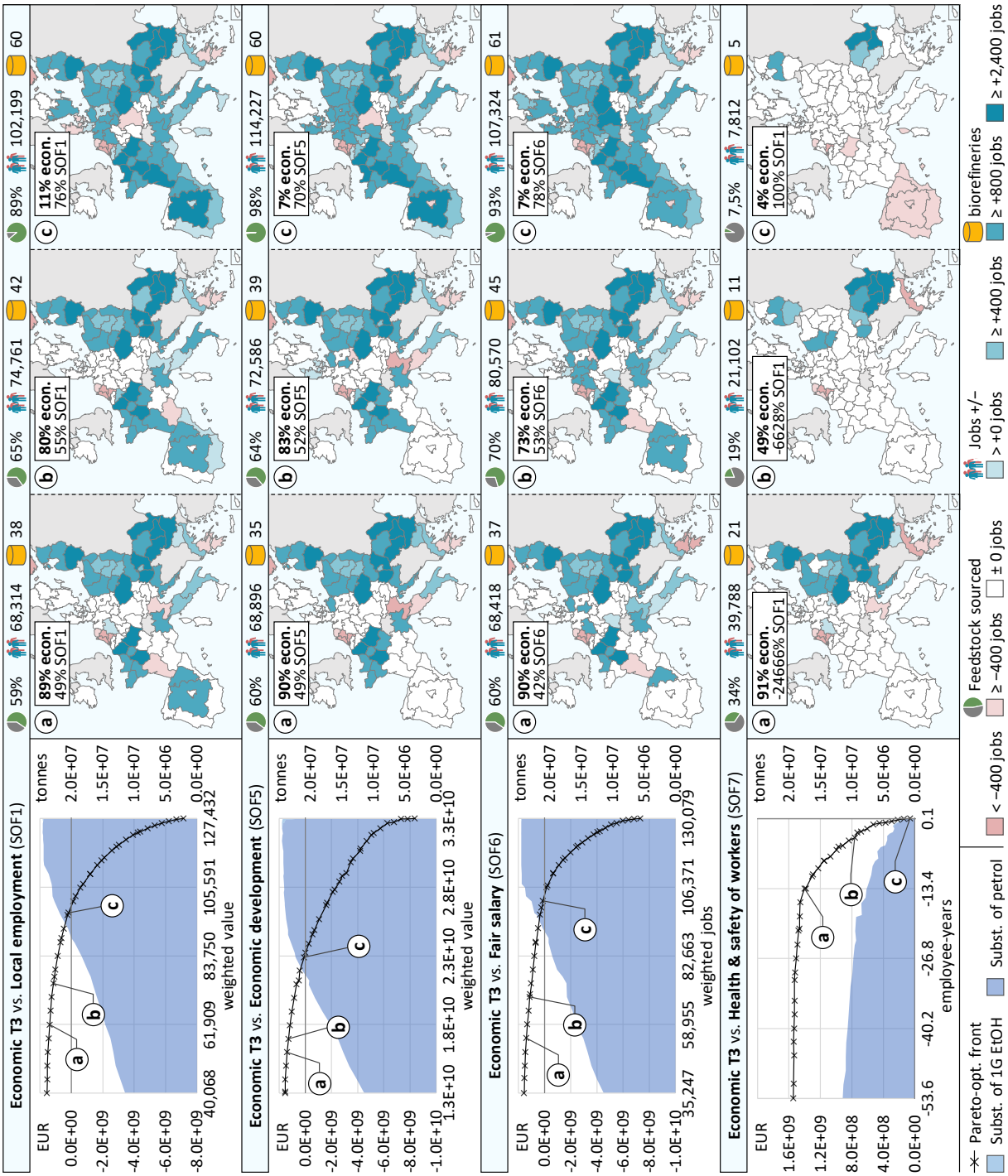

Fig. 40: Selected Pareto-optimal frontiers and EU maps
between social objective functions and the economic objective in tax scenario T3. The graphs include the substituted reference products on the secondary axes as stacked area plots. For three Pareto-optimal points, the optimal network design is displayed as maps that visualize the net number of regionally created jobs as blue/red shades. The legend also includes respective percentages of total feedstock collected, the total number of biorefineries, and the net number of jobs created and lost

The optimization towards SOF7 (*health and safety of workers*) is distinctly different from the other social objectives. While for all other SOFs, the amount of produced EtOH increases with increasing preference for them, the amount drops with preference

for SOF7. The Pareto-optimal frontier is almost level in large parts, meaning the value for SOF7 can be improved substantially without lowering profitability. At the end of the curve, the substitution benefits overcompensate health and safety issues in the bioethanol production, but the produced volumes are only a sixth of what is economically optimal (from 11.5 Mt to 1.8 Mt).

Fig. 41 shows selected Pareto frontiers between pairs of the economic (exemplified by scenario T3), environmental (exemplified by ecosystem quality), and social (exemplified by local employment) objectives. Along the Pareto-optimal fronts, the figure gives the number of biorefineries at the two respective optima and the point with the shortest relative Euclidean distance to the utopia point (cf. chapter 2.4). The graphs on the left also show volumes of substituted 1G EtOH and fossil petrol as stacked areas on the secondary axes, as substitution decisions are the key influencing element of environmental objectives. The graphs to the right (Fig. 41 b, d, and f) include the resulting values in the third objective function (secondary axes) to allow for a three-dimensional assessment.

Graph b shows a gradual increase in the number of weighted jobs with increasing emphasis on the environmental category species years, which allows to call the objectives partially congruent. A similar reasoning allows Fig. 41 d, were the value of the environmental dimension (species years) gradually grows with increasing emphasis on the number of weighted jobs. The observation of a high congruency between social and environmental objectives is further underlined by the extremely flat Pareto curve shown in Fig. 41 e and f, which means only slight detriments in one dimension for striking improvements in the respective other dimension. This observation can be explained by the fact that the substitution decision has little implication on the value of the social dimension, but very large effects on the value of the environmental dimension. Since the petroleum sector is less labor intensive, from a social perspective, a 100% substitution of petrol would be more beneficial compared to a substitution of first-generation bioethanol. However, the effect of jobs lost due to the substitution decision (either 1G EtOH or petrol) is incidental compared to the jobs created by the second-generation bioethanol production. Therefore, the solution at the strongest gradient change on the Pareto-frontier between the two objectives *weighted jobs* and *species years* seems to be a reasonable trade-off. Interestingly, Fig. 41 f also demonstrates that the profitability reaches with about minus €10 billion its minimum at this tradoff solution.

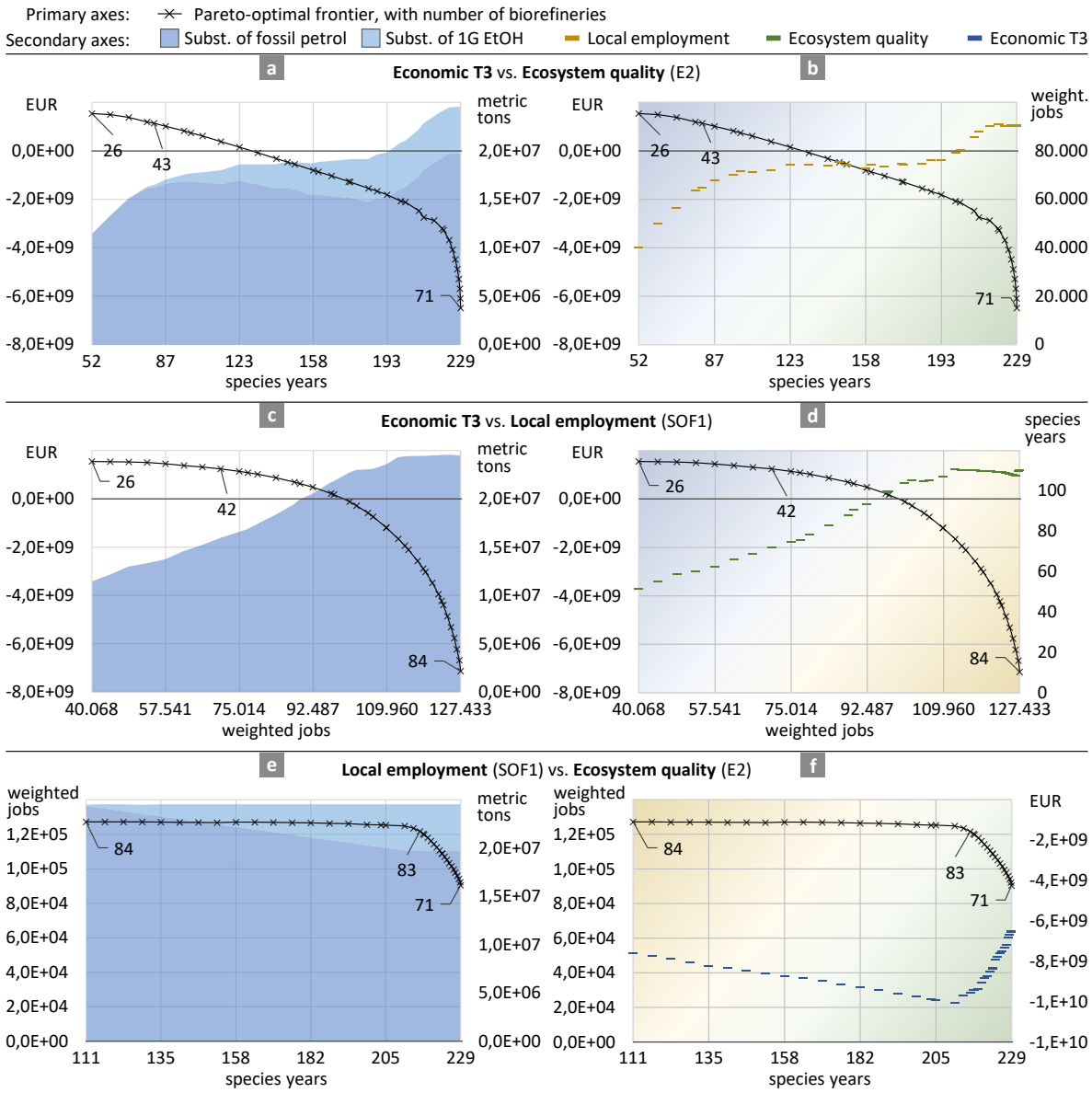

Fig. 41: Selected Pareto-optimal frontiers
between pairs of economic (T3), environmental (ecosystem quality), and social (SOF1) objectives

6.2.3 Social hotspots

Fig. 42 shows social hotspots in networks of selected objective functions. Over all objective functions, SHF13 (*injuries & fatalities*) is the most relevant hotspot, followed by SHF6 (*freedom of association, collective bargaining, right to strike*), SHF12 (*toxics & hazards*), and SHF10 (*discrimination & equal opportunities*). SHF25 (*smallholder vs. commercial farms*), SHF4 (*forced labor*), and SHF16 (*high conflict zones*) appear among the most critical hotspots occasionally. High risks in a country-sector are either due to high specific risk values or stem from a high share of network activities, which is why the feedstock sector with its high share in the overall production costs has by far the most prominent social hotspots, regardless of SHF.

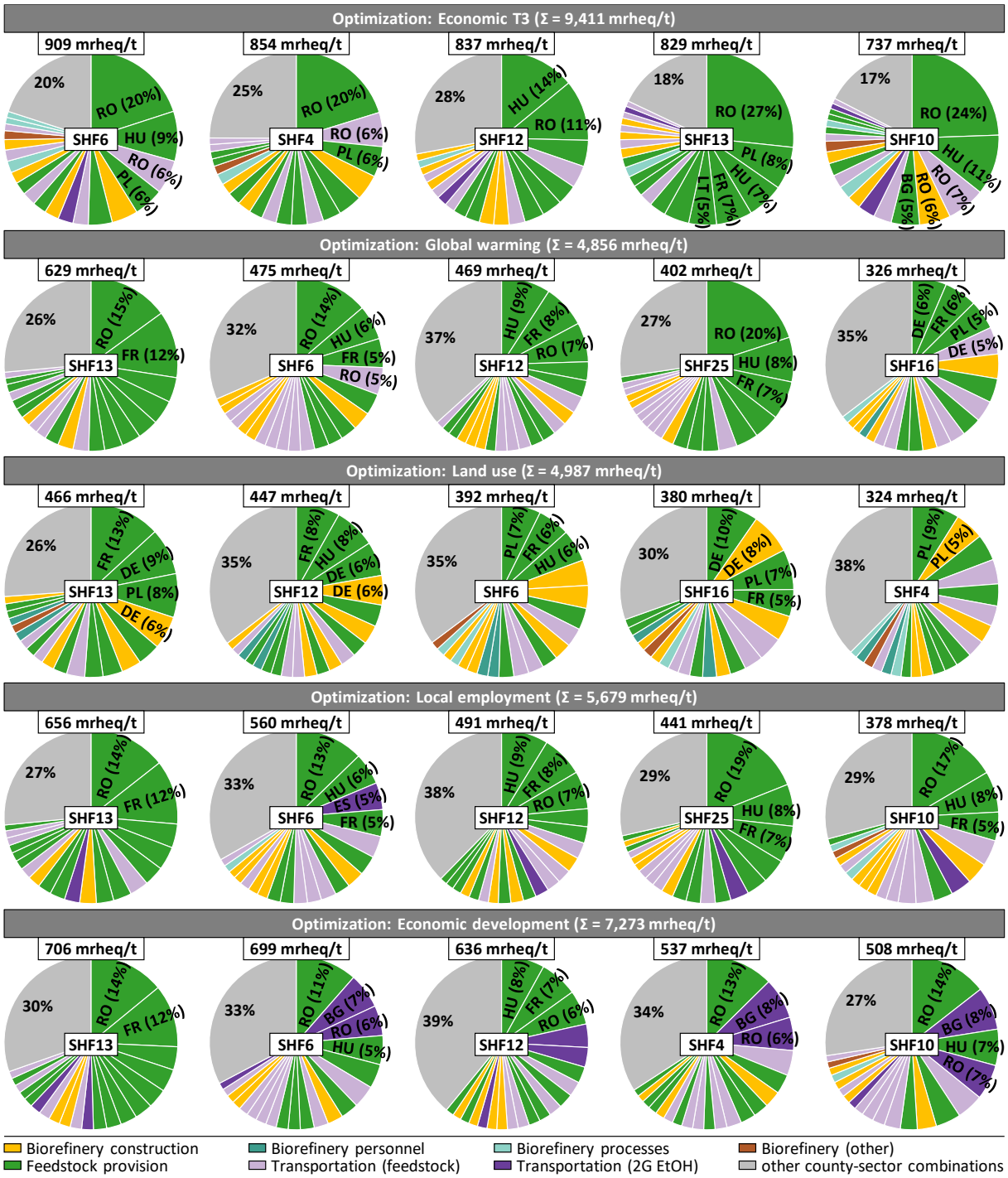

Fig. 42: Relative contributions of country- and sector-specific social risks to five SHFs, co-calculated for different objective functions. The included SHFs are the five SHFs with the highest contribution to the total risk per ton EtOH (over all SHFs) per objective function. Each pie chart provides the 20 country-sector hotspots with the highest contribution. Figures Fig. C 16, Fig. C 17, and Fig. C 18 in Appendix C.7 evaluate the category-, regional-, and process-wise aspects of the hotspot analysis on an aggregated level

The economic objective comes with the highest social risks and is about twice as exposed to risk as *global warming* (9,411 compared to 4,856 mrheq.). The relatively high risks can be explained by a focus of activities on CEE countries, which, on average,

have higher social hotspot values. The feedstock sector in Romania has the highest contribution in most of the hotspot functions, contributing up to 27% to the total *injuries & fatalities* risks (ILO, 2021d). This is mainly attributed to Romania's feedstock sector inherently and the contributing chemicals sector (fertilizer provision). Likewise afflicted with high social risks are Romania's transportation and construction sector and Hungary's feedstock sector. Networks based on the objectives *global warming* and *land use* are significantly less critical due to networks that are more widely distributed over all countries. Here, Germany, France, and Poland are also significant hotspots. This is primarily explained by their large share in the value chain (see Fig. 39) and secondarily (e.g., for SHF16) by above-average indicator values in the SHDB (e.g., in Germany due to violent xenophobic incidents and a comparably large proportion of immigrants; Benoît-Norris et al., 2018; HIIK, 2021; UNHCR, 2021). Comparing *land use* with *global warming*, the construction sector is more critical due to smaller biorefineries and resulting lower scale effects. The network of *local employment* optimization slightly emphasizes countries with higher unemployment rates like France, Spain, or Italy, wherefore they appear among the high-risk countries. *Economic development* favors economically weaker regions (esp. CEE countries, south Italy, and western Spain). Since this objective in particular involves long-distance transportation of EtOH, this sector is also subject to significant risks, especially in terms of SHF4, SHF6, and SHF10.

6.3 Implications on the Sustainable Development Goals

Together with the environmental and economic categories, the SOFs and SHFs cover 16 of the 17 Sustainable Development Goals based on our allocation scheme. Table 22 shows the matching of SOFs, SHFs, environmental and economic objective functions to individual goals, targets, and indicators of the SDGs. The SDGs are gone through by rows, and suitable objective functions are matched to the goal itself, a sub-target, or an indicator, and one objective may be matched with more than one SDG. By calculating pair-wise opportunity costs (i.e., the percental detriment in one category when optimizing another objective function; Fig. C 20), conflicts and congruencies between the different optimizable objective functions are revealed.

Table 22: Matching of all considered objective functions to SDGs.
Objective functions are clustered into the social (SOFs & SHFs), environmental and economic dimension and the SDGs are further subdivided into overall Sustainable Development Goals, Sub-Targets, and SDG Indicators.

Sustainable Development Goals (G) with adressed Targets (T) and Indicators (I)	Economic	Environment.	Social
G1 No poverty			SHF1
G2 Zero hunger			SOF4, SH15
T3 Double agricultural productivity and income of small-scale food producers			SOF8, SHF25
G3 Good health and well-being		E1, M13, M14	
T3. End the epidemics			SHF18
T4. Reduce premature mortality from non-communicable diseases		M2, M3	SHF17
T9. I1. Mortality rate due to air pollution			SOF3
Tc. Increase health financing			SHF24
G4 Quality education			
G1 Ensure free, equitable and quality primary and secondary education for all			SHF23
G5 Gender equality			SHF15
G6 Clean water and sanitation			
T1. Achieve universal and equitable access to safe and affordable drinking water			SHF21
T2. chieve access to adequate and equitable sanitation and hygiene			SHF20
T4. substantially increase water-use efficiency across all sectors		M18	
I2. Level of water stress: freshwater withdrawal as a proportion of resources			SOF2
G7 Affordable and clean energy	Economic		
G8 Decent work and economic growth			
T1. Sustain per capita economic growth			SOF5
T2. Higher levels of economic productivity	Economic		
T5. Achieve full and productive employment and decent work for all			SHF1, SHF11
I1. Average hourly earnings			SOF6
I2. Unemployment rate			SOF1
T7. Take immediate and effective measures to eradicate forced labour			SHF3, SHF4
T8. Protect labour rights and promote safe and secure working environ. for all			SHF6, SHF7
I1. Frequency rates of fatal and non-fatal occupational injuries			SOF7, SOF7b, SHF12, SHF13
G9 Industry, innovation and infrastructure			
T3. I1. Proportion of small-scale industries in total industry value added			SOF8, SHF25
G10 Reduced inequalities			
T3. I1. Equal opportunity and reduce inequalities of outcome			SHF10
G11 Sustainable cities and communities			
T3. Enhance inclusive and sustainable urbanization		M15	
T6. Reduce the adverse per capita environmental impact of cities		M5	
I1. Annual mean levels of fine particulate matter (e.g. PM2.5 and PM10) in cities			SOF3
G12 Responsible consumption and production			
T2. Achieve the sustainable management and efficient use of natural resources		E3, M16, M17	
G13 Climate action		M1	
G14 Life below water			
T1. Prevent and significantly reduce marine pollution of all kinds		E2, M9, M12	
G15 Life on land			
T1. Ensure the conservation, restoration and sustainable use of terrestrial and inland freshwater ecosystems and their services		E2, M6, M7, M8, M10, M11	
G16 Peace, justice and strong institutions			
T1. Significantly reduce all forms of violence and related death rates everywhere			SHF16
T3. Promote the rule of law at the national and international levels			SHF19
T5. Substantially reduce corruption and bribery in all their forms			SHF20

Fig. 43 shows the opportunity costs in the form of percentage detriment compared to the maximum achievable value for four social, environmental, and economic objectives. The different economic tax scenarios are most clearly missed if environmental or social goals are pursued. The *status quo* tax scenario has huge opportunity costs for optimization towards each other considered objective function. The higher the potentially achievable revenue of 2G EtOH, the lower are the detriments. For example, the optimization of global warming benefits (M1) contracts the economic optimal solution for the scenario €375 carbon tax per ton CO_2 by "only" 72%, which implies a positive profit in an environmentally optimal solution. For the environmental dimension, the magnitude of opportunity costs ranges from very low to high and is up to the substitution decisions (see chapters 5.2.1 and 5.2.2).

Category		Optimization results: Objective values	Substitution: 1G	Substitution: FF	Opportunity costs (detriment in %): T1/2	T3	T5	E2	M1	M5	M15	SOF1	SOF5	SOF6	SOF7
Economic			1G	FF											
T1/2	Status Quo / −50% tax	1.51×10^8 EUR	0%	3.5%				<−999%	<−999%	<−999%	<−999%	<−999%	<−999%	<−999%	−754%
T3	−100% excise tax abatem.	1.55×10^9 EUR	0%	11%				−520%	−414%	−511%	−316%	−592%	−674%	−574%	−96%
T5	€375 carbon tax	6.25×10^9 EUR	0%	19%				−114%	−72%	−113%	−155%	−136%	−183%	−140%	−99%
Environmental			1G	FF	T1/2	T3	T5	E2	M1	M5	M15	SOF1	SOF5	SOF6	SOF7
E2	Ecosystem quality	229 species.yrs	100%	19%	−92%	−77%	−56%	0%	−46%	0%	−43%	−52%	−18%	−52%	−95%
M1	Global warming	5.75×10^{10} kg CO_2 eq	0%	23%	−85%	−56%	−18%	−7%	0%	−8%	−87%	−7%	−9%	−7%	−94%
M5	Fine part. matter form.	1.97×10^7 kg PM2.5 eq	100%	19%	−90%	−72%	−44%	0%	−32%	0%	−55%	−46%	−21%	−48%	−96%
M15	Land use	1.12×10^{10} m^2a crop eq	100%	0%	−103%	−110%	−116%	−14%	−118%	−14%	0%	−117%	−46%	−119%	−97%
Social			1G	FF	T1/2	T3	T5	E2	M1	M5	M15	SOF1	SOF5	SOF6	SOF7
SOF1	Local employment	127k job eq.	3.7%	23%	−93%	−69%	−39%	−29%	−30%	−29%	−87%	0%	−22%	−12%	−97%
SOF5	Economic development	3.30×10^{10} value eq.	72%	20%	−94%	−59%	−44%	−28%	−28%	−28%	−86%	−15%	0%	−22%	−93%
SOF6	Fair salary	130k job eq.	2.1%	23%	−92%	−73%	−41%	−27%	−25%	−27%	−82%	−6%	−21%	0%	−96%
SOF7	Health & Safety	5.42×10^{-2} empl.yrs	4.9%	1.5%	<−999%	<−999%	<−999%	<−999%	<−999%	<−999%	<−999%	<−999%	<−999%	<−999%	0%

Fig. 43: Different social, selected relevant environmental, and economic objectives with objective values and units. The figure also includes opportunity costs in each category to optimize the other environmental categories. For example, the objective value of global warming (M1) is diminished by 87% compared to its objective value when land use (M15) is optimized. It also displays substitution decisions (in % of the 1G/fossil fuel demand substituted, pie charts), which is the most influential decision on opportunity costs between environmental categories

For socially optimal solutions, the percentage detriment of environmental decision range from 7% to almost 120%. Since SOF7 leads to very small networks, the opportunity costs are higher than for the other SOFs. The objective *global warming* contracts by only 7 to 9% for SOF1, 5, and 6, which means that pursuing those social objectives is congruent with objective global warming. The three social objective

functions, SOF1, SOF5, and SOF6, have only little detriments among each other, while social objective seven (health and safety workers) has much larger opportunity costs.

By matching objective functions to SDGs (as shown in Table 25) and calculating the opportunity costs between the objective functions (as shown in Fig. 44), the relationships among the SDGs can be evaluated. Fig. 44 displays the aggregated information on the relationships between the social, environmental, and economic objective functions on the level of their associated SDGs. Two indications are given for each pair of SDGs, representing the range between the most conflicting and the most congruent relationship between two objective functions of the associated SDGs. The colored shades indicate whether conflicts (red) or congruencies (blue) prevail qualitatively.

Optimization of objective functions associated with: / Effect on objective functions associated with:		SDG3	SDG6	SDG7	SDG8	SDG11	SDG12	SDG13	SDG14	SDG15
SDG3	Good health and well-being	−− / +++	+ / ++	−− / +	−− / ++	−− / +++	−− / +++	−− / +++	−− / +++	−− / +++
SDG6	Clean water and sanitation	+ / +++	+++	−	−− / +	+ / +++	−− / o	−−	+ / +++	+ / +++
SDG7	Affordable and clean energy	−−	−−	+++	−− / +++	−−	−− / o	−−	−−	−−
SDG8	Decent work and economic growth	−− / ++	−− / +	−− / +++	−− / +++	−− / ++	−− / ++	−− / ++	−− / ++	−− / ++
SDG11	Sustainable cities and communities	+ / +++	+ / +++	− / +	− / ++	+ / +++	− / ++	− / ++	+ / +++	+ / +++
SDG12	Responsible consumption and production	−− / ++	−− / +	−− / +	−− / ++	−− / ++	−− / +++	−− / +++	−− / ++	−− / ++
SDG13	Climate action	+ / ++	+	+	o / ++	+ / ++	o / +++	+++	+ / ++	+ / ++
SDG14	Life below water	−− / +++	+ / +++	−− / +	−− / ++	−− / +++	−− / ++	−− / ++	−− / +++	−− / +++
SDG15	Life on land	−− / +++	− / ++	−− / +	−− / ++	−− / +++	−− / ++	−− / ++	−− / +++	−− / +++

Fig. 44: Relationship between social, environmental, and economic objective function on the level of their associated SDGs, based on opportunity cost calculation (percental detriment in one category compared to its optimal value when optimizing another). SDGs with optimized objective functions are displayed on top of the table, affected ones to the left. Categories are assumed to be fully congruent with a detriment of less than −5% (+++), congruent between −5% and −50% (++), slightly congruent between −50% and −95% (+), either neutral or unrelated between −95% and −105% (o), conflicting between −105% and −150% (−), and strongly conflicting with a detriment of more than −150% (−−)

As with conflicts and congruencies on the level of different objective functions, the achievement of SDGs may be hindered or promoted by pursuing different goals. The goal of *Climate Action* (**SDG13**) profits throughout all other objective functions. Networks optimal for all other goals range from slightly to strongly co-beneficial for SDG13, yielding the more benefits, the more petrol is substituted. This finding is plausible since the life cycle assessment results indicate positive climate benefits of 2G EtOH, regardless of whether petrol or 1G EtOH is substituted. Also, for the other

SDGs, the results show that a large portion of conflicts between environmentally-oriented SDGs stems from opposing substitution decisions, wherefore affected SDGs behave ambiguously towards the others. This is the case for **SDG3**, **SDG11**, **SDG14**, **SDG15**, and, with the most pronounced tendencies, **SDG6**. A production network optimal in terms of *global warming potential* (SDG13) jeopardizes the achievement of *Clean Water and Sanitation* (SDG6) since the regional water demand increases when petrol is substituted by locally produced second-generation bioethanol. In contrast, the optimization of objective functions of *Good Health and Well-being* always leads to co-benefits for SDG6 (e.g., E1 and M13; both suggest petrol and 1G EtOH substitution, however, the production network of M13 is about half as large as for E1 optimization) and even comprises fully congruent objectives (e.g., M14 and M18; exclusive substitution of 1G EtOH for both objectives).

Fig. 44 also reveals conflicts between the three pillars of sustainability, such as with the goal *Affordable and Clean Energy* (**SDG7**; linked with the economic objective). The optimization of SDG7 entails minor benefits and some detriments for all other SDGs. Vice versa, pursuing any other of the goals compromises SDG7 strongly. This can be explained by matching the goal of *Affordable and Clean Energy* with the economic objective function. The economic objective leads to the lowest specific EtOH prices (cf., Fig. 34 in chapter 5.2.2), whereas all other objectives imply higher specific EtOH prices.

Divides may also run between different targets within one SDG, depending on the perspective and the sustainability dimension, or even within one target, depending on the context. For example, the goal *Decent Work and Economic Development* (**SDG8**) can be divided into two groups: The corporate and profit-focused economic objective (matched with target 8.2) together with health & safety issues (matched with target 8.8.1), and the second group, which is composed the societal and GDP-focused SOF5 (matched with) together with employment SOF1 (matched with target 8.1 and 8.5.2, respectively) and remuneration issues (SOF6; target 8.5.1). The first group is highly conflicting with the second group and all other SDGs, while the second group co-benefits from the others. Similarly, **SDG12** with target 12.2 (natural resources) is divided into E3 (*resource availability*) & M17 (*fossil resource scarcity*), and M16 (*mineral resource scarcity*). The former generally benefit from any bioethanol network, particularly from the substitution of petrol, while the latter is impacted by the material requirements of the network itself, with only minor substitution benefits.

The remaining SDGs are associated with non-optimizable SOFs and SHFs, for which a calculation of distinct opportunity costs is not meaningful due to non-existent optimal values. For these categories, the conflicts and congruencies are quantified by normalizing them between their best and worst values overall economic, environmental,

and social optimization. This way, the indications, and shades visualize worse-than-average and better-than-average results in these SHFs and SOFs when the (optimizable) economic, environmental, and social objectives are optimized. This is based on calculating the percental detriment in the per-liter-values of category when optimizing one of the (economic, environmental, social) objective functions, normalized between the worst and the best value over all objective functions. Categories reach values close to the best value (normalized detriment of less than −5%: +++), significantly better than average values (−5% to −25%: ++), better than average values (−25% to −45%: +), average values (−45% to −55%: o), worse-than-average values (−55% to −75%: −), and significantly-worse-than-average values (with a normalized detriment of more than −75%: −−). Indications are given as a range between the most conflicting and the most congruent relationship between categories associated with each pair of SDGs. Fig. 45 displays the relationships of SDGs associated with the non-optimizable SOFs and SHFs.

Optimization of objective functions associated with: / Effect on SHFs / SOFs associated with:	SDG3	SDG6	SDG7	SDG8	SDG11	SDG12	SDG13	SDG14	SDG15
SDG1 No poverty	+ / ++	+	+	−− / ++	++	++	++	++	+ / ++
SDG2 Zero hunger	−− / +++	− / +	o / +	−− / +++	−− / +++	−− / +++	o / +++	−− / +++	−− / +++
SDG3 Good health and well-being	−− / +++	− / +++	− / +++	−− / +++	−− / +++	− / +++	− / +	−− / +++	−− / +++
SDG4 Quality education	+ / ++	+	o	−− / ++	+	+ / ++	+	+ / ++	+
SDG5 Gender equality	− / o	−	−	−− / +	− / o	o / +	o	− / o	− / o
SDG6 Clean water and sanitation	−− / ++	−− / ++	−− / +	−− / +++	−− / ++	−− / +++	−− / o	−− / +	−− / ++
SDG8 Decent work and economic growth	−− / +	−− / −	−− / o	−− / ++	−− / +	−− / ++	−− / +	−− / +	−− / +
SDG9 Industry, innovation and infrastructure	o / ++	o	o	−− / +++	+ / ++	+ / +++	+	+	+ / ++
SDG10 Reduced inequalities	+ / ++	+	o	−− / ++	+	+ / ++	+	+ / ++	+ / ++
SDG11 Sustainable cities and communities	−− / +++	+++	+++	−− / +++	+++	+ / +++	+	+++	−− / +++
SDG16 Peace, justice and strong institutions	−− / ++	−− / +	−− / o	−− / ++	−− / +	− / ++	− / +	−− / ++	−− / ++

Fig. 45: Relationship between social, environmental, and economic objective function on the one hand (to the top), and non-optimizable SOFs and SHFs on the other hand (on the left), on the level of their associated SDGs. The colored shades indicate whether conflicts (red) or congruencies (blue) prevail qualitatively

The effect of optimizable objective functions on non-optimizable objective functions can be clustered into four groups. The first group is characterized by neutral to positive effects of all objective functions on all non-optimizable SOFs and Social Hotspot Functions relevant for the respective SDG, which applies to **SDG1**, **SDG4**, **SDG9**, and **SDG10**. The second group is characterized by negative to neutral effects, which

applies only for **SDG5**, *gender equality*. This could be attributed to the fact that a second-generation bioethanol network would mainly support industries with deficiencies in gender equity (e.g., construction sector). The third and fourth groups are characterized by a wide range from negative effects to positive effects within the same SDG. In the third group, most effects are negative, which pertains to **SDG6**, **SDG7**, and **SDG16**. The fourth group comprises SDG2, SDG3, and SDG11, and the majority of effects are positive, while a few effects are negative. For example, *zero hunger* (SDG2) belongs to this group, and especially objective functions with high substitution values of 1G EtOH (e.g., land use optimization; M15) positively affect land/food conflicts. At the same time, SHF25 *smallholder vs. commercial farms* is part of SDG2 and negatively affected by land use optimization due to a decreased demand for agricultural land.

Fig. 44 and Fig. 45 serve the purpose of visualizing tendencies in conflicts and congruencies between the various SDGs. For insights on the detailed relationships on the level of individual SOFs and SHF, the effects should be assessed individually, based on the relationships between the associated individual categories, which is displayed in Fig. C 20 and Fig. C 21.

6.4 Discussion and conclusion on the socially extended model

Chapter 6 provides a best-practice approach for a structured and transparent inclusion of a comprehensive set of social aspects. This is done by selecting applicable quantitative and operationalizable social indicators from the Guidelines for Social Life Cycle Assessment of Products and Organizations and the Social Hotspots Database. The approach is applied in a network optimization model for second-generation bioethanol in the EU. The complete set of categories encompasses economic, 21 environmental, and 34 social functions. The model thereby addresses 16 of the 17 SDGs and extends existing work, especially by operationalizing the social dimension. The results allow for identifying socially optimal decisions (social objective functions) and evaluating possible social hotspots in global value chains (social hotspot functions).

The different objective functions lead to three fundamentally different network structures, some of which are closely related to the substitution decision. First, economically optimal networks concentrate on lower-cost CEE countries to be competitive with fuel prices more expensive countries (especially in scenarios T1–T3). The higher the subsidization (excise tax abatement or carbon taxation), the more competitive bioethanol becomes, leading to more extensive production networks. Second, several environmental objectives suggest an exclusive substitution of 1G bioethanol with widely dispersed but capacity-wise small production networks (e.g., *land use*). The third principal network structure comprises environmentally optimal solutions that fully exploit the feedstock potential in large production networks.

Depending on the environmental objective, 2G bioethanol should either substitute 1G bioethanol *and* petrol (e.g., *ecosystem quality*) or petrol exclusively (e.g., *global warming*). Most of the social objective functions fall into this group due to, i.a., the benefits in employment and regional development, but the effects of substitution are less decisive than the spatial layout of the network itself. The feedstock sector of Romania constitutes the most significant social hotspot, to which *injuries & fatalities* contribute the most. It is followed by Hungary's feedstock sector, where *toxics & hazards* are particularly critical. Therefore, when a bioethanol producer decides to invest in these countries, due diligence and supplier auditions are necessary to ensure safe working conditions. In addition, construction and transportation sectors also entail notable risks that would, in practice, need to be assessed in detail.

The analysis of relationships between SDGs supports the notion that sustainability of strategic decisions is not universal but rather case-specific and varies between a plethora of interconnected social, environmental, and economic criteria. Decision-makers, be it on a corporate level and following one or more business objective functions, or on a political level and using the SDGs as a framework, need to be aware of reciprocities between the various criteria. Given the diversity of the different goals, pursuing a specific goal will necessitate concessions in others. SDG8 and SDG12 are prime examples for why one action can benefit or harm not only different sustainability goals differently but also targets and indicators within the same goal. On a more thematic level, particularly the bioeconomy is at the center of tensions between different stakeholders. European policy-makers could use the lever of taxation (cf. chapter 5.2.1) to improve the competitiveness of 1G and 2G bioethanol vis-à-vis fossil fuels to foster the achievement of inter alia SDG13 while simultaneously realizing significant benefits in terms of, i.a., employment (SDG8.5) and regional development (SDG8.1). This decision needs, however, to be taken consciously. The labor intensity of residue harvesting and transportation and the hereby accumulated risk for adverse social circumstances along the global upstream value chains could create new hotspots that must be monitored. The decision would also put further stress on land, water, mineral resources, and food security, especially in the case of 1G ethanol. The discontinuation of subsiding 1G bioethanol alleviates some of the latter tensions but prevents the full climate, employment, and regional development potential from being unlocked. Especially corporate decision-makers need to be aware of the likely hotspots in their specific value chains (section 6.2.3), but also of the potential for environmental and social benefits that adjustments of strategic decisions yield, which could be unlocked with comparably small sacrifices in profits (section 6.2.2). It bears mentioning that, while aspects of 16 of 17 SDGs are covered, this work cannot address the interrelationships between all SDGs, as the objective functions only relate to individual subordinate targets or to the goals only ideationally.

The intricacy of modeling the benefits of substitution in SOF2, SOF3, SOF4, and SOF8 implies that they cannot be optimized and thus represent cradle-to-gate approaches. At the same time, the optimizable SOFs and the environmental and economic objectives are characterized as cradle-to-tank, including avoided burdens. Further developments should be able to operationalize these aspects, too, to circumnavigate this common challenge in LCSA (Valdivia et al., 2021). Furthermore, the most readily applicable indicators are not necessarily those that society and academia should keep relying on in the medium term. While the GDP is a commonly applied indicator in similar studies and European cohesion policy (European Commission, 2017b) with undoubted advantages, the measurement of the well-being of the various societal stakeholders should arguably go beyond this metric (Hoekstra, 2019).

Lastly, this work takes only an ex-post and aggregated look at the co-calculated (i.e., not optimized) social hotspot functions, as the risk scores from the SHDB are designed to shed light on potential social grievances without inducing divestment incentives from regions with high risks (Benoit-Norris and Norris, 2015). The approach provides a valuable basis for decision-makers in strategic supply chain design by pointing at hotspots. Subsequent analyzes would be necessary in practice to elucidate the circumstances behind the values on both echelons, countries and sectors, and for each indicator. Future work could also incorporate the SHDB's risk scores ex-ante by optimizing improvements in social hotspots; here, the causality between strategic decisions and the actual improvement or deterioration of social criteria is the principal academic, interdisciplinary challenge.

7 Discussion

This dissertation is composed of four contextual chapters in which the five research questions posed at the outset are answered. Chapter 3 explicitly addresses research question 1 and investigates the agroforestry residue streams in the European Union at the regional level to identify the most promising feedstocks for bio-based value chains. The agroforestry feedstock potential is differentiated in (1) the theoretical potential that includes all parts of the harvested biomass without dedicated use in the food, feed, or industrial production, (2) the technical potential, which considers technical and sustainability factor limitations, and finally (3) the bioeconomic potential which additionally considers prioritized feedstock applications. Based on the historic agricultural production and the applied methodology, wheat straw has the highest average bioeconomic potential in the agricultural sector (46 Mt), followed by maize stover (31 Mt), barley straw (16 Mt), and rapeseed straw (14 Mt). Together, those four agricultural residues account for about 80% of the cereals and oil crops' harvesting residues. Wheat straw is most abundant in the North of France and the Czech Republic. Grain maize is most abundant in France (Sud-Ouest and Ouest) and Northeast Italy. The main barley straw potentials are in Northern France, Central Spain, and Denmark. In the forestry sector, waste bark from two coniferous species, spruce, and pine is the most promising source, with a bioeconomic potential of 15 Mt, and Scandinavia and central Europe have the largest supply.

The applied assessment approach is based on aggregated and generalized data, and the most severe limitation in the investigation of research goal 1 is the assumption of constant *residue to crop ratios* and constant *sustainable removal rate* per considered crop, since both factors partly depend on regional and terrain specific features (Scarlat et al., 2019). The *Association of German Agricultural Assessment and Research Organisations,* for example, provides a method to calculate a soil-specific humus balance and thereby provides a basis for regionalized sustainable removal rates (VDLUFA, 2014). The method requires region-specific parameters that are difficult to obtain in macro-level assessments. Comparable works on the assessment of agroforestry residue potentials, like the S2Biom project (Dees et al., 2017) and the works Scarlat et al. (2019) and Scarlat et al. (2010), achiev comparable total residue potentials but differentiate in factors like spatial resolution, considered residues, or years considered.

Chapter 4 of this work addresses the second research goal and develops an approach to forecasting the development of the four prioritized agricultural residues wheat straw (common and durum), corn stover, barley straw, and rapeseed straw until 2030 at the regional level. The future bioeconomic potential is a function of crop yields, cultivated

areas, and competing applications. Each underlying factor is forecasted based on historic data (2000 – 2016) with a set of different fitted time series models with optimized model parameters. The logistic time series model fitted the yield development very well, especially in regions with more recent EU membership, since the yield developed positively towards the maximum possible yield due to improving farming patterns. In regions where the yield fluctuated around a stable level in past years, simple exponential smoothing applied well. The annual percentage change in cultivated area was adopted from the EU Agricultural Outlook (European Commission, 2018a). The outlook also considers exogenous macro-economic factors like changing levels of subsidies, which cannot be taken into account by time series-based models.

The results of chapter 4 indicate an increasing potential of the most abundant agricultural residues, wheat straw, and corn stover, in the next decade due to their competitiveness on the world market, at the cost of reduced volumes of crops like oats or rapeseed (European Commission, 2016, 2017a). Since the cultivated area of barley is forecasted to stay constant with marginally increasing barley yields, its straw potential hardly increases. Historically strong growth rates of rapeseed production can mainly be attributed to expansions in the cultivated area, however, due to reductions in subsidization of first-generation biofuel, rapeseed straw volumes will probably decrease by 2030 (European Commission, 2018a). Chapter 4 forecasts a bioeconomic potential increase from 113.0 Mt in 2017 to approximately 127.0 Mt in 2030, mainly due to growing yields in central-eastern European countries for the four prioritized agricultural residues.

While forecasts on the EU-wide total production volumes are fairly accurate, regional divergences between forecasts and actual production volumes can be substantial due to annual weather events, which strongly impact crop yields (Lesk et al., 2016; Kahiluoto et al., 2019). On aggregated EU-wide level, shortfalls are mostly compensated, however, extreme weather events or strong deviations from annual mean values can lead to sharp regional declines, which could negatively affect the utilization of biorefinery capacities. In 2003, for example, constant drought and heatwaves significantly reduced wheat production, especially in France, Germany, and Italy (see Fig. 46; M. van der Velde et al., 2018).

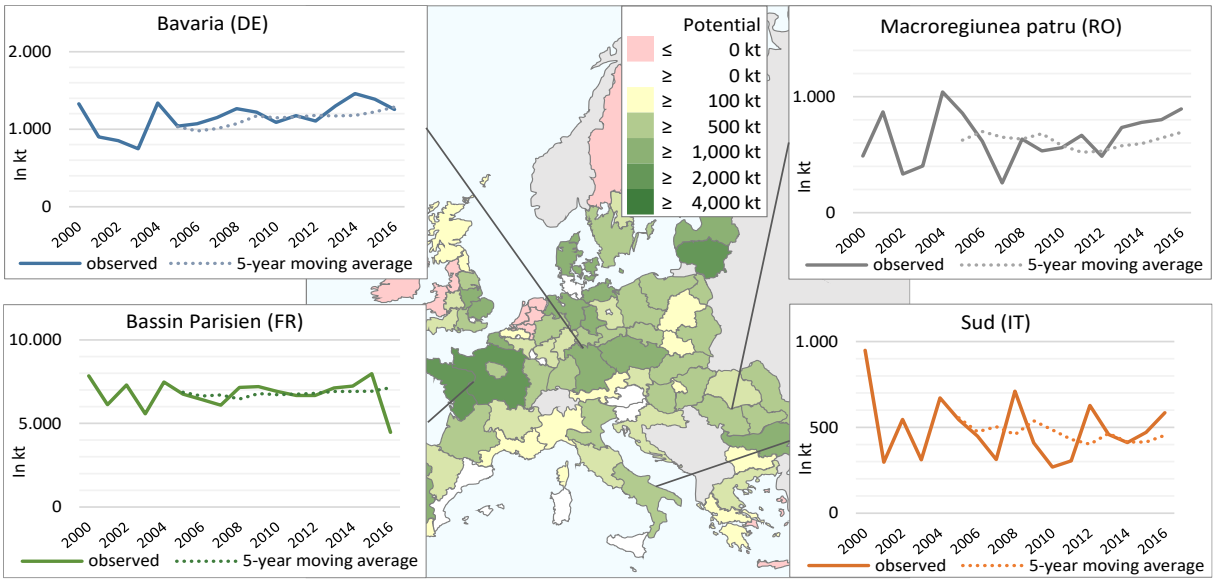

Fig. 46: Smoothed 2018 bioeconomic potential of wheat straw on NUTS1 level and annual historic bioeconomic wheat straw potential between 2000 and 2016 for selected regions

In 2016, EUs' most important cereal supply region, central northern France, faced a severe drop in wheat production volumes of up to 50% in some départments and an average drop of 30% compared to the five-year average (see Fig. 46 *Bassin Parisien*; Ben-Ari et al., 2018) due to heavy rainfalls, abnormally high minimum temperatures, and a long-lasting reduction of solar radiation (Ben-Ari et al., 2018; van der Velde et al., 2019). The two incidents described are only examples of possible weather extremes that can considerably reduce the feedstock supply. Even in the optimistic scenario of 1.5°C warming (SSP1-1.9), hot temperature extremes, heavy precipitation, and agricultural and ecological drought events are *likely* to further increase in frequency and intensity (IPCC, 2021), which could further increase annual variabilities in feedstock supply volumes in the coming decades. Long-term forecasts are difficult under those circumstances, which necessitates a constant monitoring of annual feedstock volumes and the updating of forecasts.

Chapter 5 addresses research goal 3 and develops a multi-criteria optimization model for the strategic design of bio-based value chains to integrate various economic and environmental objectives. The model is applied to the strategic network design of a large-scale second-generation bioethanol production network to substitute first-generation bioethanol and petrol in the EU. While the results point out positive environmental benefits for most impact and damage categories, the environmental categories are not concordantly congruent and in some cases even highly contradictory. The size of the biorefinery network and the substitution decision impact the environmental results most, and the objectives can be clustered in three congruency groups with similar substitution decisions and low opportunity costs. Group one distinguishes by simultaneous first-generation bioethanol and petrol substitution, group

two by exclusive petrol substitution, and group three by small production networks with exclusive first-generation ethanol substitution. The results show that bioethanol based on the considered lignocellulose residues could substitute up to 22% of today's petrol demand in the EU under optimal production networks for group two objectives (i.a., global warming). The greenhouse gas benefits could amount to about 59 Mt CO_2 eq., corresponding to about 1.35% of the EU's total emissions in 2018 (Eurostat, 2020a). With global warming benefits optimization, impact categories like *terrestrial acidification* and *particulate matter formation* show opportunity costs of up to 50% compared to their optimum, which implicates only slight improvements in those categories. Impact categories like *human non-carcinogenic toxicity*, *land use*, and *water consumption* could even be net deteriorated to optimize global warming. This implies that the environmental dimension cannot be reduced to greenhouse gases due to the risk of problem shifting (Hjuler and Hansen, 2018), but decision-making needs to consider a broader range of categories. A large-scale 2G EtOH production is not economically feasible for the time being with today's oil prices and taxes. The economically optimal networks yield costs of about 0.75 €/l 2G EtOH (production and distribution costs without excise taxes and other duties), and the environmentally optimal networks results in cost ranges from 0.88 €/l to more than 2.00 €/l. With the preconditions around 2020, only the combination of production in low wages and feedstock cost countries (e.g., Romania, Czech, or Hungary) with transportation to countries with an excise tax abatement for second-generation biofuels (e.g., Sweden, Croatia, or Austria) is close to being profitable (which is underlined by the high sensitivity of the economic result). The investigated carbon and excise tax scenarios show that a carbon tax of €50 could significantly increase the volume of profitably produced 2G ethanol to 7.0 Mt, which roughly corresponds to EUs' total ethanol consumption in 2018. An excise tax abatement of 100% for advanced biofuels would have an even greater impact. It could further increase economically feasible production volumes to 13.7 Mt. Single objective optimization reveals conflicts within the environment, and with the economic dimension, the Pareto optimization reveals interesting trade-offs between conflicting goals. Significant environmental benefits can often be realized with only small economic detriments, and vice versa, economic profitability can significantly be improved at low environmental opportunity costs. Furthermore, the applied Pareto optimization shows that the endpoints *human health* and *ecosystem quality* are suitable aggregators of the impact categories, wherefore they could serve as basis in multi-criteria decision-making. Nonetheless, a transparent consideration of a broad range of impacts and knowledge about the categories' contributions remains indispensable to reveal possible negative consequences (Rosenbaum et al., 2018).

Chapter 6 addresses research question four and five and provide a best-practice approach for a structured and transparent selection of a comprehensive set of quantitative and operationalizable social indicators based on existing frameworks. The inclusion of the social dimension into quantitative optimization models is more intricate than for the economic or environmental dimension since social repercussions of a decision are hard to estimate ex-ante. In most cases, social advantageousness is subjective, and many widely accepted social assessment categories are of qualitative nature. Furthermore, a lack of numerical data on social issues (Valdivia et al., 2021) renders the inclusion of social indicators into quantitative decision models challenging. To address these challenges, chapter 6 differentiates in *social objective functions*, which can be included in quantitative optimization models and allow the identification of socially optimal decisions, and in *social hotspot functions* which are only co-calculated and evaluate potential social hotspots in global value chains. In the context of the second-generation bioethanol case study, nine relevant and quantifiable social objective functions were identified, including the *local employment, water use, living conditions, land-food conflict, economic development, fair salary,* two objective functions on *workers' health & safety,* and *smallholder farming.* The social hotspot functions consist of the 25 indicators provided by the *Social Hotspots Database.*

Moreover, chapter 6 extends the model developed in chapter 5 by the social dimension, which eventually allows a strategic network design under consideration of the triple bottom line of sustainability. The final set of objectives covers one economic (subdivided into five taxation scenarios), 21 environmental, and nine social objective functions (plus 25 social hotspots functions). The optimization of the 34 objective functions leads to three fundamentally different network designs. The first group includes the economically optimal network structures, which tend to be implemented in lower-cost central and eastern European countries, and transportation of ethanol to countries with a biofuel high excise tax abatement. Second-generation bioethanol becomes more competitive with increasing subsidization (either excise tax abatement for biofuels or additional carbon taxation), which also yields larger networks. The second group comprises a few environmental objectives, based on which only first-generation bioethanol is substituted. Production networks of this class are widely dispersed in the EU with low-capacity biorefineries. The third group includes the most objective functions and is characterized by the entire exploitation of the available bioeconomic feedstock potential. Most environmental objective functions are part of this group, whereas those objectives can further be subdivided into objectives that prefer a simultaneous 1G bioethanol and petrol substitution and objectives that favor an exclusive petrol substitution. In addition, almost all social objectives are part of this group since larger production networks increase the total benefits in employment and regional development within EU's borders. The substitution decision is less decisive for

social objectives than the spatial network structure. The social hotspot analysis shows that the highest social risks within the feedstock sector are mainly due to a high probability of *injuries & fatalities* and high risks in the category *toxics and hazards*.

The developed multi-criteria model allows a strategic network design of bioeconomic value chains considering 35 economic, environmental, and social different objective functions, whereby 16 of the 17 SDGs are addressed (chapter 6.3). By matching the objective functions to goals and by calculating opportunity cost between the objective functions, the model is also able to unveil congruencies and conflicts between the SDGs and targets or indicators within one SDG. Thereby, the work shows how European policymakers could steer the roll-out of advanced biofuels under alignment with the SDGs. The taxation lever (cf. chapter 5.2) would improve the competitiveness of 2G bioethanol vis-à-vis fossil fuels and, depending on the taxation, also 1G EtOH. This fosters the achievement of inter alia SDG13 (climate action) while simultaneously realizing significant benefits in terms of, i.a., employment (SDG8.5) and regional development (SDG8.1).

On the contrary, the social hotspot analysis shows that the labor intensity in sectors with high risk for adverse social conditions like residue harvesting and transportation could create new hotspots that should be monitored. The decision would also put further stress on land, water, mineral resources, and food security, especially in the case of simultaneous production of 2G and 1G ethanol. Substitution of 1G by 2G bioethanol could mitigate certain adverse environmental aspects of biofuel production (inter alia land use impacts and ecosystem quality damage), but at the same time prevent the full exploitation of climate, employment, and regional development potentials. The SDG analysis supports the perception that decision-making under consideration of different sustainability criteria requires trade-offs. Decision-makers, whether at the corporate level pursuing one or more business objectives or at the policy level using the SDGs as a framework, should be aware of the reciprocities between the different criteria. Therefore, it is particularly important to show as early as in the strategic network design stage what consequences a decision will have on other aspects that might be less in the decision-maker's focus. This transparency may allow potential negative impacts of decisions on certain SDGs to be addressed timely and mitigated through appropriate measures. The European bioeconomy is subject to tensions between various stakeholders and clearly shows the lines of conflict within the SDGs. While on the one hand, it would be desirable to have quantifiable indicators for each sub-goal of the SDGs, Chapter six also illustrates the difficulty in interpreting the results when a large number of conflictory objectives exists.

With respect to chapters three and four, chapters five and six reveal the scarcity of agricultural residues regarding the prevailing demand. The annual energy provided by

the flow of solar radiation in agricultural residues is far from meeting the demand for fuels. While advanced biofuels could play a role in the private transportation sector in the medium term (~2030), battery electric vehicles and hydrogen-based engines will probably gain large shares in developed countries within the next decade. Alternative and more environmentally friendly solutions are scarce and farther behind private transportation for aviation, international navigation, and heavy-duty vehicles. Therefore, hydrocarbon-based fuels like second-generation bioethanol are viable in those applications in the next decades.

The developed strategic network design model is characterized by a central decision authority within the European Union, wherefore the approach is valuable for gaining general knowledge about economic, environmental, and social issues associated with a large-scale biorefinery network. In the fictitious planning model, one market participant acts as a centralized player that carries out the strategic network design without considering other market participants for the entire European market. The proposed approach can be characterized as a single-level model that assumes simultaneous decision-making for a large-scale production network at one point in time, which is a clear simplification of reality (Wogrin et al., 2020). This approach is legitimate for gaining general knowledge, and policy-makers are supported in deciding upon which project might be eligible for funding, which SDG benefits can be expected, and which additional risks might be induced. Furthermore, entrepreneurial decision-makers show that integrating environmental and social objectives is partly compatible with economic goals. However, the model disregards that different market participants will compete. The described model with one central player is similar to the national energy sectors until the 1980s. Many countries liberalized the energy sector and implemented electricity markets in the years after, leading to multiple producers. Bilevel programming was successfully used in this field to account for the sequential decision-making process in a market increasingly divided among different market actors (Wogrin et al., 2020), which is also a conceivable extension for the proposed model.

8 Conclusion and Outlook

This doctoral thesis assesses the economic, environmental, and social benefits of an upscaled bioeconomy in the EU on the case of second-generation bioethanol. The work starts with the investigation of the agroforestry residue potentials on a regional level and thus contributes to the frequently neglected topic of biomass availability. Based on the outcomes of this initial study, a set of feedstocks is prioritized for further in-depth analysis, and the volumes to be expected are spatially explicitly forecasted until 2030. These results are used to parametrize a strategic biorefinery production network design model applied within the European Union. The model is implemented as multi-criteria mixed-integer linear program and applies 35 economic, environmental, and social objective functions, some of which are operationalized as part of this work. These models were used to examine congruencies and conflicts within and between different Sustainable Development Goals. The following insights summarize the main results of this thesis, which are the outcome of the research questions 1 to 5 defined at the outset of the thesis:

RQ1 Agroforestry residue volumes are differentiated in a theoretical, technical, and bioeconomic potential to account for different issues that lower the feedstock volumes available for bioeconomic applications. The most promising agricultural residue in the EU is wheat straw (bioeconomic potential of 46 Mt), followed by maize stover (31 Mt), barley straw (16 Mt), and rapeseed straw (14 Mt), which together account for about 80% of the cereals and oil crops residues (average from 2010 to 2014). Central and northern France produces the largest agricultural residues volumes, followed by Central and Eastern EU regions. In forestry, waste bark from the two coniferous species, spruce and pine, are most promising, with a bioeconomic potential of 15 Mt and the highest supplies in Scandinavia and central EU.

RQ2 The future bioeconomic potential of agricultural residues is a function of the crop yields, the cultivated area, and the straw demand of competing applications. The results of the time-series-based forecast models predict a total increase of the bioeconomic potential of the prioritized feedstocks wheat, maize, barley, and rapeseed straw from about 113 Mt in 2017 to approximately 127 Mt in 2030. The forecast indicates the largest increase of all investigated crops for corn stover at up to 20% until 2030. Wheat straw potentials are forecasted to increase by 14%. Barley straw potentials are predicted to stay constant, and rapeseed straw production are forecasted to decrease in many regions within the next decade. The work identified increasing crop yields as the main driver for advancing

feedstock potentials, and Central and Eastern European countries show high growth rates.

RQ3 The strategic network design model is implemented as multi-criteria Mixed-Integer Linear Program. The economic dimension is addressed by profit maximization for five taxation scenarios, and the environmental dimension is addressed by benefit maximization of 18 impact and 3 damage categories of the LCIA method ReCiPe. The model assesses the economic and environmental benefits of optimal second-generation bioethanol production network designs based on agricultural residues to substitute petrol and/or first-generation ethanol in the EU. Optimal network decisions of the different environmental objectives can be clustered into three groups of mutual congruencies with low opportunity costs within one group and high opportunity costs between objectives of different groups, which indicates conflicting decisions. The decision to either substitute first-generation ethanol or petrol has the greatest influence on environmental performance. Taking the endpoints *human health* and *ecosystem quality* as environmental criteria, 2G bioethanol should be used to substitute 1G ethanol and petrol simultaneously (100% 1G EtOH and 18% petrol of the 2018 demand in the EU). In the case study, the impact categories *global warming potential*, *fine particulate matter formation*, and *land use* contribute most to the Areas of Protection human health and ecosystem quality. Taking the global warming potential as decision criteria, up to 22% of the 2018 petrol demand could be substituted with benefits of about 59 Mt CO_2 eq. The economic optimization shows that 2G bioethanol is barely competitive vis-à-vis petrol with current taxation. An excise tax abatement for advanced biofuels or carbon taxes would be required to allow economic viability. The results also exemplify the scarcity of agricultural residues as feedstock for advanced biofuels.

RQ4 The structured identification of quantitative and operationalizable social indicators starts with the selection of suitable social assessment frameworks, whereof relevant and quantifiable social aspects are identified, and irrelevant issues are excluded. In the next step, the selected indicators are operationalized and implemented in the MILP model. For the case of second-generation bioethanol, nine quantitative *Social Objective Functions (SOF)* from the *Guidelines for Social Life Cycle Assessment of Products and Organization*s were identified. Additionallay, 25 *Social Hotspot Functions (SHF)* were identified from the Social Hotspots Database. SOFs represent social issues, where strategic network decisions have distinctly positive or negative impacts wherefore they are included as maximization functions. SHFs are not optimized but quantified by co-calculation to unveil social risks within the supply chain. Key findings are that social optimization leads to large and labor-intensive production networks

distributed all over the EU, and the value creation slightly shifts regionally, depending on the social objective. The production network shifts to regions with high unemployment rates to optimize local employment, such as Spain, and Italy. When optimizing *economic development*, economically superior metropolitan regions are discriminated in favor of weaker regions of Central and Eastern EU. In terms of size, most socially and environmentally optimal production networks are similar, although the substitution decision has little impact on social objective realization. This means that if a decision is made based on social criteria and an environmentally advantageous substitution decision is taken in addition, trade-offs can be found that imply only minor sacrifices. Socially optimal production networks are highly unprofitable; however, Pareto optimization identifies trade-offs that yield acceptable results in both dimensions. The main *social hotspot* is induced by Injuries and Fatalities in the feedstock sectors of Central and Eastern European countries.

RQ5 By including the social objective functions into the multi-criteria model, the final set of 35 economic, environmental, and social objectives allows a strategic network design of bioeconomic value chains under consideration of 16 of the 17 SDGs. By matching the objective functions to Sustainable Development Goals, targets, and indicators and calculating opportunity cost between the objective functions, the model can unveil congruencies and conflicts between different goals, targets, and indicators. Nine SDGs can be explicitly optimized through matching to objective functions (*good health and well-being, clean water and sanitation, affordable clean energy, decent work and economic growth, sustainable cities and communities, responsible consumption and production, climate action, life below water, life on land*). Another 7 SDGs are addressed by the co-calculated *SHFs*, which means that, although no separate optimization is possible, the effects of optimizing other SDGs can be made transparent. The results of chapter 6 show how European policymakers could steer the roll-out of advanced biofuels under alignment with the SDGs. The taxation lever (cf. chapter 5.2) would improve the competitiveness of 2G bioethanol vis-à-vis fossil fuels and, depending on the taxation, also 1G EtOH. This would foster the attainment of inter alia SDG13 (climate action) while simultaneously realizing significant benefits in terms of, i.a., employment (SDG8.5) and regional development (SDG8.1). On the downside, the social hotspot analysis shows that increasing labor intensity due to 2G EtOH production in countries and sectors with high risk for adverse social conditions could create new hotspots, such as increasing risks for *injuries & fatalities* (SDG 8), that need to be monitored. The decision to subsidize biofuels could also put further stress on land, water, mineral resources, and food security, especially in the case of simultaneous production of 2G and 1G ethanol. Apart from that, the substitution

of 1G by 2G bioethanol could mitigate certain adverse environmental aspects of biofuel production (i.a., land use impacts and ecosystem quality damage), but at the same time prevent the full exploitation of climate, employment, and regional development potentials. The assessment of relationships between the different SDGs supports the perception that different aspects of sustainability are not equally directed. Sustainability, expressed by the SDGs, is rather case-specific and varies between a multitude of interdependent social, environmental, and economic criteria. Decision-makers, whether at the corporate level pursuing one or more business objectives or at the policy level using the SDGs as a framework, need to be aware of the reciprocities between the different criteria.

The introduced model is based on many parameters, most of which being uncertain and volatile over time. Besides chapter-wise sensitivity analysis of the effects of key parameter variations on the main results, this work disregards the stochastic nature of various parameters. Especially regional agricultural feedstock volumes are subject to high annual volatilities due to changing weather and thereby fluctuating growing conditions (Lesk et al., 2016). With regard to advancing climate change, an increase of regional and large-scale weather anomalies with negative impacts on crop yields are more likely to occur and probably increase in severity (IPCC, 2021), which significantly complicates forecasts. Future works could include the stochasticity of feedstock supply and the increasing probability of supply disruptions under consideration of certain climate change scenarios to set up production networks that can cope with changing conditions. With suitable models, climate resilience measures of crop production (Kahiluoto et al., 2019) and biomass supply chains (Langholtz et al., 2014) could already be considered in the strategic planning to build climate-resilient supply chains. Measures to increase the resilience of biorefineries could be the feedstock storage in warehouses to compensate annual fluctuations, keep additional pre-treatment and processing units ready flexibility in the feedstock type, or implement end-product storage (Langholtz et al., 2014). Stochastic programming is a widely applied concept in a range of disciplines to consider uncertain parameters (Hosseini et al., 2019), and the application of such approaches could be investigated for the case described. The discussed limitation of one central decision-maker could, by future works, for example, be addressed by bilevel programming to model markets with different actors. Introducing supply stochasticity and bilevel programming, or even the combination into stochastic bilevel applications, could support developing models closer to reality. A key challenge with such model extensions will be the efficient solvability (Wogrin et al., 2020) and the parametrization.

Sustainable development, which combines environmental responsibility and social stability with economic feasibility, is increasingly the focus of decision-makers in business and politics and has been summarized by the United Nations in 17 sustainable

development goals (United Nations, 2015; Valdivia et al., 2021). The transformation of our economy, which is to date highly based on fossil and mineral resources, into one subject to the SDG framework is a substantial but inevitable challenge and the use of renewable sources offers a major lever. Multi-criteria Strategic Network Design is the cornerstone for companies to achieve long-term business objectives. For policy-makers, such multi-objective models support in gaining general knowledge about economic, environmental, and social aspects of sectors that strongly rely on regional aspects such as bioeconomic value chains. Including a large set of objective functions enables decision-makers to gain insights into the reciprocities of different sustainability aspects. The integration of methods, such as Life Cycle Sustainability Assessment and Mathematical Programming, allows the investigation of interdependencies between decisions and their implication on objectives. The model developed in this thesis can map the contribution of a large-scale second-generation biorefinery network to the Sustainable Development Goals. It takes a deeper look at decisions within *one* bioeconomic segment, but policy-makers also need decision support on the most appropriate markets to use the limited agroforestry residue potentials to contribute best to the SDGs. Future work should also expand their models to include dynamic issues, such as advancing climate change, and be more closely aligned with business realities. The second-generation bioconversion industry has a great potential to contribute to sustainable development, and good decisions about using the available feedstocks, which are aligned with the SDGs, will help humanity sustain the Earth's habitat for longer.

References

Abdullah, B. *et al.* (2019) 'Fourth generation biofuel: A review on risks and mitigation strategies', *Renewable and Sustainable Energy Reviews*, 107(February), pp. 37–50. doi:10.1016/j.rser.2019.02.018.

Agrifrance (2017) 'Agrifrance 2017 Rural Report', p. 44. Available at: https://group.bnpparibas/en/news/agrifrance-2017-rural-report-wine-market.

Aguiar, A., Narayanan, B. and McDougall, R. (2016) 'An Overview of the GTAP 9 Data Base', *Journal of Global Economic Analysis*, 1(1), pp. 181–208. doi:10.21642/JGEA.010103AF.

Anderson, H. *et al.* (2004) *Meta-analysis of time-series studies and panel studies of particulate matter (PM) and ozone (O3) : report of a WHO task group*, *Report of a WHO Task group*. Copenhagen. Available at: https://apps.who.int/iris/handle/10665/107557.

Anvari, S. and Turkay, M. (2017) 'The facility location problem from the perspective of triple bottom line accounting of sustainability', *International Journal of Production Research*, 55(21), pp. 6266–6287. doi:10.1080/00207543.2017.1341064.

Arrhenius, S. (1896) 'On the influence of carbonic acid in the air upon the temperature of the ground', *The London, Edinburgh, and Dublin Philosophical Magazine and Journal of Science*, 41(251), pp. 237–276. doi:10.1080/14786449608620846.

Asia, S., OECD and FAO (2017) *OECD-FAO Agricultural Outlook 2017-2026*, *OECD Publishing*. Available at: http://dx.doi.org/10.1787/agr_outlook-2017-en.

Babazadeh, R. *et al.* (2017) 'A sustainable second-generation biodiesel supply chain network design problem under risk', *Omega*, 66, pp. 258–277. doi:10.1016/j.omega.2015.12.010.

Bairamzadeh, S., Pishvaee, M.S. and Saidi-Mehrabad, M. (2016) 'Multiobjective Robust Possibilistic Programming Approach to Sustainable Bioethanol Supply Chain Design under Multiple Uncertainties', *Industrial and Engineering Chemistry Research*, 55(1). doi:10.1021/acs.iecr.5b02875.

Bakker, R. *et al.* (2013) *Rice straw and Wheat straw. Potential feedstocks for the Biobased Economy*, *NL Agency Ministry of Economic Affairs*. Available at: http://english.rvo.nl/sites/default/files/2013/12/Straw report AgNL June 2013.pdf.

Balat, M. (2011) 'Production of bioethanol from lignocellulosic materials via the biochemical pathway: A review', *Energy Conversion and Management*, 52(2), pp. 858–875. doi:10.1016/j.enconman.2010.08.013.

Barbosa-Póvoa, A.P., da Silva, C. and Carvalho, A. (2018) 'Opportunities and challenges in sustainable supply chain: An operations research perspective', *European Journal of Operational Research*, 268(2), pp. 399–431. doi:10.1016/j.ejor.2017.10.036.

BEKW (2016) *Bioenergy plant Emsland (in German)*.

Ben-Ari, T. *et al.* (2018) 'Causes and implications of the unforeseen 2016 extreme yield loss in the breadbasket of France', *Nature Communications*, 9(1). doi:10.1038/s41467-018-04087-x.

Benoît-Norris, C., Bennema, M. and Norris, G. (2018) *The Social Hotspots Database: Supporting documentation Update 2019*.

Benoit-Norris, C., Cavan, D.A. and Norris, G. (2012) 'Identifying social impacts in product supply chains: Overview and application of the social hotspot database', *Sustainability*, 4(9), pp. 1946–1965.

doi:10.3390/su4091946.

Benoit-Norris, C. and Norris, G.A. (2015) 'Chapter 8 : The Social Hotspots Database', *The Sustainability Practitioner's Guide to Social Analysis and Assessment*, (November), pp. 52–73. Available at: https://www.researchgate.net/publication/287215286_Chapter_8_The_Social_Hotspots_Database_Context_of_the_SHDB.

Bertaud, F. *et al.* (2012) 'Development of green adhesives for fibreboard manufacturing, using tannins and lignin from pulp mill residues', *Cellulose Chemistry and Technology*, 46, pp. 449–455.

Biofuels Barometer (2019) *Biofuels Barometer*. Available at: https://www.eurobserv-er.org/category/all-biofuels-barometers/.

Bittermann, W. and Suvorov, M. (2012) *Quality standard for statistics on wood fuel consumption of households*.

Bjørn, A. *et al.* (2018) 'Scope Definition', in *Life Cycle Assessment*. Cham: Springer International Publishing, pp. 75–116. doi:10.1007/978-3-319-56475-3_8.

Borrion, A.L., McManus, M.C. and Hammond, G.P. (2012) 'Environmental life cycle assessment of lignocellulosic conversion to ethanol: A review', *Renewable and Sustainable Energy Reviews*, 16(7), pp. 4638–4650. doi:10.1016/j.rser.2012.04.016.

Bowling, I.M., Ponce-Ortega, J.M. and El-Halwagi, M.M. (2011) 'Facility Location and Supply Chain Optimization for a Biorefinery', *Industrial & Engineering Chemistry Research*, 50(10), pp. 6276–6286. doi:10.1021/ie101921y.

bp (no date) *Approximate Conversion Factors: Statistical Review of World Energy*, *Rules of Thumb for Chemical Engineers*. doi:10.1016/b978-075067856-8/50028-1.

Bright, R.M. and Strømman, A.H. (2009) 'Life cycle assessment of second generation bioethanols produced from scandinavian Boreal forest resources a regional analysis for middle Norway', *Journal of Industrial Ecology*, 13(4), pp. 514–531. doi:10.1111/j.1530-9290.2009.00149.x.

Brosowski, A.A. *et al.* (2016) 'A review of biomass potential and current utilisation – Status quo for 93 biogenic wastes and residues in Germany', *Biomass and Bioenergy*, 95, pp. 257–272. doi:10.1016/j.biombioe.2016.10.017.

Büchsenmeister, R. (2016) *Dissemination and performance of spruce in Austria (in German)*, *BFW-Praxisinformation*.

Budzinski, M. *et al.* (2019) 'Assessment of lignocellulosic biorefineries in Germany using a hybrid LCA multi-objective optimization model', *Journal of Industrial Ecology*, p. jiec.12857. doi:10.1111/jiec.12857.

Buranov, A.U. and Mazza, G. (2008) 'Lignin in straw of herbaceous crops', *Industrial Crops and Products*, 28(3), pp. 237–259. doi:10.1016/j.indcrop.2008.03.008.

Burkhard, B. *et al.* (2012) 'Mapping ecosystem service supply, demand and budgets', *Ecological Indicators*, 21, pp. 17–29. doi:10.1016/j.ecolind.2011.06.019.

CEFIC (2017) *Facts and Figures 2016*. European Chemical Industry Council.

Cherubini, F. *et al.* (2009) 'Energy- and greenhouse gas-based LCA of biofuel and bioenergy systems: Key issues, ranges and recommendations', *Resources, Conservation and Recycling*, 53(8), pp. 434–447. doi:10.1016/j.resconrec.2009.03.013.

Cherubini, F. and Strømman, A.H. (2011) 'Life cycle assessment of bioenergy systems: State of the art and future challenges', *Bioresource Technology*, 102(2), pp. 437–451. doi:10.1016/j.biortech.2010.08.010.

Cherubini, F. and Ulgiati, S. (2010) 'Crop residues as raw materials for biorefinery systems - A LCA case study', *Applied Energy*, 87(1), pp. 47–57. doi:10.1016/j.apenergy.2009.08.024.

Ciais, P. *et al.* (2005) 'Europe-wide reduction in primary productivity caused by the heat and drought in 2003', *Nature*, 437(7058), pp. 529–533. doi:10.1038/nature03972.

Ciroth, A. and Eisfeldt, F. (2016) *PSILCA – A Product Social Impact Life Cycle Assessment database. Database version 1.0. Documentation*. Available at: http://www.openlca.org/documents/14826/6d439d91-ddf5-480f-9155-e4787eaa0b6b.

Clariant (2020) *sunliquid FP7*. Available at: https://www.sunliquid-project-fp7.eu/ (Accessed: 7 September 2020).

Clariant (2021a) *Clariant completes construction of first commercial sunliquid® cellulosic ethanol plant in Podari, Romania*. Available at: https://www.sunliquid-project-fp7.eu/de/news/fertigstellung-bau (Accessed: 20 October 2021).

Clariant (2021b) *Sunliquid. Cellulosic ethanol from agricultural residues*. Straubing. Available at: https://www.clariant.com/en/Solutions/Products/2014/10/16/16/16/sunliquid?p=1 (Accessed: 25 January 2022).

Corsano, G., Vecchietti, A.R. and Montagna, J.M. (2011) 'Optimal design for sustainable bioethanol supply chain considering detailed plant performance model', *Computers & Chemical Engineering*, 35(8), pp. 1384–1398. doi:10.1016/j.compchemeng.2011.01.008.

Čuček, L., Klemeš, J.J. and Kravanja, Z. (2012) 'A review of footprint analysis tools for monitoring impacts on sustainability', *Journal of Cleaner Production*, 34, pp. 9–20. doi:10.1016/j.jclepro.2012.02.036.

DBFZ (2011) 'Basic Information for a Sustainable Utilization of Agricultural Resources in the Bioenergy Sector (in German)'.

Deb, K. and Gupta, S. (2010) 'Understanding Knee Points in Bicriteria Problems and Their Implications as Preferred Solution Principles A Knee Solution in a Bi-Objective Optimization Problem', *Engineering Optimization* [Preprint].

Dees, M. *et al.* (2016) *A spatial data base on sustainable biomass cost- supply of lignocellulosic biomass in Europe - methods & data sources .*

Dees, M. *et al.* (2017) *A spatial data base on sustainable biomass cost- supply of lignocellulosic biomass in Europe - methods & data sources. Project Report*. FNR. Available at: https://zenodo.org/record/1478483.

DESTATIS (2021) *Producing Industries (in German)*, *Fachserie 4 Reihe 6.1*.

DG Trade (2021) *Access2Markets*. Available at: https://trade.ec.europa.eu/access-to-markets/en/home (Accessed: 20 October 2021).

Dias De Oliveira, M.E., Vaughan, B.E. and Rykiel, E.J. (2005) 'Ethanol as fuel: Energy, carbon dioxide balances, and ecological footprint', *BioScience*, 55(7), pp. 593–602. doi:10.1641/0006-3568(2005)055[0593:EAFECD]2.0.CO;2.

Dobrescu, M. (2017) *Romania Grains and Feeds Update - Romania's Bumper Crop*. Bucharest.

Domschke, W. *et al.* (2015) *Introduction to Operations Research (in german)*. Berlin, Heidelberg: Springer Berlin Heidelberg. doi:10.1007/978-3-662-48216-2.

Dunnett, A.J., Adjiman, C.S. and Shah, N. (2008) 'A spatially explicit whole-system model of the lignocellulosic bioethanol supply chain: An assessment of decentralised processing potential', *Biotechnology for Biofuels*, 1, pp. 1–17. doi:10.1186/1754-6834-1-13.

Dutta, K., Daverey, A. and Lin, J.G. (2014) 'Evolution retrospective for alternative fuels: First to fourth generation', *Renewable Energy*, 69, pp. 114–122. doi:10.1016/j.renene.2014.02.044.

Duveiller, G. *et al.* (2017) 'A dataset of future daily weather data for crop modelling over Europe derived from climate change scenarios', *Theoretical and Applied Climatology*, 127(3–4), pp. 573–585. doi:10.1007/s00704-015-1650-4.

EBTP (2017) *Advanced Biofuels R&D&D Mapping*, *Accelearting deployment of advanced biofuels in Europe*. European Biofuel Technology Platform.

ECN Phyllis (2012) *ECN Phyllis, database for biomass and waste*.

Edenhofer, O. *et al.* (2013) 'On the economics of renewable energy sources', *Energy Economics*, 40, pp. S12–S23. doi:10.1016/j.eneco.2013.09.015.

Edwards, R.A.H. *et al.* (2005) 'GIS-Based Assessment of Cereal Straw Energy Resource in the European Union.', in *Proceedings of the 14th European Biomass Conference & Exhibition. Biomass for Energy, Industry and Climate Protection*. Paris.

EEA (2021) *Air quality statistics calculated by the EEA (F)*. Available at: http://aidef.apps.eea.europa.eu/?source=%7B%22query%22%3A%7B%22match_all%22%3A%7B%7D%7D%2C%22display_type%22%3A%22tabular%22%7D (Accessed: 6 October 2021).

EFI (2020) *Investing in nature to transform the post COVID-19 economy*. Available at: https://efi.int/news/investing-nature-transform-post-covid-19-economy-2020-06-10 (Accessed: 15 January 2022).

Ehrgott, M. (2005) *Multicriteria Optimization*, *Structural Optimization*. Heidelberg: Springer Berlin Heidelberg New York. doi:10.1007/978-0-387-95865-1_8.

EIA (2021) *International Energy Statistics*. Available at: https://www.eia.gov/international/overview/world (Accessed: 4 November 2021).

ePure (2018) 'European renewable ethanol – key figures 2018 EU renewable ethanol market at a glance – 2018', *Key Figures 2018*, pp. 2018–2019. Available at: https://epure.org/media/1920/190828-def-data-statistics-2018-infographic.pdf.

Ericsson, K. and Nilsson, L.J. (2006) 'Assessment of the potential biomass supply in Europe using a resource-focused approach', *Biomass and Bioenergy*, 30(1), pp. 1–15. doi:10.1016/j.biombioe.2005.09.001.

Eskandarpour, M. *et al.* (2015) 'Sustainable supply chain network design: An optimization-oriented review', *Omega (United Kingdom)*, 54, pp. 11–32. doi:10.1016/j.omega.2015.01.006.

European Commission (2007) *En Route to the Knowledge-Based Bio-Economy (Cologne Paper)*.

European Commission (2012) *Innovating for Sustainable Growth: A Bioeconomy for Europe*, *Communication*. doi:10.1017/CBO9781107415324.004.

European Commission (2016) 'EU Agricultural Outlook. Prospect for EU agricultural markets and income 2016-2026', *Agriculture and Rural Development*, (December), pp. 1–96.

European Commission (2017a) *EU Agricultural Outlook*. Brussels.

European Commission (2017b) *My Region, My Europe, Our Future. Seventh report on economic, social and territorial cohesion*, *JRC Technical Report*. Luxembourg. doi:10.2776/5244.

European Commission (2018a) *EU Agricultural Outlook for Markets and Income*. Brussels.

European Commission (2018b) *Euro area and EU working days to build Calendar Adjustment Regressor.* Available at: https://ec.europa.eu/eurostat/cros/content/euro-area-and-eu-working-days-build-

calendar-adjustment-regressor_en (Accessed: 4 February 2021).

European Commission (2018c) 'Roadmap: Update of the 2012 Bioeconomy Strategy', *Ref. Ares(2018)975361*, (2018), pp. 1–3. Available at: https://ec.europa.eu/info/law/better-regulation/initiatives/ares-2018-975361_en.

European Commission (2020) *Weekly Oil Bulletin*. Available at: https://ec.europa.eu/energy/en/data-analysis/weekly-oil-bulletin (Accessed: 29 January 2021).

European Commission (2021a) *A European Green Deeal*. Available at: https://ec.europa.eu/info/strategy/priorities-2019-2024/european-green-deal_en (Accessed: 7 April 2021).

European Commission (2021b) *Monthly and cumulative crude oil imports into the EU (2001-2019)*, *EU crude oil imports and supply cost*. Available at: https://ec.europa.eu/energy/data-analysis/eu-crude-oil-imports_en (Accessed: 12 July 2021).

European Commission and European Union (2017) *Review of the 2012 European Bioeconomy Strategy*, *The 2012 European Bioeconomy Strategy*. doi:10.2777/086770.

European Court of Auditors (2016) *Rail freight transport in the EU: still not on the right track*, *Special Report No. 8*. doi:10.2865/53961.

Eurostat (2016a) *Agricultural Statistics*. Available at: http://ec.europa.eu/eurostat/web/agriculture/data/database (Accessed: 1 March 2017).

Eurostat (2016b) *Forestry*. Available at: https://ec.europa.eu/eurostat/web/forestry/data/database (Accessed: 1 March 2017).

Eurostat (2018a) *Crop production in national humidity [apro_cpnh1]*. Available at: http://appsso.eurostat.ec.europa.eu/nui/show.do?dataset=apro_cpnh1&lang=en (Accessed: 12 April 2018).

Eurostat (2018b) *Distance nuts matrix NUTS2013*, *TERCET*. Available at: http://ec.europa.eu/eurostat/tercet/flatfiles.do (Accessed: 14 June 2018).

Eurostat (2018c) *Farms and farmland in the European Union - statistics*. Available at: https://ec.europa.eu/eurostat/statistics-explained/index.php?title=Farms_and_farmland_in_the_European_Union_-_statistics#Farms_in_2016 (Accessed: 23 July 2021).

Eurostat (2018d) *Prodcom Annual Data*, *NACE Rev. 2*.

Eurostat (2019a) *Archive:Income poverty statistics*, *Statistics Explained*. Available at: https://ec.europa.eu/eurostat/statistics-explained/index.php?title=Income_poverty_statistics&oldid=440992#At-risk-of-poverty_rate_and_threshold (Accessed: 8 October 2021).

Eurostat (2019b) *Gas price by type of user*, *TEN00118*. Available at: https://ec.europa.eu/eurostat/databrowser/view/ten00118/default/table?lang=en.

Eurostat (2019c) *Supply, transformation and consumption of oil and petroleum productsle*, *nrg_cb_oil*. Available at: https://appsso.eurostat.ec.europa.eu/nui/show.do?dataset=nrg_cb_oil&lang=en (Accessed: 10 October 2019).

Eurostat (2020a) *Greenhouse gas emissions by source sector (common reporting format, UNFCCC) - total, excluding LUILUCF and memo items, including international aviation)*, *Statistics Explained*. Available at: http://appsso.eurostat.ec.europa.eu/nui/show.do?lang=en&dataset=env_air_gge.

Eurostat (2020b) *Labour cost levels by NACE Rev. 2 activity [lc_lci_lev]*. Available at:

http://appsso.eurostat.ec.europa.eu/nui/show.do?dataset=lc_lci_lev&lang=en (Accessed: 27 March 2020).

Eurostat (2020c) *Purchasing power parities (PPPs), price level indices and real expenditures for ESA 2010 aggregates*, *prc_ppp_ind*. Available at: https://appsso.eurostat.ec.europa.eu/nui/submitViewTableAction.do (Accessed: 27 March 2020).

Eurostat (2020d) *Unemployment rate by sex and age and NUTS2 regions (%)*, *[lfst_r_lfu3rt]*. Available at: http://appsso.eurostat.ec.europa.eu/nui/show.do?lang=en&dataset=lfst_r_lfu3rt (Accessed: 4 February 2021).

Eurostat (2021a) *Accidents at work by days lost and NACE Rev. 2 activity*, *[hsw_n2_04]*. Available at: http://appsso.eurostat.ec.europa.eu/nui/show.do?dataset=hsw_n2_04&lang=en (Accessed: 18 February 2021).

Eurostat (2021b) *Accidents at work by days lost and NACE Rev. 2 activity*, *[hsw_n2_04]*. Available at: https://appsso.eurostat.ec.europa.eu/nui/show.do?dataset=hsw_n2_04&lang=en (Accessed: 18 February 2021).

Eurostat (2021c) *Average number of usual weekly hours of work in main job, by sex, professional status, full-time/part-time and economic activity (from 2008 onwards, NACE Rev. 2) - hours [lfsa_ewhun2]*. Available at: http://appsso.eurostat.ec.europa.eu/nui/show.do?dataset=lfsa_ewhun2&lang=en (Accessed: 4 February 2021).

Eurostat (2021d) *Complete energy balances [nrg_bal_c]*. Available at: https://appsso.eurostat.ec.europa.eu/nui/show.do?dataset=nrg_bal_c (Accessed: 20 October 2021).

Eurostat (2021e) *Crop production in EU standard humidity [apro_cpsh1]*. Available at: https://ec.europa.eu/eurostat/databrowser/view/apro_cpsh1/default/table?lang=en (Accessed: 20 October 2021).

Eurostat (2021f) *Crop production in national humidity by NUTS 2 regions [apro_cpnhr]*. Available at: https://ec.europa.eu/eurostat/product?code=agr_r_acs&mode=view&language=en (Accessed: 6 October 2021).

Eurostat (2021g) *Electricity prices for non-household consumers [nrg_pc_205]*, *nrg_pc_205*. Available at: https://appsso.eurostat.ec.europa.eu/nui/show.do?dataset=nrg_pc_205&lang=en (Accessed: 20 October 2021).

Eurostat (2021h) *Farm indicators by agricultural area, type of farm, standard output, legal form and NUTS 2 regions [ef_m_farmleg]*. Available at: https://appsso.eurostat.ec.europa.eu/nui/show.do?dataset=ef_m_farmleg&lang=en (Accessed: 31 January 2022).

Eurostat (2021i) *Gas prices components for non-household consumers - annual data [nrg_pc_203_c]*. Available at: http://appsso.eurostat.ec.europa.eu/nui/show.do?dataset=nrg_pc_203&lang=en.

Eurostat (2021j) *Gross domestic product (GDP) at current market prices by NUTS 2 regions*, *[nama_10r_2gdp]*. Available at: http://appsso.eurostat.ec.europa.eu/nui/show.do?lang=en&dataset=nama_10r_2gdp (Accessed: 3 February 2021).

Eurostat (2021k) *Labour cost levels by NACE Rev. 2 activity*, *[lc_lci_lev]*. Available at: https://appsso.eurostat.ec.europa.eu/nui/show.do?dataset=lc_lci_lev&lang=en (Accessed: 12 February 2021).

Eurostat (2021l) *Land cover overview by NUTS 2 regions*, *[land_lcv_ovw]*. Available at: https://appsso.eurostat.ec.europa.eu/nui/submitViewTableAction.do (Accessed: 19 October 2021).

Eurostat (2021m) *Non-fatal accidents at work by NACE Rev. 2 activity and sex*, *[hsw_n2_01]*. Available at: https://appsso.eurostat.ec.europa.eu/nui/show.do?dataset=hsw_n2_01&lang=en (Accessed: 18 February 2021).

Eurostat (2021n) *Population density by NUTS 3 region [demo_r_d3dens]*. Available at: http://appsso.eurostat.ec.europa.eu/nui/show.do?dataset=demo_r_d3dens&lang=en (Accessed: 6 October 2021).

Eurostat (2021o) *Population on 1 January by age and sex [demo_pjan]*. Available at: https://appsso.eurostat.ec.europa.eu/nui/show.do?dataset=demo_pjan&lang=en (Accessed: 16 December 2021).

FAO (2014) *Pulp and Paper Capacities*. Rome.

FAO (2015) *The economic lives of smallholder farmers*, *FAO Food And Agriculture Organization of the United Nations*. Available at: https://www.fao.org/3/i5251e/i5251e.pdf.

FAO (2017) *Agricultural Statistics*. Available at: http://www.fao.org/faostat/en/#data (Accessed: 18 October 2017).

FAO (2021) *FAO's Global Information System on Water and Agriculture.*, *AQUASTAT*. Available at: http://www.fao.org/aquastat/en/databases/ (Accessed: 10 May 2021).

Fengel, D. and Grosser, D. (1975) 'Chemical composition of coniferous and broadleaf trees (in German)', *Holz als Roh- und Werkstoff*, 33, pp. 32–34. doi:10.1007/BF02612913.

Finnish NFI (2013) *National Forest Inventory*.

Fleischmann, B., Meyr, H. and Wagner, M. (2008) 'Advanced Planning', in *Supply Chain Management and Advanced Planning*. Berlin, Heidelberg: Springer Berlin Heidelberg, pp. 81–106. doi:10.1007/978-3-540-74512-9_5.

Foulkes, M.J. *et al.* (2011) 'Raising yield potential of wheat. III. Optimizing partitioning to grain while maintaining lodging resistance', *Journal of Experimental Botany*, 62(2), pp. 469–486. doi:10.1093/jxb/erq300.

Frischknecht, R. (2020) *Textbook of Life Cycle Assessment (in German)*. Berlin, Heidelberg: Springer Berlin Heidelberg. doi:10.1007/978-3-662-54763-2.

Fürtner, D. *et al.* (2021) 'Locating Hotspots for the Social Life Cycle Assessment of Bio-Based Products from Short Rotation Coppice', *Bioenergy Research*, 14(2), pp. 510–533. doi:10.1007/s12155-021-10261-9.

Georgescu-Roegen, N. (1971) 'The Entropy Law and the Economic Problem', *The University of Alabama Distinguished Lecture Series* [Preprint], (1).

Georgescu-Roegen, N. (1975) 'Selections from "Energy and Economic Myths"', *Southern Economic Journal*, 41(1).

Gerbrandt, K. *et al.* (2016) 'Life cycle assessment of lignocellulosic ethanol: A review of key factors and methods affecting calculated GHG emissions and energy use', *Current Opinion in Biotechnology*, 38, pp. 63–70. doi:10.1016/j.copbio.2015.12.021.

German Federal Government (2012) *Roadmap Biorefinery*. Berlin. Available at: https://www.bmbf.de/pub/Roadmap_Bioraffinerien.pdf.

Ghaderi, H., Moini, A. and Pishvaee, M.S. (2018) 'A multi-objective robust possibilistic programming approach to sustainable switchgrass-based bioethanol supply chain network design', *Journal of Cleaner Production*, 179, pp. 368–406. doi:10.1016/j.jclepro.2017.12.218.

Ghaffar, S.H. and Fan, M. (2014) 'Lignin in straw and its applications as an adhesive', *International Journal of Adhesion and Adhesives*, 48(September), pp. 92–101. doi:10.1016/j.ijadhadh.2013.09.001.

Giuntoli, J. (2018) *Advanced biofuel policies in selected EU member states: 2018 update*.

Global Carbon Project (2021) *Global Carbon Atlas*. Available at: http://www.globalcarbonatlas.org/en/CO2-emissions (Accessed: 16 December 2021).

Goedkoop, M. and Spriensma, R. (2001) *The Eco-Indicator 99: A Damage Oriented Method for Life Cycle Impact Assessment.* Amersfoort. Available at: https://www.researchgate.net/publication/247848113_The_Eco-Indicator_99_A_Damage_Oriented_Method_for_Life_Cycle_Impact_Assessment.

Goetschalcks, M. and Fleischmann, B. (2008) 'Strategic Network Design', in Stadtler, H., Kilger, C., and Meyr, H. (eds) *Supply Chain Management and Advanced Planning*. Berlin, Heidelberg: Springer Berlin Heidelberg, pp. 117–132. doi:10.1007/978-3-540-74512-9_7.

Gong, J. and You, F. (2014) 'Global optimization for sustainable design and synthesis of algae processing network for CO 2 mitigation and biofuel production using life cycle optimization', *AIChE Journal*, 60(9), pp. 3195–3210. doi:10.1002/aic.14504.

González-García, S. *et al.* (2009) 'Life cycle assessment of flax shives derived second generation ethanol fueled automobiles in Spain', *Renewable and Sustainable Energy Reviews*, 13(8), pp. 1922–1933. doi:10.1016/j.rser.2009.02.003.

González-García, S. *et al.* (2012) 'Life cycle assessment of hemp hurds use in second generation ethanol production', *Biomass and Bioenergy*, 36, pp. 268–279. doi:10.1016/j.biombioe.2011.10.041.

Govindan, K., Jha, P.C. and Garg, K. (2016) 'Product recovery optimization in closed-loop supply chain to improve sustainability in manufacturing', *International Journal of Production Research*, 54(5), pp. 1463–1486. doi:10.1080/00207543.2015.1083625.

Govindan, K., Soleimani, H. and Kannan, D. (2015) 'Reverse logistics and closed-loop supply chain: A comprehensive review to explore the future', *European Journal of Operational Research*, 240(3), pp. 603–626. doi:10.1016/j.ejor.2014.07.012.

Gregg, J.S. *et al.* (2017) 'Value chain structures that define European cellulosic ethanol production', *Sustainability (Switzerland)*, 9(1), pp. 1–17. doi:10.3390/su9010118.

GRI (2021) *Global Reporting Standards*. Available at: https://www.globalreporting.org/standards/ (Accessed: 6 October 2021).

Gryparis, A. *et al.* (2004) 'Acute Effects of Ozone on Mortality from the "Air Pollution and Health', *American Journal of Respiratory and Critical Care Medicine*, 170(10), pp. 1080–1087. doi:10.1164/rccm.200403-333OC.

Gupta, A. and Verma, J.P. (2015) 'Sustainable bio-ethanol production from agro-residues: A review', *Renewable and Sustainable Energy Reviews*, 41, pp. 550–567. doi:10.1016/j.rser.2014.08.032.

Hamelinck, C.N., Van Hooijdonk, G. and Faaij, A.P.C. (2005) 'Ethanol from lignocellulosic biomass: Techno-economic performance in short-, middle- and long-term', *Biomass and Bioenergy*, 28(4), pp. 384–410. doi:10.1016/j.biombioe.2004.09.002.

Harkin, J.M. and Rowe, J.W. (1971) *Bark And Its Possible Uses*. U.S. Department of Agriculture.

Harms, R. (2020) *Straw price calculator (in German)*. Available at: https://www.lwk-niedersachsen.de/index.cfm/portal/betriebumwelt/nav/360/article/35680.html (Accessed: 22 November 2018).

Hauschild, M.Z. (2018) 'Introduction to LCA Methodology', in *Life Cycle Assessment*. Cham: Springer

International Publishing, pp. 59–66. doi:10.1007/978-3-319-56475-3_6.

Hauschild, M.Z., Bonou, A. and Olsen, S.I. (2018) 'Life Cycle Interpretation', in *Life Cycle Assessment*. Cham: Springer International Publishing, pp. 323–334. doi:10.1007/978-3-319-56475-3_12.

Hauschild, M.Z., Rosenbaum, R.K. and Olsen, S.I. (eds) (2018) *Life Cycle Assessment*. Cham: Springer International Publishing. doi:10.1007/978-3-319-56475-3.

Heijungs, R. and Guinée, J.B. (2007) 'Allocation and "what-if" scenarios in life cycle assessment of waste management systems', *Waste Management*, 27(8), pp. 997–1005. doi:10.1016/j.wasman.2007.02.013.

Heimann, T. (2019) 'Bioeconomy and SDGs: Does the Bioeconomy Support the Achievement of the SDGs?', *Earth's Future*, 7(1), pp. 43–57. doi:10.1029/2018EF001014.

Hein, F., Peter, F. and Graichen, P. (2020) *The German Power Market: State of Affairs in 2019*. Available at: https://www.agora-energiewende.de/en/publications/the-german-power-market-state-of-affairs-in-2019/.

Helwig, T. *et al.* (2002) *Agricultural Biomass Residue Inventories and Conversion Systems for Energy Production in Eastern Canada*.

Hennig, C., Brosowski, A. and Majer, S. (2016) 'Sustainable feedstock potential – a limitation for the bio-based economy?', *Journal of Cleaner Production*, 123(August), pp. 200–202. doi:10.1016/j.jclepro.2015.06.130.

Henrich, E., Dahmen, N. and Dinjus, E. (2009) 'Cost estimate for biosynfuel production via biosyncrude gasification', *Biofuels, Bioproducts and Biorefining*, 3(1), pp. 28–41. doi:10.1002/bbb.126.

Hertwich, E.G. *et al.* (2015) 'Integrated life-cycle assessment of electricity-supply scenarios confirms global environmental benefit of low-carbon technologies', *Proceedings of the National Academy of Sciences of the United States of America*, 112(20), pp. 6277–6282. doi:10.1073/pnas.1312753111.

Heuzé *et al.* (2017) *Straws*, *Feedpedia, a programme by INRAE, CIRAD, AFZ and FAO.* Available at: https://www.feedipedia.org/node/60 (Accessed: 1 March 2017).

HIIK (2021) *Conflict Barometer 2020*, *Heidelberg Institute for International Conflict Research*.

Hjuler, S.V. and Hansen, S.B. (2018) 'LCA of Biofuels and Biomaterials', in *Life Cycle Assessment*. Cham: Springer International Publishing, pp. 755–782. doi:10.1007/978-3-319-56475-3_30.

Hoekstra, R. (2019) *Replacing GDP by 2030*. Cambridge University Press. doi:10.1017/9781108608558.

Hosseini, S., Ivanov, D. and Dolgui, A. (2019) 'Review of quantitative methods for supply chain resilience analysis', *Transportation Research Part E: Logistics and Transportation Review*, 125(March), pp. 285–307. doi:10.1016/j.tre.2019.03.001.

Houghton, T. (2018) *French 2017/18 wheat production revised down 1% to 36.6 million mt*. Available at: https://www.agricensus.com/Article/French-2017-18-wheat-production-revised-down-1-to-36-6-million-mt-838.html (Accessed: 7 May 2018).

Huang, Y., Chen, C.W. and Fan, Y. (2010) 'Multistage optimization of the supply chains of biofuels', *Transportation Research Part E: Logistics and Transportation Review*, 46(6), pp. 820–830. doi:10.1016/j.tre.2010.03.002.

Huijbregts, M. *et al.* (2016) *ReCiPe 2016 - A harmonized life cycle impact assessment method at midpoint and endpoint level. Report I: Characterization*, *National Institute for Public Health and the Environment*. Available at: https://www.rivm.nl/bibliotheek/rapporten/2016-0104.pdf.

Huijbregts, M.A.J. *et al.* (2017) 'ReCiPe2016: a harmonised life cycle impact assessment method at

midpoint and endpoint level', *The International Journal of Life Cycle Assessment*, 22(2), pp. 138–147. doi:10.1007/s11367-016-1246-y.

Humbird, D. *et al.* (2011) 'Process Design and Economics for Biochemical Conversion of Lignocellulosic Biomass to Ethanol: Dilute-Acid Pretreatment and Enzymatic Hydrolysis of Corn Stover', *National Renewable Energy Laboratory*, (May), pp. 1–147. doi:10.2172/1107470.

Hyndman, R.J. and Athanasopoulos, G. (2013) *Forecasting: principles and practices*. OTexts.

IEA (2021) *Data and Statistics*. Available at: https://www.iea.org/data-and-statistics (Accessed: 20 October 2021).

IGN (2015) *National Forest Inventory (in French)*. Institute National de L'Information Geographique et Forestiere.

ILO (2021a) *Days lost due to cases of occupational injury with temporary incapacity for work by economic activity - Annual*. Available at: https://www.ilo.org/shinyapps/bulkexplorer41/?lang=en&segment=indicator&id=INJ_DAYS_ECO_NB_A (Accessed: 6 October 2021).

ILO (2021b) *Employees by sex and economic activity (thousands)*. Available at: https://www.ilo.org/shinyapps/bulkexplorer41/?lang=en&segment=indicator&id=EES_TEES_SEX_ECO_NB_A (Accessed: 6 October 2021).

ILO (2021c) *International Labour Organization (2021). Fatal occupational injuries per 100'000 workers by economic activity - Annual.* Available at: https://www.ilo.org/shinyapps/bulkexplorer41/?lang=en&segment=indicator&id=INJ_DAYS_ECO_NB_A (Accessed: 6 October 2021).

ILO (2021d) *Statistics and databases*. Available at: https://www.ilo.org/global/statistics-and-databases/lang--en/index.htm (Accessed: 16 October 2021).

IMF (2021) *World Economic Outlook Update, January 2021*. Available at: https://www.imf.org/en/Publications/WEO/weo-database/2020/October/ (Accessed: 6 October 2021).

IPCC (1992) *Climate change: The IPCC 1990 and 1992 Assessments*, *IPCC First Assessment Report*.

IPCC (1996) 'Revised 1996 IPCC Guidelines for National Greenhouse Gas Inventories', (1993), pp. 76–95. Available at: http://www.ipcc-nggip.iges.or.jp/public/gl/invs1.html.

IPCC (2014) *Climate Change 2014: Synthesis Report. Contribution of Working Groups I, II and III to the Fifth Assessment Report of the Intergovernmental Panel on Climate Change*. Geneva, Switzerland.

IPCC (2021) *Climate Change 2021: The Physical Science Basis. Contribution of Working Group I to the Sixth Assessment Report of the Intergovernmental Panel on Climate Change*. Edited by V. Masson-Delmotte et al. Cambridge: Cambridge University Press.

IRG - Rail (2019) *Seventh IRG-Rail Market Monitoring report*. Available at: https://www.irg-rail.eu/irg/documents/market-monitoring/220,2019.html.

ISO (2006a) *ISO 14040 (2006) Environmental management – life cycle assessment – principles and framework*. Available at: https://www.iso.org/standard/37456.html.

ISO (2006b) *ISO 14044 Environmental management — Life cycle assessment — Requirements and guidelines*. Available at: https://www.iso.org/standard/38498.html.

ISO (2011) *ISO 26000 Social Responsibility*. Available at: https://www.iso.org/iso-26000-social-responsibility.html (Accessed: 6 October 2021).

Jakhar, S.K. (2015) 'Performance evaluation and a flow allocation decision model for a sustainable supply chain of an apparel industry', *Journal of Cleaner Production*, 87, pp. 391–413. doi:10.1016/j.jclepro.2014.09.089.

Jones, D. (2015) *Ireland leads the world in wheat yields*. Farmers weekly. Available at: https://www.fwi.co.uk/arable/ireland-leads-world-wheat-yields (Accessed: 19 April 2018).

Jungbluth, N. *et al.* (2007) *Life Cycle Inventories of Bioenergy*. Uster. Available at: http://www.researchgate.net/publication/230725648_Life_Cycle_Inventories_of_Bioenergy._ecoinvent_report_No._17/file/9c96051b76e2fb8dce.pdf.

Kahiluoto, H. *et al.* (2019) 'Decline in climate resilience of european wheat', *Proceedings of the National Academy of Sciences of the United States of America*, 116(1), pp. 123–128. doi:10.1073/pnas.1804387115.

Kaltschmitt, M., Hartmann, H. and Hofbauer, H. (2016) *Energy from biomass (in German)*. 3rd edn. Edited by M. Kaltschmitt, H. Hartmann, and H. Hofbauer. Berlin, Heidelberg: Springer Vieweg. doi:10.1007/978-3-662-47438-9.

Kamm, B., Gruber, P.R. and Kamm, M. (2010) *Biorefineries - Industrial Processes and Products*. 2nd edn. Edited by B. Kamm, P.R. Gruber, and M. Kamm. Weinheim: WILEY-VCH Verlag GmbH & Co. KGaA.

Kamm, B. and Kamm, M. (2004) 'Principles of biorefineries', *Applied Microbiology and Biotechnology*, 64(2), pp. 137–145. doi:10.1007/s00253-003-1537-7.

Kavalov, B. (2009) *Market Perspectives for Products from Future Energy Driven Biorefineries by 2020*. doi:10.2790/159.

Kemppainen, K. *et al.* (2014) 'Spruce bark as an industrial source of condensed tannins and non-cellulosic sugars', *Industrial Crops and Products*, 52, pp. 158–168. doi:10.1016/j.indcrop.2013.10.009.

Kenneth, C. and Zammit-Mangion, D. (2013) 'On e-Constraint Based Methods for the Generation of Pareto Frontiers', *Journal of Mechanics Engineering and Automation*, (3), pp. 279–289. doi:10.1017/CBO9781107415324.004.

Khamphet, T., Tandjo, D. and Penner, M.H. (1997) 'Influence of extractives on the chemical analysis of switchgrass', *Journal of Agricultural and Food Chemistry*, 45(1994), pp. 437–443.

Kim, J. *et al.* (2011) 'Design of biomass processing network for biofuel production using an MILP model', *Biomass and Bioenergy*, 35(2), pp. 853–871. doi:10.1016/j.biombioe.2010.11.008.

Kim, S. and Dale, B.E. (2004) 'Global potential bioethanol production from wasted crops and crop residues', *Biomass and Bioenergy*, 26(4), pp. 361–375. doi:10.1016/j.biombioe.2003.08.002.

Kim, S. and Dale, B.E. (2005) 'Life cycle assessment of various cropping systems utilized for producing biofuels: Bioethanol and biodiesel', *Biomass and Bioenergy*, 29(6), pp. 426–439. doi:10.1016/j.biombioe.2005.06.004.

Kolotzek, C. *et al.* (2018) 'A company-oriented model for the assessment of raw material supply risks, environmental impact and social implications', *Journal of Cleaner Production*, 176, pp. 566–580. doi:10.1016/j.jclepro.2017.12.162.

Kost, C. *et al.* (2021) 'Study: Levelized Cost of Electricity- Renewable Energy Technologies', (June), pp. 1–45.

Krauß, H. (2017) *Harvest 2017: Cereal yields heterogeneous, rapeseed 18 % below average (in German)*. Available at: https://www.agrarheute.com/pflanze/ernte-2017-getreideertraege-heterogen-raps-18-schnitt-537547 (Accessed: 25 May 2018).

Kretschmer, B., Allen, B. and Hart, K. (2012) 'Mobilising cereal straw in the EU to feed advanced biofuel

production', *Report produced for Novozymes*, (May), p. 61. doi:10.1017/CBO9781107415324.004.

Kühnen, M. and Hahn, R. (2017) 'Indicators in Social Life Cycle Assessment: A Review of Frameworks, Theories, and Empirical Experience', *Journal of Industrial Ecology*, 21(6), pp. 1547–1565. doi:10.1111/jiec.12663.

Lacoste, C. *et al.* (2015) 'Biobased foams from condensed tannin extracts from Norway spruce (Picea abies) bark', *Industrial Crops and Products*, 73, pp. 144–153. doi:10.1016/j.indcrop.2015.03.089.

Lal, R. (2005) 'World crop residues production and implications of its use as a biofuel', *Environment International*, 31(4), pp. 575–584. doi:10.1016/j.envint.2004.09.005.

Landwirtschaftskammer NRW (2015) 'Target rates for the assessment of agricultural crops (in German)', (September), p. 2.

Langholtz, M. *et al.* (2014) 'Climate risk management for the U.S. cellulosic biofuels supply chain', *Climate Risk Management*, 3, pp. 96–115. doi:10.1016/j.crm.2014.05.001.

Lauven, L.-P. (2014) 'An optimization approach to biorefinery setup planning', *Biomass and Bioenergy*, 70, pp. 440–451. doi:10.1016/j.biombioe.2014.07.026.

Lauven, L.-P., Karschin, I. and Geldermann, J. (2018) 'Simultaneously optimizing the capacity and configuration of biorefineries', *Computers & Industrial Engineering*, 124(March 2017), pp. 12–23. doi:10.1016/j.cie.2018.07.014.

Lavoie, J.-M. *et al.* (2011) 'Biorefining Lignocellulosic Biomass via the Feedstock Impregnation Rapid and Sequential Steam Treatment', in *Biofuel's Engineering Process Technology*. InTech. doi:10.5772/18186.

Leduc, S. *et al.* (2010) 'Optimal location of lignocellulosic ethanol refineries with polygeneration in Sweden', *Energy*, 35(6), pp. 2709–2716. doi:10.1016/j.energy.2009.07.018.

Lee, J., Nam, D.S. and Kong, C. (2016) 'Variability in nutrient composition of cereal grains from different origins', *SpringerPlus*, 5(1), p. 419. doi:10.1186/s40064-016-2046-3.

Lee, R.A. and Lavoie, J.M. (2013) 'From first- to third-generation biofuels: Challenges of producing a commodity from a biomass of increasing complexity', *Animal Frontiers*, 3(2), pp. 6–11. doi:10.2527/af.2013-0010.

Lesk, C., Rowhani, P. and Ramankutty, N. (2016) 'Influence of extreme wheater disasters on global crop production', *Nature*, 529(7584), pp. 84–87. doi:10.1038/nature16467.

Lewandowski, I. (2015) 'Securing a sustainable biomass supply in a growing bioeconomy', *Global Food Security*, 6, pp. 34–42. doi:10.1016/j.gfs.2015.10.001.

Life Cycle Initiative (2021) *The Guidelines for Social Life Cycle Assessment (S-LCA) of Products 2020*.

Lin, C.-C., Liu, W.-Y. and Huang, G.-L. (2019) 'Fuzzy Multi-objective Forest Biomass-to-biofuel Facility Location Problem with Social Consideration', *Energy Procedia*, 158, pp. 4067–4072. doi:10.1016/j.egypro.2019.01.830.

Lin, M.H. *et al.* (2013) 'A review of piecewise linearization methods', *Mathematical Problems in Engineering*, 2013. doi:10.1155/2013/101376.

López, S. *et al.* (2005) 'Assessment of nutritive value of cereal and legume straws based on chemical composition and in vitro digestibility', *Journal of the Science of Food and Agriculture*, 85(9), pp. 1550–1557. doi:10.1002/jsfa.2136.

Majeau-Bettez, G. *et al.* (2018) 'Choice of Allocations and Constructs for Attributional or Consequential Life Cycle Assessment and Input-Output Analysis', *Journal of Industrial Ecology*, 22(4), pp. 656–670.

doi:10.1111/jiec.12604.

Marvin, W.A., Schmidt, L.D. and Daoutidis, P. (2013) 'Biorefinery location and technology selection through supply chain optimization', *Industrial and Engineering Chemistry Research*, 52(9), pp. 3192–3208. doi:10.1021/ie3010463.

Mavrotas, G. (2009) 'Effective implementation of the ε-constraint method in Multi-Objective Mathematical Programming problems', *Applied Mathematics and Computation*, 213(2), pp. 455–465. doi:10.1016/j.amc.2009.03.037.

McCormick, K. and Kautto, N. (2013) 'The Bioeconomy in Europe: An Overview', *Sustainability (Switzerland)*, 5(6), pp. 2589–2608. doi:10.3390/su5062589.

McKean, W.T. and Jacobs, R.S. (1997) *Wheat Straw as a Paper Fiber Source*. Seattle: The Clean Washington Center.

Meadows, D.H. *et al.* (1972) *The Limits to Growth: A report for the Club of Rome's Project on the Predicament of Mankind*, *Demography*. Universe Books. doi:10.1349/ddlp.1.

Messmann, L. *et al.* (2019) 'Economic and environmental benefits of recovery networks for WEEE in Europe', *Journal of Cleaner Production*, 222, pp. 655–668. doi:10.1016/j.jclepro.2019.02.244.

Messmann, L. *et al.* (2020) 'How to quantify social impacts in strategic supply chain optimization: State of the art', *Journal of Cleaner Production*, 257, p. 120459. doi:10.1016/j.jclepro.2020.120459.

Ministerstvo Zemedelstvi (2012) 'Information on Forests and Forestry in the Czech Republic by 2012', p. 29. doi:10.1051/forest:2008043.

Miret, C. *et al.* (2016) 'Design of bioethanol green supply chain: Comparison between first and second generation biomass concerning economic, environmental and social criteria', *Computers and Chemical Engineering*, 85, pp. 16–35. doi:10.1016/j.compchemeng.2015.10.008.

Mok, W.S.L. and Antal, M.J. (1992) 'Uncatalyzed Solvolysis of Whole Biomass Hemicellulose by Hot Compressed Liquid Water', *Industrial and Engineering Chemistry Research*, 31(4), pp. 1157–1161. doi:10.1021/ie00004a026.

Monteil-Rivera, F. *et al.* (2013) 'Isolation and characterization of herbaceous lignins for applications in biomaterials', *Industrial Crops and Products*, 41(1), pp. 356–364. doi:10.1016/j.indcrop.2012.04.049.

Morales, M. *et al.* (2015) 'Life cycle assessment of lignocellulosic bioethanol: Environmental impacts and energy balance', *Renewable and Sustainable Energy Reviews*, 42, pp. 1349–1361. doi:10.1016/j.rser.2014.10.097.

Moreno, A.D. *et al.* (2017) 'Production of Ethanol from Lignocellulosic Biomass', in Fang, Z., Smith, J.R., and Qi, X. (eds) *Production of Platform Chemicals from Sustainable Resources*. Singapor, pp. 375–410. doi:10.1007/978-981-10-4172-3_12.

Mota, B., Gomes, M.I., Carvalho, A. and Barbosa-Póvoa, A. (2015) 'Supply chain design and planning accounting for the Triple Bottom Line', in, pp. 1841–1846. doi:10.1016/B978-0-444-63576-1.50001-7.

Mota, B., Gomes, M.I., Carvalho, A. and Barbosa-Povoa, A.P. (2015) 'Towards supply chain sustainability: economic, environmental and social design and planning', *Journal of Cleaner Production*, 105, pp. 14–27. doi:10.1016/j.jclepro.2014.07.052.

Mota, B. *et al.* (2018) 'Sustainable supply chains: An integrated modeling approach under uncertainty', *Omega*, 77, pp. 32–57. doi:10.1016/j.omega.2017.05.006.

Mousavi Ahranjani, P. *et al.* (2018) 'Hybrid Multiobjective Robust Possibilistic Programming Approach to a Sustainable Bioethanol Supply Chain Network Design', *Industrial and Engineering Chemistry Research*, 57(44), pp. 15066–15083. doi:10.1021/acs.iecr.8b02869.

Mujkic, Z., Qorri, A. and Kraslawski, A. (2018) 'Sustainability and Optimization of Supply Chains: a Literature Review', *Operations and Supply Chain Management: An International Journal*, pp. 186–199. doi:10.31387/oscm0350213.

Münch, J. (2008) 'Sustainably usable wheat straw in Germany (in German)'.

Muñoz, I. *et al.* (2014) 'Life cycle assessment of bio-based ethanol produced from different agricultural feedstocks', *International Journal of Life Cycle Assessment*, 19(1), pp. 109–119. doi:10.1007/s11367-013-0613-1.

Müssig, J. and Carus, M. (2014) *Marktanalyse Nachwachsende Rohstoffe Teil II*.

National Forest Holding (2015) 'The National Forest Inventory'.

Nguyen, T.L.T., Hermansen, J.E. and Mogensen, L. (2013) 'Environmental performance of crop residues as an energy source for electricity production: The case of wheat straw in Denmark', *Applied Energy*, 104, pp. 633–641. doi:10.1016/j.apenergy.2012.11.057.

norwegianpetroleum (2021) *Everything you need to know about Norwegian petroleum activities*. Available at: https://www.norskpetroleum.no/en/economy/employment/%0A.

NREL & PNNL (2004) *Top Value Added Chemicals from Biomass*. doi:10.2172/15008859.

OECD (2009) 'The Bioeconomy to 2030 - Main Findings and Conclusions', p. 18.

OECD and FAO (2015) *Aglink-Cosimo Model Documentation; A partial equilibrium model of world agricultural markets*.

Ogunwusi, A.A. (2013) 'Potentials of Industrial Utilization of Bark', *Journal of Natural Sciences Research*, 3(5), pp. 2225–921. Available at: www.iiste.org.

Osmani, A. and Zhang, J. (2013) 'Stochastic optimization of a multi-feedstock lignocellulosic-based bioethanol supply chain under multiple uncertainties', *Energy*, 59, pp. 157–172. doi:10.1016/j.energy.2013.07.043.

Osmani, A. and Zhang, J. (2014) 'Economic and environmental optimization of a large scale sustainable dual feedstock lignocellulosic-based bioethanol supply chain in a stochastic environment', *Applied Energy*, 114, pp. 572–587. doi:10.1016/j.apenergy.2013.10.024.

Palo, R.T. (1984) 'Distribution of birch (Betula SPP.), willow (Salix SPP.), and poplar (Populus SPP.) secondary metabolites and their potential role as chemical defense against herbivores', *Journal of Chemical Ecology*, 10(3).

Pannonpower (2014) *Dalkia's straw fuelled power plant in Pécs named best in Europe*.

Papatheofanous, M.G. *et al.* (1998) 'Optimizing multisteps mechanical-chemical fractionation of wheat straw components', *Industrial Crops and Products*, 7(2–3), pp. 249–256. doi:10.1016/S0926-6690(97)00055-1.

Patel, M., Zhang, X. and Kumar, A. (2016) 'Techno-economic and life cycle assessment on lignocellulosic biomass thermochemical conversion technologies: A review', *Renewable and Sustainable Energy Reviews*, 53, pp. 1486–1489. doi:10.1016/j.rser.2015.09.070.

Persyn, D. *et al.* (2020) 'Territorial Development - JRC Policy Insights A NEW DATASET OF DISTANCE AND TIME RELATED TRANSPORT COSTS FOR EU REGIONS', *Territorial Development Insights Series* [Preprint], (January).

Pfau, S.F. *et al.* (2014) 'Visions of sustainability in bioeconomy research', *Sustainability (Switzerland)*, 6(3), pp. 1222–1249. doi:10.3390/su6031222.

Pishvaee, M.S., Razmi, J. and Torabi, S.A. (2014) 'An accelerated Benders decomposition algorithm for

sustainable supply chain network design under uncertainty: A case study of medical needle and syringe supply chain', *Transportation Research Part E: Logistics and Transportation Review*, 67, pp. 14–38. doi:10.1016/j.tre.2014.04.001.

ProMods (2017) *List of truck speed limits for all countries in Europe*. Available at: https://promods.net/viewtopic.php?f=7&t=18254.

Pronyk, C., Mazza, G. and Tamaki, Y. (2011) 'Production of carbohydrates, lignins, and minor components from triticale straw by hydrothermal treatment', *Journal of Agricultural and Food Chemistry*, 59(8), pp. 3788–3796. doi:10.1021/jf104543a.

PwC (2019) *Creating a strategy for a better world. How the Sustainable Development Goals can provide the framework for business do deliver progess on our global challenges*.

Quaschning, V. (2020) *Renewable Energies and Climate Protection: Background - Techniques and Planning - Economy and Ecology - Energy transition*. Hanser.

Ragauskas, A.J. *et al.* (2006) 'From wood to fuels: Integrating biofuels and pulp production', *Industrial Biotechnology*, 2(1), pp. 55–65. doi:10.1089/ind.2006.2.55.

Ragauskas, A.J. *et al.* (2014) 'Lignin valorization: Improving lignin processing in the biorefinery', *Science*, 344(6185). doi:10.1126/science.1246843.

Räisenen, T. and Athanassiadis, D. (2013) *Basic chemical composition of the biomass components of pine, spruce and birch*. Forest Refine.

Rehman, S.U. (2017) *EU cuts cereal crop outlook as drought in Spain hits barley*. Available at: https://www.brecorder.com/2017/06/01/351827/eu-cuts-cereal-crop-outlook-as-drought-in-spain-hits-barley/ (Accessed: 25 May 2018).

Ren, J. *et al.* (2015) 'Prioritization of bioethanol production pathways in China based on life cycle sustainability assessment and multicriteria decision-making', *The International Journal of Life Cycle Assessment*, 20(6), pp. 842–853. doi:10.1007/s11367-015-0877-8.

Ricke, K. *et al.* (2018) 'Country-level social cost of carbon', *Nature Climate Change*, 8(10), pp. 895–900. doi:10.1038/s41558-018-0282-y.

Rockström, J. *et al.* (2009) 'Planetary Boundaries: Exploring the Safe Operating Space for Humanity Johan', *Nature*, 461(7263), pp. 472–475. doi:10.1038/461472a.

Roni, M.S. *et al.* (2017) 'A multi-objective, hub-and-spoke model to design and manage biofuel supply chains', *Annals of Operations Research*, 249(1–2), pp. 351–380. doi:10.1007/s10479-015-2102-3.

Rosenbaum, R.K. *et al.* (2018) 'Life Cycle Impact Assessment', in Hauschild, Michael Z., Rosenbaum, R.K., and Olsen, S.I. (eds) *Life Cycle Assessment*. Springer, pp. 167–270. doi:10.1007/978-3-319-56475-3.

RPS-MCOS (2004) 'The Renewable Energy Resource Potential of Dry Agricultural Residues in Ireland'.

Rye, C. *et al.* (2013) 'Environmental Limits to Population Growth', in *Biology*. Houston, Texas: openstax, pp. 1326–1331.

S2Biom (2015) *S2Biom Database*, *Biomass Chain Data*. Available at: https://s2biom.wenr.wur.nl/.

Sahebjamnia, N., Fathollahi-Fard, A.M. and Hajiaghaei-Keshteli, M. (2018) 'Sustainable tire closed-loop supply chain network design: Hybrid metaheuristic algorithms for large-scale networks', *Journal of Cleaner Production*, 196, pp. 273–296. doi:10.1016/j.jclepro.2018.05.245.

SAI (1997) *SA8000® Standard*. Available at: https://sa-intl.org/programs/sa8000/ (Accessed: 6 October 2021).

Sangnark, A. and Noomhorm, A. (2004) 'Chemical, physical and baking properties of dietary fiber prepared from rice straw', *Food Research International*, 37(1), pp. 66–74. doi:10.1016/j.foodres.2003.09.007.

De Santi, G. *et al.* (2008) 'Biofuels in the European Context: Facts and Uncertainties', p. 0. doi:10.2788/69274.

Santibañez-Aguilar, J.E. *et al.* (2011) 'Optimal Planning of a Biomass Conversion System Considering Economic and Environmental Aspects', *Industrial & Engineering Chemistry Research*, 50(14), pp. 8558–8570. doi:10.1021/ie102195g.

Santibañez-Aguilar, J.E. *et al.* (2014) 'Optimal planning and site selection for distributed multiproduct biorefineries involving economic, environmental and social objectives', *Journal of Cleaner Production*, 65, pp. 270–294. doi:10.1016/j.jclepro.2013.08.004.

Scarlat, N. *et al.* (2019) 'Integrated and spatially explicit assessment of sustainable crop residues potential in Europe', *Biomass and Bioenergy*, 122(February), pp. 257–269. doi:10.1016/j.biombioe.2019.01.021.

Scarlat, N., Martinov, M. and Dallemand, J.-F. (2010) 'Assessment of the availability of agricultural crop residues in the European Union: Potential and limitations for bioenergy use', *Waste Management*, 30(10), pp. 1889–1897. doi:10.1016/j.wasman.2010.04.016.

Schaidle, J.A., Moline, C.J. and Savage, P.E. (2011) 'Biorefinery sustainability assessment', *Environmental Progress & Sustainable Energy*, 30(4), pp. 743–753. doi:10.1002/ep.10516.

Schlittgen and Streitberg (2001) *Time Series Analysis (in German)*. 9. München: Oldenbourg.

Schmid, K., Hadwiger, F. and Wilke, P. (2019) *Branchenanalyse Mineralölindustrie*.

Schweitzer (1994) *Industrial Operations (in german)*. 2nd edn. Edited by P.D.G.S. Prof. Dr. Marcell Schweitzer, Prof. Dr. Herbert Kargl, Prof. Dr. Erich Frese, Prof. Dr. Oskar Grün, Prof. Dr. Hartmut Kreikebaum, Prof. Dr. Marcell Schweitzer, Prof. Dr. Hans-Ulrich Küpper, Prof. Dr. Heinz Strebel, Prof. Dr. Gerhard Seicht. Vahlen.

Scottish Government (2017) *Review of Legislation Governing Small Landholdings in Scotland*. Available at: https://www.gov.scot/publications/review-legislation-governing-small-landholdings-scotland/documents/.

Sheehan, J. *et al.* (2003) 'Energy and environmental aspects of using corn stover for fuel ethanol', *Journal of Industrial Ecology*, 7(3–4), pp. 117–146. doi:10.1162/108819803323059433.

Shokouhyar, S. and Aalirezaei, A. (2017) 'Designing a sustainable recovery network for waste from electrical and electronic equipment using a genetic algorithm', *International Journal of Environment and Sustainable Development*, 16(1), p. 60. doi:10.1504/IJESD.2017.080851.

Singh, A., Chu, Y. and You, F. (2014) 'Biorefinery supply chain network design under competitive feedstock markets: An agent-based simulation and optimization approach', *Industrial and Engineering Chemistry Research*, 53(39), pp. 15111–15126. doi:10.1021/ie5020519.

Soleimani, H. *et al.* (2017) 'Fuzzy multi-objective sustainable and green closed-loop supply chain network design', *Computers & Industrial Engineering*, 109, pp. 191–203. doi:10.1016/j.cie.2017.04.038.

Staffas, L., Gustavsson, M. and McCormick, K. (2013) 'Strategies and policies for the bioeconomy and bio-based economy: An analysis of official national approaches', *Sustainability (Switzerland)*, 5(6), pp. 2751–2769. doi:10.3390/su5062751.

Stefansdottir, B. *et al.* (2018) 'Impact of shelf life on the trade-off between economic and

environmental objectives: A dairy case', *International Journal of Production Economics*, 201(February), pp. 136–148. doi:10.1016/j.ijpe.2018.04.009.

Stegmann, P., Londo, M. and Junginger, M. (2020) 'The circular bioeconomy: Its elements and role in European bioeconomy clusters', *Resources, Conservation and Recycling: X*, 6(July 2019), p. 100029. doi:10.1016/j.rcrx.2019.100029.

Strom-Report (2021) *Electricity price composition (in German)*. Available at: https://strom-report.de/strompreise/strompreis-zusammensetzung/.

Suhl, L. and Mellouli, T. (2013) *Optimization Systems (in german)*. Berlin, Heidelberg: Springer Berlin Heidelberg (Springer-Lehrbuch). doi:10.1007/978-3-642-38937-5.

Sun, R.-C. and Tomkinson, J. (2000) 'Essential Guides for Isolation / Purification of Drug Metabolites', *Encyclopedia of Separation Science*, (1991), pp. 4568–4574.

Sun, Y. and Cheng, J. (2002) 'Hydrolysis of lignocellulosic materials for ethanol production : a review q', *Bioresource technology*, 83(1), pp. 1–11. doi:10.1016/S0960-8524(01)00212-7.

Sunliquid (2019) *Cellulosic ethanol made from agricultural residues*. Available at: www.sunliquid-project-fp7.eu (Accessed: 29 September 2019).

Swedish NFI (2016) *Fellings*.

Taherzadeh, M.J. and Karimi, K. (2008) *Pretreatment of lignocellulosic wastes to improve ethanol and biogas production: A review*, *International Journal of Molecular Sciences*. doi:10.3390/ijms9091621.

Thangavelu, S.K., Ahmed, A.S. and Ani, F.N. (2016) 'Review on bioethanol as alternative fuel for spark ignition engines', *Renewable and Sustainable Energy Reviews*, 56, pp. 820–835. doi:10.1016/j.rser.2015.11.089.

Theil, H. (1966) *Applied Economic Forecasting*. Amsterdam: North Holland.

Thonemann, U. (2010) *Operations Management*. 2nd edn. Pearson Studium.

Thorenz, A. *et al.* (2018) 'Assessment of agroforestry residue potentials for the bioeconomy in the European Union', *Journal of Cleaner Production*, 176(December), pp. 348–359. doi:10.1016/j.jclepro.2017.12.143.

Thrän, D. and Pfeiffer, D. (2015) 'Method Handbook: Material flow-oriented assessment of greenhouse gas effects', p. 161.

Tilman, D. *et al.* (2009) 'Beneficial biofuels - The food, energy, and environment trilemma', *Science*, 325(5938), pp. 270–271. doi:10.1126/science.1177970.

Towler, G.P. and Sinnott, R.K. (2013) 'Chemical engineering design. Principles, Practice and Economics of Plant and Process Design', in *Chemical Engineering Design*. Elsevier, p. i. doi:10.1016/B978-0-08-096659-5.00022-5.

Trompiz, G. (2017) *France heading for record rapeseed yield - crop institute*. Available at: https://www.agriculture.com/markets/newswire/france-heading-for-record-rapeseed-yield-crop-institute (Accessed: 25 May 2018).

Tühnen (2016) *Third Natrional Forest Inventory*, *Bundeswaldinventur*.

Tuyttens, F.A.M. (2005) 'The importance of straw for pig and cattle welfare: A review', *Applied Animal Behaviour Science*, 92(3), pp. 261–282. doi:10.1016/j.applanim.2005.05.007.

UKEITI (2021) *Oil & Gas in the UK*. Available at: https://www.ukeiti.org/oil-gas.

UN Comtrade (2016) *UN Comtrade*.

UNEP (2011) *Towards a Life Cycle Sustainability Assessment*. doi:DTI/1412/PA.

UNEP (2020) *Guidelines for Social Life Cycle Assessment of Products and Organizations*. Edited by C. Benoît-Norris et al. Available at: http://www.unep.fr/shared/publications/pdf/DTIx1164xPA-guidelines_sLCA.pdf.

UNEP SETAC (2013) *The Methodological Sheets for Subcategories in Social Life Cicle Assessment (S-LCA)*, *Pre-Publication-Version.* Edited by C. Benoît-Norris et al. Available at: http://link.springer.com/10.1007/978-1-4419-8825-6.

UNFCCC (2015) *Paris Agreement*. Available at: https://unfccc.int/process-and-meetings/the-paris-agreement/the-paris-agreement (Accessed: 23 December 2021).

UNHCR (2021) *Figures at a Glance*. Available at: https://www.unhcr.org/en-us/figures-at-a-glance.html (Accessed: 12 October 2021).

United Nations (2015) *Sustainable Development Goals*. Available at: https://sdgs.un.org/goals (Accessed: 6 October 2021).

Valdivia, S. *et al.* (2021) 'Principles for the application of life cycle sustainability assessment', *The International Journal of Life Cycle Assessment*, 26(9), pp. 1900–1905. doi:10.1007/s11367-021-01958-2.

VDLUFA (2014) *Humus balancing; A Method for the analysis and assessment of the humus provision of cultivated farmland (in German)*. Speyer.

van der Velde, M. *et al.* (2018) 'In-season performance of European Union wheat forecasts during extreme impacts', *Scientific Reports*, 8(1), pp. 1–10. doi:10.1038/s41598-018-33688-1.

van der Velde, M. *et al.* (2019) 'Assessing the France 2016 extreme wheat production loss-evaluating our operational capacity to predict complex compound events', *Climate Extremes and Their Implications for Impact and Risk Assessment*, (July), pp. 139–158. doi:10.1016/B978-0-12-814895-2.00009-4.

Ververis, C. *et al.* (2004) 'Fiber dimensions, lignin and cellulose content of various plant materials and their suitability for paper production', *Industrial Crops and Products*, 19(3), pp. 245–254. doi:10.1016/j.indcrop.2003.10.006.

VHE (2014) *Strohverkauf und Kompostdüngung*. Aachen: Verband der Humus- und Erdenwirtschaft e.V.

Villegas, J.D. and Gnansounou, E. (2008) 'Techno-economic and environmental evaluation of lignocellulosic biochemical refineries: Need for a modular platform for integrated assessment (MPIA)', *Journal of Scientific and Industrial Research*, 67(11), pp. 927–940.

Vis, M.W. and van den Berg, D. (2010) 'Harmonization of biomass resource assessments Volume I - Best Practices and Methods Handbook', I, p. 220. doi:10.13140/2.1.4643.8084.

VLK (2015) *Bodenfruchtbarkeit – Grundlage erfolgreicher Landwirtschaft Bodenfruchtbarkeit – Grundlage erfolgreicher Landwirtschaft*. Würzburg: Verband der Landwirschaftskammern.

Walther, G., Schatka, A. and Spengler, T.S. (2012) 'Design of regional production networks for second generation synthetic bio-fuel - A case study in Northern Germany', *European Journal of Operational Research*, 218(1), pp. 280–292. doi:10.1016/j.ejor.2011.09.050.

Wang, L., Littlewood, J. and Murphy, R.J. (2013) 'Environmental sustainability of bioethanol production from wheat straw in the UK', *Renewable and Sustainable Energy Reviews*, 28, pp. 715–725. doi:10.1080/00036846.2013.835479.

Watanabe, M.D.B. *et al.* (2016) 'Hybrid Input-Output Life Cycle Assessment of First- and Second-

Generation Ethanol Production Technologies in Brazil', *Journal of Industrial Ecology*, 20(4), pp. 764–774. doi:10.1111/jiec.12325.

Weisstein, E.W. (2018) *Disk Line Picking*, *Math World*. Available at: http://mathworld.wolfram.com/DiskLinePicking.html (Accessed: 14 September 2018).

Wernet, G. *et al.* (2016) 'The ecoinvent database version 3 (part I): overview and methodology', *The International Journal of Life Cycle Assessment*, 21(9), pp. 1218–1230. doi:10.1007/s11367-016-1087-8.

Wheeler, J. *et al.* (2018) 'Combining multi-attribute decision-making methods with multi-objective optimization in the design of biomass supply chains', *Computers & Chemical Engineering* [Preprint]. doi:10.1016/j.compchemeng.2018.02.010.

WHO (2013) *Health risks of air pollution in Europe – HRAPIE project*, *World Heath Organization (WHO)*. Available at: http://tinyurl.com/oe8wmc6%0A.

WHO (2021) *AirQ+: software tool for health risk assessment of air pollution*. Available at: https://www.euro.who.int/en/health-topics/environment-and-health/air-quality/activities/airq-software-tool-for-health-risk-assessment-of-air-pollution (Accessed: 6 October 2021).

Wietschel, L. *et al.* (2021) 'Environmental benefits of large-scale second-generation bioethanol production in the EU: An integrated supply chain network optimization and life cycle assessment approach', *Journal of Industrial Ecology*, 25(3), pp. 677–692. doi:10.1111/jiec.13083.

Wietschel, L., Thorenz, A. and Tuma, A. (2019) 'Spatially explicit forecast of feedstock potentials for second generation bioconversion industry from the EU agricultural sector until the year 2030', *Journal of Cleaner Production*, 209, pp. 1533–1544. doi:10.1016/j.jclepro.2018.11.072.

Wiloso, E.I., Heijungs, R. and De Snoo, G.R. (2012) 'LCA of second generation bioethanol: A review and some issues to be resolved for good LCA practice', *Renewable and Sustainable Energy Reviews*, 16(7), pp. 5295–5308. doi:10.1016/j.rser.2012.04.035.

Wogrin, S., Pineda, S. and Tejada-Arango, D.A. (2020) 'Applications of Bilevel Optimization in Energy and Electricity Markets', in, pp. 139–168. doi:10.1007/978-3-030-52119-6_5.

World Bank (2019) *State and Trends of Carbon Pricing 2019*, *State and Trends of Carbon Pricing*. Washington, DC: The World Bank. doi:10.1596/978-1-4648-1435-8.

World Bank (2021a) *CO2 emissions (kt) - European Union*. Available at: https://data.worldbank.org/indicator/EN.ATM.CO2E.KT?locations=EU (Accessed: 4 November 2021).

World Bank (2021b) *Employing Workers*. Available at: https://www.worldbank.org/en/research/employing-workers/data/working-hours (Accessed: 8 October 2021).

World Bank (2021c) *Survey mean consumption or income per capita, bottom 40% of population (2011 PPP $ per day)*. Available at: https://data.worldbank.org/indicator/SI.SPR.PC40 (Accessed: 6 October 2021).

World Bank (2021d) *Unemployment, total (% of total labor force)*. Available at: https://data.worldbank.org/indicator/SL.UEM.TOTL.ZS?name_desc=false (Accessed: 6 October 2021).

Wright, M. and Brown, R.C. (2007) 'Establishing the optimal sizes of different kinds of biorefineries', *Biofuels, Bioproducts and Biorefining*, 1(3), pp. 191–200. doi:10.1002/bbb.25.

Xu, F. *et al.* (2006) 'Comparative study of organosolv lignins from wheat straw', *Industrial Crops and Products*, 23(2), pp. 180–193. doi:10.1016/j.indcrop.2005.05.008.

Xu, Z. *et al.* (2007) 'Enzymatic hydrolysis of pretreated soybean straw', *Biomass and Bioenergy*, 31(2–3), pp. 162–167. doi:10.1016/j.biombioe.2006.06.015.

You, F. *et al.* (2012) 'Optimal design of sustainable cellulosic biofuel supply chains: Multiobjective optimization coupled with life cycle assessment and input-output analysis', *AIChE Journal*, 58(4), pp. 1157–1180. doi:10.1002/aic.12637.

You, F. and Wang, B. (2011) 'Life cycle optimization of biomass-to-liquid supply chains with distributed-centralized processing networks', *Industrial and Engineering Chemistry Research*, 50(17), pp. 10102–10127. doi:10.1021/ie200850t.

Yrjölä, T. (2002) 'Forest management guidelines and practices in Finland, Sweden and Norway', *European Forest Institute Internal Report*, (11), p. 46.

Yue, D., Pandya, S. and You, F. (2016) 'Integrating Hybrid Life Cycle Assessment with Multiobjective Optimization: A Modeling Framework', *Environmental Science and Technology*, 50(3), pp. 1501–1509. doi:10.1021/acs.est.5b04279.

Zahiri, B., Zhuang, J. and Mohammadi, M. (2017) 'Toward an integrated sustainable-resilient supply chain: A pharmaceutical case study', *Transportation Research Part E: Logistics and Transportation Review*, 103, pp. 109–142. doi:10.1016/j.tre.2017.04.009.

Zamboni, A., Shah, N. and Bezzo, F. (2009) 'Spatially explicit static model for the strategic design of future bioethanol production systems. 1. cost minimization', *Energy and Fuels*, 23(10), pp. 5121–5133. doi:10.1021/ef9004779.

Zhalechian, M. *et al.* (2016) 'Sustainable design of a closed-loop location-routing-inventory supply chain network under mixed uncertainty', *Transportation Research Part E: Logistics and Transportation Review*, 89, pp. 182–214. doi:10.1016/j.tre.2016.02.011.

Zhou, M. *et al.* (2014) 'Particulate air pollution and mortality in a cohort of Chinese men', *Environmental Pollution*, 186, pp. 1–6. doi:10.1016/j.envpol.2013.11.010.

Zhu, L. and Hu, D. (2017) 'Sustainable Logistics Network Modeling for Enterprise Supply Chain', *Mathematical Problems in Engineering*, 2017, pp. 1–11. doi:10.1155/2017/9897850.

Ziebell, A.L. *et al.* (2013) 'Sunflower as a biofuels crop: An analysis oflignocellulosic chemical properties', *Biomass and Bioenergy*, 59, pp. 208–217. doi:10.1016/j.biombioe.2013.06.009.

Zimmermann, H.-J. and Gutsche, L. (1991) *Multi-Criteria Analyse*. Berlin, Heidelberg: Springer Berlin Heidelberg (Heidelberger Lehrtexte Wirtschaftswissenschaften). doi:10.1007/978-3-642-58198-4.

Appendix A

Parts of Appendix A are based on the Supplementary Data of Thorenz et al. (2018) and can be found only (https://doi.org/10.1016/j.jclepro.2017.12.143).

A.1 Literature review on agroforestry residue potentials

Table A 1: Literature review on residue to crop ratio of different agricultural plants

Crop	Average	σ	Lower bound	Upper bound	Sample size	Source
Cereals						
Wheat	1.00	0.35	0.80	1.60	4	(Helwig et al., 2002; Scarlat et al., 2010; Landwirtschaftskammer NRW, 2015; Kaltschmitt et al., 2016)
Maize (corn)	1.13	0.17	0.90	1.30	3	(Helwig et al., 2002; Scarlat et al., 2010; Kaltschmitt et al., 2016)
Green maize (silage)	Whole plant for silage production					
Barley	0.93	0.23	0.70	1.30	4	(Helwig et al., 2002; Scarlat et al., 2010; Landwirtschaftskammer NRW, 2015; Kaltschmitt et al., 2016)
Oats	1.13	0.18	0.90	1.40	4	(Helwig et al., 2002; Scarlat et al., 2010; Landwirtschaftskammer NRW, 2015; Kaltschmitt et al., 2016)
Triticale	0.95	0.05	0.90	1.00	2	(Helwig et al., 2002; Landwirtschaftskammer NRW, 2015; Kaltschmitt et al., 2016)
Rye	1.10	0.29	0.90	1.60	4	(Helwig et al., 2002; Scarlat et al., 2010; Landwirtschaftskammer NRW, 2015; Kaltschmitt et al., 2016)
Rice	1.70	0.50	1.20	2.20	2	(Scarlat et al., 2010)
Sorghum	1.30		1.30	1.30	1	(Kim and Dale, 2004)
Legumes						
Soybean	1.50	0.00	0.00	0.00	1	(Helwig et al., 2002)
Oil Crops						
Rapeseed	1.70	0.24	1.40	2.00	3	(Helwig et al., 2002; Scarlat et al., 2010; Kaltschmitt et al., 2016)
Sunflower	2.70	0.50	2.20	3.20	3	(Helwig et al., 2002; Scarlat et al., 2010)
Sugar crops						
Sugar beet pulp	0.23	0.25	0.20	0.25	2	(IPCC, 1996; Lal, 2005)
Fibre Plants						
Hemp hurds	1.75	0.25	1.50	2.00	2	(González-García et al., 2012)
Flax shives	0.30	0.00	0.00	0.00	1	(González-García et al., 2009)
Cotton fibre	2.20	0.80	1.40	3.00	2	(Lal, 2005)
Other						
Miscanthus	Whole plant for biorefinery					
Switchgrass	Whole plant for biorefinery					

Table A 2: Literature study on biochemical composition of agricultural residues

	Lignin			Cellulose			Hemicellulose			
Crop	**Mean**	**σ**	**#**	**Mean**	**σ**	**#**	**Mean**	**σ**	**#**	**Source**
Wheat Straw	17.8	4.4	22	37.3	6.2	22	28.7	6.2	22	(ECN Phyllis, 2012 (18 samples); Papatheofanous et al., 1998; Sun and Tomkinson, 2000; Sun and Cheng, 2002; Xu et al., 2006)
Barley Straw	17.2	3.3	4	39.6	5.6	4	24.7	1.4	4	(ECN Phyllis, 2012 (3 samples); Sun and Tomkinson, 2000)
Corn Cob	12.7	4.3	6	40.9	7.4	7	30.8	3.5	6	(ECN Phyllis, 2012 (5 samples), Sun and Cheng, 2002)
Corn Stover	16.7	2.5	10	37.3	5.6	10	25.5	4.4	10	(ECN Phyllis, 2012 (5 samples); Buranov and Mazza, 2008; Khamphet et al., 1997; Ragauskas et al., 2014; Sun and Tomkinson, 2000; Villegas and Gnansounou, 2008)
Rape Straw	19.8	0.9	4	40.9	3.9	4	24.4	3.3	4	(ECN Phyllis, 2012 (3 samples); Sun and Tomkinson, 2000)
Rice Straw	15.2	5.3	10	37.1	5.6	10	25.1	3.3	9	(ECN Phyllis, 2012 (6 samples); Buranov and Mazza, 2008; Sangnark and Noomhorm, 2004; Sun and Tomkinson, 2000)
Rye Straw	12.3	6.5	7	37.0	6.6	7	24.0	5.4	7	(ECN Phyllis, 2012 (6 samples); Sun and Tomkinson, 2000)
Sunflower Straw	25.2	0.5	3	34.8	2.8	4	21.8	2.2	3	(ECN Phyllis, 2012 (1 sample); Ziebell et al., 2013)
Oats Straw	16.1	1.0	2	37.8	1.0	2	28.3	4.8	2	(ECN Phyllis, 2012 (1 samples); Sun and Tomkinson, 2000)
Switchgrass	17.3	3.4	5	36.6	6	6	27.2	5	5	(Khamphet et al., 1997; Sun and Cheng, 2002; Ververis et al., 2004; Villegas and Gnansounou, 2008; Ragauskas et al., 2014)
Bagasse	26.8	4.9	1	19.2	3	2	44	13.9	2	(Sun and Tomkinson, 2000)
Nut Shells	35	7.1	2	27.5	3.5	2	27.5	3.5	2	(Sun and Cheng, 2002)
Miscanthus	16.6	9.8	3	46.3	5.2	3	28.5	6.4	2	(Ververis et al., 2004; Ragauskas et al., 2014)
Sorghum Straw	15.5	0.5	2	36	0	1	18	0	1	(Mok and Antal, 1992; Kim and Dale, 2004)
Triticale	19.2	0	1	21	0	1	36.28	0	1	(Pronyk et al., 2011)
Soybean	17.6	0	1	25	0	1	11.9	0	1	(Xu et al., 2007)
Hemp	24.6	0	1	46.33	0	1	16.07	0	1	(Monteil-Rivera et al., 2013)
Flax Shives	25.3	0	1	38.4	0	1	18	0	1	(Monteil-Rivera et al., 2013)
Cotton Fibre	17.6	0	1	43.8	0	1				(Ververis et al., 2004)

Table A 3: Literature study on the biochemical composition of forestry sources

Reference	Lignin	Cellulose	Hemicellulose	(Condensed) Tannin (%)	Extractives	Source
Coniferous Wood						
Spruce	27.4	42.0	27.3	0	2	(Räisenen and Athanassiadis, 2013)
Scots Pine	27.0	40.7	26.09		5	(Räisenen and Athanassiadis, 2013)
Average Conif.	29.8	41.2	26.8			(Ragauskas et al., 2006)
Average Conif.	27.5					(Harkin and Rowe, 1971)
Average Conif.	25.0–35.0	45.0–50.0	25.0–35.0			(Sun and Cheng, 2002)
Broadleaf Wood						
Birch	20.2	44.70	28.72			(Räisenen and Athanassiadis, 2013)
Beech	22.0	45.0	29.0			(Ragauskas et al., 2006)
Birch	27.33	40.91				(Fengel and Grosser, 1975)
Beech	22.88	45.97				
Coniferous Bark						
Spruce (Picea Abies)				11.0	26.6	(Bertaud et al., 2012)
Aleppo Pine				16.6	30.1	(Bertaud et al., 2012)
Douglas Fir				6.7	22.8	(Bertaud et al., 2012)
Maritime Pine				1.2	10.2	(Bertaud et al., 2012)
Spruce (Picea Abies)	29.3-36.1	19.0–35.3	N/A	8.3–10.7		(Kemppainen et al., 2014)
Spruce (Picea Abies)	11.80	26.6	9.2			(Räisenen and Athanassiadis, 2013)
Scots Pine	13.1	22.2	8.1			(Räisenen and Athanassiadis, 2013)
Average Conif.	45.0–50.0				2-25	(Harkin and Rowe, 1971)
Broadleaf Bark						
Average Broadleaf	40.0-50.0				5-10	(Harkin and Rowe, 1971)
Birch	14.7	10.7	11.2		25.6	(Räisenen and Athanassiadis, 2013)
Birch				4.1–6.2		(Palo, 1984)

Table A 4: Applied sustainable removal rates (based on Scarlat et al., 2010)

Crop	**Sustainable removal rate**
Wheat straw	40 %
Rye straw	40 %
Barley straw	40 %
Oats straw	40 %
Triticale straw[a]	40 %
Maize stover	50 %
Rice straw	50 %
Rapeseed stover	50 %
Sunflower straw	50 %

[a]: Own assumption

Table A 5: Literature review about roundwood production ratios

Country	**Spruce (%)**	**Pine (%)**	**Information**	**Source**
Sweden	63.4	36.6	Mean Fellings 2005-2015	(Swedish NFI, 2016)
Germany	69.3	23.3	Mean Fellings 2002-2012	(Tühnen, 2016)
Finland	16.6	83.4	Dominant species	(Finnish NFI, 2013)
Finland (1999)	52.0	48.0	Felling Data	(Yrjölä, 2002)
Poland	9.1	84.6	Standing trees	(National Forest Holding, 2015)
France	21.1	30.1	Production shares	(IGN, 2015)
Austria	69.0		Production share	(Büchsenmeister, 2016)
Czech Republic	51.5	16.7	Timber land in %	(Ministerstvo Zemedelstvi, 2012)

Table A 6: List of combined heat & power (CHP) straw plants in the EU

Country	**Number of plants**	**Annual straw demand (1000 t)**	**Reference**
Denmark	11	1023	(Scarlat et al., (2010)
United Kingdom	1 (Ely)	166	(Scarlat et al., 2010)
Spain	1 (Sanguesa)	131	(Scarlat et al., 2010)
Hungary	1 (Pècs)	240	(Pannonpower, 2014)
Germany	1 (Emsland)	62.5	(BEKW, 2016)
Total	15	1622.5	

A.2 Agroforestry residue prices analysis

In addition to feedstock availability, the cost of raw materials is one of the most important factors for the economically viable use of agroforestry residues. The profitability of new technologies that valorize agroforestry residues into high-added-value products depends on raw material prices. Neither agricultural residues nor forestry residues have a transparent market in the European Union. Therefore, feedstock prices that have to be paid by an upcoming bioeconomy are difficult to assess. Furthermore, emerging markets will lead to additional competition, influencing future prices. This section introduces an approach for evaluating agricultural residue prices (wheat straw, maize stover, barley straw, rapeseed straw) and forestry residue prices (pine bark, spruce bark).

Straw price analysis

Today's main uses of straw comprise its use as fertilizer to sustain soil quality and its use as bedding material which often means that straw is harvested and used within the same farm. Large markets for straw do not exist, and the regional demand determines the price. In regions with a large share of horses, prices rise due to competition and customers willing to pay higher costs. This approach for calculating feedstock prices is based on the straw price calculator of Harms (2018). The price is based on the value of the feedstock specific nutrients, a profit margin of 50 % based on the value of the nutrients, labor, and machinery costs for the harvesting and baling (square bales with 1,2m x 0,9m x 2,4m), labor and machinery costs for the loading, transportation (assumed average traveled distance is 3 km) and unloading at the farm. Additionally, covered storage at the farm from one to twelve months can be considered in the final straw price. Detailed information regarding the storage can be found in chapter 0.

The feedstock-specific nutrient price is calculated based on the specific nutrient mass and the specific nutrient price. Nutrient prices are subject to price variations, wherefore prices need to be updated regularly. Table A 7 shows the nutrient prices of June 2018 and the feedstock-specific content (Harms, 2020). According to Harms (2018), we assume a profit margin of 50 % based on the nutrient price as an economic incentive.

Table A 7: Feedstock specific nutrient prices

Nutrients	Price (€/kg)	Wheat straw (kg/t)	Maize stover (kg/t)	Barley straw (kg/t)	Rape straw (kg/t)
Nitrogen	0.82	5.00	9.00	5.00	11.00
Phosphor	0.56	3.00	2.00	3.00	6.00
Potassium*	0.60	7.00	10.00	9.00	12.50
Magnesium	1.19	2.00	2.00	2.00	2.00
Sulfur	0.05	1.80	2.00	1.80	1.80
Humus	0.04	100.00	80.00	100.00	80.00
Sum (€/t)		17.90	21.92	19.20	28.40
50 % profit margin (€/t)		8.23	10.09	8.83	12.78

*Potassium-specific values are based on the assumption that half of the potassium is washed out, wherefore, only half of the specific potassium mass is used in the calculation (Harms, 2020).

The harvesting and baling costs consist of labor- and machinery costs for baling into square bales (1,2m x 0,9m x 2,4m). We assume country-specific labor costs with distinctive leverage on the total price (Eurostat, 2020b). Additionally, machinery costs arise for a hauler and the press machine, which we assume is independent of the sourcing country. As the properties of the different feedstock types are comparable, labor and machinery costs are separate from the feedstock. The logistic costs are again composed of labor and machinery costs. Labor costs for logistics on field and farm are also based on country-specific labor costs (Eurostat, 2020b). Machinery costs for field to farm logistics are composed of in-field loading (telescopic handler with trailer), transportation (telescopic handler with trailer, assumed average traveled distance from field to farm is 3 km), and unloading at the farm (telescopic with pliers for square bales).

Table A 8 contains the calculated feedstock prices for the different straws at the farm gate without storage. The feedstock storage costs add up to the final expenses at the farm gate. Summarizing the results, the nutrients make up the largest share of the overall straw costs with little over one-third of the total costs. Harvesting and baling also accounts for nearly one-third. Logistic cost accounts for about 20 % and profit margin for 17 %.

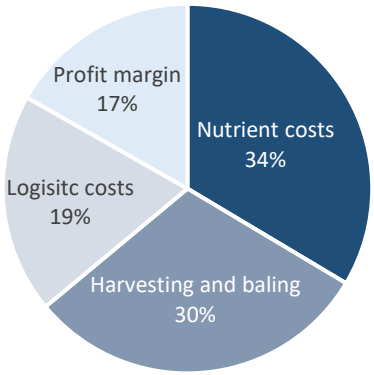

Fig. A 1: Average composition of straw prices (based on Harms, 2020)

Table A 8: Expected agricultural residue prices in the EU 28.

Country (NUTS Code)	Wheat straw (€/t)	Maize stover (€/t)	Barley straw (€/t)	Rapeseed straw (€/t)
AT	58.6	64.2	60.4	72.2
BE	61.0	66.6	62.8	74.6
BG	48.0	53.6	49.8	61.6
CY	52.3	57.9	54.1	65.9
CZ	50.2	55.8	52.0	63.8
DE	58.7	64.3	60.5	72.3
DK	62.1	67.7	63.9	75.7
EE	50.5	56.1	52.3	64.1
EL	51.7	57.3	53.5	65.3
ES	54.3	59.9	56.1	67.9
FI	58.9	64.5	60.7	72.5
FR	59.7	65.3	61.5	73.3
HR	50.1	55.7	51.9	63.7
HU	49.4	55.0	51.2	63.0
IE	57.8	63.4	59.6	71.4
IT	56.8	62.4	58.6	70.4
LT	49.1	54.7	50.9	62.7
LU	60.1	65.7	61.9	73.7
LV	49.2	54.8	51.0	62.8
MT	51.3	56.9	53.1	64.9
NT	59.2	64.8	61.0	72.8
PL	49.6	55.2	51.4	63.2
PT	51.5	57.1	53.3	65.1
RO	48.5	54.1	50.3	62.1
SE	60.6	66.2	62.4	74.2
SI	52.5	58.1	54.3	66.1
SK	50.3	55.9	52.1	63.9
UK	56.4	62.0	58.2	70.0
Average	54.2	59.8	56.0	67.9

Bark price analysis

Bark arises as residue in large amounts at sawmills and pulp and paper mills. Currently, the bark is used as fuel in CHP units or as bark mulch. A market price for bark does not exist, wherefore we calculate bark prices on the price for wood chips. Air dry bark has a moisture content of about 50 %. The energy content of air-dry matter is 8.2 to 8.3 GJ/t, comparable to chippings from sawmills which also contain 50 % moisture (Bittermann and Suvorov, 2012). Eurostat's PRODOM database provides data on the annual produced coniferous wood in chips or particles (PRODCOM Code: 16102503) volume and the generated revenue (Eurostat, 2018d). Information on the assumed water content is not available, and we assume a moisture content of 50 % of coniferous wood in chips or particles corresponding to air dry matter (Bittermann and Suvorov, 2012). We assume the same price for all different coniferous barks (spruce bark, pine

bark, and all other bark). As pine bark is more suitable for bark mulch due to its higher resin content, pine bark prices could, in reality, be slightly higher than the price of other bark[4]. Additionally, a substitution-based value can be found in Table A 9 in which we assume the substitution of bark as fuel in CHP units to provide heat and electric energy by gas, and additionally purchased electricity.

Table A 9: Bark prices

Country (NUTS Code)	Based on wood chips price, average 2015-2017 (€/t with 50 % moisture content)	Based on substitution of electric energy (2018) (€/t with 50 % moisture content)	Based on substitution of gas (2018) (€/t with 50 % moisture content)
AT	57.8	63.7	43.4
BE	53.1	47.6	48.1
BG	52.4	43.1	48.1
CY	-	47.4	70.1
CZ	49.0	88.1	59.6
DE	49.3	50.8	57.5
DK	55.2	77.6	64.3
EE	24.4	60.4	0.0
EL	-	62.2	54.5
ES	41.6	57.7	66.2
FI	68.6	58.4	48.1
FR	45.5	83.6	53.8
HR	37.7	82.5	0.0
HU	38.8	61.0	56.4
IE	54.4	49.2	61.3
IT	57.0	48.9	60.0
LT	45.7	49.4	45.7
LU	-	79.1	0.0
LV	35.5	50.7	72.2
MT	-	58.6	60.9
NT	-	51.5	57.2
PL	53.0	66.0	51.3
PT	42.5	48.8	48.3
RO	65.5	50.5	59.8
SE	43.4	68.5	54.3
SI	43.2	40.0	112.2
SK	62.9	40.2	90.1
UK	54.0	79.0	49.3
Average	49.1	59.4	53.3

Storage cost

For the storage of straw and bark, we assume a covered shed with 42m x 22m x 7m. The cost information is based on Harms (2018) and is available monthly. The storage cost has a considerable share of the overall costs, and 12-month storage adds up to about 50 €/t. As a wide range of options exists to realize storage sheds, the storage

4 Personal correspondence with Brüning Group.

cost is highly uncertain. For the different feedstock types, the same specific storage costs are assumed (see table 5).

Table 5: Storage cost

Storage period (month)	**Storage costs without VAT (€/t)**
0	0.0
1	4.3
2	8.7
3	13.0
4	17.3
5	21.6
6	26.0
7	30.3
8	34.6
9	39.0
10	43.3
11	47.6
12	51.9
Average	25.96

Appendix B

Parts of Appendix B corresponds to the Supporting Information of Wietschel et al. (2021).

B.1 General data, parameters, and assumptions

This section provides the nomenclature in Table B 1: General data and parameters, as well as a detailed description of general data and parameters of the model, their background, the underlying assumptions, calculations, and references in the following sub-sections. Values for these parameters are given in the Data Repository D.2 (sheet Data 1).

Table B 1: General data and parameters

Data	Unit	Definition
$\delta_{r,s}$	km	distance between regions $r \in R$ and $s \in R$
ζ_r^{1G}	t	current demand for 1G bioethanol in region $r \in R$
ζ_r^{FF}	t EtOH eq.	current demand for petrol in region $r \in R$ expressed in metric tons EtOH equivalent
$\psi_{r,f}$	t	total available feedstock $f \in F$ in region $r \in R$
$\mu_{r,f}$	t / km^2	specific feedstock potential for feedstock $f \in F$ in region $r \in R$
θ_f	t EtOH / t	transformation factor from feedstock $f \in F$ to bioethanol
θ_p^{byp}	x / t EtOH	co-production factor from bioethanol to by-product $p \in P$ (MJ for electricity, and m^3 for biomethane)
σ_c	t EtOH	capacity of a biorefinery with capacity level $c \in C$
τ_r		regional road network tortuosity factor of region $r \in R$
ρ	km	width of sourcing annuli
υ_m		geometric factor for the average distance between the center and annulus $m \in M$

Transportation-related data

$\delta_{r,s}$: is a distance matrix of all 98 NUTS-1 regions $r, s \in R$ of the EU-28. The distances are aggregated from NUTS-3 to NUTS-1 based on Eurostat (2018a) which gives road distance for each pair of the 1453 regions on NUTS-3 level. The distance between two NUTS-1 regions is calculated as the average distance between each NUTS-3 region of the one NUTS-1 region and all NUTS-3 regions of the other NUTS-1 region. For the calculation of the average distance *within* one region (i.e., the diagonal of the distance matrix), we use the disk line picking method (Weisstein, 2018).

τ_r: represents the tortuosity of the regional road network in NUTS-1 region $r \in R$. The tortuosity factor is calculated as the average road distance between two NUTS-3 regions derived from Eurostat (2018a), divided by the average beeline between two points in

the respective NUTS-1 region. We assume each NUTS-1 region to be a circle and calculate the $average\ beeline$ by the disk line picking method (Weisstein, 2018).

$$\tau_r = \frac{average\ road\ distance\ between\ NUTS3\ regions\ of\ NUTS1\ region_r}{average\ beeline_r} \quad (36)$$

As this calculation is a rough estimation, we set a lower bound of 1.2 (corresponds to a well-developed road network) and an upper bound of 2 (corresponds to a less developed road network).

ρ: is the width of a sourcing annulus for sourcing within a region in km. This auxiliary parameter is required for the stepwise linearization of the non-linear transport costs (see 0) when sourcing from "around" a biorefinery in a region. A low value for ρ means a more accurate resolution of the linearized curve, which, however, entails high computation times of the mixed-integer linear programming (MILP) model. A high value for ρ means a more imprecise resolution of the linearization, but has the advantage of shorter computation times. Experiments showed a reasonable trade-off between accuracy and computation times for $\rho = 5$ km.

v_m: represents a geometric factor for the average distance between the center and an annulus m, see Eq. (27).

Reference products

ζ_r^{1G}: is the current demand for first-generation bioethanol (1G EtOH) in each region $r \in R$, and thus the upper bound for the substitution of 1G EtOH by second-generation bioethanol (2G EtOH). The consumption of bioethanol on NUTS-1 level is disaggregated from NUTS-0 level, based on population share. The whole fuel and industrial bioethanol demand is considered and the values are based on the Biofuels Barometer (2019) and ePure (2018).

ζ_r^{FF}: is the current demand for fossil petrol in each region $r \in R$, and thus the upper bound for the substitution of petrol by 2G EtOH. The demand for petrol on NUTS-1 level is disaggregated from NUTS-0 level, based on population share. The NUTS-0 petrol demand is based on the year 2018 (Eurostat, 2019a).

Feedstock and process-related

$\psi_{r,f}$ and $\mu_{r,f}$: are the total and specific available bioeconomic feedstock potential of feedstock $f \in F$ of each NUTS-1 region $r \in R$ for the year 2018 in metric tons and metric tons/km^2 respectively. In the 2030 scenario in section 5.3.3, these parameters assume the 2030 values. Both the 2018 and the 2030 values are based on the findings of chapter 4. Based on the findings of chapter 4, the regional feedstock potentials could theoretically also be negative due to a high demand of other straw applications

compared to the supply. However, in the study at hand, the supply is assumed to be zero in these regions.

θ_f: is the transformation factor from feedstock $f \in F$ to bioethanol. As straw is mainly composed of cellulose (30 – 40%), hemicellulose (20 – 30%), and lignin (20%) (see Table B 2) we assume 35% cellulose and 25% hemicellulose in the dry matter content. The considered feedstocks are wheat straw, maize stover, barley straw, and rapeseed straw. This work assumes the same transformation factor for all considered feedstocks. The transformation efficiencies of cellulose to glucose and hemicellulose to xylose, as well as the fermentation efficiency are assumed to be 85%. These assumptions translate to 0.2211 t ethanol per t straw, which is congruent with literature sources (Clariant, 2018; Santibañez-Aguilar et al., 2011; Wang et al., 2013) (Further information on the process can be found in 0).

θ_p^{byp}: is the co-production factor for the by-products $p \in P$ in relation to 1 metric ton of produced bioethanol. The hydrothermal cracking separates cellulose, hemicellulose, and lignin. In the enzymatic hydrolysis, lignin and other unconverted solids are separated from the carbohydrates and can either be combusted for the production of electricity and heat (Gupta & Verma, 2015) or sold for the production of other bio-based products. This study assumes a co-generation of electricity and steam to supply the whole energy demand of the biorefinery with the sale of excess electricity to the regional grid. Lignin is separated in the enzymatic hydrolysis (0.2 kg dry matter (d.m.) lignin per kg straw) and burned in a co-generation plant to produce electricity and heat. The lower heating value of lignin amounts to about 25 MJ/kg (d.m.) and the combustion releases all chemically available energy of lignin. The hot gases are converted in a boiler to steam at an efficiency of 88% (McKendry, 2002), which yields steam with an enthalpy of 19.9 MJ/kg EtOH (Humbird et al., 2011). The steam can either directly be used in the production process or further be converted into electric energy by a turbo generator at an efficiency of 85%. The steam required for the production process is discharged and accounts for approx. 47% of the evaporation enthalpy. The remaining steam energy of 9.6 MJ is converted into 8.16 MJ of electrical energy (per kg produced ethanol) in a turbo-generator with an efficiency of 85% (Humbird et al., 2011). 7.2 MJ electric energy are consumed directly by the biorefinery, i.e., 0.96 MJ/kg EtOH are available as excess electricity. The excess electricity is fed in the regional grid, where the regional electricity mix of the same function is substituted.

Table B 2: Chemical composition of crop residues
(common wheat straw, maize stover, barley straw, rapeseed straw)

Material	**Average fraction**
Cellulose	35% ± 5%
Glucan (C6)	35% ± 5%
Hemicellulose	25% ± 5%
Xylan (C5)	20%
Arabinan (C5)	2%
Galactan (C6)	0.75%
Mannan (C6)	0.41%
Lignin	20%
Acids	4.84%
Extractives	4.78%
Ash	8.59%
C	46.7%
H	5.49%
O	38.4%
N	0.67%
S	0.10%
LHV	17.6 MJ/kg

The second by-product considered is stillage, which is the residue from the fermentation process. Based on results of a second-generation bioethanol producer, we assume 1kg stillage per 1kg wheat straw. In principle, stillage can further be utilized as either animal fodder, fertilizer, or for the production of biogas (Tonini et al., 2016). In this study we assume biogas production from the by-product stillage. Stillage of bioethanol production from wheat straw contains between 10.2% and 17.8% versatile solids (VS) (Kaparaju et al., 2009). With an ultimate CH4 yield of 0.324 ± 0.03 (m^3/kg of VS), 5.37 MJ CH4 can be produced as by-product per kg EtOH. We assume a substitution of the natural gas equivalent in the regional grid. The resulting values for environmental and economic parameters on a regional level and the respective modelling can be found in Data Repository D.2.

Table B 3: Energy balance in the production process
of second-generation bioethanol with energy inputs, energy outputs and excess energy sold to grid.

Inputs	LHV (MJ kg-1)	MJ kg-1 Straw	MJ MJ-1 EtOH	MJ kg-1 EtOH	Comment
Wheat straw	17.50	17.50	2.97	79.16	Converted by 4.523 kg EtOH per 1 kg straw
Steam				10.30	Total steam demand for EtOH production
Electricity				7.20	Total electricity demand for EtOH production
Outputs					
EtOH			1.00	26.70	
Lignin	25.00	5.00		22.62	
steam by lignin co-generation				19.90	conversion in steal boiler at 88% efficiency (McKendry, 2002)
Lignin co-generation in electricity				8.16	conversion in turbo generator at 85% efficiency (Humbird et al., 2011)
Lignin co-generation in steam				10.30	12% steam pickup at 175 psig and 268°C and 35% pickup at 125 psig and 164°C (Humbird et al., 2011)
Versatile solids (VT)		0.102 kg kg^{-1} Straw	0.461 kg kg^{-1} EtOH	6.78	10.2% of total weight converted to versatile solids (other units then for the rest of the diagram!)
CH_4 yield of VT		1.186	0.201	5.37	CH4 yield of 0.324 ± 0.03 (m3/kg of VS)
Methane based on VT sold to grid				5.37	Excess energy (CH_4); calculation
Electricity sold to grid				0.958	Excess energy (electricity); calculation

B.2 Economic parameters

This section provides a detailed description of the economic parameters of the model, their background, the underlying assumptions, calculations, and references in the following sub-sections. Values for the economic parameters are given in the online data repository D.2.

Revenue

α_r^{1G}: is the competitive revenue in region $r \in R$ when second-generation bioethanol (2G EtOH) substitutes first-generation bioethanol (1G EtOH).

α_r^{FF}: is the competitive revenue in region $r \in R$ when second-generation bioethanol replaces fossil petrol. Fuel revenues and excise taxes for fossil petrol and biofuels are derived from European Commission (2020) and are averaged from the beginning of 2018 to July 2019. Petrol prices are very volatile, wherefore this parameter should be treated with caution.

$\alpha_{r,p}^{byp}$: are the revenues of by-products electricity and biogas in region $r \in R$. The prices are derived from Eurostat (2019) and Eurostat (2019c)

Biorefinery-related cost

κ_c^{depr}: are the annualized investment costs of installing a biorefinery with capacity level $c \in C$. We assume a depreciation time of 20 years and a constant depreciation rate per year. The reference value for Romania is derived from the German Federal Government (2014) and Sunliquid (2019) and then regionalized for every region $r \in R$ by the regionalization factor γ_r^{inv}, which is based on the Purchasing Power Parity for gross fixed capital formation derived from (Eurostat, 2020c).

κ_c^{pers}: annual costs for personnel of a biorefinery with capacity level $c \in C$. The number of employees is derived from Sunliquid (2019). The costs (reference value for Germany) are regionalized by the regionalization factor γ_r^{lab} which is based on the Labor Cost Index (compensation of employees plus taxes minus subsidies) for the activity industry (except construction) (Eurostat, 2020b)

κ_c^{oper}: are the annual costs of operating a biorefinery with capacity level $c \in C$. It includes 2% maintenance cost, 0.5% administration cost, 1% insurance cost, and 0.75% for unforeseen expenditures of the total investment cost for a biorefinery with capacity $c \in C$ (German Federal Government, 2012).

The aforementioned parameters κ_c^{depr}, κ_c^{pers}, and κ_c^{oper} include a cost degression with a scaling coefficient λ of 0.8, based on literature values (Towler and Sinnott, 2013; Lauven et al., 2018). The relation between costs and capacity is illustrated by the following equation. For example, doubling the capacity leads to about 1.7411 times the investment costs and construction impacts:

$$Investment\ costs_c = \left(\frac{capacity_c}{capacity_0}\right)^{\lambda} \times Investment\ costs_0 \quad (37)$$

κ^{var}: are the variable costs (per metric ton) of refining bioethanol at a biorefinery (German Federal Government, 2012).

Feedstock cost

$\varphi_{r,f}$: are the costs for feedstock $f \in F$ at farms in region $r \in R$. The feedstock-specific nutrient price is calculated based on the specific nutrient mass and the specific nutrient price. Table B 4 shows nutrient prices in June 2018 and the feedstock-specific content (Harms, 2020). As economic incentive, we assume, according to Harms (2018), a profit margin of 50% based on the nutrient price.

Table B 4: Feedstock specific nutrient prices

Nutrients	**Price (€/kg)**	**Wheat straw (kg/t)**	**Maize stover (kg/t)**	**Barley straw (kg/t)**	**Rapeseed straw (kg/t)**
Nitrogen	0.82	5.00	9.00	5.00	11.00
Phosphorus	0.56	3.00	2.00	3.00	6.00
Potassium*	0.60	7.00	10.00	9.00	12.50
Magnesium	1.19	2.00	2.00	2.00	2.00
Sulfur	0.05	1.80	2.00	1.80	1.80
Humus	0.04	100.00	80.00	100.00	80.00
Sum (€/t)		17.90	21.92	19.20	28.40
50% profit margin (€/t)		8.23	10.09	8.83	12.78

*Potassium specific values are based on the assumption that half of the potassium is washed out, wherefore only half of the specific potassium mass is used in the calculation (Harms, 2020).

The harvesting and baling costs consist of labor and machinery costs for baling straw into square bales (1.2m x 0.9m x 2.4m). We assume country-specific labor costs (Eurostat, 2020c). Additionally, machinery costs arise for a hauler and the press machine, which we assume to be independent from the sourcing country. As the properties of the different feedstock types are comparable, labor and machinery costs are independent of the feedstock type. The logistics costs again comprise labor and machinery costs. Labor costs for logistics on field and farm are also affected by country-specific labor costs (Eurostat, 2020b). Machinery costs for field-to-farm logistics comprise in-field loading (telescopic handler with trailer), transportation (telescopic handler with trailer; the assumed average traveled distance from field to farm is 3 km) and unloading at the farm (telescopic with pliers for square bales).

Transportation cost

ε_t^{fix}: are the fixed costs (per metric ton) of transporting feedstock with transport mode $t \in T$, derived from Henrich et al. (2009), and inflation-adjusted to the year 2019. The fixed transportation costs for $t = rail$ include a 30km pendulum tour truck transport.

ε_t^{var}: are the variable costs (per ton kilometer) of transporting feedstock with transport mode $t \in T$. The variable feedstock transportation cost are derived from Henrich et al. (2009) for Germany and inflation-adjusted to the year 2019. The costs are further regionalized by the regionalization factor γ_r^{tra}, which is based on the Purchasing Power Parity index for transportation derived from (Eurostat, 2020c).

η_t^{fix}: are the fixed costs (per metric ton) of transporting bioethanol with transport mode $t \in T$, derived from Henrich et al. (2009), and inflation-adjusted to the year 2019. We assume that the biorefinery has as direct access to the railway system.

η_t^{var}: variable costs (per ton kilometer) of transporting bioethanol with transport mode $t \in T$. The variable ethanol transportation cost are derived from Henrich et al. (2009) and inflation-adjusted to the year 2019.

B.3 Environmental parameters

This section provides the nomenclature of the 21 environmental categories in Table B 5 as well as a detailed description of the environmental parameters of the model, their background, the underlying assumptions, calculations, and references in the following sub-sections. Values for the environmental parameters as well as the Life Cycle Inventory are given in the Supporting Information S2 (sheets Data 3 and Data 4 respectively). The Life Cycle Inventory (LCI), i.e., the inputs and emissions associated with the environmental parameters, is modeled in SimaPro 9, assessing the ecoinvent database version 3.5 (Wernet et al., 2016). For the impact allocation, the procedure "allocation at the point of substitution" (APOS) is chosen. The Life Cycle Impact Assessment (LCIA), i.e., the characterization of the life cycle inventory in terms of impact and damage categories, is carried out using ReCiPe 2016 (H) v1.1 (Huijbregts et al., 2017).

Table B 5: Environmental midpoint and endpoint categories (set $\boldsymbol{L}$) according to Huijbregts et al. (2017)

Tag	Impact category / midpoint	Impact unit	Endpoint aggregation	Midpoint-to-endpoint factor
M1	Global warming	kg CO_2 eq	E1 & E2	9.28E-07 & 2.80E-09
M2	Stratospheric ozone depletion	kg CFC11 eq	E1	5.31E-04
M3	Ionizing radiation	kBq Co-60 eq	E1	8.50E-09
M4	Ozone formation, Human health	kg NO_x eq	E1	9.10E-07
M5	Fine particulate matter formation	kg PM2.5 eq	E1	6.29E-04
M6	Ozone formation, Terrestrial ecosystems	kg NO_x eq	E2	1.29E-07
M7	Terrestrial acidification	kg SO_2 eq	E2	2.12E-07
M8	Freshwater eutrophication	kg P eq	E2	6.71E-07
M9	Marine eutrophication	kg N eq	E2	1.70E-09
M10	Terrestrial ecotoxicity	kg 1,4-DCB	E2	1.14E-11
M11	Freshwater ecotoxicity	kg 1,4-DCB	E2	6.95E-10
M12	Marine ecotoxicity	kg 1,4-DCB	E2	1.05E-10
M13	Human carcinogenic toxicity	kg 1,4-DCB	E1	3.32E-06
M14	Human non-carcinogenic toxicity	kg 1,4-DCB	E1	2.28E-07
M15	Land use	m^2a crop eq	E2	8.88E-09
M16	Mineral resource scarcity	kg Cu eq	E3	2.31E-01
M17	Fossil resource scarcity	kg oil eq	E3	4.57E-01
M18	Water consumption	m^3	E1 & E2	2.22E-06 & 6.04E-13
Tag	**Area of protection / endpoint**	**Damage unit**		
E1	Human health	DALY		
E2	Ecosystem quality	Species.yrs		
E3	Resource scarcity	USD2013		

Reference products

$\tilde{\alpha}_l^{1G}$: is the impact of first-generation bioethanol equivalent for the calculation of the benefits through substitution. Based on the EU Agricultural Outlook 2018 (European Commission, 2018a), the EU's average ethanol consists of about 24% sugar beet and molasses, 32% wheat grain, and 44% other cereals (mainly maize). First-generation bioethanol is modelled based on this information and data from the ecoinvent database (*Ethanol, without water, in 99.7% solution state, from fermentation, at service station {CH}| market for | APOS, U*).

$\tilde{\alpha}_l^{FF}$: is the impact of the fossil petrol equivalent for the calculation of the benefits through substitution. The LCA is based on the respective ecoinvent process (*Petrol, low-sulfur {Europe without Switzerland}| market for | APOS, U*).

$\tilde{\alpha}_{l,r,p}^{byp}$: is impact of application substituted by by-product $p \in P$ in region $r \in R$. As described in section 0, this study considers co-produced electricity and biomethane. Ecoinvent provides Life Cycle Inventories (LCI) for the average electricity mix of each

European country. We assume that each MJ of co-produced electricity substitutes one MJ of the regional electricity mix. Ecoinvent provides the LCIs for natural gas for most EU countries and we assume that a co-produced 1 m^3 biogas substitutes the energy equivalent of natural gas (0.65 m^3). For all missing countries, this study assumes the average European natural gas mix provided by ecoinvent.

$\widetilde{\omega}_l^{CO2}, \widetilde{\omega}_l^{CH4}$: benefit from stored CO_2 in second-generation biofuel and biomethane. To enable a fair comparison between fossil based and bio-based fuels, CO_2 stored in the bio-based fuel (released during combustion) flows negatively into the carbon balance.

Table B 6 shows the carbon balance of the 2G bioethanol production. We assume the same balance for every type of straw, and values are based on the average feedstock composition. The intake of biogenic carbon takes place during the growth phase of the plant. Carbon dioxide is released in the two process steps fermentation and combustion. The remaining carbon is assumed to be stored in the bioethanol and its by-product biomethane. To allow a comparison with the two fossil references petrol and natural gas, the biogenic carbon stored in the products is modeled as carbon dioxide 'credit'. While combusting petrol releases carbon that has been locked up for millions of years, burning bioethanol and biomethane emits carbon that is part of the biogenic carbon cycle.

Table B 6: Biogenic carbon balance of 2G bioethanol production

C biogenic	**kg C kg-1 straw**	**kg C MJ-1 EtOH**	**kg C kg-1 EtOH**
Input			
C in straw	4.00E-01	6.77E-02	1.81E+00
Output			
C stored in EtOH	1.23E-01	1.95E-02	5.21E-01
Co-fermentation			
C-CO_2 (released CO_2 in fermentation)	7.24E-02	1.23E-02	3.28E-01
Stillage (upgraded to bio-methane)	6.01E-02	1.02E-02	2.72E-01
Combustion in CHP (total)	1.44E-01	2.44E-02	6.51E-01
C-CH_4	6.00E-07	1.02E-07	2.71E-06
C-CO	6.00E-06	1.02E-06	2.71E-05
C-non-methane organic compounds	1.20E-05	2.03E-06	5.43E-05
C-CO_2	1.44E-01	2.44E-02	6.51E-01

Biorefinery-related impacts

$\widetilde{\kappa}_{l,c}^{depr}$: are the annual impacts of installing a biorefinery with capacity level $c \in C$, the affiliated co-generation system, and the affiliated biogas system. The biorefinery is modelled according to Jungbluth et al. (2007). This work assumes a biorefinery

operation time of 20 years, wherefore the installing impacts are evenly allocated annually over 20 years. Analogous to the biorefinery costs, the impacts include a "cost degression", using the scale coefficient λ (see 0).

$\widetilde{\kappa}_l^{var}$: are variable impacts of refining bioethanol at a biorefinery. The following paragraph summarizes the biorefinery production process:

Pretreatment: The cleaning and mechanical shredding of the fibers to between 1 and 3 mm large particles is the first processing step. The energy needed for the shredding is provided by the co-produced electricity. It is followed by the hydrothermal cracking (autohydrolysis) to disrupt lignin and other non-cellulose components to separate cellulose and hemicellulose in subsequent steps (Gupta and Verma, 2015). Most LCA studies on cellulose ethanol still adopt the US Department of Energy's National Renewable Energy Laboratory's (NREL) process dilute acid pretreatment, followed by steam explosion (Gerbrandt et al., 2016). Processes that use acids or bases as catalysts for the pretreatment require a neutralization step, which increases the waste production and the process energy requirements, although research identified pretreatment options for commercial plants with fewer environmental impacts and costs (Gerbrandt et al., 2016). The study at hand assumes chemical free steam explosion pre-treatment, which can be considered the state-of-the-art production process in commercial plants (Sunliquid, 2019).

Enzyme production: Enzymes, which are required for the enzymatic hydrolysis, are produced from the pre-treated feedstock in an integrated step of the production process, wherefore the enzymes are optimized to the type of straw. All inputs for the enzyme production are taken from Humbird et al. (2011).

Saccharification: Subsequently, the enzyme mixture hydrolyzes cellulose and hemicellulose chains to form sugar monomers (hexoses and pentoses) in the saccharification process.

$$\text{cellulose} + \text{water} + \text{enzymes (cellulase)} \rightarrow \text{glucose (hexoses)} \tag{38}$$

$$\text{hemicellulose} + \text{water} + \text{enzymes (hemicellulase)} \rightarrow \text{xylose (pentoses)} \tag{39}$$

Fermentation: Hexose (C6 sugars) and pentose (C5 sugars) are fermented to a fermentation broth and CO_2. The maximum theoretical fermentation efficiency is 0.51 kg ethanol per kg hexose/pentose.

$$\begin{gathered}3 \text{ pentose} \rightarrow 5 \text{ ethanol} + 5 \text{ carbon dioxide } (3C_5H_{10}O_5 \\ \rightarrow 5\,C_2H_5OH + 5\,CO_2)\end{gathered} \tag{40}$$

$$\text{hexose} \rightarrow 2 \text{ ethanol} + 2 \text{ carbon dioxide } (C_6H_{12}O_6 \rightarrow 2\,C_2H_5OH + 2\,CO_2) \tag{41}$$

Purification: Ethanol is then recovered from the fermentation broth by micro-sieves to a purity of 99.7 vol.%. The transformation efficiency of cellulose to glucose and hemicellulose to xylose, as well as the fermentation efficiency is assumed to be 85%. These assumptions translate to 0.2211 t ethanol per t straw, which is congruent with literature sources on similar technologies (Clariant, 2018; Santibañez-Aguilar et al., 2011; Wang et al., 2013).

Cogeneration: The energy (electric and thermal) consumed by the biorefinery is produced by the combustion of lignin in a co-generation plant. Emissions from the co-generation to produce process energy are the main sources for environmental impacts.

Feedstock impacts

$\widetilde{\varphi}_{l,f}$: are the impacts of feedstock $f \in F$ at farm. The effect of the agricultural residue removal and the associated environmental impacts is a controversial topic in the scientific literature. Many studies on energy use of agricultural residues ignore the environmental consequences of residue removal (Cherubini and Strømman, 2011). The work of Cherubini and Ulgiati (2010) and Nguyen et al. (2013) investigated the effects of crop residue removal on the soil quality and observed long-range consequences like decreasing yield due to nutrient removal, a change in soil N_2O emissions, and a decrease of soil organic carbon. Also Lal (2005) showed that a complete removal of straw has a negative impact on the soil organic carbon (SOC) and soil erosion. Table B 7 shows the SOC loss and the resulting CO_2 emissions in case of 100% residue removal (Cherubini and Ulgiati, 2010). Different studies suggest a so called *sustainable removal rate* at which the SOC share is not significantly changed over time due to saturation effects. Sheehan et al. (2004) stated a removal of 40% straw under conventional mulch till and 70% under no-till as sustainable. The bioeconomic feedstock potential applied in this work takes into account the sustainable removal rate with the assumption that a removal of 40% (and 50% for maize) does not affect the SOC (Scarlat et al., 2010; Wietschel et al., 2019).

In addition to the SOC balance, straw removal leads to a removal of the nutrients nitrogen, phosphorous and potassium, which entails a decrease in grain yields (Cherubini and Ulgiati, 2010). To account for additional environmental impacts by straw removal, we compare a 100% straw incorporation without additional fertilization with a residue removal of 40 to 50% plus additional fertilization to compensate for the loss of the nutrients nitrogen, phosphorous and potassium. Table B 8 features the nutrient requirement per removed metric ton of straw.

Table B 7: Loss of soil organic carbon and its impact on CO_2 emissions

Material	Residue removal rate	SOC loss	CO_2 emissions	Source
Cereal straw	100%	0.039 t C/t_{straw}	0.143 t CO_2/t_{straw}	Cherubini and Ulgiati, 2010
Wheat straw	40%	-	-	Scarlat et al., 2010
Maize stover	50%	-	-	Scarlat et al., 2010
Barley straw	40%	-	-	Scarlat et al., 2010
Rapeseed straw	40%	-	-	Scarlat et al., 2010

Table B 8: Additional fertilizer requirement per removed metric ton of straw (based on Cherubini & Ulgiati, 2010; Harms, 2018)

Material	Wheat straw	Maize stover	Barley straw	Rapeseed straw	Comment
N - CAN*	1.5 kg/t	2.7 kg/t	1.5 kg/t	3.3 kg/t	30% of total N in straw
P – P_2O_5	3.0 kg/t	2.0 kg/t	3.0 kg/t	6.0 kg/t	100% of total P in straw
K – K_2O	7 kg/t	10 kg/t	9 kg/t	12.5 kg/t	50% of total K in straw

* calcium ammonium nitrate fertilizer

Transportation impacts

$\tilde{\varepsilon}_{l,t}^{fix}$: are fixed impacts (per metric ton) of transporting feedstock with transport mode $t \in T$. For $t = tractor$, we do assume no additional fixed impacts, for $t = truck$, we assume a single bale loading. For $t = rail$, we assume a 30 km pendulum tour truck transport and two bale loadings (loading of the transport truck and loading of the train).

$\tilde{\varepsilon}_{l,t}^{var}$: are variable impacts (per ton kilometer) of transporting feedstock with transport mode $t \in T$. For $t = truck$, we assume 50% with EURO5 and 50% EURO6 transport. According to the European average rail system, we assume a share of 44% diesel train and 56% electric train. Tractor, truck, and rail transport is modeled with the respective ecoinvent LCI processes.

$\tilde{\eta}_{l,t}^{fix}$: fixed impacts (per metric ton) of transporting bioethanol with transport mode $t \in T$. The fixed bioethanol transport impacts include all activities needed to offer the bioethanol at the market.

$\tilde{\eta}_{l,t}^{var}$: variable impacts (per ton kilometer) of transporting bioethanol with transport mode $t \in T$. The transportation with $t = truck$ assumes a 32 t truck.

Appendix C

Parts of Appendix C corresponds to the Supporting Information 1 of Messmann et al., which is currently under review at the Journal of Industrial Ecology.

C.1 Modeling

Table C 1: Changelog of the model between chapter 5 and chapter 6

Geography
a. Changed set R from NUTS2013 to NUTS2021 classification* (composition of FR and PL regions, order of EL regions, otherwise mostly name or code changes), which implied the following updates: i. Updated bioeconomic feedstock potential: reallocation based on the feedstock production shares of newly introduced NUTS2021 region, method based on Wietschel et al., 2019. ii. Corrected a few insignificant errors in the ratios between the 2030 and 2018 potentials (the 2030 scenario is not part of chapter 6) iii. Region geometries: Updated the region sizes (in km^2; for the calculation of the region-specific feedstock potentials) and the tortuosity factors accordingly iv. Distance matrix now following the Persyn et al. (2020) for NUTS-2 regions (instead of own aggregation from NUTS-3 + disk line picking), and then aggregating to NUTS-1 from there (as before). v. Updated gasoline and 1G EtOH demands accordingly: 1. Based on the 2019 population (instead of 2018/2017) and NUTS2021 classification 2. Updated country-level demand values from 2017 to 2018 (gasoline) and from 2017 to 2019 (EtOH)
b. Removed UK-Regions and region FRY (Départements d'Outre-Mer) from set R→ new set size: 91 (was 98 in chapter 5), and 104 after NUTS2021
c. Changed (where applicable) EU28 averages in parameters to EU27.
Capacities of biorefineries
a. The cardinality of set C increased from 37 to 38 (addition a "0" capacity level for modeling purposes)
b. Constraint (2) (ensured sufficient BR capacity) is now obsolete, as this is now covered by the newly added constraints.
Revenues and costs
a. Updated data on labor cost indices and price levels of gross capital formation and transport cost levels (04.02.2021)
b. γ_r^{inv} now also applies to *refinery costs others* (administration, insurance, maintenance), as these are calculated as percentages of the overall construction costs.
c. Updated oil prices (both for calculation of competitive 2G revenues and import factors), based on averages Jan 2018 - Dec 2020 (previously: mid-2018 – mid-2019).
d. Adjusted reference employee number for biorefineries from 120 to 100, based on https://www.sunliquid-project-fp7.eu/news/construction-progress-podari/
e. Reinterpreted annual fixed biorefinery as annuities (instead of mere depreciation), with values changing marginally.
f. Updated the annual labor costs per biorefinery employee (in the background calculation) from 50.000 EUR to 80.869 EUR in Germany, leading to different values of κ_c^{pers}. Updated the γ_r^{lab} accordingly (Germany = 1)
MILP Constraints
a. Introduced new constraints and parameters to facilitate social optimization
Error fixes

a. The labor cost factor was mistakenly normalized to EU28, even though it is stated in Appendix B.2 that it is normalized to Germany.
b. Tractor, truck, train were erroneously modeled as consequential LCI processes. Therefore, the three processes are replaced by the corresponding APOS processes.
c. Feedstock transport: for each mode, the impacts of one-time baling are considered.
d. Fixed unit conversation errors in theta. The factor theta for the by-products was mistakenly specified in MJ/kg EtOH; however, the model was calculated based on t EtOH. In the course of correcting this error, the assumptions for the energy flows have been revised, too.

C.2 Social parameters

This section provides the nomenclature of model parameters associated with the social objective functions and social hotspot functions. It distinguishes between model parameters that are the direct operationalization of the social indicators (e.g., unemployment rate) and "basic quantities", to which the indicators are applied and which give the indicators a dimension. In a way, these "basic quantities" could be interpreted analogously to a social inventory, which is then characterized by the indicators. Thus, for example, social objective function $SOF1$ (local employment) weights the number of jobs created in the network with the regional unemployment rates, and in $SOF6$ (fair salary), the parameter for wages paid is multiplied by the number of jobs that are created (i.e., that are compensated with this wage).

The "basic quantities" are directly linked to and given per unit of the respective decision variable. They divide into jobs created by the network (used by $SOF1$, $SOF6$, $SOF7$, $SOF7b$), amount of water consumed in the network ($SOF2$), amount of pollutants emitted in the network ($SOF3$), area of land occupied by the network ($SOF4$), and economic value of network activities ($\triangleq$ economic parameters; $SOF5$, $SOF8$).

The following section details the calculation of parameters from the social indicators as given in Table C 2 and offers numerical examples for the region "BE1" (Belgium, Brussels). The resulting parameter values are given in D.3 (sheets Data 1, Data 2). Section *Basic quantities* provides the calculation of the basic quantities as given in Table C 2. They are provided in the online data repository D.3 (sheets Data 3a, Data 3b).

Table C 2: Parameters from operationalized social indicators

Parameter	Definition
ξ_r^{ump}	model parameter for the indicator "unemployment rate" in region $r \in R$
ξ_r^{water}	model parameter for the indicator "water stress level" in region $r \in R$
$\xi^{water,EU}$	model parameter for the indicator "water stress level", EU27 average
$\xi_{r,q}^{air}$	model parameter for the indicator "air pollution" for pollutant $q \in Q$ in region $r \in R$
$\xi_q^{air,EU}$	model parameter for the indicator "air pollution" for pollutant $q \in Q$, EU27 average
ξ_r^{land}	model parameter for the indicator "caloric yield" in region $r \in R$
$\xi^{land,EU}$	model parameter for the indicator "caloric yield", EU27 average
ξ_r^{GDP}	model parameter for the indicator "GDP per capita" in region $r \in R$
$\xi_r^{wage,i}$	model parameter for the indicators "wage" and "poverty line" for industry sector $i \in I$ in region $r \in R$
$\xi_{r,f}^{wage,feed}$	model parameter for the indicators "wage" and "poverty line" for feedstock $f \in F$ in region $r \in R$
$\xi_r^{lda,i}$	model parameter for the indicator "occupational injuries" for industry sector $i \in I$ in region $r \in R$
$\xi_r^{lla,i}$	model parameter for the indicator "occupational fatalities" for industry sector $i \in I$ in region $r \in R$
ξ_r^{shf}	model parameter for the indicator "smallholder farming" in region $r \in R$
$\chi_r^{ump,1G}$	model parameter for the indicator "unemployment rate" in region $r \in R$, substituting 1G EtOH
$\chi_r^{ump,FF}$	model parameter for the indicator "unemployment rate" in region $r \in R$, substituting fossil petrol
$\chi_{r,p}^{ump,byp}$	model parameter for the indicator "unemployment rate" in region $r \in R$, substituting by-product $p \in P$
$\chi_r^{GDP,1G}$	model parameter for the indicator "GDP per capita" in region $r \in R$, substituting 1G EtOH
$\chi_r^{GDP,FF}$	model parameter for the indicator "GDP per capita" in region $r \in R$, substituting fossil petrol
$\chi_{r,p}^{GDP,byp}$	model parameter for the indicator "GDP per capita" in region $r \in R$, substituting by-product $p \in P$
$\chi_r^{wage,1G}$	model parameter for the indicators "wage" and "poverty line" in region $r \in R$, substituting 1G EtOH
$\chi_r^{wage,FF}$	model parameter for the indicators "wage" and "poverty line" in region $r \in R$, substituting fossil petrol
$\chi_{r,p}^{wage,byp}$	model parameter for the indicators "wage" and "poverty line" in region $r \in R$, subst. by-product $p \in P$
$\chi_r^{lda,1G}$	model parameter for the indicator "occupational injuries" in region $r \in R$, substituting 1G EtOH
$\chi_r^{lda,FF}$	model parameter for the indicator "occupational injuries" in region $r \in R$, substituting fossil petrol
$\chi_{r,p}^{lda,byp}$	model parameter for the indicator "occupational injuries" in region $r \in R$, substituting by-product $p \in P$
$\chi_r^{lla,1G}$	model parameter for the indicator "occupational fatalities" in region $r \in R$, substituting 1G EtOH
$\chi_r^{lla,FF}$	model parameter for the indicator "occupational fatalities" in region $r \in R$, substituting fossil petrol
$\chi_{r,p}^{lla,byp}$	model parameter for the indicator "occupational fatalities" in region $r \in R$, subst. by-product $p \in P$
o_r^i	social risk (SHDB; in mrheq) for industry sector $i \in I$ in region $r \in R$

Table C 3: Parameters for basic quantities

Parameter	Unit	Definition
$\iota_{r,t}^{v.t.feed}$	jobs / tkm	variable jobs from feedstock transportation in region $r \in R$ with transport mode $t \in T$
$\iota_{r,t}^{f.t.feed}$	jobs / t	fixed jobs from feedstock transportation in region $r \in R$ with transport mode $t \in T$
$\iota_{r,t}^{v.t.etoh}$	jobs / tkm	variable jobs from bioethanol transportation in region $r \in R$ with transport mode $t \in T$
$\iota_{r,t}^{f.t.etoh}$	jobs / t	fixed jobs from bioethanol transportation in region $r \in R$ with transport mode $t \in T$
$\iota^{feedstock}$	jobs / t	agricultural jobs from feedstock baling and loading in region $r \in R$
ι_c^{const}	jobs / BR	jobs from construction of biorefineries with capacity level $c \in C$
ι_c^{pers}	jobs / BR	jobs in biorefineries with capacity level $c \in C$
$\iota^{subst.1G}$	jobs / t	jobs lost due to substitution of 1G EtOH by 2G EtOH
$\iota^{subst.FF}$	jobs / t	jobs lost due to substitution of fossil petrol by 2G EtOH
$\iota_p^{subst.byp}$	jobs / t	jobs lost due to substitution of electricity and natural gas by-products $p \in P$ respectively
$\tilde{v}$, $\ddot{v}_q$, $\bar{v}$ represent locally arising water use [m^3], air emissions [kg of pollutant $q \in Q$], and land occupation [m^2a], respectively, derived from the Life Cycle Inventory of the environmental parameters (see Appendix D.3, Data 2; and Appendix D.3, Data 3b):		
$\tilde{v}_t^{v.t.feed}$, $\ddot{v}_{t,q}^{v.t.feed}$, $\bar{v}_t^{v.t.feed}$	... / tkm	from variable feedstock transportation with transport mode $t \in T$
$\tilde{v}_t^{f.t.feed}$, $\ddot{v}_{t,q}^{f.t.feed}$, $\bar{v}_t^{f.t.feed}$	... / t	from fixed feedstock transportation with transport mode $t \in T$
$\tilde{v}_t^{v.t.etoh}$, $\ddot{v}_{t,q}^{v.t.etoh}$, $\bar{v}_t^{v.t.etoh}$	... / tkm	from variable bioethanol transportation with transport mode $t \in T$
$\tilde{v}_t^{f.t.etoh}$, $\ddot{v}_{t,q}^{f.t.etoh}$, $\bar{v}_t^{f.t.etoh}$	... / t	from fixed bioethanol transportation with transport mode $t \in T$
$\tilde{v}_f^{feedstock}$, $\ddot{v}_{f,q}^{feedstock}$, $\bar{v}_f^{feedstock}$	... / t	from feedstock provision of feedstock $f \in F$
$\tilde{v}_c^{const}$, $\ddot{v}_{c,q}^{const}$, $\bar{v}_c^{const}$	... / BR	from the construction of biorefineries with capacity level $c \in C$
$\tilde{v}^{var}$, $\ddot{v}_q^{var}$, $\bar{v}^{var}$	... / t	from processing 2G EtOH in biorefineries

Social indicators

This section details how the selected social indicators are operationalized into model parameters. It bears mentioning that in most cases, not always; however, indicators on a regional level are put into relation to an EU27 average. The goal behind the individual calculation variant is to remain true and consistent to the respective basic quantities to achieve meaningful objective values, which is a shortcoming in many studies (Messmann et al., 2020). For example, jobs created in a region are not multiplied by the bare regional unemployment rate, as the resulting value would hardly be interpretable, but with the unemployment rate relative to the EU27 average (see below). This way, a job created in a region with, e.g., 1.89 times the average unemployment rate is assumed to be 1.89 more beneficial. Thus, the unit of the objective value can be interpreted as "job equivalents". This is in line with several studies in this field (unemployment-weighted jobs: e.g., Mota et al., 2015; Zhalechian et al., 2016; economic value weighted by an indicator for regional economic development: e.g., Ghaderi et al., 2018; Mota et al., 2018; Zhu & Hu, 2017). Likewise, the parameter for occupational fatalities is given in fatalities per employee; hence, it

does not require to be weighted against an EU27 average to be meaningful when multiplied with the respective basic quantity (created jobs).

ξ_r^{ump} is the parameter that operationalizes the social indicator (regional unemployment rate) of the social objective function $SOF1$ (*Local employment*). It gives the unemployment rate in region $r \in R$ relative to the EU27 average (Eurostat, 2020d), i.e., jobs created in regions with higher unemployment rates are favored.

$$\xi_r^{ump} = \frac{unemployment\ rate_r}{unemployment\ rate_{EU27}}$$

$$\text{e.g., } \xi_{BE1}^{ump} = \frac{unemployment\ rate_{BE1}}{unemployment\ rate_{EU27}} = \frac{12.5\%}{6.6\%} = 1.89$$

ξ_r^{water} is the parameter that operationalizes the social indicator (water stress level) of the social objective function $SOF2$ (*Water use*). It is the country-specific water stress level in region $r \in R$ relative to the European average, i.e., water use in regions with higher water stress is penalized. The water stress level (in 2018) is given by Aquastat (FAO, 2021) and defined as the total freshwater withdrawal divided by the total renewable water resources less environmental flow requirements.

$$\xi_r^{water} = \frac{FAO\ Aquastat\ water\ stress\ level_r}{FAO\ Aquastat\ water\ stress\ level_{Europe}}$$

$$\text{e.g., } \xi_{BE1}^{water} = \frac{FAO\ Aquastat\ water\ stress\ level_{BE1}}{FAO\ Aquastat\ water\ stress\ level_{Europe}} = \frac{49.07\%}{8.51\%} = 5.77$$

$\xi_{r,q}^{air}$ is the parameter that operationalizes the social indicator (air pollution) of the social objective function $SOF3$ (*Living conditions*). It takes into account the statistical excess mortality risk from each of the pollutants $q \in Q$ (PM2.5, PM10, NO_X, O_3, and BC (black carbon/soot)), weights it by the population density of region $r \in R$ (Eurostat, 2021n) and puts everything into relation with the EU27 average. The excess mortality is assumed to be a function of the concentration of the respective pollutant in $\frac{\mu g}{m^3}$ (cf. Anderson et al., 2004; Gryparis et al., 2004; WHO, 2013; Zhou et al., 2014). In this way, pollutant emissions in regions with a higher statistical excess mortality attributable to higher pollutant concentrations, as well as in regions with a higher population density, are penalized. The concentrations (~68,000 data points, measured by ~5,000 stations across the EU) are taken from EEA (2021) GIS-matched to NUTS-1 regions $r \in R$, and aggregated. For PM2.5, NO_X, O_3, and BC, the corresponding statistical excess mortality was retrieved from the WHO tool AirQ+ (WHO, 2021) For PM10, for which a general mortality is not available in AirQ+, we calculated the excess mortality based on the meta-analysis and regression by (Anderson et al., 2004), who estimate a marginal mortality risk of $\frac{0.60\%}{10\frac{\mu g}{m^3}}$.

$$\xi_{r,q}^{air} = \frac{mortality\ risk(concentration_{r,q})_{r,q} * population\ density_r}{mortality\ risk(concentration_{EU27,q})_{EU27,q} * population\ density_{EU27}}$$

$$\text{e.g., } \xi_{BE1}^{air,PM2.5} = \frac{mortality\ risk\left(12.03\frac{\mu g}{m^3}\right)*7{,}552\frac{1}{km^2}}{mortality\ risk\left(12.16\frac{\mu g}{m^3}\right)*108\frac{1}{km^2}} = \frac{1.29\%*7{,}552\frac{1}{km^2}}{1.21\%*108\frac{1}{km^2}} = 65.75$$

ξ_r^{land} is the parameter that operationalizes the social indicator (caloric yield) of the social objective function $SOF4$ (*Land-food conflict*). It represents the agricultural yield (in kcal wheat eq. per m^2a; (Lee et al., 2016; Eurostat, 2021f) in region $r \in R$ so as to penalize the use of land in regions more strongly, the more yielding the hypothetical alternative use of the land for food production would be.

$$\xi_r^{land} = yield_r * caloric\ value\ of\ wheat$$

$$\text{e.g., } \xi_{BE1}^{land} = 9.32\,\frac{kg}{m^2} * 4{,}000\,\frac{kcal}{kg} = 37{,}282\,\frac{kcal}{m^2}$$

ξ_r^{GDP} is the parameter that operationalizes the social indicator (regional GDP per capita) of the social objective function $SOF5$ (*Economic development*). It gives the gross domestic product (GDP) per capita (in purchasing power standards, which is also in line with the EU's cohesion report; European Commission (2017) in region $r \in R$ inversely relative to the EU27 average (Eurostat, 2021j), so as to favor economic activities in regions with a lower GDP per capita.

$$\xi_r^{GDP} = \frac{GDP\ per\ capita_{EU27}}{GDP\ per\ capita_r}$$

$$\text{e.g., } \xi_{BE1}^{GDP} = \frac{GDP\ per\ capita_{EU27}}{GDP\ per\ capita_{BE1}} = \frac{30{,}200}{61{,}300} = 0.49$$

$\xi_r^{wage,i}$ is the parameter that operationalizes the social indicators (poverty line and wages paid) of the social objective function $SOF6$ (*Fair salary*). It takes into account the hourly wage in industry sector $i \in I$ in region $r \in R$ (Benoît Norris et al., 2018; converted to EUR2020 from USD2011), the daily income at the 40% poverty line ($\triangleq$ 40% of mean equivalized income[5]; (World Bank, 2021c) and the number of daily workhours in region $r \in R$ (World Bank, 2021b) to calculate the ratio between the expectable daily wage and the poverty line, to then put the latter in relation to the same ratio on EU27 level. This favors jobs in regions in which the expectable wage is well above the poverty line.

$$\xi_r^{wage,i} = \frac{\frac{hourly\ wage_r^i * daily\ workhours_r}{40\%\ poverty\ line_r}}{\frac{hourly\ wage_{EU27}^i * daily\ workhours_{EU27}}{40\%\ poverty\ line_{EU27}}}$$

5 The EU defines the poverty threshold at 60% of the median equivalized income (Eurostat, 2019a); however, for consistency with worldwide data, where only values for the 40% mean equivalized income exist, the latter was chosen here, too.

$$\text{e.g., } \xi_{BE1}^{wage,const} = \frac{\frac{hourly\ wage_{BE}^{const} * daily\ workhours_{BE1}}{40\%\ poverty\ line_{BE1}}}{\frac{hourly\ wage_{EU27}^{const} * daily\ workhours_{EU27}}{40\%\ poverty\ line_{EU27}}} = \frac{\frac{21.66\frac{USD2011}{h} * 7.6\frac{h}{d}}{28.95\frac{USD2011}{d} * 0.7961\frac{EUR2020}{USD2011}}}{\frac{13.44\frac{USD2011}{h} * 8\frac{h}{d}}{21.10\frac{USD2011}{d} * 0.7961\frac{EUR2020}{USD2011}}} = \frac{5.69}{5.10} = 1.12$$

$\xi_r^{lda,i}$ is the parameter that operationalizes the social indicator (occupational injuries) of social objective function $SOF7$ (Workers' health & safety). It takes into account lost days due to accidents $lda_{r,i,y}$, as well as the number of employees in region $r \in R$, industry sector $i \in I$ for each year y between 2010 and 2019. (Eurostat, 2021b) gives the number of accidents (per country and sector, i.e., NACE Rev. 2 Activity) by days lost (given in ranges j, e.g., "from 4 to 6 days"). $lda_{r,i,y}$ is thus calculated as the sum product of the number of accidents in region $r \in R$, industry sector $i \in I$, year y and range of days j, and the mean value of range j (e.g., the mean of "from 4 to 6 days" is 5 days). The number of employees is calculated, retaining consistency within the data, as the total number of accidents in region $r \in R$, industry sector $i \in I$ (in 100,000 accidents), and year y, divided by the incidence rate (in accidents per 100,000 employees) (Eurostat, 2021m). Finally, $\xi_r^{lda,i}$ (in lost employee-years due to accidents per employee and year) is the annual average over $lda_{r,i,y}$ divided by the number of employees. Note: For other jobs associated with the operation of a biorefinery (insurance, administration, maintenance; 1.0%, 0.5%, 2.0% of annual fixed costs respectively), the parameter is calculated as a cost-weighted average.

$$lda_{r,i,y} = \sum_j (\#accidents_{r,i,y,j} * mean\ days_j)$$

$$employees_{r,i,y} = \frac{\#accidents_{r,i,y} * 100{,}000}{incidence_{r,i,y}}$$

$$\xi_r^{lda,i} = \frac{1}{2019-2010+1} * \sum_y \frac{lda_{r,i,y}}{365 * employees_{r,i,y}}$$

$$\text{e.g., } \xi_{BE}^{lda,construction} = 2.04 * 10^{-3}$$

$\xi_r^{lla,i}$ is the parameter that operationalizes the social indicator (occupational fatalities) of social objective function $SOF7b$ (Workers' health & safety). It takes into account the number of fatal accidents $lla_{r,i,y}$ (Eurostat, 2021b), as well as the number of employees in region $r \in R$, industry sector $i \in I$ for each year y between 2010 and 2019. The latter is calculated analogously to the calculation for $\xi_r^{lda,i}$. Finally, $\xi_r^{lla,i}$ (in lost lives due to accidents per employee and year) is the annual average over $lla_{r,i,y}$ divided by the number of employees. Note: For other jobs associated with the operation of a biorefinery (insurance, administration, maintenance; 1.0%, 0.5%, 2.0% of annual fixed costs, respectively), the parameter is calculated as a cost-weighted average.

$$\xi_r^{lla,i} = \frac{1}{2019-2010+1} * \sum_y \frac{lla_{r,i,y}}{employees_{r,i,y}}$$

$$\text{e.g., } \xi_{BE}^{lla,construction} = 6.94 * 10^{-5}$$

ξ_r^{shf} is the parameter that operationalizes the social indicator of $SOF8$ (Smallholder farming). It takes into account the share of privately owned (natural persons or common land unit, in contrast to legal persons) smallholder farms in the total number of farms (Eurostat, 2021h). The term "smallholder", however, is not unambiguously defined. Globally, and with a focus on the global south, "smallholder farming" connotes subsistence agriculture with a farming area of less than two hectares (FAO, 2015). However, in Europe, with a history of land consolidation and industrialized agriculture, the term is sometimes used differently. For example, in Scotland, smallholdings are defined as under 50 acres (~20 hectares, Scottish Government, 2017)). In the EU in 2016, two-thirds of farms are under five hectares, but in many countries, farms with 100 hectares or more are the only category in which the number of farms increases, implying a further consolidation, and the mean farm size is 16.6 ha (Eurostat, 2018c). Since $SOF8$ is bound to network decisions in the EU, we set the threshold at 20 hectares, but depending on goal and scope of the study, other values may be equally justified. In this way, feedstock sourcing is favored in regions with a large fraction of smallholder farms.

$$\xi_r^{shf} = \frac{farms\ (<20ha)\ in\ private\ or\ common\ ownership_r}{total\ number\ of\ farms_r}$$

$$\text{e.g., } \xi_{BE1}^{shf} = \frac{0}{50} = 0\%$$

Substitution

In principle, the effects of substitution are calculated analogously to the impacts of the network decisions, i.e., with corresponding basic quantities and the same idea behind the social indicators. However, substitution effects are not necessarily (exclusively) felt in the region in which substitution occurs. Therefore, the social indicators need to be adjusted with the elements presented in Table C 4 to provide the indicators (e.g., unemployment rate) as a weighted average. Generally, the following information is given: Production and import volumes of the substitutable products, their composition (taxes, refinement/processing, precursors) in terms of value, the share (in terms of kg) that every worldwide country has in the imports of the aforementioned products in the EU27 country with region r (retrieved from the Access2Markets database; DG Trade, 2021), as well as the social indicators for country w, determined analogously to the network ones (see above), but with other data sources.

Table C 4: Elements of the calculation of the social indicators for substitution

Element	Description	Data source
$w \in W$	auxiliary set for countries worldwide	
p_r^{EtOH}	production of EtOH in region r	Eurostat (2021b)
p_r^{petrol}	production of petrol in region r	Eurostat (2021b)
$p_r^{electr.}$	production of electricity in region r	IEA (2021)
p_r^{NG}	production of natural gas in region r	Eurostat (2021b)
p_r^{wheat}	production of wheat in region r	Eurostat (2021c)
p_r^{maize}	production of maize in region r	Eurostat (2021c)
$p_r^{sugarbeet}$	production of sugar beet in region r	Eurostat (2021c)
$p_r^{crude\ oil}$	production of crude oil in region r	Eurostat (2021b)
ti_r^{EtOH}	total import of EtOH in region r	Eurostat (2021b)
ti_r^{petrol}	total import of petrol in region r	Eurostat (2021b)
$ti_r^{electr.}$	total import of electricity in region r	IEA (2021)
ti_r^{NG}	total import of natural gas in region r	Eurostat (2021b)
ti_r^{wheat}	total import of wheat in region r	DG Trade (2021)
ti_r^{maize}	total import of maize in region r	DG Trade (2021)
$ti_r^{sugarbeet}$	total import of sugar beet in region r	DG Trade (2021)
$ti_r^{crude\ oil}$	total import of crude oil in region r	Eurostat (2021b)
$ps\ (refining)_r^{EtOH}$	price share of refining in the EtOH price in region r	own calculation
$ps\ (taxes)_r^{EtOH}$	price share of taxes in the EtOH price in region r	European Commission (2020)
$ps\ (wheat)_r^{EtOH}$	price share of the precursor wheat in the EtOH price in region r	Wietschel et al. (2021)
$ps\ (maize)_r^{EtOH}$	price share of the precursor maize in the EtOH price in region r	Wietschel et al. (2021)
$ps\ (sugarbeet)_r^{EtOH}$	price share of the precursor sugar beet in the EtOH price in region r	Wietschel et al. (2021)
$ps\ (refining)_r^{petrol}$	price share of refining in the petrol price in region r	own calculation
$ps\ (taxes)_r^{petrol}$	price share of taxes in the petrol price in region r	European Commission (2020)
$ps\ (crude\ oil)_r^{petrol}$	price share of the precursor crude oil in the petrol price in region r	European Commission (2020, 2021)
$ps\ (prod.\&transm.)_r^{electr.}$	price share of generation & transmission in the electricity price in region r	Eurostat (2021e)
$ps\ (taxes)_r^{electr.}$	price share of taxes in the electricity price in region r	Eurostat (2021e)
$ps\ (prod.\&transm.)_r^{NG}$	price share of generation & transmission in the natural gas price in region r	Eurostat (2021f)
$ps\ (taxes)_r^{NG}$	price share of taxes in the natural gas price in region r	Eurostat (2021f)
$is_{w,r}^{EtOH}$	import share of country w in the EtOH imports of region r	DG Trade (2021)
$is_{w,r}^{petrol}$	import share of country w in the petrol imports of region r	DG Trade (2021)
$is_{w,r}^{electr.}$	import share of country w in the electricity imports of region r	DG Trade (2021)
$is_{w,r}^{NG}$	import share of country w in the natural gas imports of region r	DG Trade (2021)
$is_{w,r}^{wheat}$	import share of country w in the wheat imports of region r	DG Trade (2021)
$is_{w,r}^{maize}$	import share of country w in the maize imports of region r	DG Trade (2021)
$is_{w,r}^{sugarbeet}$	import share of country w in the sugar beet imports of region r	DG Trade (2021)
$is_{w,r}^{crude\ oil}$	import share of country w in the crude oil imports of region r	DG Trade (2021)
$unemployment\ rate_w$		World Bank (2021c)
$GDP\ per\ capita_w$		IMF (2021)
$hourly\ wage_w^i$		Benoît-Norris et al. (2018)
$daily\ workhours_w$		World Bank (2021a)
$40\%\ poverty\ line_w$		World Bank (2021b)
$\xi_w^{lda,i}$	calculated analogously to $\xi_r^{lda,i}$	ILO (2021a, 2021b)
$\xi_w^{lla,i}$	calculated analogously to $\xi_r^{lla,i}$	ILO (2021c, 2021b)

The substitution parameters for SOF1 ($\chi_r^{ump,1G}$, $\chi_r^{ump,FF}$, $\chi_{r,p}^{ump,byp}$), SOF6 ($\chi_r^{wage,1G}$, $\chi_r^{wage,FF}$, $\chi_{r,p}^{wage,byp}$), SOF7 ($\chi_r^{lda,1G}$, $\chi_r^{lda,FF}$, $\chi_{r,p}^{lda,byp}$), and SOF7b ($\chi_r^{lla,1G}$, $\chi_r^{lla,FF}$, $\chi_{r,p}^{lla,byp}$) are determined analogously. For imported products, a weighted average over the import shares of countries W and their indicator values (e.g., unemployment rate) is calculated. This weighted average is then used in a weighted average over the production share in (country with) region r with the indicator value of r, and the import share in (country with) region r with the weighted indicator value mentioned afore.

$$\chi_r^{ump,1G} = \frac{p_r^{EtOH}}{p_r^{EtOH} + ti_r^{EtOH}} * \frac{unemployment\ rate_r}{unemployment\ rate_{EU27}} + \frac{ti_r^{EtOH}}{p_r^{EtOH} + ti_r^{EtOH}} * \frac{\sum_w (is_{w,r}^{EtOH} * unemployment\ rate_w)}{unemployment\ rate_{EU27}}$$

e.g., $\chi_{AT}^{ump,1G} = \frac{74.64\% * 4.78 + 25.36\% * 3.72}{6.6} = \frac{4.51}{6.6} = 0.68$

Analogously for fossil petrol ($\chi_r^{ump,FF}$), electricity, and natural gas ($\chi_{r,p}^{ump,byp}$).

$$\chi_r^{wage,1G} = \frac{p_r^{EtOH}}{p_r^{EtOH}+ti_r^{EtOH}} * \frac{\frac{hourly\ wage_r^{chemicals} * daily\ workhours_r}{40\%\ poverty\ line_r}}{\frac{hourly\ wage_{EU27}^{chemicals} * daily\ workhours_{EU27}}{40\%\ poverty\ line_{EU27}}} + \frac{ti_r^{EtOH}}{p_r^{EtOH}+ti_r^{EtOH}} * \frac{\sum_w is_{w,r}^{EtOH} * \frac{hourly\ wage_w^{chemicals} * daily\ workhours_w}{40\%\ poverty\ line_w}}{\frac{hourly\ wage_{EU27}^{chemicals} * daily\ workhours_{EU27}}{40\%\ poverty\ line_{EU27}}}$$

e.g., $\chi_{AT}^{wage,1G} = \frac{74.64\% * 8.53 + 25.36\% * 9.97}{10.38} = \frac{8.89}{10.38} = 0.86$

Analogously for fossil petrol ($\chi_r^{wage,FF}$), electricity, and natural gas ($\chi_{r,p}^{wage,byp}$).

$$\chi_r^{lda,1G} = \frac{p_r^{EtOH}}{p_r^{EtOH}+ti_r^{EtOH}} * \xi_r^{lda,chemicals} + \frac{ti_r^{EtOH}}{p_r^{EtOH}+ti_r^{EtOH}} * \xi_w^{lda,chemicals}$$

e.g., $\chi_{AT}^{lda,1G} = 74.64\% * 6.47 * 10^{-4} + 25.36\% * 6.24 * 10^{-4} = 6.41 * 10^{-4}$

Analogously for fossil petrol ($\chi_r^{lda,FF}$), electricity, and natural gas ($\chi_{r,p}^{lda,byp}$) as well as for $\chi_r^{lla,1G}$, $\chi_r^{lla,FF}$, and $\chi_{r,p}^{lla,byp}$.

As the price structure of the reference products has a more direct impact on the GDP indicator (e.g., excise tax), the weighted sum above is extended for $\chi_r^{wage,1G}$, $\chi_r^{wage,FF}$, and $\chi_{r,p}^{wage,byp}$ and includes the price structure (taxes, refining/processing, precursors), as well as another weighted sum for the import shares of the precursors (for $\chi_{r,p}^{wage,byp}$, it is only differentiated between processing (+ transmission) and taxes).

$$\begin{aligned}
&\chi_r^{GDP,1G} = GDP\ per\ capita_{EU27}\ /\ (\\
&ps\ (taxes)_r^{EtOH} * GDP\ per\ cap_r\\
&+(1 - ps\ (taxes)_r^{EtOH}) * \frac{ti_r^{EtOH}}{p_r^{EtOH}+ti_r^{EtOH}} * \sum_w \left(is_{w,r}^{EtOH} * GDP\ per\ cap_w\right)\\
&+(1 - ps\ (taxes)_r^{EtOH}) * \frac{p_r^{EtOH}}{p_r^{EtOH}+ti_r^{EtOH}} * \frac{ps\ (refining)_r^{EtOH}}{ps\ (refining)_r^{EtOH}+ps\ (wheat)_r^{EtOH}+ps\ (maize)_r^{EtOH}+ps\ (sugarbeet)_r^{EtOH}} * GDP\ per\ cap_r\\
&+(1 - ps\ (taxes)_r^{EtOH}) * \frac{p_r^{EtOH}}{p_r^{EtOH}+ti_r^{EtOH}} * \frac{ti_r^{wheat}}{p_r^{wheat}+ti_r^{wheat}} * \frac{ps\ (wheat)_r^{EtOH}}{ps\ (refining)_r^{EtOH}+ps\ (wheat)_r^{EtOH}+ps\ (maize)_r^{EtOH}+ps\ (sugarbeet)_r^{EtOH}}\\
&\quad * \sum_w \left(is_{w,r}^{wheat} * GDP\ per\ cap_w\right)
\end{aligned}$$

$$+(1-ps\ (taxes)_r^{EtOH}) * \frac{p_r^{EtOH}}{p_r^{EtOH}+ti_r^{EtOH}} * \frac{p_r^{wheat}}{p_r^{wheat}+ti_r^{wheat}} * \frac{ps\ (wheat)_r^{EtOH}}{ps\ (refining)_r^{EtOH}+ps\ (wheat)_r^{EtOH}+ps\ (maize)_r^{EtOH}+ps\ (sugarbeet)_r^{EtOH}}$$
$$* GDP\ per\ cap_r$$

$$+(1-ps\ (taxes)_r^{EtOH}) * \frac{p_r^{EtOH}}{p_r^{EtOH}+ti_r^{EtOH}} * \frac{ti_r^{maize}}{p_r^{maize}+ti_r^{maize}} * \frac{ps(maize)_r^{EtOH}}{ps\ (refining)_r^{EtOH}+ps\ (wheat)_r^{EtOH}+ps\ (maize)_r^{EtOH}+ps\ (sugarbeet)_r^{EtOH}}$$
$$* \sum_w \left(is_{w,r}^{maize} * GDP\ per\ cap_w\right)$$

$$+(1-ps\ (taxes)_r^{EtOH}) * \frac{p_r^{EtOH}}{p_r^{EtOH}+ti_r^{EtOH}} * \frac{p_r^{maize}}{p_r^{maize}+ti_r^{maize}} * \frac{ps\ (maize)_r^{EtOH}}{ps\ (refining)_r^{EtOH}+ps\ (wheat)_r^{EtOH}+ps\ (maize)_r^{EtOH}+ps\ (sugarbeet)_r^{EtOH}}$$
$$* GDP\ per\ cap_r$$

$$+(1-ps\ (taxes)_r^{EtOH}) * \frac{p_r^{EtOH}}{p_r^{EtOH}+ti_r^{EtOH}} * \frac{ti_r^{sugarbeet}}{p_r^{sugarbeet}+ti_r^{sugarbeet}} * \frac{ps\ (sugarbeet)_r^{EtOH}}{ps\ (refining)_r^{EtOH}+ps\ (wheat)_r^{EtOH}+ps\ (maize)_r^{EtOH}+ps\ (sugarbeet)_r^{EtOH}}$$
$$* \sum_w \left(is_{w,r}^{sugarbeet} * GDP\ per\ cap_w\right)$$

$$+(1-ps\ (taxes)_r^{EtOH}) * \frac{p_r^{EtOH}}{p_r^{EtOH}+ti_r^{EtOH}} * \frac{p_r^{sugarbeet}}{p_r^{sugarbeet}+ti_r^{sugarbeet}} * \frac{ps\ (sugarbeet)_r^{EtOH}}{ps\ (refining)_r^{EtOH}+ps\ (wheat)_r^{EtOH}+ps\ (maize)_r^{EtOH}+ps\ (sugarbeet)_r^{EtOH}}$$
$$* GDP\ per\ cap_r$$

)

e.g., $\chi_{AT}^{GDP,1G} = 30{,}200€ / (0\% * 55{,}406€$

$$+(1-0\%) * 25.36\% * 40{,}833€$$
$$+(1-0\%) * 74.64\% * 37.06\% * 55{,}406€$$
$$+(1-0\%) * 74.64\% * 62.35\% * 23.88\% * 37{,}049€$$
$$+(1-0\%) * 74.64\% * 37.65\% * 23.88\% * 55{,}406€$$
$$+(1-0\%) * 74.64\% * 55.90\% * 27.18\% * 33{,}170€$$
$$+(1-0\%) * 74.64\% * 44.10\% * 27.18\% * 55{,}406€$$
$$+(1-0\%) * 74.64\% * 4.30\% * 11.88\% * 32{,}331€$$
$$+(1-0\%) * 74.64\% * 95.70\% * 11.88\% * 55{,}406€)$$

$$= \frac{30{,}200€}{47{,}061€} = 0.64$$

$$\chi_r^{GDP,FF} = GDP\ per\ capita_{EU27} / (ps\ (taxes)_r^{petrol} * GDP\ per\ cap_r$$

$$+(1-ps\ (taxes)_r^{petrol}) * \frac{ti_r^{petrol}}{p_r^{petrol}+ti_r^{petrol}} * \sum_w \left(is_{w,r}^{petrol} * GDP\ per\ cap_w\right)$$

$$+(1-ps\ (taxes)_r^{petrol}) * \frac{p_r^{petrol}}{p_r^{petrol}+ti_r^{petrol}} * \frac{ps\ (refining)_r^{petrol}}{ps\ (refining)_r^{petrol}+ps\ (crude\ oil)_r^{petrol}} * GDP\ per\ cap_r$$

$$+(1-ps\ (taxes)_r^{EtOH}) * \frac{p_r^{petrol}}{p_r^{petrol}+ti_r^{petrol}} * \frac{ti_r^{crude\ oil}}{p_r^{crude\ oil}+ti_r^{crude\ oil}} * \frac{ps\ (crude\ oil)_r^{petrol}}{ps\ (refining)_r^{petrol}+ps\ (crude\ oil)_r^{petrol}}$$
$$* \sum_w \left(is_{w,r}^{crude\ oil} * GDP\ per\ cap_w\right)$$

$$+(1-ps\ (taxes)_r^{EtOH}) * \frac{p_r^{petrol}}{p_r^{petrol}+ti_r^{petrol}} * \frac{p_r^{crude\ oil}}{p_r^{crude\ oil}+ti_r^{crude\ oil}} * \frac{ps\ (wheat)_r^{petrol}}{ps\ (refining)_r^{petrol}+ps\ (crude\ oil)_r^{petrol}} * GDP\ per\ cap_r)$$

e.g., $\chi_{AT}^{GDP,FF} = 30{,}200€ / (57.85\% * 55{,}406€$

$$+(1-57.85\%) * 24.77\% * 59{,}146€$$

$$+(1-57.85\%)*75.23\%*28.56\%*55{,}406€$$
$$+(1-57.85\%)*75.23\%*93.12\%*71.44\%*16{,}661€$$
$$+(1-57.85\%)*75.23\%*6.88\%*71.44\%*55{,}406€)$$
$$=\frac{30{,}200€}{47{,}624€}=0.63$$

$$\chi_{r,electr.}^{GDP,byp} = GDP\ per\ capita_{EU27} \,/\, (ps\ (taxes)_r^{electr.} * GDP\ per\ cap_r$$
$$+ps\ (prod.\&transm.)_r^{electr.} * \frac{ti_r^{electr.}}{p_r^{electr.}+ti_r^{electr.}} * \sum_w \left(is_{w,r}^{electricity} * GDP\ per\ cap_w\right)$$
$$+ps\ (prod.\&transm.)_r^{electr.} * \frac{p_r^{electr.}}{p_r^{electr.}+ti_r^{electr.}} * GDP\ per\ cap_r)$$

e.g., $\chi_{AT,electr.}^{GDP,byp} = 30{,}200€ \,/\, (36.85\% * 55{,}406€$
$$+63.15\% * 29.04\% * 48{,}829€$$
$$+63.15\% * 70.96\% * 55{,}406€)$$
$$=\frac{30{,}200€}{54{,}200€}=0.56$$

Analogously for natural gas ($\chi_{r,natural\ gas.}^{GDP,byp}$).

This approach makes several assumptions, including: 1) that the composition in terms of value is a valid approximation; 2) that exports (unlike production and imports) can be disregarded; 3) that HS codes (tariff nomenclature) for data from Access2Markets roughly matches the focal products; 4) that imports from country w are valorized in this country, and that country w is not only a transit country.

The elaborate calculation approach does not aim at feigning a non-existent precision (given the assumptions). Its goal is rather to account for larger effects, e.g., a very high unemployment rate in a significant import country. In our opinion, this is more meaningful than naively assuming that substitution only affects the country in which it occurs or not quantifying substitution in the SOFs at all. In a further development, this approach could be extended to include a full input-output model, which would entail its own challenges (e.g., the discrepancy between actual products and aggregated sector values).

Basic quantities

$\iota_{r,t}^{v.t.feed}$ is the job factor (variable, per tkm) for feedstock transportation in region $r \in R$ with transport mode $t \in T$. It takes into account the average speed of vehicles v_t, the average load of vehicles l_t, the average operation time per workday of vehicles o_t (assumption: o_1, o_2 = ½, o_3 = ⅔), as well as the average annual workhours in region $r \in R$:

$$\iota_{r,t}^{v.t.feed} = \frac{1}{v_t * l_t * o_t * workhours\ p.a._r}$$

$\iota_{r,t}^{f.t.feed}$ is the job factor (fixed, per ton) for feedstock transportation in region $r \in R$ with transport mode $t \in T$. The job factor for transportation by trucks ($t = 2$) represents the loading of straw bales onto lorries. It takes into account the amount b of bales (in tons) loaded by a telehandler per hour, as well as the average annual workhours in region $r \in R$. For fixed jobs from train transportation ($t = 3$), we assume two times bale loading and a pendulum tour by truck of 30 km. This is in line with the calculation of fixed costs and impacts in the economic and environmental categories.

$$\iota_{r,1}^{f.t.feed} = 0$$

$$\iota_{r,2}^{f.t.feed} = \frac{1}{b * workhours\ p.a._r}$$

$$\iota_{r,3}^{f.t.feed} = 2 * \iota_{r,2}^{f.t.f.} + 2 * 30 * \iota_{r,2}^{v.t.f.}$$

$\iota_{r,t}^{v.t.etoh}$ is the job factor (variable, per tkm) for EtOH transportation in region $r \in R$ with transport mode $t \in T$. It takes into account the average speed of vehicles v_t, the average load of vehicles l_t, the average operation time per workday of vehicles o_t (assumption: o_1, o_2 = 50%, o_3 = 80%), the number of drivers per unit as well as the average annual workhours in region $r \in R$:

$$\iota_{r,t}^{v.t.etoh} = \frac{1}{v_t * l_t * d_t * o_t * workhours\ p.a._r}$$

$\iota_{r,t}^{f.t.etoh}$ is the job factor (fixed, per ton) for EtOH transportation in region $r \in R$ with transport mode $t \in T$. However, this factor is zero because these jobs are assumed to be jobs at gas stations, which are unaffected by substituting one fuel with another.

$$\iota_{r,t}^{f.t.etoh} = 0\ \forall \mathrm{r,t}$$

Table C 5: Value and references for the calculation of transportation job factors

Modi	Description	Unit	Value	Source
Bale loading	b bales (in tons) loaded by a telehandler per hour	t/h	50	(S2Biom, 2015)
Tractor	speed limit	km/h	40	Average general limit in EU countries
	tractor load	ton	18	(S2Biom, 2015)
	v_t average speed (80% of limit)	km/h	32,0	Estimation
	l_t average load (80% of load limit)	ton	14,4	Estimation
	d_t drivers per unit	job	1	Estimation
	o_t Share of driving time per worktime		0,5	Estimation
Truck	speed limit	km/h	80	(ProMods, 2017)
	tractor load	ton	25	(S2Biom, 2015)
	v_t average speed (80% of limit)	km/h	64,0	Estimation based on (ProMods, 2017)
	l_t average load (80% of load limit)	ton	20,0	(S2Biom, 2015)
	d_t drivers per unit	job	1	Estimation
	o_t Share of driving time per worktime		0,5	Estimation
Train	average speed	km/h	25	Estimation based on (European Court of Auditors, 2016)
	train load	ton	533	(IRG - Rail, 2019)
	d_t drivers per unit	job	2	Estimation
	o_t Share of driving time per worktime		0,80	Estimation

$\iota^{feedstock}$ is the job factor (per ton of feedstock) for jobs generated by feedstock provision. It is based on the assumed share of labor costs in the average feedstock costs φ_r (in €/ton) in region $r \in R$ (Appendix D.2), divided by the total annual labor costs (annual wages & salaries + annual labor costs other than wages & salaries; (Eurostat, 2021k)) per agricultural employee and year in region $r \in R$. The annual labor costs are based on hourly wages in industry sector $i \in I$ in region $r \in R$ (Benoît-Norris et al., 2018, converted to EUR2020 from USD2011), the weekly number of workhours in region $r \in R$ (Eurostat, 2021b, five workdays per week, and the number of yearly workdays in region $r \in R$ (European Commission, 2018b), and are modified by the labor-costs-to-wages ratio of region $r \in R$ (Eurostat, 2020b). The personnel cost of feedstock provision can be ascribed to baling, as well as loading and unloading bales and transporting them from the field to the on-sight feedstock storage (Harms, 2020). Harms (2020) quantifies the labor cost share of the total feedstock cost for Germany; for all other countries, it is adjusted by the ratio of annual labor costs per job in regions $r \in R$ and $r = Germany\ (DE)$. This regionalization, however, cancels out in the final fraction, resulting in the same job factor for all regions.

$$\iota^{feedstock} = \frac{\varphi_r * share\ of\ labor\ costs\ in\ feedstock\ costs_r}{annual\ labor\ costs\ per\ empl._r}$$

$$= \frac{\varphi_r}{annual\ labor\ costs\ per\ empl._r} * \frac{\frac{annual\ labor\ costs\ per\ empl.r}{annual\ labor\ costs\ per\ empl._{DE}} * (baling\ costs_{DE} + loading\ costs_{DE})}{\varphi_r}$$

$$= \frac{baling\ costs_{DE} + loading\ costs_{DE}}{annual\ labor\ costs\ per\ empl._{DE}} = \frac{\frac{17.40€+5.00€}{1t}}{43{,}519€} = 5.15 * 10^{-4}$$

ι_c^{const} is the job factor for jobs generated by the construction of a biorefinery. It is based on Clariant (2020), who estimate the total number of construction workers associated with constructing their second-generation biorefinery (capacity of about 50.000 tons of second-generation bioethanol per year) to range between 300 and 800, varying over the construction period of three years. The construction started in 2018 and finished in October 2021 (Clariant, 2021a). Based on this, we assume an average of 600 construction workers for the duration of three years for a biorefinery with a capacity of 50.000 tons and annualize those jobs for an expected lifetime of the biorefinery of 20 years. As for capacity-dependent economic and environmental parameters, the number of required construction workers is assumed to scale with the capacity σ_c at capacity level $c \in C$, and we apply a scaling coefficient λ of 0.8 (Towler and Sinnott, 2013).

$$\iota_c^{const} = \left(\frac{cap_c}{50{,}000t}\right)^{\lambda} * \frac{600\ jobs * 3\ years}{20\ years}$$

ι_c^{pers} is the job factor for the number of jobs created as biorefinery personnel of a biorefinery. It is also based on Clariant (2020), who estimate the total annual number of employees associated with the operation of their second-generation biorefinery (capacity of about 50.000 tons of second-generation bioethanol per year) to be about 100 workers. As for capacity-dependent economic and environmental parameters, the number of employees is assumed to scale with the capacity σ_c at capacity level $c \in C$, and we apply a scaling coefficient λ of 0.8 (Towler and Sinnott, 2013).

$$\iota_c^{pers} = \left(\frac{cap_c}{50{,}000t}\right)^{\lambda} * \ 100\frac{jobs}{year}$$

$\iota^{subst.1G}$ is the job factor for direct jobs lost by the substitution of first-generation bioethanol. Schaidle et al. (2011) report that first-generation ethanol production generates half the jobs compared to second-generation bioethanol production. The value is based on the assumption of 100 direct jobs for a second-generation bioethanol refinery of 50.000 t per year (Clariant, 2020). Direct jobs only cover jobs directly involved in the EtOH production process (without indirect jobs like logistic jobs or feedstock provision).

$$\iota^{subst.1G} = \frac{1}{2} * \frac{100\ jobs}{50.000\ t\ EtOH}$$

$\iota^{subst.FF}$ is the job factor for direct jobs lost by the substitution of petrol. The factor separates the affected jobs in *mining and production jobs* of crude oil and *refining jobs* to produce end products (e.g., petrol). For the direct jobs in mining and production, we take the mean of Norway 2020 and UK 2019; for the direct jobs in the oil refining sector, we take Germany as basis.

$$\iota^{subst.\mathrm{FF}} = \frac{mining\ and\ production\ direct\ jobs}{ton\ oil\ eq.} + \frac{refining\ direct\ jobs}{ton\ petrol}$$

$\iota_{gas}^{subst.byp}$ is the job factor for direct jobs lost by the substitution of natural gas. The factor bases on the same assumptions as $\iota^{subst.FF}$ and is also the average of Norway 2020 and UK 2019.

$\iota_{electricity}^{subst.byp}$ is the job factor for direct jobs lost by the substitution of electricity. The factor is based on the *direct jobs* associated with the total electricity production of Germany in 2019. The calculation of the direct jobs related to electricity production is based on the total employees in the electric energy supply weighted by the electricity price composition (share of production costs).

$$\iota_{electricity}^{subst.byp} = \frac{Employees\ in\ electric\ energy\ supply * production\ cost\ share}{Electic\ endenergy\ consumption}$$

Table C 6: Value and references for the calculation of the lost jobs by substation

	Description	Unit	Value	Source
Fossil fuel	Direct jobs in the oil and gas sector (Norway 2020)	jobs	57.700	(norwegianpetroleum, 2021)
	Oil equivalent oil and gas production (Norway 2020)	m^3	$226{,}5x10^6$	(norwegianpetroleum, 2021)
	Direct jobs in the oil and gas sector (UK 2019)	jobs	40.000	(UKEITI, 2021)
	Oil equivalent oil and gas production (UK 2019)	m^3	$104{,}7x10^6$	(UKEITI, 2021)
	Total jobs in the oil refining sector (GER 2017)	jobs	25.000	(Schmid et al., 2019)
	Total production in oil refining sector (GER 2017)	Tons	$105x10^6$	(Schmid et al., 2019)
	Specific job factor associated with mining, production, and refining of oil	jobs/ ton petrol	$6{,}09x10^{-4}$	Calculatory jobs factor
Electricity	Employees in electricity energy supply (GER 2019)	Jobs	215.176	(DESTATIS, 2021)
	Electricity price composition - production	%	24,10	(Strom-Report, 2021)
	Electricity price composition - transmission network	%	24,50	(Strom-Report, 2021)
	Electricity price composition - taxes, fees, reallocation charge	%	51,40	(Strom-Report, 2021)
	Direct jobs in electric energy production (GER2019)	jobs	106.702,5	Calculatory jobs
	kWh end energy consumption electricity in (GER 2019)	kWh	$569x10^9$	(Hein et al., 2020)
	Specific job factor associated with electricity supply	jobs/kWh	$1{,}88x10^{-7}$	Calculatory job factor
Nat. gas	m^3 natural gas per 1 m^3 oil eq.		$9{,}84x10^2$	(bp, no date)
	Specific job factors for mining and production of natural gas	Jobs/m^3	$3{,}28x10^{-7}$	Calculatory job factor

The values of $\tilde{v}$, $\ddot{v}_q$, and $\bar{v}$ (and their derivatives) were derived from the Life Cycle Inventories of chapter 5 (see Appendix D.2). This was done by removing those technosphere inputs that arguably do not take place regionally. In this way, only those LCI elements that occur (or comprise LCI elements that occur) in the same region remained. The Life Cycle Inventory itself is detailed in Appendix B.3 (reasoning and qualitative description) and Appendix D.2 (inputs and outputs incl. values). The exclusion of non-regional elements for the determination of $\tilde{v}$, $\ddot{v}_q$, and $\bar{v}$ is documented in Supporting Information S2 (Data 3b) of this work.

C.3 Social objective functions

Table C 7: Formulation of decision expressions of social objective functions ***SOF1***, ***SOF6***, ***SOF7***, and ***SOF7b*** (basic quantity: jobs)

Decision expression	**Formulation**
	$maximize\ SOF1$ (Local employment)
$refinery\ installation$	$= \sum_{r\in R}\sum_{c\in C} B_{r,c}\ \iota_c^{const}\ \xi_r^{ump}$
$refinery\ personnel$	$+ \sum_{r\in R}\sum_{c\in C}\ (B_{r,c}\ \iota_{c-1}^{pers} + C_{r,c}\frac{\iota_c^{pers} - \iota_{c-1}^{pers}}{\sigma_c - \sigma_{c-1}})\ \xi_r^{ump}$
$feedstock\ provison$	$+ (\sum_{r\in R}\sum_{m\in M}\sum_{f\in F}\sum_{t\in T} F_{r,m,f,t}^{in}\ \iota^{feedstock}\ \xi_r^{ump}$ $+ \sum_{r\in R}\sum_{s\in R}\sum_{f\in F}\sum_{t\in T} F_{r,s,f,t}^{out}\ \iota^{feedstock}\ \xi_r^{ump})$
$feedstock\ collection\ fixed$	$+ (\sum_{r\in R}\sum_{m\in M}\sum_{f\in F}\sum_{t\in T} F_{r,m,f,t}^{in}\ \iota_{r,t}^{f.t.feed}\ \xi_r^{ump}$ $+ \sum_{r\in R}\sum_{s\in R}\sum_{f\in F}\sum_{t\in T} F_{r,s,f,t}^{out}\ \iota_{s,t}^{f.t.feed}\ \xi_s^{ump})$
$feedstock\ collection\ var.$	$+ (\sum_{r\in R}\sum_{m\in M}\sum_{f\in F}\sum_{t\in T} 2\ F_{r,m,f,t}^{in}\ \upsilon_m\ \rho\ \tau_r\ \iota_{r,t}^{v.t.feed}\ \xi_r^{ump}$ $+ \sum_{r\in R}\sum_{s\in R}\sum_{f\in F}\sum_{t\in T} 2\ F_{r,s,f,t}^{out}\ \delta_{r,s}\ \iota_{s,t}^{v.t.feed}\ \xi_s^{ump})$
$EtOH\ distribution\ fixed$	$+ \sum_{r\in R}\sum_{s\in R}\sum_{t\in T}\ (P_{r,s,t}^{1G} + P_{r,s,t}^{FF})\ \iota_{r,t}^{f.t.etoh}\ \xi_r^{ump}$
$EtOH\ distribution\ var.$	$+ \sum_{r\in R}\sum_{s\in R}\sum_{t\in T} 2\ (P_{r,s,t}^{1G} + P_{r,s,t}^{FF})\ \delta_{r,s}\ \iota_{r,t}^{v.t.etoh}\ \xi_r^{ump}$
$substitution\ (1G)$	$- \sum_{r\in R}\sum_{s\in R}\sum_{t\in T} P_{r,s,t}^{1G}\ \iota^{subst.1G}\ \chi_s^{ump,1G}$
$substitution\ (FF)$	$- \sum_{r\in R}\sum_{s\in R}\sum_{t\in T} P_{r,s,t}^{FF}\ \iota^{subst.FF}\ \chi_s^{ump,FF}$
$substitution\ (by\text{-}products)$	$- \sum_{r\in R}\sum_{s\in R}\sum_{t\in T}\sum_{p\in P}\ \ (P_{r,s,t}^{1G} + P_{r,s,t}^{FF})\ \theta_p^{byp}\ \iota_p^{subst.byp}\ \chi_{r,p}^{ump,byp}$

Table continued

$maximize\ SOF6$ (Fair salary)	$maximize\ SOF7$[1] (Workers' health & safety – injuries)
$= \sum_{r\in R}\sum_{c\in C} B_{r,c}\ \iota_c^{const}\ \xi_r^{wage,cns}$	$= -\sum_{r\in R}\sum_{c\in C} B_{r,c}\ \iota_c^{const}\ \xi_r^{lda,F41}$
$+ \sum_{r\in R}\sum_{c\in C}\ (B_{r,c}\ \iota_{c-1}^{pers} + C_{r,c}\frac{\iota_c^{pers} - \iota_{c-1}^{pers}}{\sigma_c - \sigma_{c-1}})\ \xi_r^{wage,chm}$	$- \sum_{r\in R}\sum_{c\in C}\ (B_{r,c}\ \iota_{c-1}^{pers} + C_{r,c}\frac{\iota_c^{pers} - \iota_{c-1}^{pers}}{\sigma_c - \sigma_{c-1}})\ \xi_r^{lda,C20}$
$+ (\sum_{r\in R}\sum_{m\in M}\sum_{f\in F}\sum_{t\in T} F_{r,m,f,t}^{in}\ \iota^{feedstock}\ \xi_{r,f}^{wage,feed}$ $+ \sum_{r\in R}\sum_{s\in R}\sum_{f\in F}\sum_{t\in T} F_{r,s,f,t}^{out}\ \iota^{feedstock}\ \xi_{r,f}^{wage,feed})$	$- (\sum_{r\in R}\sum_{m\in M}\sum_{f\in F}\sum_{t\in T} F_{r,m,f,t}^{in}\ \iota^{feedstock}\ \xi_r^{lda,A01}$ $+ \sum_{r\in R}\sum_{s\in R}\sum_{f\in F}\sum_{t\in T} F_{r,s,f,t}^{out}\ \iota^{feedstock}\ \xi_r^{lda,A01})$
$+ (\sum_{r\in R}\sum_{m\in M}\sum_{f\in F}\sum_{t\in T} F_{r,m,f,t}^{in}\ \iota_{r,t}^{f.t.feed}\ \xi_r^{wage,otp}$ $+ \sum_{r\in R}\sum_{s\in R}\sum_{f\in F}\sum_{t\in T} F_{r,s,f,t}^{out}\ \iota_{s,t}^{f.t.feed}\ \xi_s^{wage,otp})$	$- (\sum_{r\in R}\sum_{m\in M}\sum_{f\in F}\sum_{t\in T} F_{r,m,f,t}^{in}\ \iota_{r,t}^{f.t.feed}\ \xi_r^{lda,H49}$ $+ \sum_{r\in R}\sum_{s\in R}\sum_{f\in F}\sum_{t\in T} F_{r,s,f,t}^{out}\ \iota_{s,t}^{f.t.feed}\ \xi_s^{lda,H49})$
$+ (\sum_{r\in R}\sum_{m\in M}\sum_{f\in F}\sum_{t\in T} 2\ F_{r,m,f,t}^{in}\ \upsilon_m \rho\tau_r\ \iota_{r,t}^{v.t.feed}\ \xi_r^{wage,otp}$ $+ \sum_{r\in R}\sum_{s\in R}\sum_{f\in F}\sum_{t\in T} 2\ F_{r,s,f,t}^{out}\ \delta_{r,s}\ \iota_{s,t}^{v.t.feed}\ \xi_s^{wage,otp})$	$- (\sum_{r\in R}\sum_{m\in M}\sum_{f\in F}\sum_{t\in T} 2\ F_{r,m,f,t}^{in}\ \upsilon_m\ \rho\ \tau_r\ \iota_{r,t}^{v.t.feed}\ \xi_r^{lda,H49}$ $+ \sum_{r\in R}\sum_{s\in R}\sum_{f\in F}\sum_{t\in T} 2\ F_{r,s,f,t}^{out}\ \delta_{r,s}\ \iota_{s,t}^{v.t.feed}\ \xi_s^{lda,H49})$
$+ \sum_{r\in R}\sum_{s\in R}\sum_{t\in T}\ (P_{r,s,t}^{1G} + P_{r,s,t}^{FF})\ \iota_{r,t}^{f.t.etoh}\xi_r^{wage,otp}$	$- \sum_{r\in R}\sum_{s\in R}\sum_{t\in T}\ (P_{r,s,t}^{1G} + P_{r,s,t}^{FF})\ \iota_{r,t}^{f.t.etoh}\ \xi_r^{lda,H49}$
$+ \sum_{r\in R}\sum_{s\in R}\sum_{t\in T} 2\ (P_{r,s,t}^{1G} + P_{r,s,t}^{FF})\ \delta_{r,s}\ \iota_{r,t}^{v.t.etoh}\ \xi_r^{wage,otp}$	$- \sum_{r\in R}\sum_{s\in R}\sum_{t\in T} 2\ (P_{r,s,t}^{1G} + P_{r,s,t}^{FF})\ \delta_{r,s}\ \iota_{r,t}^{v.t.etoh}\ \xi_r^{lda,H49}$
$- \sum_{r\in R}\sum_{s\in R}\sum_{t\in T} P_{r,s,t}^{1G}\ \iota^{subst.1G}\ \chi_s^{wage,1G}$	$+ \sum_{r\in R}\sum_{s\in R}\sum_{t\in T} P_{r,s,t}^{1G}\ \iota^{subst.1G}\ \chi_s^{lda,1G}$
$- \sum_{r\in R}\sum_{s\in R}\sum_{t\in T} P_{r,s,t}^{FF}\ \iota^{subst.FF}\ \chi_s^{wage,FF}$	$+ \sum_{r\in R}\sum_{s\in R}\sum_{t\in T} P_{r,s,t}^{FF}\ \iota^{subst.FF}\ \chi_s^{lda,FF}$
$- \sum_{r\in R}\sum_{s\in R}\sum_{t\in T}\sum_{p\in P}\ \ (P_{r,s,t}^{1G} + P_{r,s,t}^{FF})\ \theta_p^{byp}\ \iota_p^{subst.byp}\ \chi_{r,p}^{wage,byp}$	$+ \sum_{r\in R}\sum_{s\in R}\sum_{t\in T}\sum_{p\in P}\ \ (P_{r,s,t}^{1G} + P_{r,s,t}^{FF})\ \theta_p^{byp}\ \iota_p^{subst.byp}\ \chi_{r,p}^{lda,byp}$

[1] Analogously for $SOF7b$ (Workers' health & safety – fatalities) with $\xi_r^{lla,i}$ and $\chi_r^{lda,i}$ in place of $\xi_r^{lda,i}$ and $\chi_r^{lda,i}$.

Table C 8: Formulation of decision expressions of social objective functions
SOF2, ***SOF3***, and ***SOF4*** (basic quantity: local water use, local air emissions, local land occupation)

Decision expression	**Formulation**
	$SOF2$ (Water use)
$refinery\ installation$	$= \sum_{r\in R}\sum_{c\in C} B_{r,c}\ \tilde{v}_c^{const}\ \xi_r^{water}$
$refinery\ processes$	$+ \sum_{r\in R}\sum_{s\in R}\sum_{t\in T}\ \left(P_{r,s,t}^{1G} + P_{r,s,t}^{FF}\right)\tilde{v}_t^{f.t.etoh}\ \xi_r^{water}$
$feedstock\ provison$	$+ (\sum_{r\in R}\sum_{m\in M}\sum_{f\in F}\sum_{t\in T} F_{r,m,f,t}^{in}\ \tilde{v}_f^{feedstock}\ \xi_r^{water}$
	$+ \sum_{r\in R}\sum_{s\in R}\sum_{f\in F}\sum_{t\in T} F_{r,s,f,t}^{out}\ \tilde{v}_f^{feedstock}\ \xi_r^{water})$
$feedstock\ collection\ fixed$	$+ (\sum_{r\in R}\sum_{m\in M}\sum_{f\in F}\sum_{t\in T} F_{r,m,f,t}^{in}\tilde{v}_t^{f.t.feed}\ \xi_r^{water}$
	$+ \sum_{r\in R}\sum_{s\in R}\sum_{f\in F}\sum_{t\in T} F_{r,s,f,t}^{out}\ \tilde{v}_t^{f.t.feed}\ \xi_s^{water})$
$feedstock\ collection\ var.$	$+ (\sum_{r\in R}\sum_{m\in M}\sum_{f\in F}\sum_{t\in T} 2\ F_{r,m,f,t}^{in}\ v_m\ \rho\ \tau_r\ \tilde{v}_t^{v.t.feed}\ \xi_r^{water}$
	$+ \sum_{r\in R}\sum_{s\in R}\sum_{f\in F}\sum_{t\in T} 2\ F_{r,s,f,t}^{out}\ \delta_{r,s}\ \tilde{v}_t^{v.t.feed}\ \xi_s^{water})$
$EtOH\ distribution\ fixed$	$+ \sum_{r\in R}\sum_{s\in R}\sum_{t\in T}\ \left(P_{r,s,t}^{1G} + P_{r,s,t}^{FF}\right)\tilde{v}_t^{f.t.etoh}\ \xi^{water,EU}$
$EtOH\ distribution\ var.$	$+ \sum_{r\in R}\sum_{s\in R}\sum_{t\in T} 2\left(P_{r,s,t}^{1G} + P_{r,s,t}^{FF}\right)\delta_{r,s}\ \tilde{v}_t^{v.t.etoh}\ \xi^{water,EU}$

Table continued

$SOF3$ (Living conditions)	$SOF4$ (Land/food conflict)
$= \sum_{r\in R}\sum_{c\in C}\sum_{q\in Q} B_{r,c}\ \ddot{v}_{c,q}^{const}\ \xi_{r,q}^{air}$	$= \sum_{r\in R}\sum_{c\in C} B_{r,c}\ \bar{v}_c^{const}\ \xi_r^{land}$
$+ \sum_{r\in R}\sum_{s\in R}\sum_{t\in T}\sum_{q\in Q}\ \left(P_{r,s,t}^{1G} + P_{r,s,t}^{FF}\right)\ddot{v}_q^{var}\ \xi_{r,q}^{air}$	$+ \sum_{r\in R}\sum_{s\in R}\sum_{t\in T}\ \left(P_{r,s,t}^{1G} + P_{r,s,t}^{FF}\right)\bar{v}^{var}\ \xi_r^{land}$
$+ (\sum_{r\in R}\sum_{m\in M}\sum_{f\in F}\sum_{t\in T}\sum_{q\in Q} F_{r,m,f,t}^{in}\ \ddot{v}_{f,q}^{feedstock}\ \xi_{r,q}^{air}$	$+ (\sum_{r\in R}\sum_{m\in M}\sum_{f\in F}\sum_{t\in T} F_{r,m,f,t}^{in}\ \bar{v}_f^{feedstock}\ \xi_r^{land}$
$+ \sum_{r\in R}\sum_{s\in R}\sum_{f\in F}\sum_{t\in T}\sum_{q\in Q} F_{r,s,f,t}^{out}\ \ddot{v}_{f,q}^{feedstock}\ \xi_{r,q}^{air})$	$+ \sum_{r\in R}\sum_{s\in R}\sum_{f\in F}\sum_{t\in T} F_{r,s,f,t}^{out}\ \bar{v}_f^{feedstock}\ \xi_r^{land})$
$+ (\sum_{r\in R}\sum_{m\in M}\sum_{f\in F}\sum_{t\in T}\sum_{q\in Q} F_{r,m,f,t}^{in}\ \ddot{v}_{t,q}^{f.t.feed}\ \xi_{r,q}^{air}$	$+ (\sum_{r\in R}\sum_{m\in M}\sum_{f\in F}\sum_{t\in T} F_{r,m,f,t}^{in}\ \bar{v}_t^{f.t.feed}\ \xi_r^{land}$
$+ \sum_{r\in R}\sum_{s\in R}\sum_{f\in F}\sum_{t\in T}\sum_{q\in Q} F_{r,s,f,t}^{out}\ \ddot{v}_{t,q}^{f.t.feed}\ \xi_{s,q}^{air})$	$+ \sum_{r\in R}\sum_{s\in R}\sum_{f\in F}\sum_{t\in T} F_{r,s,f,t}^{out}\ \bar{v}_t^{f.t.feed}\ \xi_s^{land})$
$+ (\sum_{r\in R}\sum_{m\in M}\sum_{f\in F}\sum_{t\in T}\sum_{q\in Q} 2\ F_{r,m,f,t}^{in}\ v_m\ \rho\ \tau_r\ \ddot{v}_{t,q}^{v.t.feed}\ \xi_{r,q}^{air}$	$+ (\sum_{r\in R}\sum_{m\in M}\sum_{f\in F}\sum_{t\in T} 2\ F_{r,m,f,t}^{in}\ v_m\ \rho\ \tau_r\ \bar{v}_t^{v.t.feed}\ \xi_r^{land}$
$+ \sum_{r\in R}\sum_{s\in R}\sum_{f\in F}\sum_{t\in T}\sum_{q\in Q} 2\ F_{r,s,f,t}^{out}\ \delta_{r,s}\ \ddot{v}_{t,q}^{v.t.feed}\ \xi_{s,q}^{air})$	$+ \sum_{r\in R}\sum_{s\in R}\sum_{f\in F}\sum_{t\in T} 2\ F_{r,s,f,t}^{out}\ \delta_{r,s}\ \bar{v}_t^{v.t.feed}\ \xi_s^{land})$
$+ \sum_{r\in R}\sum_{s\in R}\sum_{t\in T}\sum_{q\in Q}\ \left(P_{r,s,t}^{1G} + P_{r,s,t}^{FF}\right)\ddot{v}_{t,q}^{f.t.etoh}\ \xi_q^{air,EU}$	$+ \sum_{r\in R}\sum_{s\in R}\sum_{t\in T}\ \left(P_{r,s,t}^{1G} + P_{r,s,t}^{FF}\right)\bar{v}_t^{f.t.etoh}\ \xi^{land,EU}$
$+ \sum_{r\in R}\sum_{s\in R}\sum_{t\in T}\sum_{q\in Q} 2\left(P_{r,s,t}^{1G} + P_{r,s,t}^{FF}\right)\delta_{r,s}\ \ddot{v}_{t,q}^{v.t.etoh}\ \xi_q^{air,EU}$	$+ \sum_{r\in R}\sum_{s\in R}\sum_{t\in T} 2\left(P_{r,s,t}^{1G} + P_{r,s,t}^{FF}\right)\delta_{r,s}\ \bar{v}_t^{v.t.etoh}\ \xi^{land,EU}$

Table C 9: Formulation of decision expressions of social objective functions ***SOF5*** and ***SOF8*** (basic quantity: economic value)

Decision expression	**Formulation**	
	$maximize\ SOF5$ (Economic development)	$SOF8$ (Smallholder farming)
$refinery\ installation$	$= \sum_{r\in R} \sum_{c\in C} B_{r,c}\ \kappa_c^{depr}\ \gamma_r^{inv}\ \xi_r^{GDP}$	
$refinery\ personnel$	$+ \sum_{r\in R} \sum_{c\in C}\ (B_{r,c}\ \kappa_{c-1}^{pers} + C_{r,c}\ \frac{\kappa_c^{pers} - \kappa_{c-1}^{pers}}{\sigma_c - \sigma_{c-1}})\ \gamma_r^{lab}\ \xi_r^{GDP}$	
$other\ refinery\ operation$	$+ \sum_{r\in R} \sum_{c\in C} B_{r,c}\ \kappa_c^{oper}\ \xi_r^{GDP}$	
$refinery\ processes$	$+ \sum_{r\in R} \sum_{s\in R} \sum_{t\in T} \left(P_{r,s,t}^{1G} + P_{r,s,t}^{FF}\right) \kappa^{var}\ \xi_r^{GDP}$	
$feedstock\ provison$	$+ (\sum_{r\in R} \sum_{m\in M} \sum_{f\in F} \sum_{t\in T} F_{r,m,f,t}^{in}\ \varphi_{r,f}\ \xi_r^{GDP}$ $+ \sum_{r\in R} \sum_{s\in R} \sum_{f\in F} \sum_{t\in T} F_{r,s,f,t}^{out}\ \varphi_{r,f}\ \xi_r^{GDP})$	$= (\sum_{r\in R} \sum_{m\in M} \sum_{f\in F} \sum_{t\in T} F_{r,m,f,t}^{in}\ \varphi_{r,f}\ \xi_r^{shf}$ $+ \sum_{r\in R} \sum_{s\in R} \sum_{f\in F} \sum_{t\in T} F_{r,s,f,t}^{out}\ \varphi_{r,f}\ \xi_r^{shf})$
$feedstock\ collection\ fixed$	$+ (\sum_{r\in R} \sum_{m\in M} \sum_{f\in F} \sum_{t\in T} F_{r,m,f,t}^{in}\ \varepsilon_t^{fix}\ \xi_r^{GDP}$ $+ \sum_{r\in R} \sum_{s\in R} \sum_{f\in F} \sum_{t\in T} F_{r,s,f,t}^{out}\ \varepsilon_t^{fix}\ \xi_s^{GDP})$	
$feedstock\ collection\ var.$	$+ (\sum_{r\in R} \sum_{m\in M} \sum_{f\in F} \sum_{t\in T} 2\ F_{r,m,f,t}^{in}\ \varepsilon_t^{var}\ \gamma_r^{tra}\ \upsilon_m\ \rho\ \tau_r\ \xi_r^{GDP}$ $+ \sum_{r\in R} \sum_{s\in R} \sum_{f\in F} \sum_{t\in T} 2\ F_{r,s,f,t}^{out}\ \varepsilon_t^{var}\ \gamma_s^{tra}\ \delta_{r,s}\ \xi_s^{GDP})$	
$EtOH\ distribution\ fixed$	$+ \sum_{r\in R} \sum_{s\in R} \sum_{t\in T} \left(P_{r,s,t}^{1G} + P_{r,s,t}^{FF}\right) \eta_t^{fix}\ \xi_r^{GDP}$	
$EtOH\ distribution\ var.$	$+ \sum_{r\in R} \sum_{s\in R} \sum_{t\in T} 2\left(P_{r,s,t}^{1G} + P_{r,s,t}^{FF}\right) \eta_t^{var}\ \delta_{r,s}\ \xi_r^{GDP}$	
$substitution\ (1G)$	$- \sum_{r\in R} \sum_{s\in R} \sum_{t\in T} P_{r,s,t}^{1G}\ \alpha_s^{1G}\ \chi_s^{GDP,1G}$	
$substitution\ (FF)$	$- \sum_{r\in R} \sum_{s\in R} \sum_{t\in T} P_{r,s,t}^{FF}\ \alpha_s^{FF}\ \chi_s^{GDP,FF}$	
$substitution\ (by\text{-}products)$	$- \sum_{r\in R} \sum_{s\in R} \sum_{t\in T} \sum_{p\in P} \left(P_{r,s,t}^{1G} + P_{r,s,t}^{FF}\right) \alpha_{r,p}^{byp}\ \theta_p^{byp}\ \chi_r^{GDP,byp}$	

C.4 Social hotspot functions

The social hotspot functions $SHF1$ to $SHF25$ calculate the social hotspots, i.e., the risk for adverse social conditions in the global supply chain to be reinforced by the bioethanol production network. In contrast to the social objective functions, where one unit of a decision variable has distinctly positive or negative effects on its respective social indicator, the social hotspots are more ambivalent, as the existence of a risk for e.g., forced labor in a country and sector does not necessarily mean that forced labor is employed in the global upstream supply chains, but necessitates due diligence of the respective operating companies.

The risk values for each sector $i \in I$ and country (here: regions $r \in R$) are retrieved from the Social Hotspots Database (Benoît-Norris et al., 2018). The SHDB is based on the input-output model of the Global Trade Analysis Project (Aguiar et al., 2016) and uses 160 indicators and country- and sector-specific data on labor intensity to calculate social risk values in medium risk hour equivalents (mrheq) per USD2011. We convert this value to mrheq/EUR2020 (see Data Repository D.2, Data 2), the result of which is the model parameter o_r^i. For the social hotspot functions $SHF1$ to $SHF25$, this value is multiplied with the economic value (in EUR) of the various activities within the bioethanol network to calculate the accumulated risk of the respective environmentally, socially, or economically optimal network. The economic value of network activities is assumed to be equivalent to the parameters of the economic objective function (cf. $SOF5$). Values and calculation of o_r^i is given in Supporting Information S2, Data 2.

Table C 10 lists the 25 hotspot subcategories $h \in H$, for which social hotspot functions exist, as well as their respective top categories in the SHDB. Table 19 details the mathematical formulation of the SHFs in the model. Due to their aforementioned parameter-wise relation with the economic objective function, the calculation is based on the latter.

Table C 10: Social hotpots functions (SHDB subcategories)
and corresponding, aggregating SHDB categories (Benoît-Norris et al., 2018)

Function	SHDB Subcategory	SHDB Category	Unit
*SHF*1	Wage assessment	Labor rights & decent work	mrheq
*SHF*2	Poverty	Labor rights & decent work	mrheq
*SHF*3	Child labor	Labor rights & decent work	mrheq
*SHF*4	Forced labor	Labor rights & decent work	mrheq
*SHF*5	Excessive overtime	Labor rights & decent work	mrheq
*SHF*6	Freedom of association, collective bargaining, and right to strike	Labor rights & decent work	mrheq
*SHF*7	Migrant workers	Labor rights & decent work	mrheq
*SHF*8	Social benefits	Labor rights & decent work	mrheq
*SHF*9	Labor laws & conventions	Labor rights & decent work	mrheq
*SHF*10	Discrimination and equal opportunities	Labor rights & decent work	mrheq
*SHF*11	Unemployment	Labor rights & decent work	mrheq
*SHF*12	Occupational toxics and hazards	Health & safety	mrheq
*SHF*13	Occupational injuries and deaths	Health & safety	mrheq
*SHF*14	Indigenous rights	Human rights	mrheq
*SHF*15	Gender equity	Human rights	mrheq
*SHF*16	High conflict	Human rights	mrheq
*SHF*17	Human health, non-communicable and health issues	Human rights	mrheq
*SHF*18	Human health: communicable diseases	Human rights	mrheq
*SHF*19	Legal system	Governance	mrheq
*SHF*20	Corruption	Governance	mrheq
*SHF*21	Access to improved drinking water source	Community	mrheq
*SHF*22	Access to improved sanitation	Community	mrheq
*SHF*23	Children out of school	Community	mrheq
*SHF*24	Hospital bed access	Community	mrheq
*SHF*25	Smallholder vs. commercial farms	Community	mrheq
*SHF*1-11	Labor rights & decent work	-	pts
*SHF*12-13	Health & safety	-	pts
*SHF*14-18	Human rights	-	pts
*SHF*19-20	Governance	-	pts
*SHF*21-25	Community	-	pts

C.5 Results

The sheets Results 1 - Results 4 of D.3 provide the numerical results on which the results sections of this Appendix C and the chapter 6 are based. The actual data used in the figures are also explicitly listed on the sheets "Figure data (manuscript)" and "Figure Data (S1)".

Category relevance

Each midpoint contributes to its respective endpoint differently. These contributions result from the parameters used (resulting from Life Cycle Inventories and Life Cycle Impact Assessment) and decisions taken in this application case on the one hand, and the aggregation factors between midpoints/endpoints given by the ReCiPe 2016 method on the other hand. For example, for optimization of SOF7, the values of the midpoints *mineral resource scarcity* (M16) and *fossil resource scarcity* (M17) are (in the unit of their respective endpoint *resource scarcity* (E3)) $|-1.73\times10^{6}|$ and $|6.63\times10^{8}|$ USD2013 respectively, the sum of magnitudes of all contributions to E3 is 6.65×10^{8} USD2013, which means a relative contribution by M16 and M17 of −0.26% and 99.74% respectively to the endpoint value. Fig. C 1 shows the relative contribution of each midpoint to its respective endpoint (i.e., to the total of magnitudes of relative contributions) over all economic, environmental, and social optimization runs.

In our opinion, this provides a reasonable estimate of the relevance of each midpoint/subcategory in this application case and a set of midpoints on which this work should focus. The main body of this work thus includes only those environmental categories that contribute at least 10% (positively or negatively) to the respective endpoint in any optimization run. These are most notably *global warming* (M1), *fine particulate matter formation* (M5), *land use* (M15), and *fossil resource scarcity* (M17). However, the latter is almost identical to its endpoint *resource availability* (E3) and thus not displayed separately.

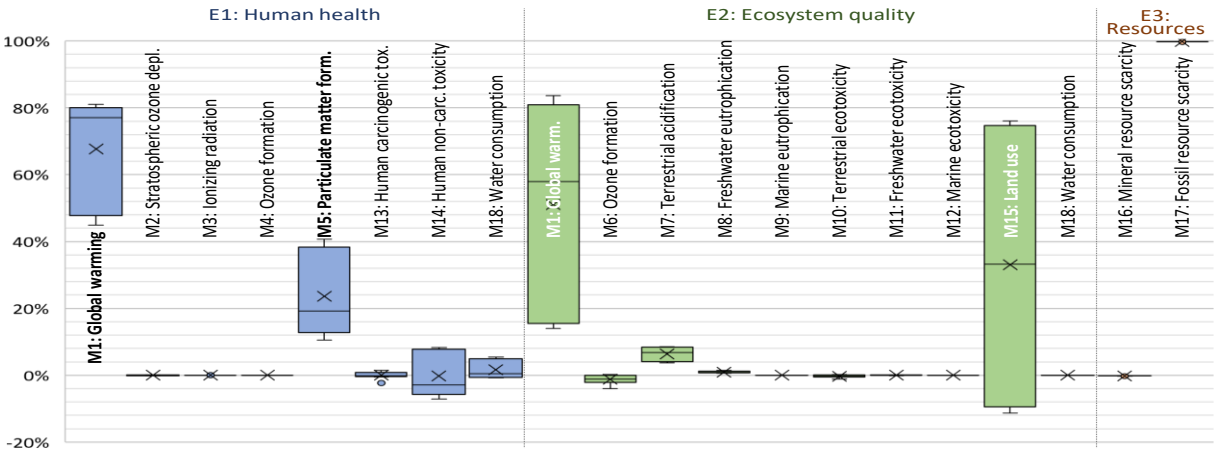

Fig. C 1: Relative contribution of each midpoint to the respective endpoint over all optimizations (i.e., share of midpoints to the sum of magnitudes of contributions to respective endpoints)

Fig. C 2 shows similar results for the SHFs (SHDB subcategories) but in absolute values (mrheq per metric ton of 2G EtOH produced). The SHDB subcategories belong to the five categories *Labor rights & decent work*, *Health & safety*, *Human rights*, *Governance*, and *Community*. For the SHFs, the question of relevance is more intricate. Not only are their values negative (meaning an overall risk increase due to network activities) in the vast majority of optimization runs, but also are the differences in the magnitudes much less pronounced between the categories. SHF4, SHF6, SHF10, SHF12, SHF13, SHF16, SHF20, SHF23, and SHF25 are the most important (see Fig. 42 of chapter 6.2.3). When evaluating the relevance of subcategories within their respective superordinate category, SHF16 (*High conflict zones*) dominates its category *Human rights* most markedly. Notably, SHF21 (*Access to drinking water*) is the only subcategory with positive values in about half of the optimization runs (meaning an overall risk reduction due to substitution), however, only in small magnitudes.

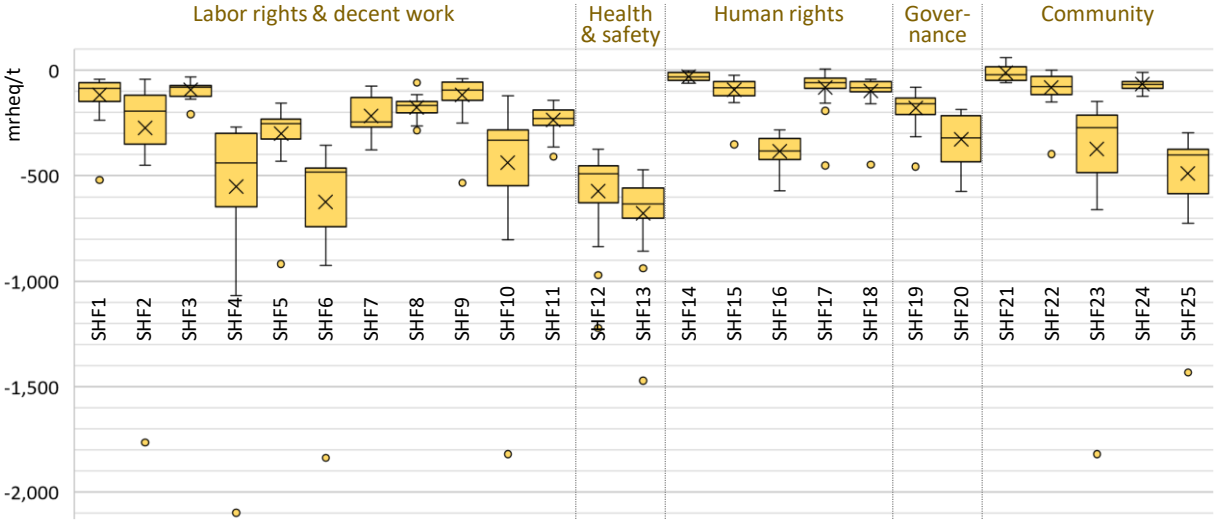

Fig. C 2: Result (in mrheq per ton 2G EtOH) in each SHF (SHDB subcategory) over all optimization runs

Feedstock sourced

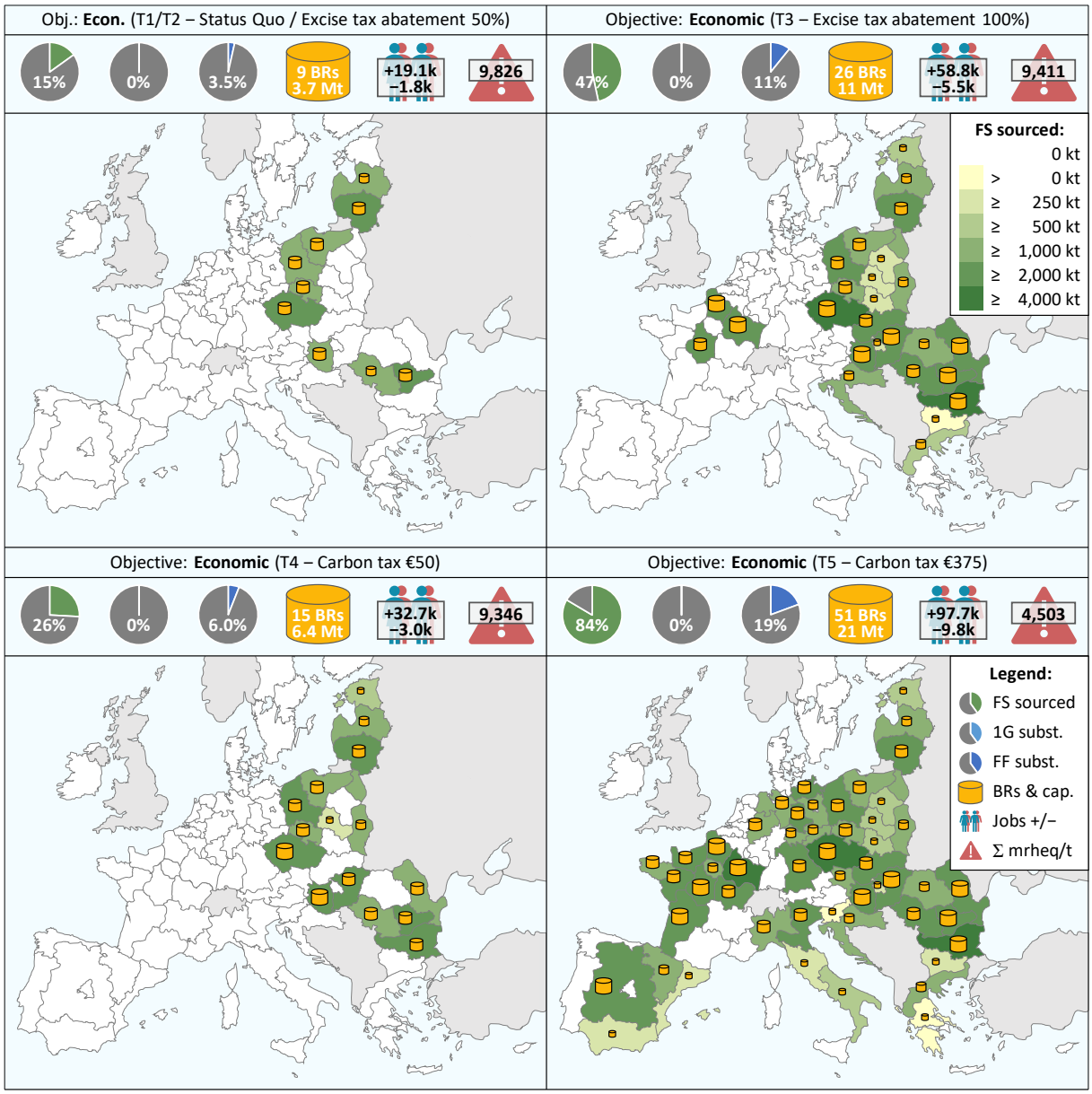

Fig. C 3: Feedstock sourced: Economically optimal biorefinery location and capacity (the size of cylinders corresponds to the capacity) and regional amounts of feedstock sourced (green shades, in metric kilotons) for economic objectives in five tax scenarios (with identical networks for T1 and T2). The legend also includes respective percentages of total feedstock collected (FS sourced), the percentage of 1G demand substituted, the percentage of fossil petrol demand substituted (subst. 1G and subst. FF, pie charts), the total number and total capacity of biorefineries (BRs & cap.), the net number of jobs added, as well as the total risk increase over all SHDB categories (in pts per ton)

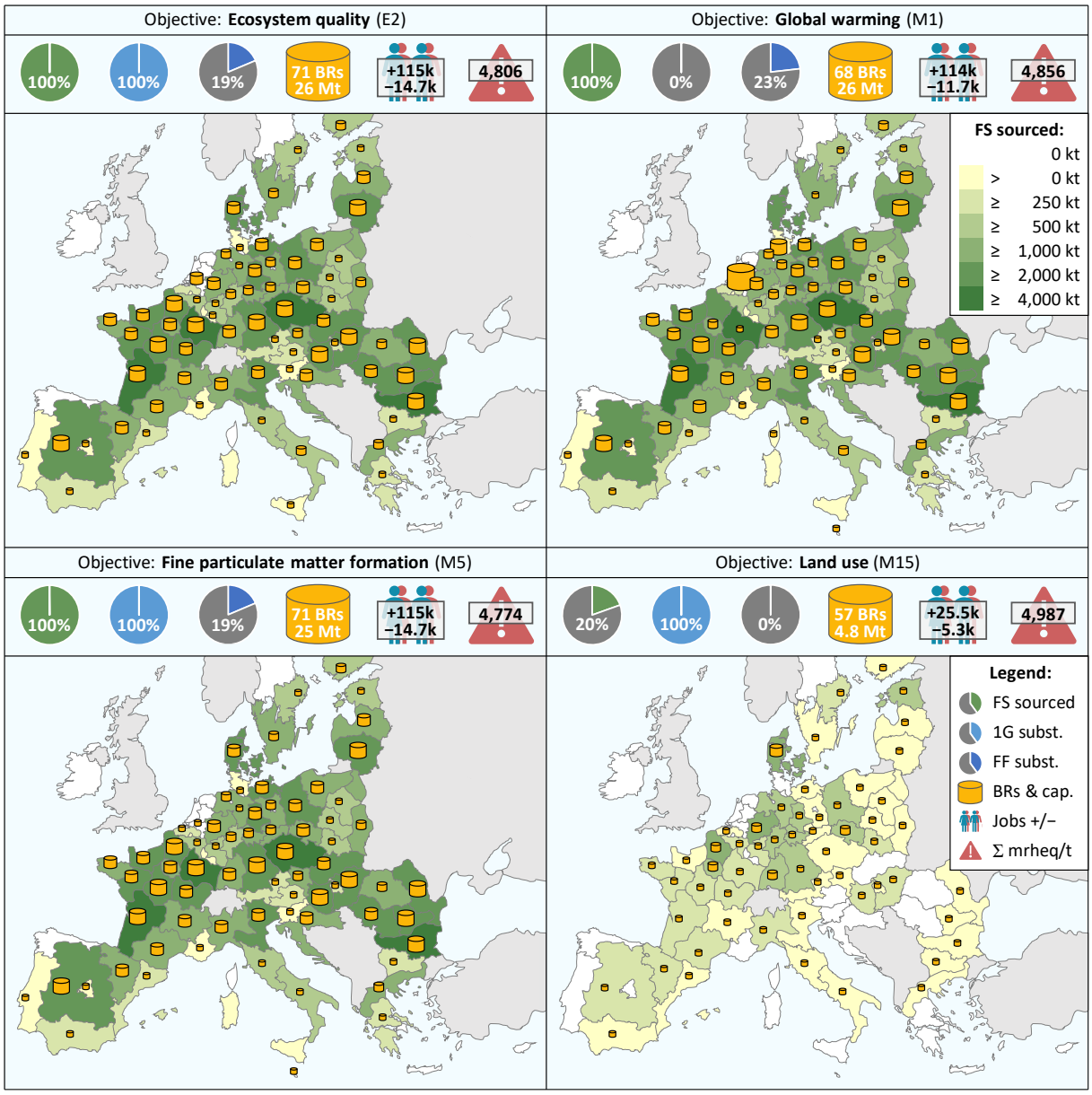

Fig. C 4: Feedstock sourced: Environmentally optimal biorefinery location and capacity (the size of cylinders corresponds to the capacity) and regional amounts of feedstock sourced (green shades, in metric kilotons) for four environmental objectives (endpoint *ecosystem quality* and three of the most relevant midpoints, see section 0). The legend also includes respective percentages of total feedstock collected (FS sourced), the percentage of 1G demand substituted, the percentage of fossil petrol demand substituted (subst. 1G and subst. FF, pie charts), the total number and total capacity of biorefineries (BRs & cap.), the net number of jobs added, as well as the total risk increase over all SHDB categories (in pts per ton)

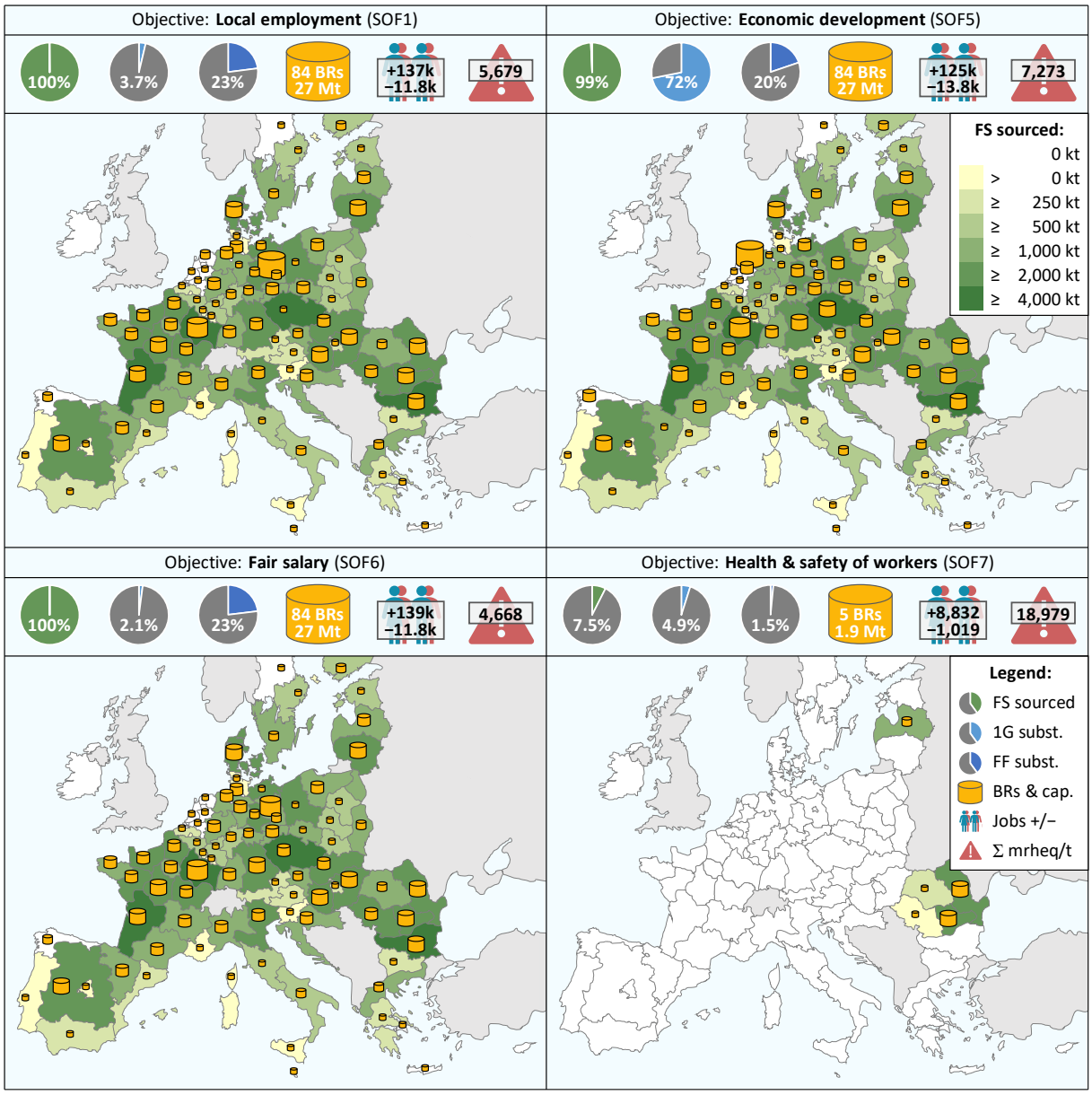

Fig. C 5: Feedstock sourced: Socially optimal biorefinery location and capacity (the size of cylinders corresponds to the capacity) and regional amounts of feedstock sourced (green shades, in metric kilotons) for four social objectives. The legend also includes respective percentages of total feedstock collected (FS sourced), the percentage of 1G demand substituted, the percentage of fossil petrol demand substituted (subst. 1G and subst. FF, pie charts), the total number and total capacity of biorefineries (BRs & cap.), the net number of jobs added, as well as the total risk increase over all SHDB categories (in pts per ton)

Jobs created

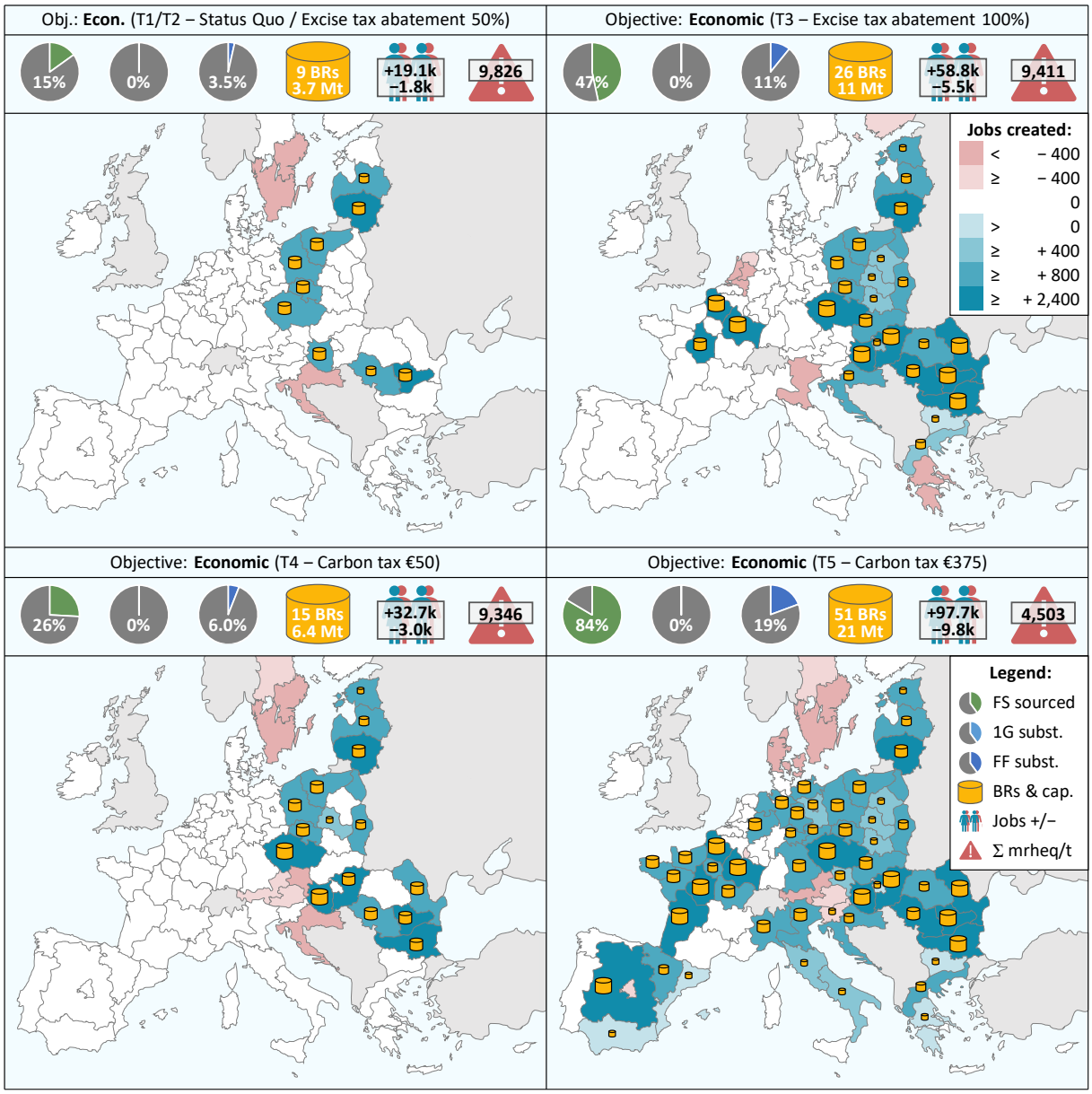

Fig. C 6: Jobs created: Economically optimal biorefinery location and capacity (the size of cylinders corresponds to the capacity) and the net number of regionally created jobs (blue/red shades) for economic objectives in five tax scenarios (with identical networks for T1 and T2). The legend also includes respective percentages of total feedstock collected (FS sourced), the percentage of 1G demand substituted, the percentage of fossil petrol demand substituted (subst. 1G and subst. FF, pie charts), the total number and total capacity of biorefineries (BRs & cap.), the net number of jobs added, as well as the total risk increase over all SHDB categories (in pts per ton)

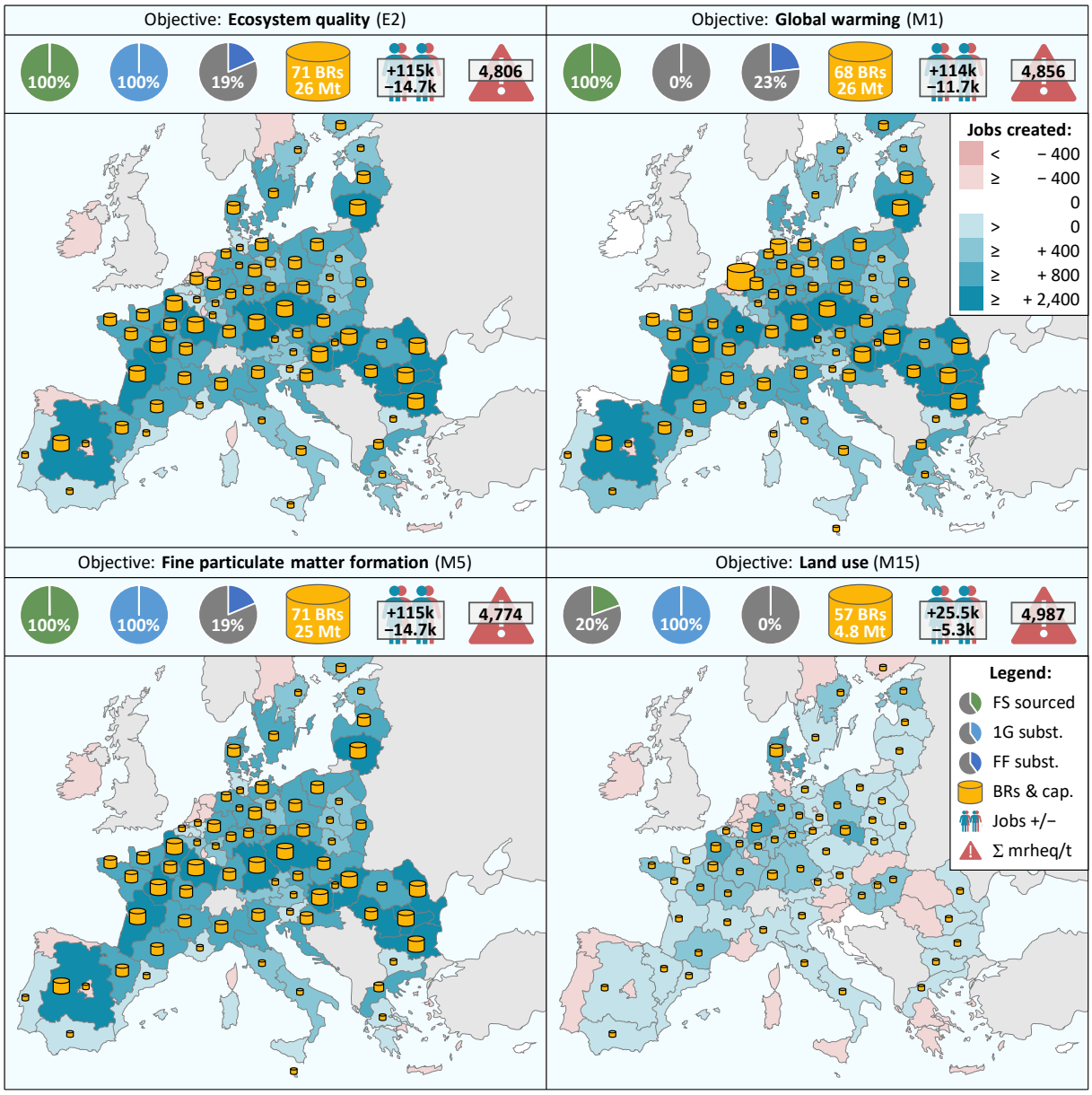

Fig. C 7: Jobs created: Environmentally optimal biorefinery location and capacity (the size of cylinders corresponds to the capacity) and the net number of regionally created jobs (blue/red shades) for four environmental objectives (endpoint *ecosystem quality* and three of the most relevant midpoints, see section 0). The legend also includes respective percentages of total feedstock collected (FS sourced), the percentage of 1G demand substituted, the percentage of fossil petrol demand substituted (subst. 1G and subst. FF, pie charts), the total number and total capacity of biorefineries (BRs & cap.), the net number of jobs added, as well as the total risk increase over all SHDB categories (in pts per ton)

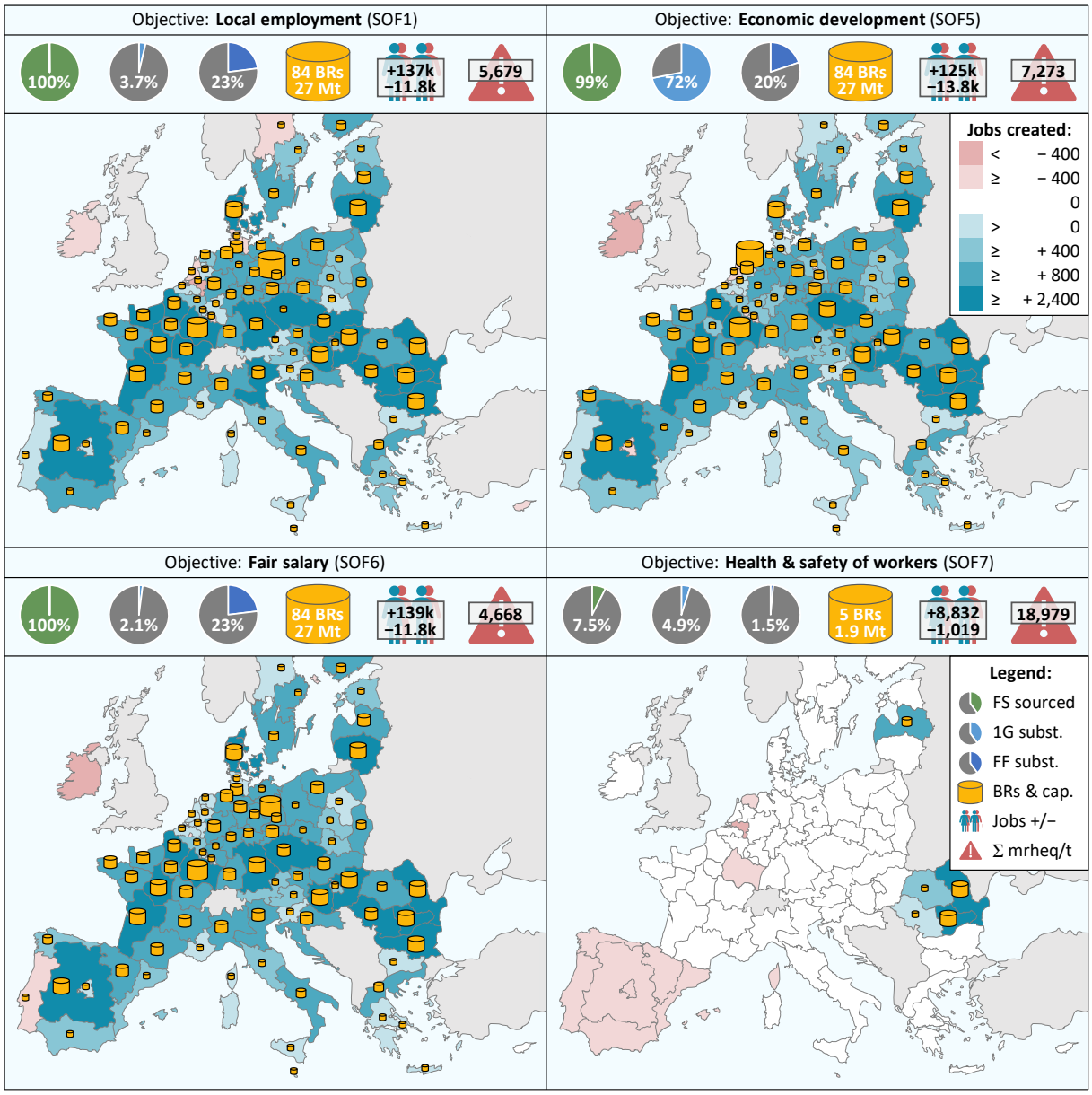

Fig. C 8: Jobs created: Socially optimal biorefinery location and capacity (the size of cylinders corresponds to the capacity) and the net number of regionally created jobs (blue/red shades) for four social objectives. The legend also includes respective percentages of total feedstock collected (FS sourced), the percentage of 1G demand substituted, the percentage of fossil petrol demand substituted (subst. 1G and subst. FF, pie charts), the total number and total capacity of biorefineries (BRs & cap.), the net number of jobs added, as well as the total risk increase over all SHDB categories (in pts per ton)

Economic value created

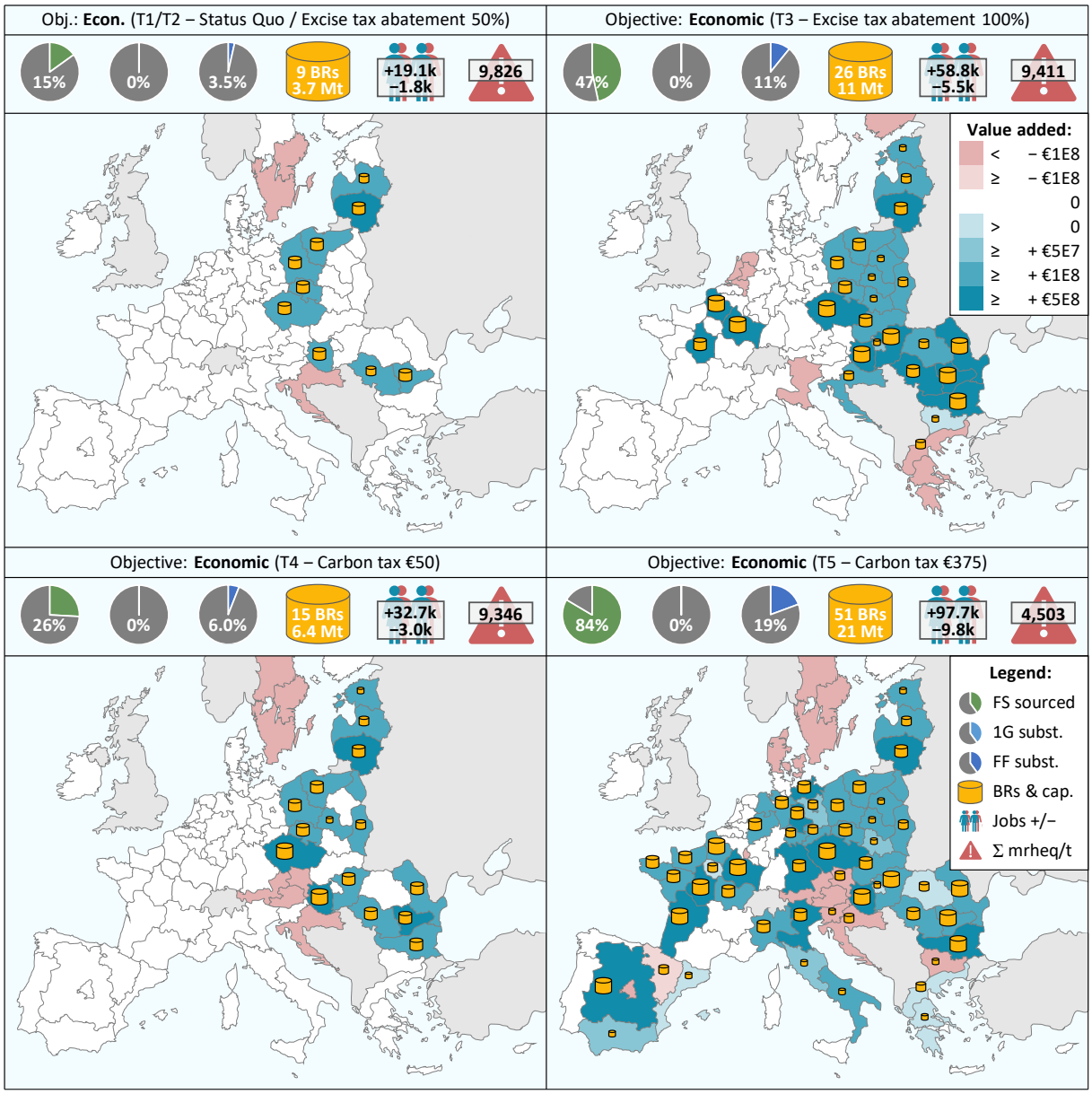

Fig. C 9: Economic value: Economically optimal biorefinery location and capacity (the size of cylinders corresponds to the capacity) and the regionally created/substituted economic value (blue/red shades) for economic objectives in five tax scenarios (with identical networks for T1 and T2). The legend also includes respective percentages of total feedstock collected (FS sourced), the percentage of 1G demand substituted, the percentage of fossil petrol demand substituted (subst. 1G and subst. FF, pie charts), the total number and total capacity of biorefineries (BRs & cap.), the net number of jobs added, as well as the total risk increase over all SHDB categories (in pts per ton)

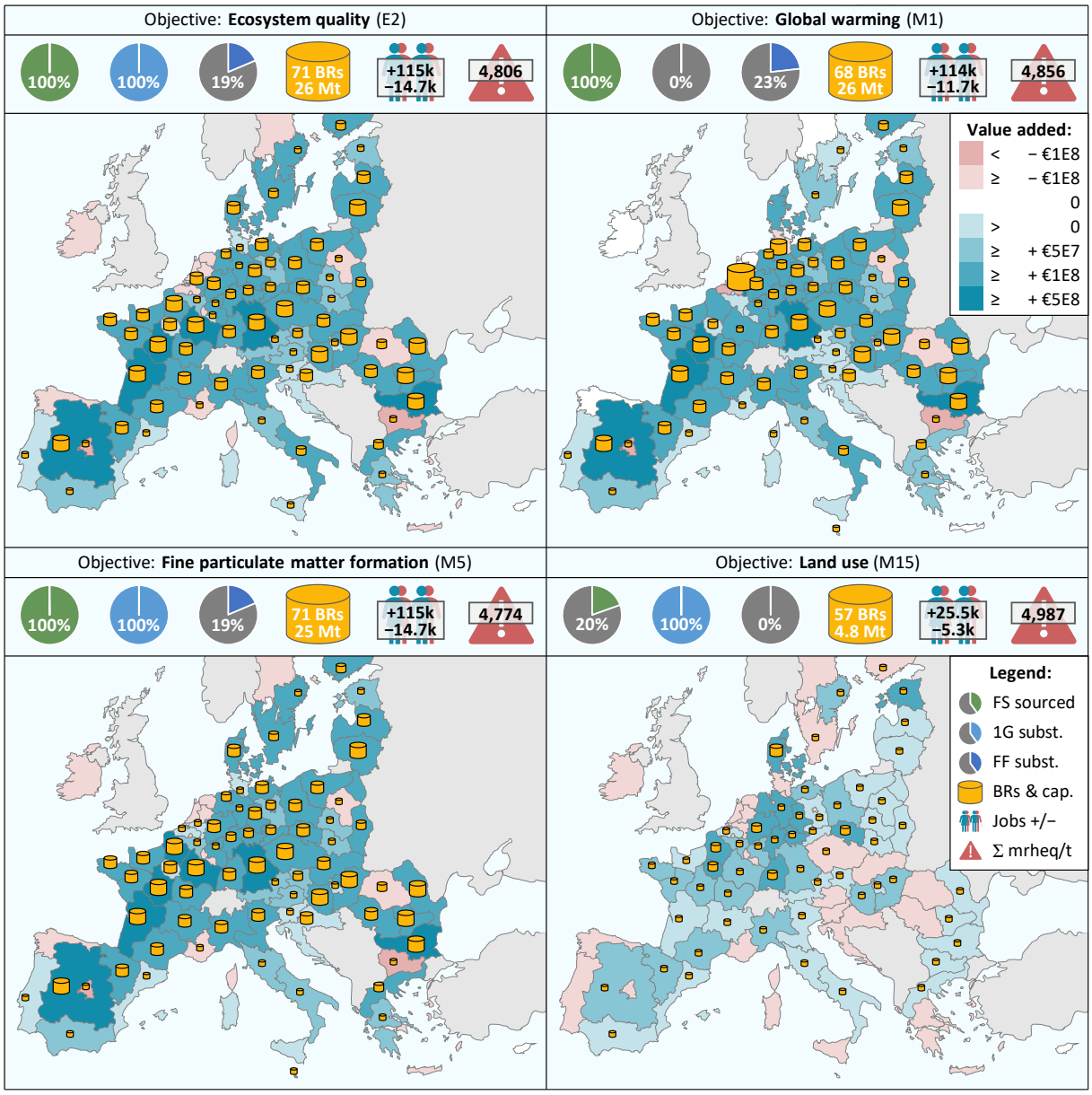

Fig. C 10: Economic value: Environmentally optimal biorefinery location and capacity (the size of cylinders corresponds to the capacity) and the regionally created/substituted economic value (blue/red shades) for four environmental objectives (endpoint *ecosystem quality* and three of the most relevant midpoints, see section 0). The legend also includes respective percentages of total feedstock collected (FS sourced), the percentage of 1G demand substituted, the percentage of fossil petrol demand substituted (subst. 1G and subst. FF, pie charts), the total number and total capacity of biorefineries (BRs & cap.), the net number of jobs added, as well as the total risk increase over all SHDB categories (in pts per ton)

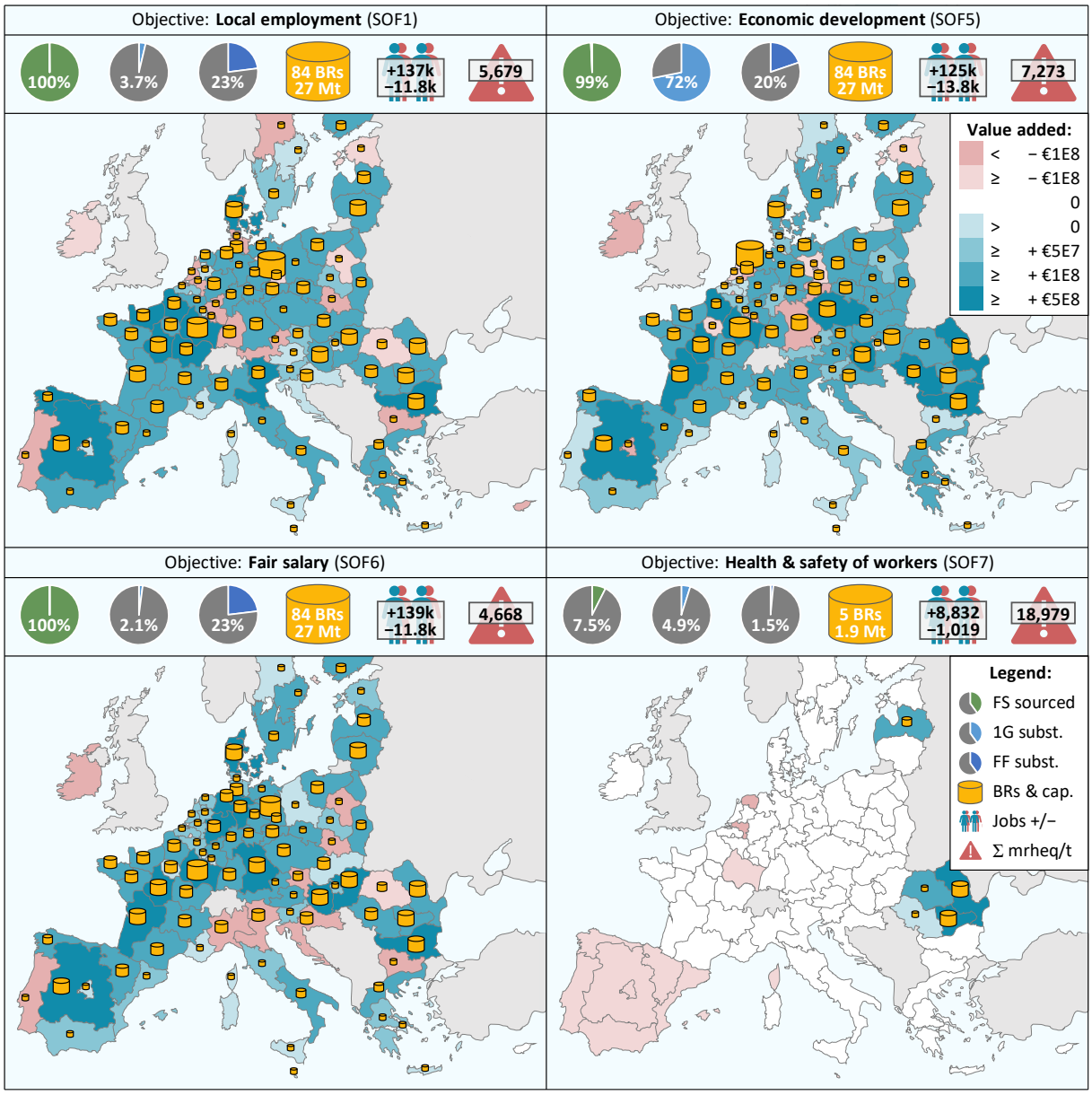

Fig. C 11: Economic value: Socially optimal biorefinery location and capacity (the size of cylinders corresponds to the capacity) and the regionally created/substituted economic value (blue/red shades) for four social objectives. The legend also includes respective percentages of total feedstock collected (FS sourced), the percentage of 1G demand substituted, the percentage of fossil petrol demand substituted (subst. 1G and subst. FF, pie charts), the total number and total capacity of biorefineries (BRs & cap.), the net number of jobs added, as well as the total risk increase over all SHDB categories (in pts per ton)

Social risk increased

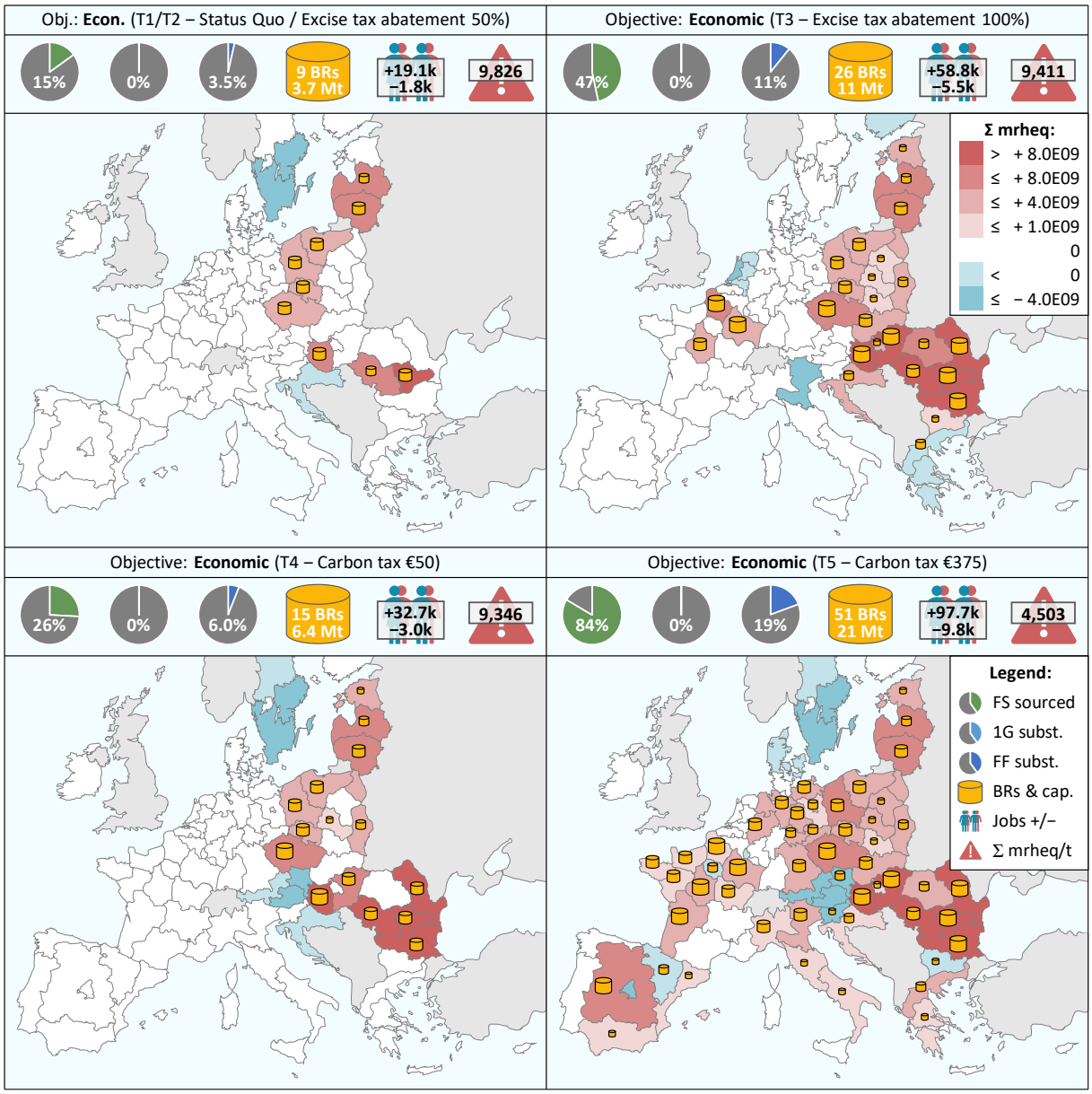

Fig. C 12: Social risk: Economically optimal biorefinery location and capacity (the size of cylinders corresponds to the capacity) and the regional total increase/decrease of the global social risk (over all SHDB categories, in pts; red/blue shades) for economic objectives in five tax scenarios (with identical networks for T1 and T2). The legend also includes respective percentages of total feedstock collected (FS sourced), the percentage of 1G demand substituted, the percentage of fossil petrol demand substituted (subst. 1G and subst. FF, pie charts), the total number and total capacity of biorefineries (BRs & cap.), the net number of jobs added, as well as the total risk increase over all SHDB categories (in pts per ton)

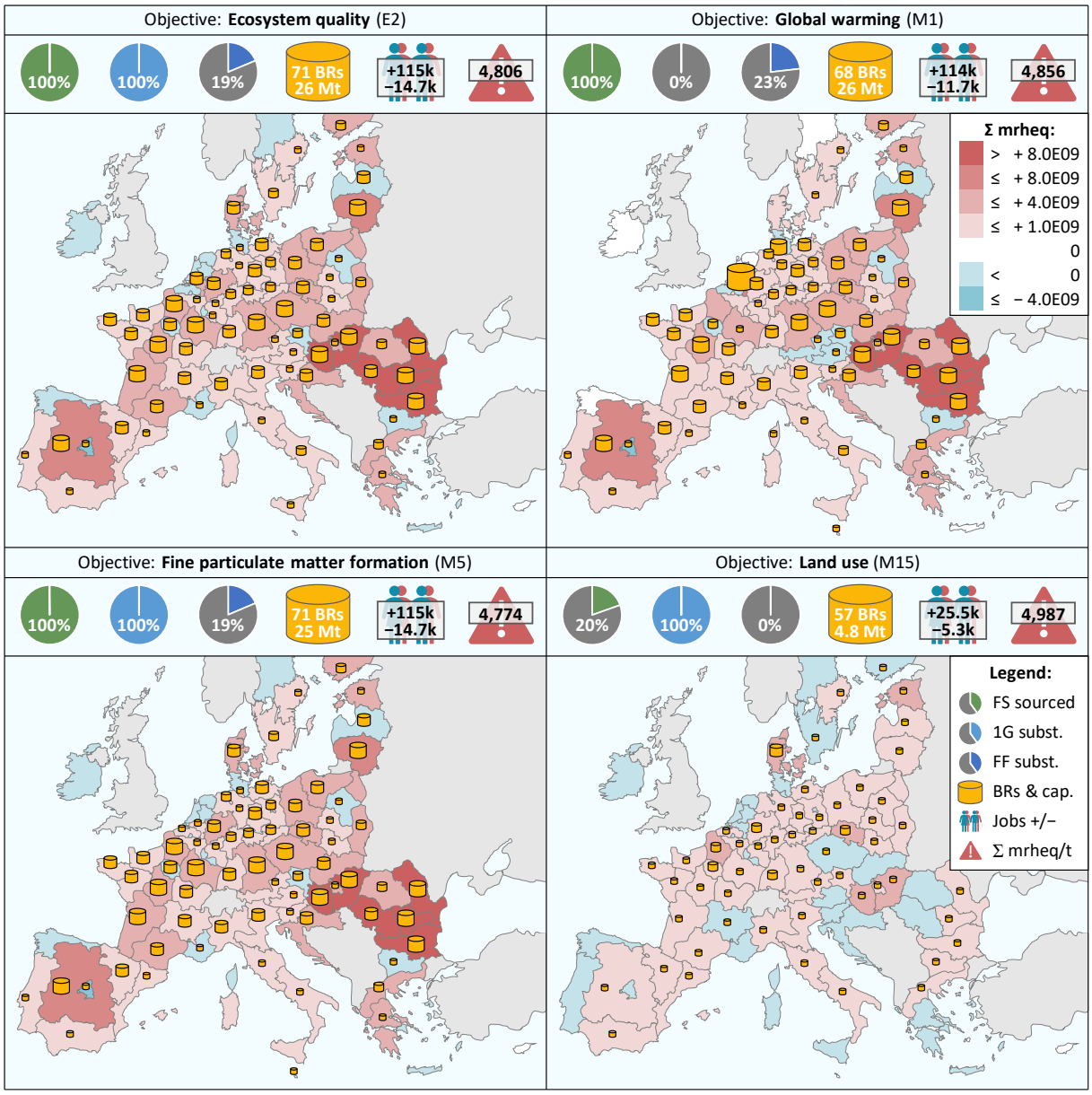

Fig. C 13: Social risk: Environmentally optimal biorefinery location and capacity (the size of cylinders corresponds to the capacity) and the regional total increase/decrease of the global social risk (over all SHDB categories, in pts; red/blue shades) for four environmental objectives (endpoint *ecosystem quality* and three of the most relevant midpoints, see section 0). The legend also includes respective percentages of total feedstock collected (FS sourced), the percentage of 1G demand substituted, the percentage of fossil petrol demand substituted (subst. 1G and subst. FF, pie charts), the total number and total capacity of biorefineries (BRs & cap.), the net number of jobs added, as well as the total risk increase over all SHDB categories (in pts per ton)

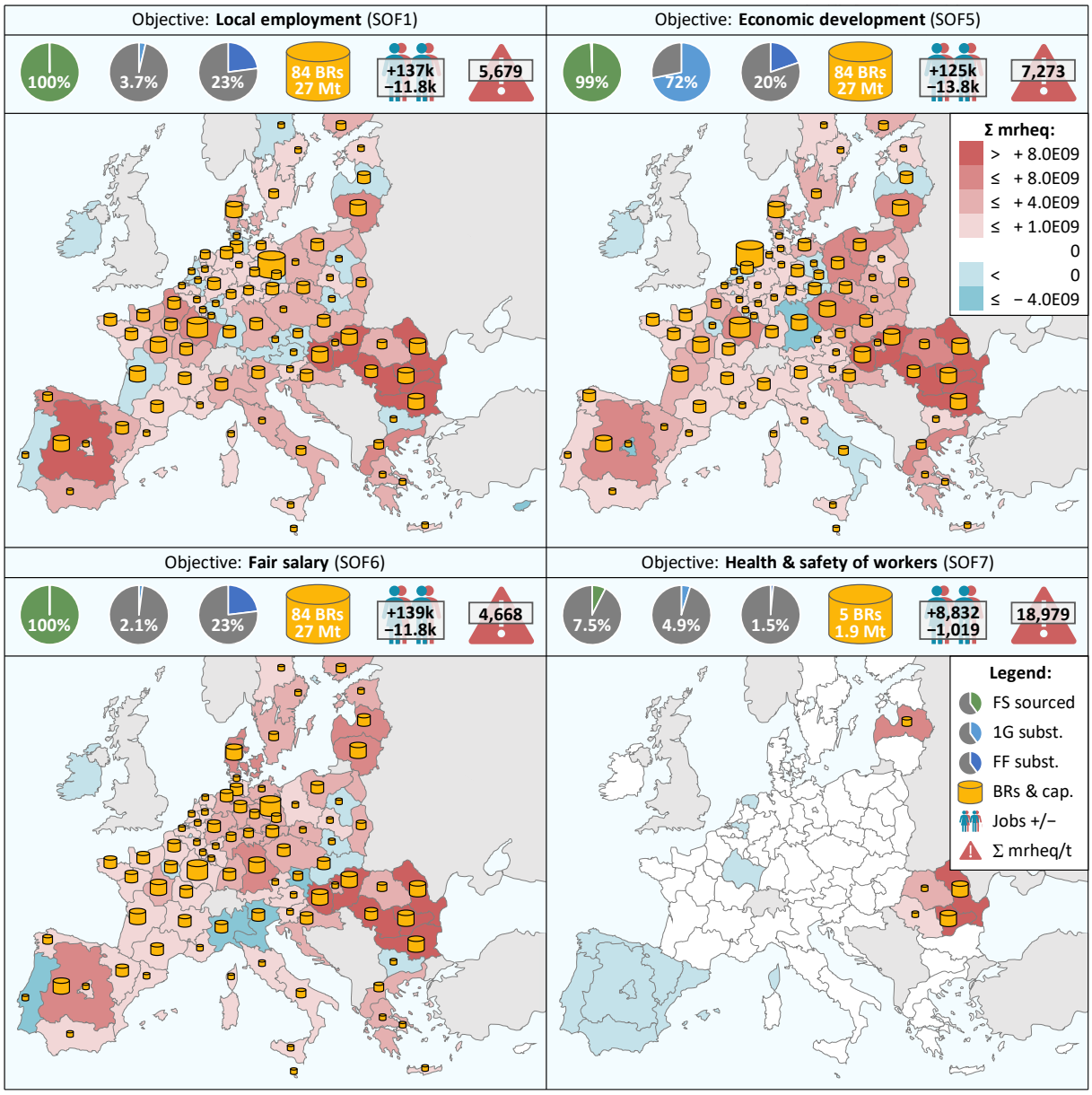

Fig. C 14: Social risk: Socially optimal biorefinery location and capacity (the size of cylinders corresponds to the capacity) and the regional total increase/decrease of the global social risk (over all SHDB categories, in pts; red/blue shades) for four social objectives. The legend also includes respective percentages of total feedstock collected (FS sourced), the percentage of 1G demand substituted, the percentage of fossil petrol demand substituted (subst. 1G and subst. FF, pie charts), the total number and total capacity of biorefineries (BRs & cap.), the net number of jobs added, as well as the total risk increase over all SHDB categories (in pts per ton)

Process contribution

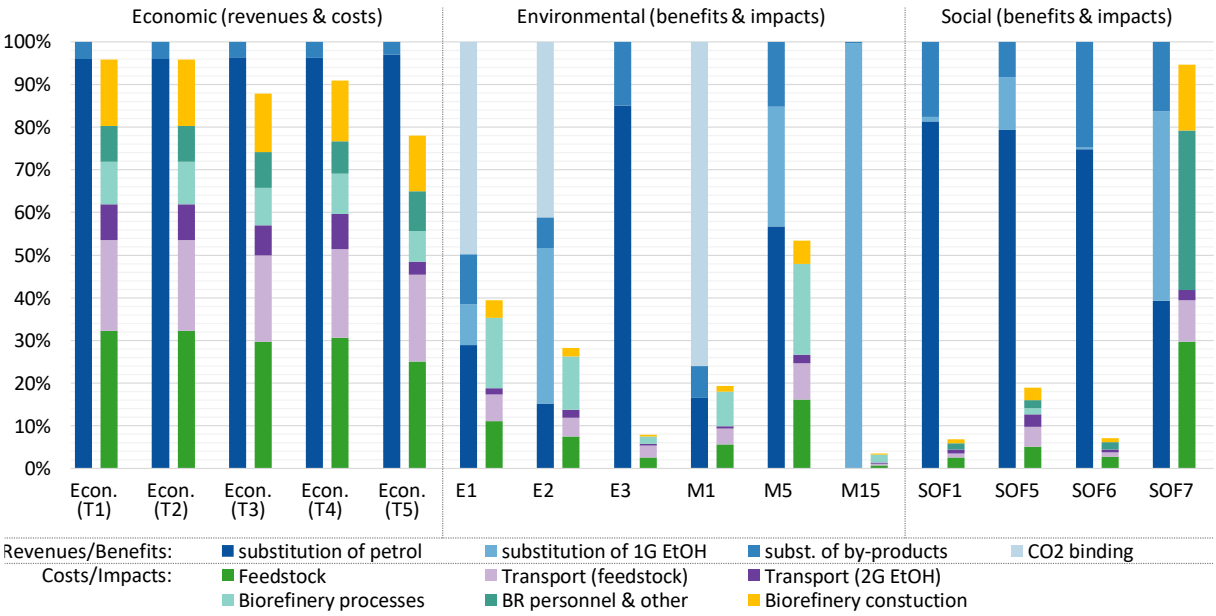

Fig. C 15: Composition (revenues/benefits vs. costs/impacts) of selected objectives for economic, environmental, and social objective values, and relative contribution of different revenues/benefits and costs/impacts

Hotspots by process (sector)

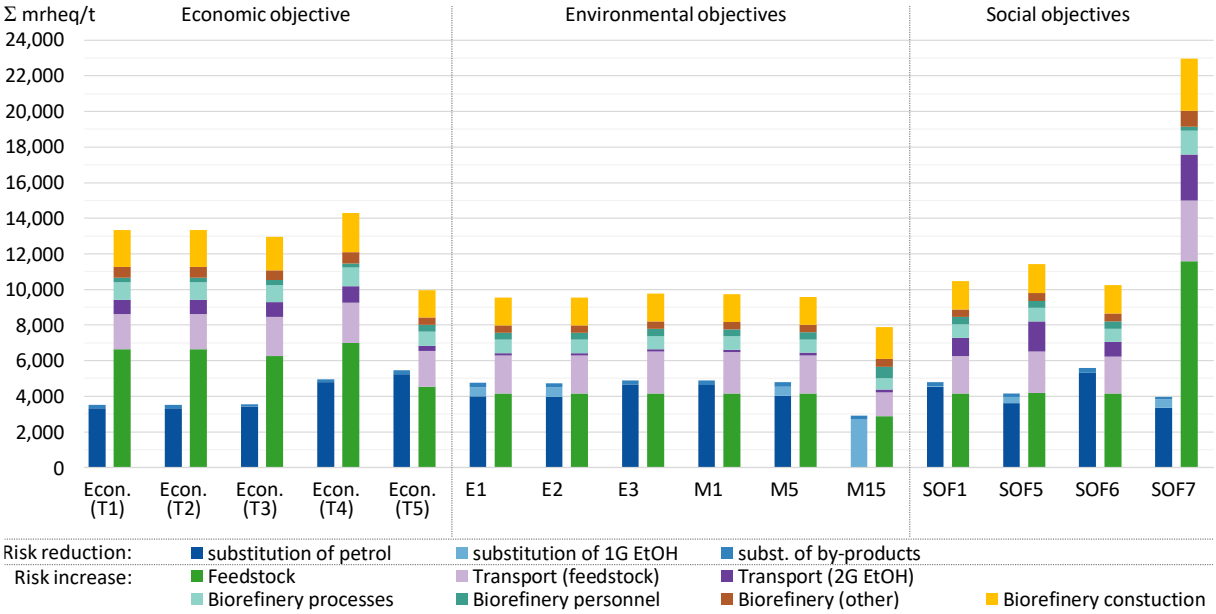

Fig. C 16: Social hotspots by process for selected economic, environmental, and social objective functions, given as the sum of mrheq / t over all SHFs

Hotspots by country

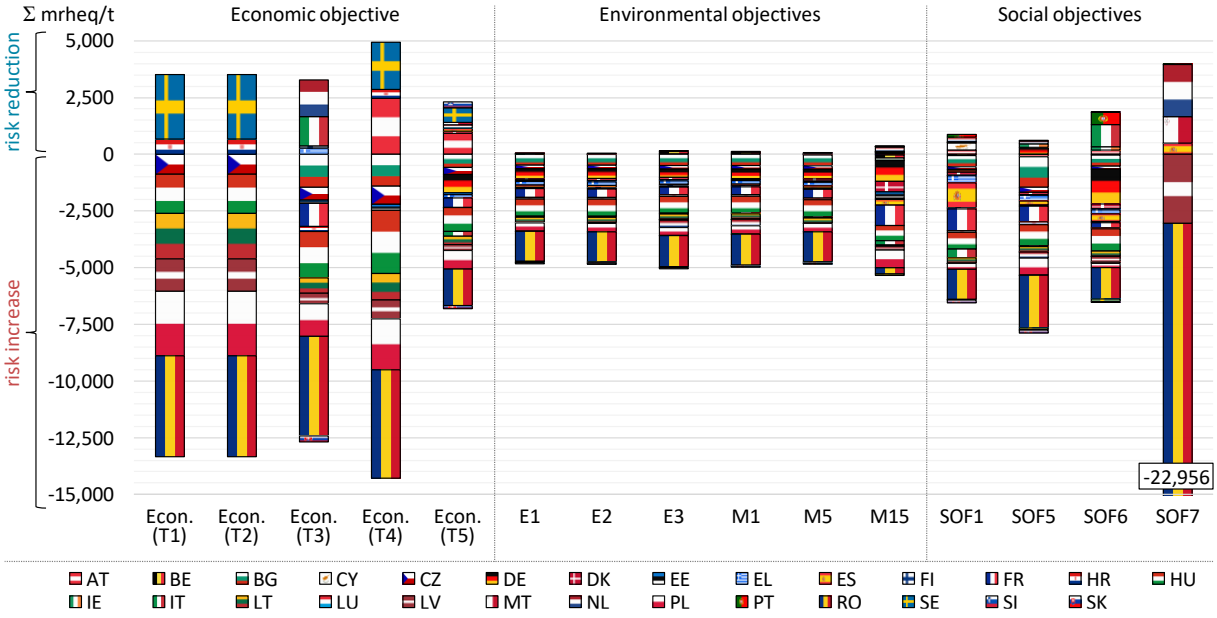

Fig. C 17: Social hotspots by country
for selected economic, environmental, and social objective functions, given as the sum of mrheq / t over all SHFs

Hotspots by subcategory

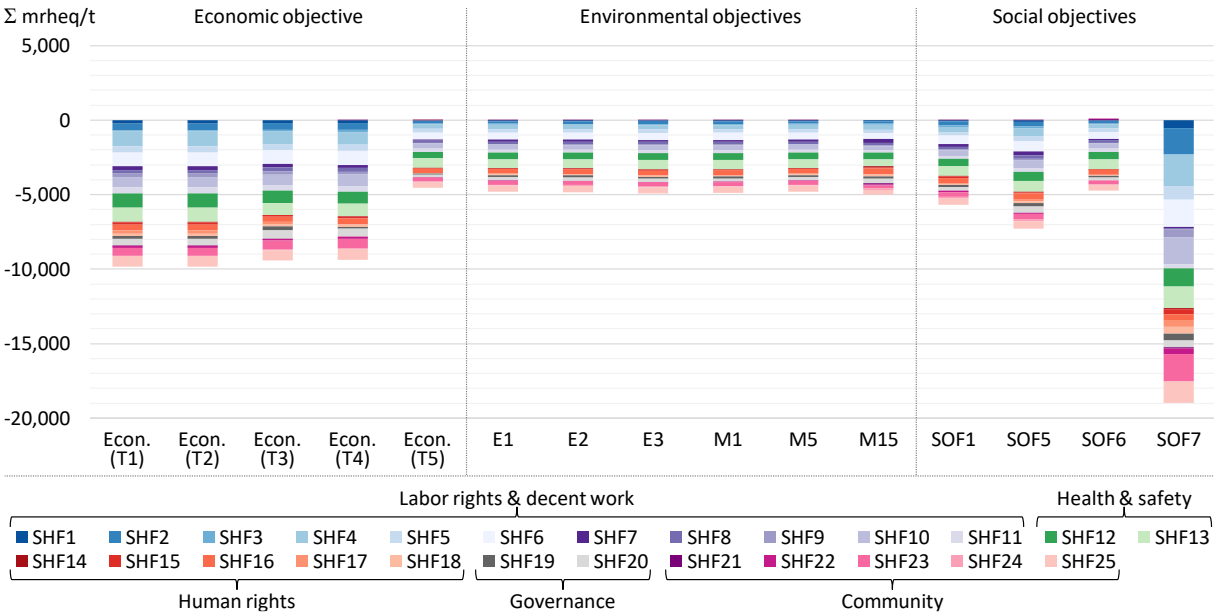

Fig. C 18: Social hotspots by SHDB subcategory (SHF)
for selected economic, environmental, and social objective functions, given in mrheq / t

Regional impacts (SOF2, SOF3, SOF4) & benefits (SOF8)

Fig. C 19 displays the co-calculated results of SOF2, SOF3, SOF4, SOF8, and, for the sake of comparison, of the hotspot functions (as the sum over all SHFs). They are

presented as normalized values, between the worst (0%) and the best (100%) value per ton of produced 2G EtOH in the respective economic, environmental, or social optimization. For SOF2, SOF3, and SOF4, "good" results are those with small co-calculated values per ton of EtOH, i.e., with few regional impacts in terms of water use, air emissions, or land occupation per ton of EtOH. For SOF8, larger objective values represent a higher economic value from feedstock sourcing at small and family-owned farms and are thus preferred.

For **SOF2**, the worst result (0%) corresponds to a value of -30.2 [stress-level-weighted m^3 water per metric ton of 2G EtOH] when optimizing M9 (*Marine eutrophication*), the best corresponds to -4.9 when optimizing SOF7 (*Health & safety*; see Supporting Information S2, Results 1).

For **SOF3**, the worst result (0%) corresponds to a value of -22.8 [excess-mortality- and population-density-weighted air emissions per ton 2G EtOH] when optimizing M8 (*Freshwater eutrophication*), the best corresponds to -1.2 when optimizing M10 (*Terrestrial ecotoxicity*; see Supporting Information S2, Results 1).

For **SOF4**, the worst result (0%) corresponds to a value of -663 [yield weighted m^2 of land occupied per ton 2G EtOH] when optimizing M18 (*Water consumption*), the best corresponds to -224 when optimizing E1 (*Human health*; see SI S2, Results 1).

For **SOF8**, the worst result (0%) corresponds to a value of 140 [feedstock value in EUR weighted with the share of small and family-owned farms per ton 2G EtOH] when optimizing M10 (*Terrestrial ecotoxicity*), the best corresponds to 350 when optimizing SOF7 (*Health & safety*; see Supporting Information S2, Results 1).

For the **sum of SHFs**, the highest risk (0%) corresponds to a value of -18,979 [mrheq per ton 2G EtOH] when optimizing SOF7 (*Health & safety*), the lowest risk corresponds to -4,503 when optimizing Econ. T5 (see Supporting Information S2, Results 1).

The results show that different economic, environmental, and social objective functions differently affect the five displayed categories. Economic optimization up to T4 leads to above-average results for all SOF, especially SOF3. From T5 onwards, the tendencies are heterogeneous. SOF2 and SOF8 are most comparable: T5 and the selected environmental and three of the social objective functions lead to below-average values (i.e., above-average per-ton impacts for SOF2 and below-average per-ton values of feedstock sourcing at small farms), with M15 being the most detrimental. This is explained by comparably low water stress levels (SOF2) and a relatively high fraction of small farms (SOF8) in CEE countries on which economic networks concentrate.

SOF3 shows similar tendencies but with much more pronounced differences. It also profits from the CEE-focused networks (economic optimization and SOF7) and is negatively impacted by the larger and more widely spread networks of many of the

environmental categories, where more Western European countries with partially higher population densities are included. This reason is most notable for the differences between SOF1, SOF5, and SOF6. All objectives feature similar (cf. Figure S5) and extensive networks in which the feedstock potential is fully exploited. However, when possible, SOF1 and SOF6 favor metropolitan regions with higher unemployment rates and higher wages but also higher population densities, while SOF5 focuses on often less developed and less densely populated regions. This leads to the fact that SOF5 optimization leads to one of the best results for SOF3, despite comparably long transportation distances.

In contrast, SOF4 shows the best results for the displayed environmental optimizations. On the one hand, the widely spread network of, e.g., E1 includes many countries with high yields (e.g., Germany, France, Netherlands), meaning that areas with a notable (caloric) potential for food production are occupied. On the other hand, the dispersed network also means that transportation distances can be relatively short, and the environmental preference for rail instead of lorry transports leads to lower land requirements in the environmental cases. This also explains why, despite similar optimal networks (capacities, locations, and production amounts), M15 (*land use*) leads to much fewer impacts in SOF4 compared to M18 (*water consumption*; not part of the figure, corresponds to 0% for SOF4).

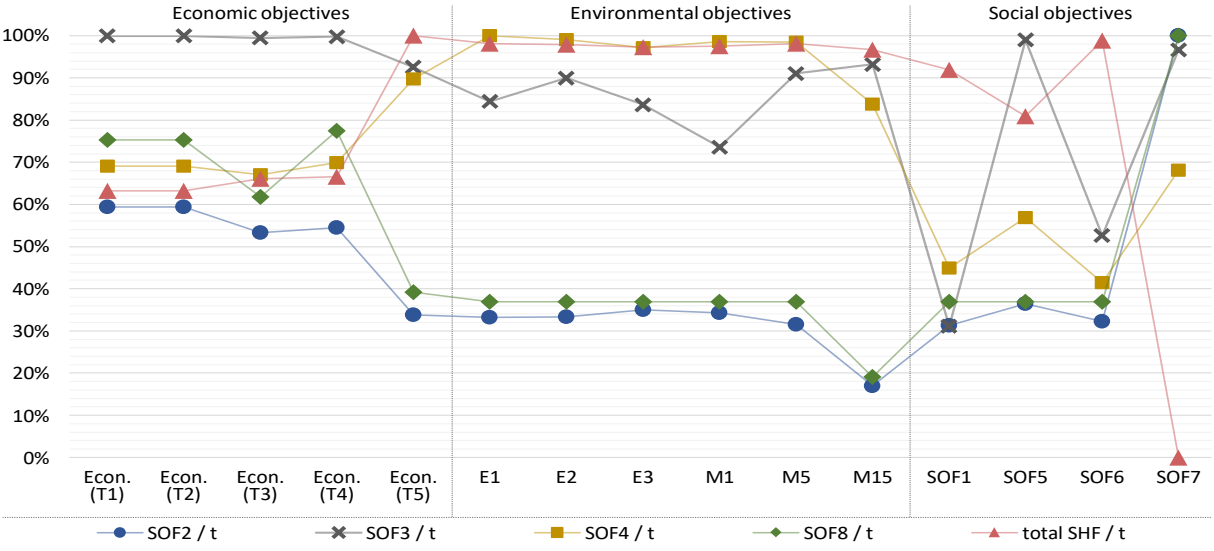

Fig. C 19: Results of SOF2, SOF3, SOF4, SOF8
and the sum over all SHFs, co-calculated for selected economic, environmental, and social objective functions. The results are given as per-ton values, normalized between the worst (0%) and best (100%) value over all economic, environmental, and optimizable social objective functions

C.7 Implications on SDGs

Fig. C 20 and Fig. C 21 show the relationships of the SDGs towards each other on the level of individual objective functions. Those two figures are the basis of Fig. 44 and Fig. 45.

SDG3 and its target 3.4 are linked to the results of E1 (*human health*), M13 & M14 (*human toxicity*), M2 (*ozone depletion*), M3 (*ionizing radiation*), and M4 (*ozone formation*), but these range from conflicting (−−) to highly congruent (+++), depending on which objective is optimized. Thus, for example, E1 profits from the exclusive substitution of 1G EtOH when optimizing M13, while the substitution benefits when optimizing E1 are not sufficient to compensate for the impacts of the larger network itself, leading to a deterioration of M13. In general, categories associated with **SDG3** are, for a slight majority of pair-wise comparisons, positively affected by objectives of SDG6 (e.g., M18 *water consumption*), SDG11 (e.g., M15 *land use*), SDG14 (e.g., M9 *marine eutrophication*), and SDG15 (e.g., M10 *terrestrial ecotoxicity*), as well as among themselves, but hindered mainly by SDG7 (with the associated profit-oriented *economic objective function*), SDG8, SDG12 (e.g., E3 *resource availability*), or SDG13 (M1 *global warming*).

The relationships are similar for **SDG6** (especially target 6.4, with the associated midpoint M18 water consumption), SDG14, and SDG15, but positive and negative tendencies are more pronounced. Again, this is predominantly due to the different substitution decisions. A bioethanol production network entails severe impacts in terms of water consumption, which can only be overcompensated when substituting 1G EtOH, hence the conflicts with, e.g., M1 or E3.

Most notably, the achievement of **SDG7** (Affordable and clean energy) is adversely affected by all other categories. On the one hand, the topic of bioeconomy is inherently linked to this goal, with second-generation biofuels being comparably "clean" vis-à-vis fossil fuels and their first-generation. On the other hand, the single optimization of most social and environmental objectives leads to economically highly inviable networks with uncompetitively high 2G EtOH prices (hence the need for multi-criteria optimization, cf. Fig. 36, Fig. 40, and Fig. 41).

SDG8 (Decent work and economic growth) shows more ambiguous relationships with the other goals. Its associated categories can be divided into two groups: The (corporate and profit-focused) economic objective (see above; target 8.2) as well as health & safety issues (SOF7, SOF7b; target 8.8.1) on the one hand, and (the GDP-focused) SOF5, as well as issues of employment (SOF1; target 8.5.2) and remuneration (SOF6; target 8.5.1) on the other. The first group is highly conflicting with the second group and all objectives associated with the other SDGs, while the second co-benefits from all other

goals. Similarly, **SDG12** (Responsible consumption and production) with target 12.2 (natural resources) is divided into E3 (*resource availability*) & M17 (*fossil resource scarcity*), and M16 (*mineral resource scarcity*). The former generally benefit from any bioethanol network, particularly from the substitution of fossil petrol. The latter is impacted by the material needs of the network itself, with next to no substitution benefits regardless of the reference product. SDG8 and SDG12 are prime examples of why the same action can benefit *and* harm different sustainability goals, targets, and indicators within the same goal, which is why both policy-makers and corporate decision-makers need to be aware of these interdependencies when pursuing social, environmental, or economic objectives.

Lastly, **SDG11** (Sustainable cities and communities, mainly target 11.6) and **SDG13** (Climate action) range from slightly to highly (with fossil petrol substitution) congruent with the other SDGs and their associated objectives.

Effect on objectives:	Optimization of objectives:	SDG3	SDG3	SDG3	SDG3.4	SDG3.4	SDG3.4	SDG6.4	SDG7	SDG8.1	SDG8.2	SDG8.5.1	SDG8.5.2	SDG8.8.1	SDG8.8.1	SDG11.3	SDG11.6	SDG12.2	SDG12.2	SDG13	SDG14.1	SDG14.1	SDG14.1	SDG15.1	SDG15.1	SDG15.1	SDG15.1	SDG15.1	SDG15.1
		E1	M13	M14	M2	M3	M4	M18	EC-t3	SOF5	EC-t3	SOF6	SOF1	SOF7	SOF7b	M15	M5	E3	M16	M1	E2	M9	M12	E2	M6	M7	M8	M10	M11
SDG3	E1	0%	-47%	-76%	-76%	-6%	-76%	-78%	-59%	-9%	-59%	-17%	-16%	-94%	-100%	-76%	0%	-5%	-100%	-5%	0%	-77%	-75%	0%	-77%	-1%	-36%	-77%	-76%
SDG3	M13	-132%	0%	-59%	-85%	-104%	-64%	-58%	-151%	-191%	-151%	-182%	-181%	-131%	-100%	-82%	-59%	-168%	-100%	-168%	-133%	-39%	-59%	-133%	-64%	-114%	-49%	-95%	-42%
SDG3	M14	-249%	-94%	0%	-8%	-275%	-11%	-16%	-255%	-321%	-255%	-452%	-447%	-120%	-100%	-82%	-59%	-397%	-100%	-547%	-249%	-7%	0%	249%	-12%	-253%	-143%	-13%	-3%
SDG3.4	M2	-369%	-149%	-3%	0%	-374%	-4%	-9%	-312%	-420%	-312%	-552%	-548%	-126%	-100%	-1%	-1%	-547%	-100%	-547%	-369%	-3%	-3%	369%	-6%	-369%	-215%	-2%	-4%
SDG3.4	M3	-7%	-61%	-85%	-82%	0%	-76%	-83%	-67%	-17%	-67%	-14%	-15%	-98%	-100%	-76%	-7%	-28%	-100%	-29%	-8%	-82%	-85%	-8%	-76%	-5%	-59%	-71%	-84%
SDG3.4	M4	-534%	-170%	-67%	-57%	-520%	0%	-58%	533%	-741%	-533%	-842%	-835%	-220%	-100%	-23%	-524%	753%	-749%	-100%	532%	-41%	-60%	-1%	-500%	-414%	-57%	-41%	
SDG6.4	M18	-57%	-21%	-2%	-5%	-59%	-3%	0%	128%	-87%	-128%	-164%	-162%	-100%	-100%	-4%	-56%	165%	-165%	165%	-56%	-2%	-3%	-56%	-5%	-56%	-32%	-5%	-2%
SDG7	EC-t3	-521%	-397%	-305%	-323%	-550%	-315%	-335%	0%	-674%	0%	-574%	-592%	-96%	-100%	-316%	-511%	-409%	-100%	-421%	-520%	-346%	-304%	-520%	-310%	-557%	-586%	-295%	-347%
SDG8.1	SOF5	-28%	-61%	-86%	-86%	-27%	-85%	-81%	-59%	0%	-59%	-22%	-15%	-93%	-100%	-86%	-28%	-27%	-100%	-28%	-28%	-81%	-86%	-28%	-85%	-25%	-49%	-84%	-82%
SDG8.2	EC-t3	-521%	-397%	-305%	-323%	-550%	-315%	-335%	0%	-674%	0%	-574%	-592%	-96%	-100%	-316%	-511%	-409%	-100%	-414%	-520%	-346%	-304%	-520%	-310%	-557%	-586%	-295%	-347%
SDG8.5.1	SOF6	-27%	-60%	-84%	-82%	-15%	-82%	-86%	-73%	-21%	-73%	0%	-6%	-96%	-100%	-82%	-27%	-25%	-100%	-25%	-27%	-81%	-84%	-27%	-83%	-24%	-47%	-87%	-82%
SDG8.5.2	SOF1	-29%	-73%	-92%	-88%	-18%	-85%	-89%	-69%	-22%	-69%	-12%	0%	-97%	-100%	-87%	-29%	-30%	-100%	-30%	-29%	-87%	-91%	-29%	-86%	-27%	-63%	-86%	-90%
SDG8.8.1	SOF7	<-999%	<-999%	<-999%	<-999%	<-999%	<-999%	<-999%	<-999%	<-999%	<-999%	<-999%	<-999%	0%	-100%	<-999%	<-999%	<-999%	-100%	<-999%	<-999%	<-999%	<-999%	<-999%	<-999%	<-999%	<-999%	<-999%	<-999%
SDG8.8.1	SOF7b	<-999%	<-999%	<-999%	<-999%	<-999%	<-999%	<-999%	<-999%	<-999%	<-999%	<-999%	<-999%	<-999%	0%	<-999%	<-999%	<-999%	-100%	<-999%	<-999%	<-999%	<-999%	<-999%	<-999%	<-999%	<-999%	<-999%	<-999%
SDG11.3	M15	-14%	-7%	0%	0%	-16%	0%	-1%	-110%	-46%	-110%	-119%	-117%	-97%	-100%	0%	-14%	-118%	-100%	-118%	-14%	-1%	0%	-14%	-2%	-15%	-10%	0%	-1%
SDG11.6	M5	0%	-32%	-55%	-56%	-8%	-54%	-56%	-72%	-21%	-72%	-48%	-46%	-96%	-100%	-55%	0%	-33%	-100%	-32%	0%	-56%	-55%	0%	-55%	0%	-29%	-57%	-55%
SDG12.2	E3	-12%	-64%	-92%	-92%	-16%	-92%	-94%	-56%	-12%	-56%	-7%	-7%	-93%	-100%	-92%	-12%	0%	-100%	0%	-12%	-93%	-92%	-12%	-92%	-13%	-50%	-92%	-93%
SDG12.2	M16	<-999%	<-999%	<-999%	<-999%	<-999%	<-999%	<-999%	<-999%	<-999%	<-999%	<-999%	<-999%	<-999%	-100%	<-999%	<-999%	<-999%	0%	<-999%	<-999%	<-999%	<-999%	<-999%	<-999%	<-999%	<-999%	<-999%	<-999%
SDG12.2	M17	-10%	-61%	-90%	-90%	-13%	-90%	-92%	-56%	-11%	-56%	-7%	-7%	-93%	-100%	-90%	-10%	0%	-100%	0%	-10%	-91%	-90%	-10%	-90%	-11%	-47%	-90%	-90%
SDG13	M1	-7%	-58%	-87%	-87%	-11%	-88%	-89%	-56%	-9%	-56%	-7%	-7%	-94%	-100%	-87%	-8%	0%	-100%	0%	-7%	-88%	-87%	-7%	-88%	-8%	-44%	-88%	-87%
SDG14.1	E2	0%	-28%	-43%	-43%	-4%	-43%	-45%	-77%	-18%	-77%	-52%	-52%	-95%	-100%	-43%	0%	-46%	-100%	-46%	0%	-44%	-43%	0%	-44%	-1%	-21%	-44%	-43%
SDG14.1	M9	-11%	-5%	0%	0%	-11%	0%	0%	106%	-40%	-106%	-111%	-110%	-96%	-100%	0%	-11%	-114%	-100%	-113%	-11%	0%	0%	-11%	-2%	-11%	-6%	0%	0%
SDG14.1	M12	-318%	-116%	0%	-22%	-398%	-27%	-50%	331%	-462%	-331%	-636%	-628%	-141%	-100%	-24%	-320%	-474%	-100%	-465%	-319%	-21%	0%	319%	-27%	-329%	-198%	-31%	-6%
SDG15.1	E2	0%	-28%	-43%	-43%	-4%	-43%	-45%	-77%	-18%	-77%	-52%	-52%	-95%	-100%	-43%	0%	-46%	-100%	-46%	-46%	-44%	-43%	0%	-44%	-1%	-21%	-44%	-43%
SDG15.1	M6	<-999%	-434%	-120%	-102%	<-999%	-1%	-110%	<-999%	<-999%	<-999%	<-999%	<-999%	-349%	-100%	-40%	<-999%	<-999%	<-999%	<-999%	<-999%	-77%	-107%	<-999%	0%	<-999%	-939%	-103%	-77%
SDG15.1	M7	0%	-21%	-35%	-37%	-4%	-35%	-36%	-81%	-22%	-81%	-62%	-60%	-96%	-100%	-36%	0%	-55%	-100%	-55%	0%	-36%	-35%	0%	-37%	0%	-18%	-37%	-35%
SDG15.1	M8	-27%	-8%	-40%	-54%	-25%	-53%	-45%	-73%	-45%	-73%	-65%	-65%	-97%	-100%	-58%	-28%	-64%	-100%	-59%	-28%	-37%	-41%	-28%	-54%	-26%	0%	-61%	-38%
SDG15.1	M10	-305%	-289%	-5%	-5%	-578%	-48%	-141%	-392%	-572%	-392%	-918%	-900%	-128%	-100%	-5%	-310%	-473%	-100%	-474%	-304%	-114%	-5%	-304%	-47%	-383%	-369%	0%	-68%
SDG15.1	M11	-126%	-37%	-2%	-10%	-143%	-9%	-14%	-186%	-189%	-186%	-287%	-283%	-114%	-100%	-11%	-127%	-247%	-100%	-244%	-127%	-3%	-1%	-127%	-11%	-126%	-69%	-14%	0%

Fig. C 20: Opportunity costs

(percental detriment in one category compared to its optimal value when optimizing another) between social, environmental, and economic objective functions, matched with the SDGs. Optimized objective functions and their SDGs are displayed on top of the table, affected ones to the left

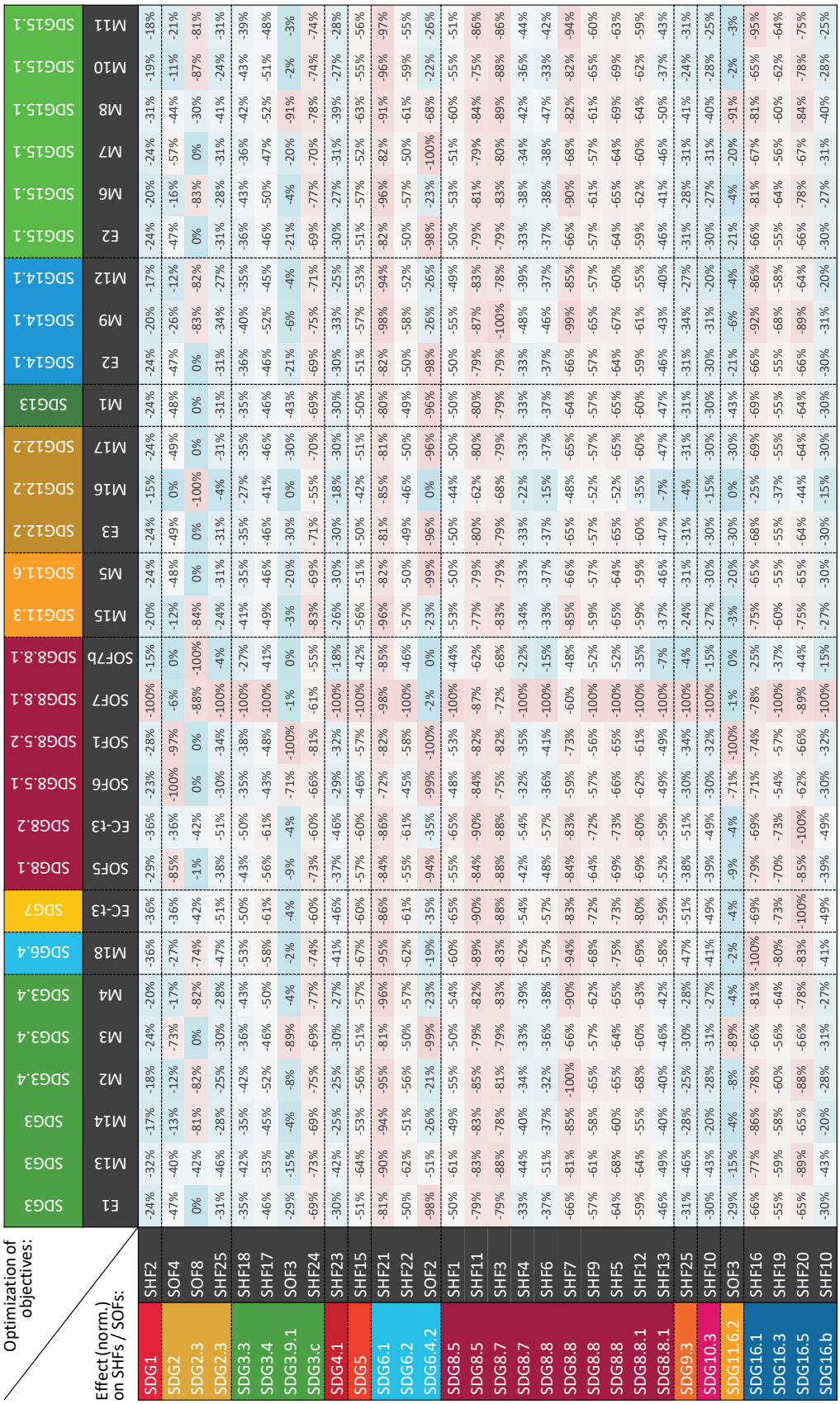

Fig. C 21: Detriment in the categories
to the left (bottom) when optimizing the objective functions to the top (left), normalized between the worst and best values

Appendix D

Appendix D includes the links to the online data repositories

D.1 Online data repository for Chapter 4

Data for: Spatially explicit forecast of feedstock potentials for second generation bioconversion industry from the EU agricultural sector until the year 2030

https://data.mendeley.com/datasets/3r7nd7gb56/1

D.2 Online data repository for Chapter 5

Supporting Information: Assessing the Social Dimension in Strategic Network Design for a Sustainable Development: The Case of Bioethanol Production in the EU

https://doi.org/10.5281/zenodo.3941996

D.3 Online data repository for Chapter 6

Supporting Information: Assessing the Social Dimension in Strategic Network Design for a Sustainable Development: The Case of Bioethanol Production in the EU

Link to the data repository at manuscript submission (available):

https://doi.org/10.5281/zenodo.5886754

Link to the final data repository (available after publication):

https://doi.org/10.5281/zenodo.5589667